

Information Circular 9448

Proceedings of the Second International Workshop on Coal Pillar Mechanics and Design

**Edited by Christopher Mark, Ph.D., Keith A. Heasley, Ph.D.,
Anthony T. Iannacchione, Ph.D., and Robert J. Tuchman**

U.S. DEPARTMENT OF HEALTH AND HUMAN SERVICES
Public Health Service
Centers for Disease Control and Prevention
National Institute for Occupational Safety and Health
Pittsburgh Research Laboratory
Pittsburgh, PA

June 1999

International Standard Serial Number
ISSN 1066-5552

CONTENTS

	<i>Page</i>
Abstract	1
Introduction	2
A unique approach to determining the time-dependent in situ strength of coal pillars, by K. Biswas, Ph.D. (University of Ballarat), Australia, C. Mark, Ph.D. (National Institute for Occupational Safety and Health), and S. S. Peng, Ph.D. (West Virginia University), U.S.A	5
Developments in coal pillar design at Smoky River Coal Ltd., Alberta, Canada, by P. Cain, Ph.D., P.Eng. (Smoky River Coal Ltd.), Canada	15
Coal pillar design for longwall gate entries, by J. W. Cassie, P. F. R. Altounyan, Ph.D., and P. B. Cartwright (Rock Mechanics Technology Ltd.), United Kingdom	23
Analysis of longwall tailgate serviceability (ALTS): a chain pillar design methodology for Australian conditions, by M. Colwell (Colwell Geotechnical Services), R. Frith, Ph.D. (Strata Engineering), Australia, and C. Mark, Ph.D. (National Institute for Occupational Safety and Health), U.S.A.	33
Experience of field measurement and computer simulation methods for pillar design, by W. J. Gale, Ph.D. (Strata Control Technology), Australia	49
University of New South Wales coal pillar strength determinations for Australian and South African mining conditions, by J. M. Galvin, Ph.D., B. K. Hebblewhite, Ph.D. (University of New South Wales), Australia, and M. D. G. Salamon, Ph.D. (Colorado School of Mines), U.S.A.	63
Practical boundary-element modeling for mine planning, by K. A. Heasley, Ph.D., and G. J. Chekan (National Institute for Occupational Safety and Health), U.S.A	73
Experience with the boundary-element method of numerical modeling to resolve complex ground control problems, by G. J. Karabin, P.E., and M. A. Evanto, P.G. (Mine Safety and Health Administration), U.S.A.	89
The fracture mechanics approach to understanding supports in underground coal mines, by J. M. Kramer, Ph.D., G. J. Karabin, P.E., and M. T. Hoch (Mine Safety and Health Administration), U.S.A.	115
A hybrid statistical-analytical method for assessing violent failure in U.S. coal mines, by H. Maleki, Ph.D. (Maleki Technologies, Inc.), E. G. Zahl, and J. P. Dunford (National Institute for Occupational Safety and Health), U.S.A.	139
Empirical methods for coal pillar design, by C. Mark, Ph.D. (National Institute for Occupational Safety and Health), U.S.A.	145
Coal pillar strength and practical coal pillar design considerations, by D. W. H. Su, Ph.D., and G. J. Hasenus (CONSOL, Inc.), U.S.A.	155
New strength formula for coal pillars in South Africa, by J. N. van der Merwe, Ph.D. (Itasca Africa (Pty.) Ltd.), Republic of South Africa	163
The role of overburden integrity in pillar failure, by J. N. van der Merwe, Ph.D. (Itasca Africa (Pty.) Ltd.), Republic of South Africa	173
Using a postfailure stability criterion in pillar design, by R. K. Zipf, Jr., Ph.D. (University of Missouri-Rolla), U.S.A	181

UNIT OF MEASURE ABBREVIATIONS USED IN THIS REPORT

ft	foot (feet)	kPa/m	kilopascal per meter
GPa	gigapascal	m	meter
ha	hectare	mm	millimeter
hr	hour	MN/m	meganewton per meter
in	inch	MN/m ³	meganewton per cubic meter
in/in	inch per inch	MPa	megapascal
kg/cm ²	kilogram per square centimeter	psi	pound (force) per square inch
kg/m ³	kilogram per cubic meter	psi/ft	pound (force) per square inch per foot
km	kilometer	sec	second
km ²	square kilometer	%	percent
kN/m ³	kilonewton per cubic meter	°	degree

The views expressed by non-NIOSH authors in these proceedings are not necessarily those of the National Institute for Occupational Safety and Health.

Mention of any company name or product does not constitute endorsement by the National Institute for Occupational Safety and Health.

To receive other information about occupational safety and health problems, call 1-800-35-NIOSH (1-800-356-4674), or visit the NIOSH Home Page on the World Wide Web at <http://www.cdc.gov/niosh>

PROCEEDINGS OF THE SECOND INTERNATIONAL WORKSHOP ON COAL PILLAR MECHANICS AND DESIGN

Edited by Christopher Mark, Ph.D.,¹ Keith A. Heasley, Ph.D.,¹
Anthony T. Iannacchione, Ph.D.,² and Robert J. Tuchman³

ABSTRACT

Pillar design is the first line of defense against rock falls—the greatest single safety hazard faced by underground coal miners in the United States and abroad. To help advance the state of the art in this fundamental mining science, the National Institute for Occupational Safety and Health organized the Second International Workshop on Coal Pillar Mechanics and Design. The workshop was held in Vail, CO, on June 6, 1999, in association with the 37th U.S. Rock Mechanics Symposium. The proceedings include 15 papers from leading ground control specialists in the United States, Canada, Australia, the United Kingdom, and the Republic of South Africa. The papers address the entire range of issues associated with coal pillars and have a decidedly practical flavor. Topics include numerical modeling, empirical design formulas based on case histories, field measurements, and postfailure mechanics.

¹Supervisory physical scientist.

²Deputy director.

³Technical writer-editor.

Pittsburgh Research Laboratory, National Institute for Occupational Safety and Health, Pittsburgh, PA.

INTRODUCTION

By Christopher Mark, Ph.D.¹

Pillar design is one of the oldest and most fundamental of the mining sciences. Without pillars to support the great weight of the overburden, underground coal mining would be practically impossible. Coal pillars are employed in a wide variety of mining operations, from shallow room-and-pillar mines to deep longwall mines. Yet despite more than 100 years of research and experience, pillar failures continue to occur, placing miners' lives at risk. Some recent examples are [Mark et al. 1998]:

Massive collapses: In 1992, miners were splitting pillars at a mine in southern West Virginia when the fenders in a 2.3-ha area suddenly collapsed. The miners were knocked to floor by the resulting airblast; 103 ventilation stoppings were destroyed. At least 12 similar events have occurred in recent years in the United States and 15 others in Australia, fortuitously without a fatality.

Pillar squeezes: At a coal mine in Kentucky, pillars were being extracted in the main entries under 270 m of cover. The pillars began to crush in response to the vertical load, resulting in a roof fall that killed two miners. This incident is an extreme example of hazardous conditions that can be associated with slow pillar failure. At least 45 recent instances of pillar squeezes in room-and-pillar mines have been identified.

Longwall tailgate blockages: In 1984, 26 miners at the Wilberg Mine in Utah could not escape a deadly fire because of a tailgate roof fall. Similar blockages were common in the 1980s, and 50 cases have been documented.

Pillar bumps: Extracting the initial lift from a standing pillar at a deep operation in eastern Kentucky resulted in a bump that killed two miners. However, bumps are not confined to pillars; another fatal bump occurred at a longwall face in Utah just days later.

Multiple-seam interactions: Some studies indicate that most remaining coal reserves will experience multiple-seam interactions. At a mine in West Virginia where four seams had been previously extracted, one fatality occurred when the roof collapsed without warning beneath a remnant barrier pillar.

Abandoned mine subsidence: As suburban development expands into historic coal mining areas, unplanned subsidence has become an important issue. In one case, residents above 50-year-old workings were disturbed by seismicity emanating from collapsing pillars. In the Republic of South Africa, collapsing pillars in the Vaal Basin are creating large sinkholes that threaten many homes.

To help reduce the safety hazards of pillar failures, this *Second International Workshop on Coal Pillar Mechanics and*

Design was organized. (The first workshop was held in Santa Fe, NM, in 1992.) The proceedings of the second workshop feature 15 invited papers from leading rock mechanics experts in the United States, Australia, the Republic of South Africa, the United Kingdom, and Canada. Mines in these five countries employ increasingly similar methods, including:

- Retreat longwall mining, usually using large chain pillars;
- Room-and-pillar mining with continuous mining machines; and
- Roof bolts for primary roof support.

The similarity of mining methods means that it is easier and more valuable to transfer safety technologies like pillar design from one country to another. Indeed, one of the striking features of these proceedings is the convergence of research results across international borders.

Other trends affecting the mining industries of the five countries are also reflected in these proceedings, some of which have been less positive. In the 7 years since the first workshop, underground production has risen in Australia and the Republic of South Africa, declined in the United Kingdom and Canada, and remained steady in the United States. However, great employment losses have occurred in all five countries because of technological advances and dramatic productivity increases.

One consequence has been a significant decline in institutional support for mining research. Since 1992, the U.S. Bureau of Mines (USBM), the Canada Centre for Mineral and Energy Technology's (CANMET) Coal Research Laboratory, British Coal's Headquarters Technical Division, and the South African Chamber of Mines research department have all closed their doors. Government funding for mining research is now indirect and open for competition everywhere, except in the United States. In the United States, the National Institute for Occupational Safety and Health (NIOSH) has taken up the USBM's traditional mine safety research role, although at a reduced level, and continues to receive direct funding from the U.S. Congress.

University mining departments have also been under pressure due to fluctuating student enrollments, reduced research funding, and a shortage of qualified junior faculty. Lower profit margins and a renewed emphasis on the bottom line has meant that few mining companies now maintain any in-house research capability. As the traditional sources of mining research have faltered, in many cases private consulting firms have taken up the challenge. Often staffed by former government researchers and sometimes supported in part by government contracts, consultants are now often on the cutting edge of research.

¹Supervisory physical scientist, Pittsburgh Research Laboratory, National Institute for Occupational Safety and Health, Pittsburgh, PA.

In comparing the proceedings of the second workshop with those of the first [Iannacchione et al. 1992], the most obvious difference is that the current collection of papers is a slimmer volume. There are 15 papers in these proceedings, compared with 23 in 1992. Australia, which in many ways has the healthiest mining research community, is the only country to see its representation increase (see table 1). Although the number of papers from industry, government, and academia all decreased by at least 50%, the number of papers from private consultants more than doubled.

Another consequence of the changed research environment is reflected in the proceedings' pervasive emphasis on practical problem-solving. Although about one-half of the papers at the first workshop addressed issues of a more theoretical nature, nearly every paper in the current collection uses case histories, field measurements, and/or practical experience to develop techniques for solving real-world pillar design problems.

The papers divide almost evenly between those that focus primarily on the application of numerical modeling and those that discuss empirical formulas derived from statistical analysis of case histories (table 1). Of the numerical modelers, two used finite-difference methods (Gale, Cassie et al.), four used boundary elements (Heasley-Chekan, Maleki et al., Zipf, Karabin-Evanto), and one used finite elements (Su-Hasenfus). Field measurements feature prominently in six papers, with Cassie et al., Colwell et al., and Gale monitoring stress and deformation, Heasley-Chekan and Karabin-Evanto mapping underground conditions, and Biswas et al. measuring changes in rock strength.

In general, however, the similarities between the papers are more striking than their dissimilarities despite the variety of countries, author affiliations, and research methods. For example, new empirical formulas are presented for the Republic of South Africa (van der Merwe), the United States (Mark), and Australia (Galvin et al.). Derived independently from different sets of case histories from around the world, the three formulas are within 15% of each other (see figure 1).

Five papers (Su-Hasenfus, Gale, Cassie et al., Mark, and Colwell et al.) explicitly address the design of squat (large width-to-height (w/h) ratio) pillars, primarily for protection of longwall gate entries. All agree that the strength of these pillars can vary widely depending on the roof, floor, and seam parting characteristics. Moreover, the strength of the roof is often just as important to the design process as the strength of the pillar itself. The degree of consensus that has been achieved on this complex topic is an important advance. At the other end of the w/h scale, van der Merwe, Zipf, and Mark address slender pillars and their potential for sudden collapse. Again, all three reach similar conclusions regarding the importance of pillar geometry and postfailure pillar stiffness.

The beginnings of a consensus are also evident in one of the oldest pillar design controversies—the value of compressive

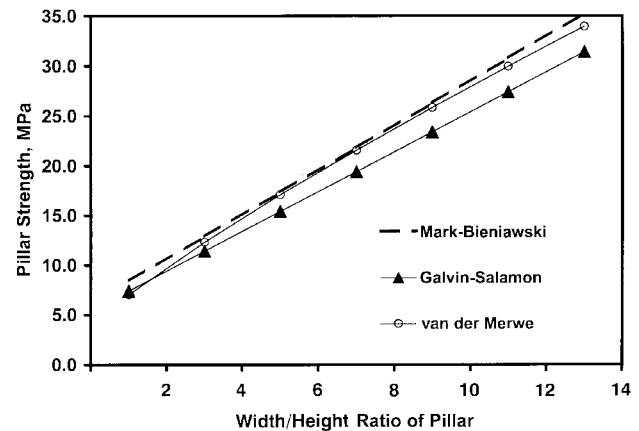


Figure 1.—Empirical pillar strength formulas derived from case histories by Mark (U.S.A.), Galvin (Australia), and van der Merwe (Republic of South Africa).

strength tests on coal specimens. Only two papers (Karabin-Evanto and Maleki et al.) make use of laboratory tests to evaluate seam strength. On the other hand, van der Merwe, Su-Hasenfus, Cassie et al., Galvin et al., Gale, and Mark all conclude that variations in the uniaxial compressive strength have little effect on the in situ pillar strength.

With the focus on pillar strength, it is important not to overlook the other half of the design equation—the load. Gale and Colwell et al. describe field measurements that shed new light on the loads that occur during longwall mining. Heasley-Chekan and van der Merwe address the effect of overburden behavior on the pillar loading. Kramer et al. have extended their fracture mechanics approach for estimating load distribution to consider the effects of other kinds of supports.

Other special topics that are discussed in these proceedings include the effect of weathering on long-term pillar strength (Biswas et al.), the geologic and geotechnical factors that affect the potential for coal bumps (Maleki et al.), thick-seam room-and-pillar mining (Cain), multiple-seam mine design (Heasley-Chekan), and the strength of rectangular pillars (Galvin et al. and Mark).

One final comparison between the first and second workshops is perhaps in order. The proceedings of the first workshop [Iannacchione et al. 1992] included papers from a number of now retired individuals whose names have been synonymous with pillar design for nearly 3 decades: Salamon, Bieniawski, Wagner, Barron, and Carr. In many ways, their contributions laid the foundation upon which rests much of our current understanding of coal pillars. Their retirement has left a large gap that cannot be filled (although it is hoped that they will continue to contribute to the profession!). To paraphrase Sir Isaac Newton, it is only by standing on the shoulders of such giants that we can hope to achieve further progress.

**Table 1.—Summary of papers for the Second International Workshop
on Coal Pillar Mechanics and Design**

Primary author	Country	Affiliation	Method
Biswas	Australia	University	Empirical.
Cain	Canada	Mining company	Empirical.
Cassie	U.K.	Consultant	Numerical.
Colwell	Australia	Consultant	Empirical.
Gale	Australia	Consultant	Numerical.
Galvin	Australia	University	Empirical.
Heasley	U.S.A.	Government	Numerical.
Karabin	U.S.A.	Government	Numerical.
Kramer	U.S.A.	Government	Numerical.
Maleki	U.S.A.	Consultant	Empirical/numerical.
Mark	U.S.A.	Government	Empirical.
Su	U.S.A.	Mining company	Numerical.
van der Merwe	South Africa	Consultant	Empirical.
Zipf	U.S.A.	University	Numerical.

REFERENCES

Iannacchione AT, Mark C, Repsher RC, Tuchman RJ, Jones CC, eds. [1992]. Proceedings of the Workshop on Coal Pillar Mechanics and Design. Pittsburgh, PA: U.S. Department of the Interior, Bureau of Mines, IC 9315.

Mark C, Su D, Heasley KA [1998]. Recent developments in coal pillar design in the United States. In: Aziz NI, Indraratna B, eds. Proceedings of the

International Conference on Geomechanics/Ground Control in Mining and Underground Construction. Wollongong, New South Wales, Australia: University of Wollongong, Vol. 2, pp. 309-324.

A UNIQUE APPROACH TO DETERMINING THE TIME-DEPENDENT IN SITU STRENGTH OF COAL PILLARS

By Kousick Biswas, Ph.D.,¹ Christopher Mark, Ph.D.,²
and Syd S. Peng, Ph.D.³

ABSTRACT

In general, it cannot be assumed that the strength of coal pillars remains constant over long periods of time. Field observations indicate that a coal seam, especially when it contains a parting layer, deteriorates over time, reducing the load-bearing capacity of the pillars. This paper discusses a unique approach to determining the time-dependent strength of coal pillars in the field. Three coal pillars that were developed 5, 15, and 50 years ago were chosen for the study. Holes were drilled in coal and parting layers in each pillar, and the strength profiles were determined for each hole using a borehole penetrometer. The strength data were treated statistically to establish time-dependent strength equations for different layers. The results can be used to help estimate the loss of pillar capacity over time.

¹Lecturer, School of Engineering, University of Ballarat, Victoria, Australia.

²Supervisory physical scientist, Pittsburgh Research Laboratory, National Institute for Occupational Safety and Health, Pittsburgh, PA.

³Chairman and Charles T. Holland professor, Department of Mining Engineering, West Virginia University, Morgantown, WV.

INTRODUCTION

All manmade structures deteriorate over time; pillars in underground coal mines are no exception. There are numerous examples of coal pillars failing many years after they were developed. Scrutiny of existing pillar design theories indicates that few make any attempt to consider the effect of time. Similarly, there is rarely an attempt to consider the inhomogeneous nature of most coal seams. For example, the classic pillar design methodology involves the following three steps:

1. Calculate the vertical stress on the pillar:

$$S_v = \frac{(H(W\%W_e)(L\%W_e))}{(WL)}, \quad (1)$$

where S_v = vertical stress,

C = unit weight of the overburden,

H = depth of the seam,

W = pillar width (minimum pillar dimension),

L = pillar length (maximum pillar dimension),

and W_e = entry width.

2. Calculate the pillar strength using Bieniawski's formula [Bieniawski 1992]:

$$S_p = S_1 \left(0.64 \% \left(0.36 \frac{W}{h} \right) \right), \quad (2)$$

where S_p = pillar strength,

S_1 = in situ seam strength,

and h = seam height.

3. Calculate the stability factor (SF) as

$$SF = \frac{\text{Pillar strength}}{\text{Pillar stress}} = \frac{S_p}{S_v}. \quad (3)$$

The stability factor that is calculated using equations 1-3 assumes that—

- The coal strength is constant and does not deteriorate over time; and
- Coal seams are homogenous.

Back-analyses of subsidence above abandoned mines using the classic methodology have found that pillar failures have occurred over a broad range of stability factors [Marino and Bauer 1989; Craft and Crandall 1988]. The implication is that over time the standard pillar design methodology loses its ability to accurately predict the strength of coal pillars.

One recent South African study focused on the phenomenon of pillar scaling over time [van der Merwe 1998]. Twenty-seven case histories of pillar failure, occurring as long as 15 years after mining, were included in the database. Three parameters were found to be statistically significant: coal seam, pillar height, and time to failure. The study concluded that the scaling rate decreases exponentially over time and further hypothesized that "the inner portions of the pillar, being protected from the atmosphere, would then weather at a lower rate."

This paper describes a detailed study of the time-dependent structural deterioration of coal pillars and proposes a means to estimate the strength reduction of the coal seam in situ by taking into account the seam heterogeneity.

FIELD OBSERVATIONS

A survey conducted by West Virginia University, Department of Mining Engineering, of room-and-pillar mines in the eastern Appalachian region found that some of the coal seams contain one or more mudstone or claystone layers with variable thicknesses [Tsang et al. 1996]. For example, the Pittsburgh and Twin Freeport Seams contain parting layers in the coal seam. During field visits to several coal mines developed in these seams, the conditions of many pillars in worked-out

districts, some as much as 100 years old, were visually inspected. Most of the pillars did not show any apparent sign of instability because of their large size compared to their depth (stability factors ranged from 2 to 12).

A more detailed inspection revealed several kinds of weathering actions on the different layers of the coal seam with varying degrees of severity. The following structural deteriorations were noticed on older pillars:

- Conversion of mudstone/claystone layer to clay due to prolonged exposure to the mine moisture;
- Squeezing of the softer parting layer by the top and bottom portion of the coal;
- Major peeling of the parting layer;
- Separation of the parting from the host coal along the slick interfaces (perhaps the result of differential slippage); and
- Minor peeling of the top and bottom portion of the coal.

Figure 1 illustrates this deterioration in the structure of a pillar.

From the field observations, it was concluded that the structural deteriorations in both coal and parting are dependent on time. From these observations, aided by some laboratory studies and finite-element modeling [Biswas 1997], it was possible to postulate a conceptual model of the time-dependent strength profiles in the coal and parting layers (figures 2 and 3). Its assumptions are that—

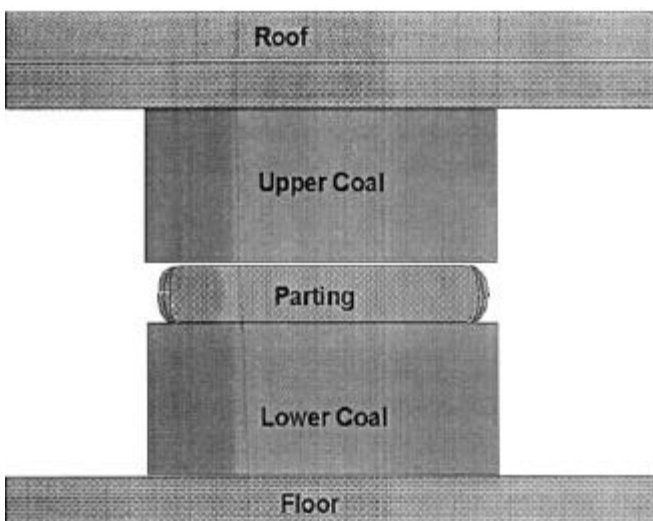


Figure 1.—Peeling of weathered parting in coal seam.

- The pillars are not affected by any mining activity in their vicinity; and
- The majority of the yield zones depicted in figures 2 and 3 are the result of the weathering action on the different layers in the pillar.

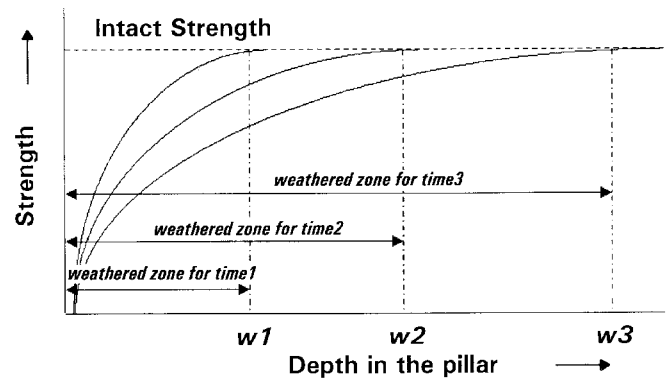


Figure 2.—Conceptualization for strength deterioration for parting. (Note: time1 < time2 < time3.)

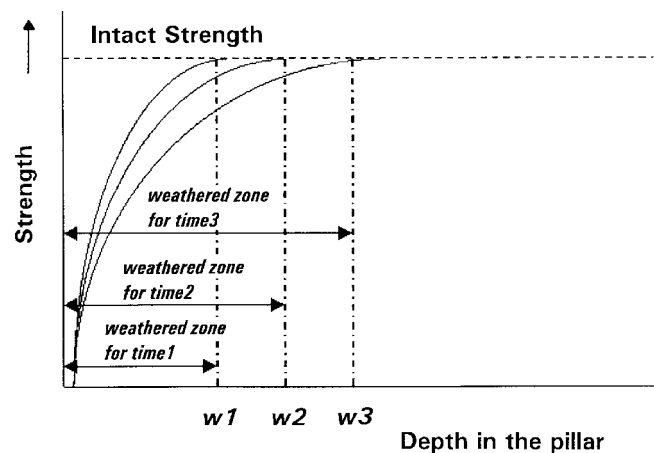


Figure 3.—Conceptualization for strength deterioration for coal. (Note: time1 < time2 < time3.)

IN SITU DETERMINATION OF TIME-DEPENDENT STRENGTH

The goal of this study was to determine one set of time-dependent strength profiles under in situ conditions. A detailed testing program was designed to establish the strength reduction in various layers of a pillar in situ over time.

THE STUDY SITE

The study was conducted at the Safety Research Coal Mine at the National Institute for Occupational Safety and Health's (NIOSH) Pittsburgh Research Laboratory. The Safety Research Coal Mine was selected for the following reasons:

- The overburden depth is very shallow, ranging from 15 to 18 m (50 to 60 ft); thus, any deterioration of the pillars is attributable to the effect of weathering rather than stress.
- The mine is developed in the Pittsburgh Seam, and it contains a parting of varying thickness (from 0.15 to 0.3 m (6 to 12 in)).
- The mine has accessible pillars developed as recently as 1991 and as long ago as the 1940s.
- The mine remains more or less inactive in terms of mining activities.

Three pillars were chosen in the mine based on their current conditions and the thickness of the parting. The three pillars were developed 5, 15, and 50 years ago. Due to other technical difficulties, more faces could not be chosen for this experiment. Figure 4 shows the mine plan and the location of the study sites.

THE APPARATUS

A borehole penetrometer (BPT) was used to measure the strength profiles in the coal and parting layers. The basic principle followed by the BPT is to fracture the borehole wall by means of an indenter and record the pressure that initiates the first fracture [Hladysz 1995]. The recorded failure pressure is then converted by a formula to determine the uniaxial

compressive strength (UCS) at that location in the borehole. The BPT's great advantages are that the rock strength is tested in situ, and multiple tests can be conducted within a single borehole [Zhang et al. 1996].

The BPT consists of the following components:

- Head
- Hydraulic pump with oil reservoirs and pressure transducers
- Displacement indicator
- Four-wire electric cable
- High-pressure hydraulic hose with quick couplers
- Set of extension rods

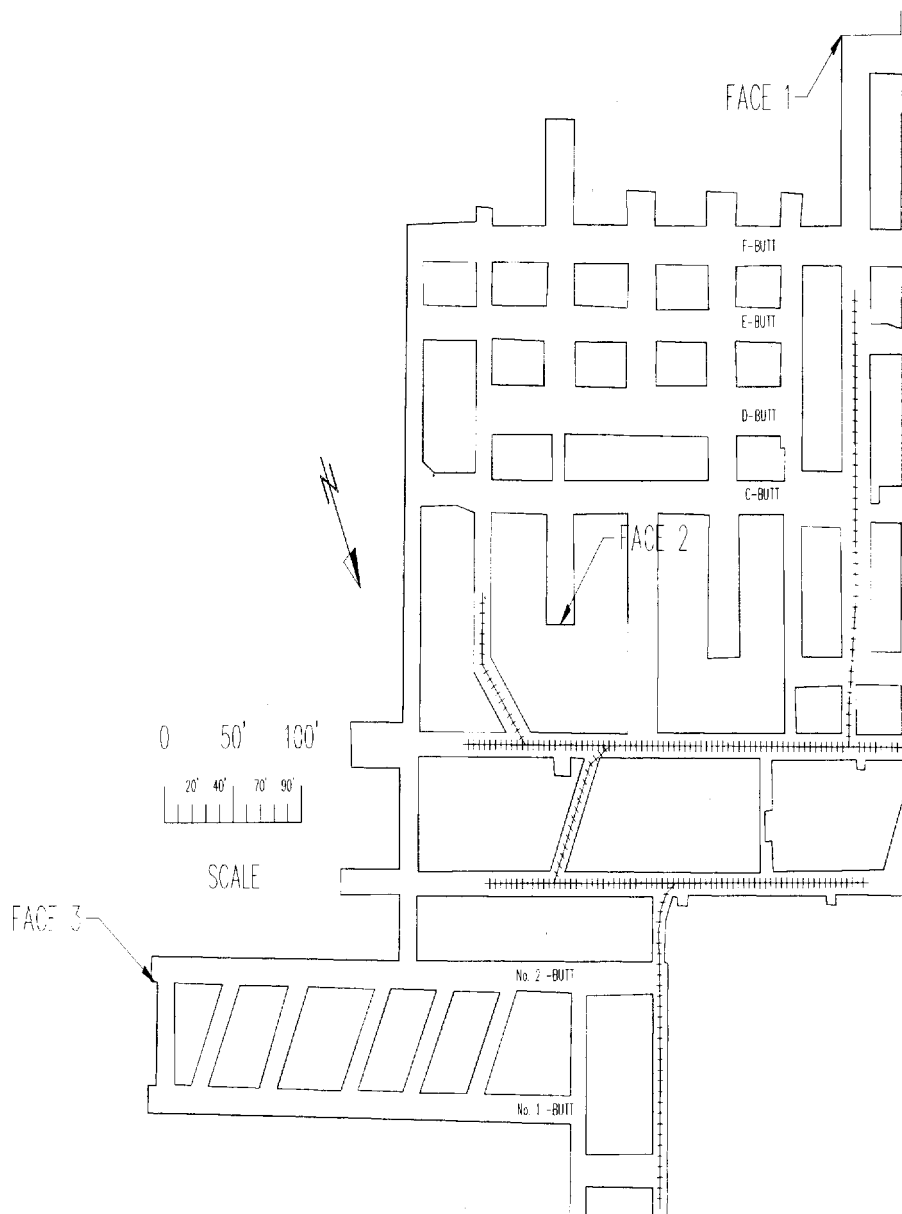


Figure 4.—Mine plan indicating three faces chosen for the BPT tests.

The BPT test setup is illustrated in figure 5. To perform the test, the head of the device is inserted into a standard NX drill hole with the help of a set of extension rods. When the head is positioned at the desired depth, the indenter is forced into the borehole wall using the hydraulic pump. At the critical pressure, the indenter penetrates the rock rapidly, making a small crater around the indenter's tip. This event is indicated by a rapid movement of the needle on the displacement indicator and by a sudden drop in pressure (figure 6). In hard and brittle rock, an audible sound is often associated with rock failure. The critical pressure causing the rock to break is a function of rock separation resistance (or penetration resistance). Penetration resistance is proportional to the material properties of the rock mass and the state of stresses. By repositioning the head and repeating the test procedures along the entire length of the hole, a penetration profile (or strength profile) for the tested section of the rock mass can be determined.

To achieve accuracy, a pressure transducer, a data acquisition module, and a digital readout unit are used. The failure pressure and ram displacement data recorded at a specified time interval are stored during an individual test and later transferred to a computer to determine the failure pressure. A portable battery-operated recorder unit records the collected data. The pressure transducer that is connected to the hydraulic pump generates the pressure signal; the displacement signal comes from a linear variable differential transformer (LVDT) that is linked to the indenter. The recorded data are stored in the data logger unit memory and later played back using a personal computer driven by application software. The data from a typical BPT test include the pressure, displacement of ram or indenter, time and an identification for the hole No., test depth, test date, etc. More details about the instrument, its specifications, principles, and testing procedure can be found elsewhere [Hladysz 1995].

THE EXPERIMENT

For each BPT test, the following steps were conducted:

1. Connect the hydraulic hoses to the head and to the pump.

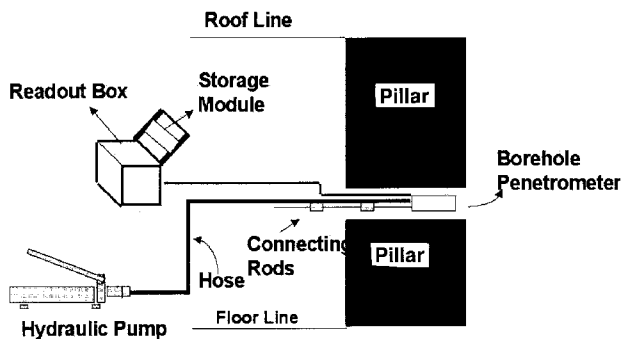


Figure 5.—BPT test setup.

2. Connect the cable to the head and to the data acquisition displacement input terminals.
3. Connect the cable to the pressure transducer and to the data acquisition pressure input terminals.
4. Set up the recording session parameters in the data logger unit (e.g. date, ID No., etc.).
5. Insert the head into the borehole and position the device at the desired depth.
6. Close the main valve of the pump.
7. Initiate a data recording session.
8. Increase pressure slowly at a constant rate, continuing to pump until failure occurs.
9. Open the valve to allow the indenter to retract fully and stop recording.
10. Reposition the penetrometer head and repeat steps 4 to 9.

Two NX boreholes were drilled in each test pillar, one in coal and one in the parting. The holes were each 3 m (10 ft) long. About 15-20 tests were conducted along each borehole. The testing frequency was higher near the pillar edge; it was postulated that the rib edge would be more disturbed than the intact central portion of the pillar. All of the data for each test were collected in the storage module during the tests and later transferred to a computer for more detailed analysis. The data for each test point were manipulated in a spreadsheet program; finally, a graph was plotted for each test point. The graph consists of time on the X-axis, failure pressure on the primary Y-axis, and the relative displacement rate of the indenter on the secondary Y-axis. Typical graphs for the parting and the coal are shown in figures 6 and 7, respectively. The failure pressure in the hard rock, in general, is characterized by a distinct jump (increase) in the ram displacement.

DATA ANALYSIS

The first step in analyzing the data was to determine the failure pressures at all test points. Then, the following conversion formula was used to convert the failure pressure to the UCS:

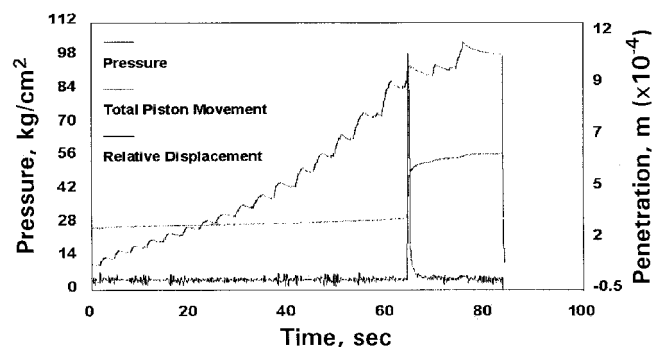


Figure 6.—Typical raw BPT test data analysis for parting.

$$UCS = (F_s)P_f, \tag{4}$$

where F_s = strength factor,

and P_f = failure pressure from the BPT test.

For coal, the value of the strength factor was 1.25, as suggested by Zhang et al. [1996]. For the parting, a value of 1.00 was used based on laboratory studies of the cores of the parting obtained from the BPT test holes [Biswas 1997].

The scatter plots of the converted strength values were obtained for each hole in each face. Because these scatter plots showed considerable variability in the trend of the strength deterioration, which is a typical characteristic of any experiment conducted in situ, a curve-fitting program called Curve Expert was used to fit the best curve with the highest correlation coefficient. Figures 8-10 illustrate the best-fit curves for the parting, and figures 11-13 illustrate the best-fit curves for the coal for all three faces.

The general form of all of the best-fit equations for both coal and parting is

$$y = a(1.01 - e^{-bx}), \tag{5}$$

where a and b are the coefficients,

y is the failure pressure or the strength,

and x is the depth (in this case, the range is from 0.06 to 3 m (0.2 to 10 ft)).

The negative exponential and its negative power give the best-fit curves their asymptotic form. The correlation coefficients for the best-fit equations for the parting and coal for each age group are 0.84, 0.85, 0.89 and 0.96, 0.88, 0.94, respectively.

For the parting, the gradient in the weathered zone for the younger face is initially steeper, but the slope flattens as the age increases. This change in strength gradient before it reaches the intact or stabilized strength is considerable. The weathered zone apparently expands from 1 to 3 m (3.2 to 10 ft) over the 50 years. For coal, the strength gradient for all of the age groups is steeper than that of the parting, and the expansion of

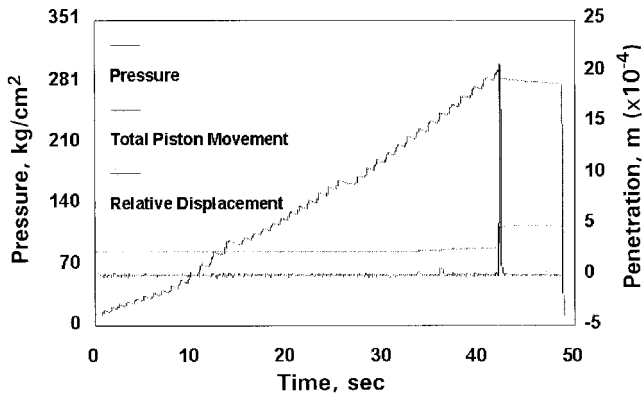


Figure 7.—Typical raw BPT test data analysis for coal.

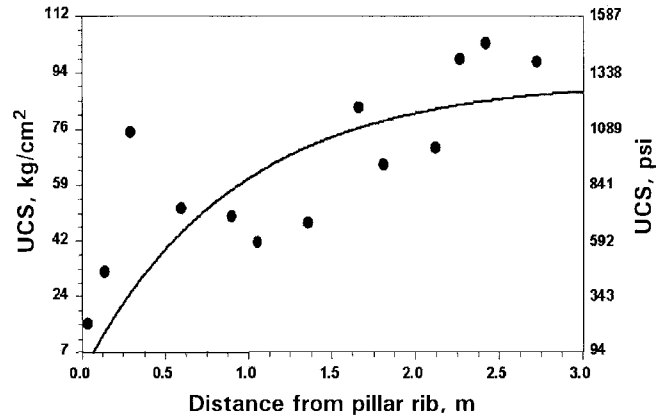


Figure 9.—Best-fit curve for 15-year-old parting.

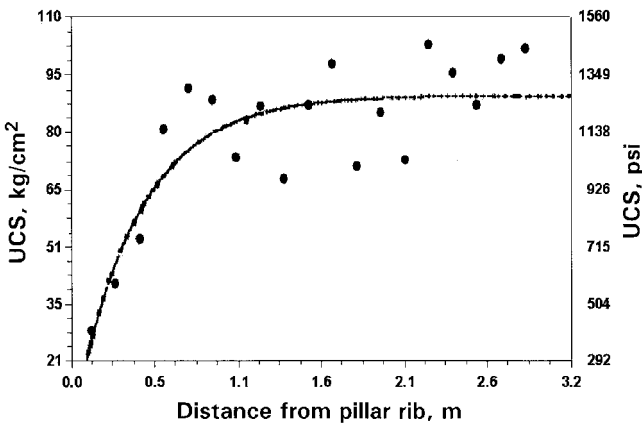


Figure 8.—Best-fit curve for 5-year-old parting.

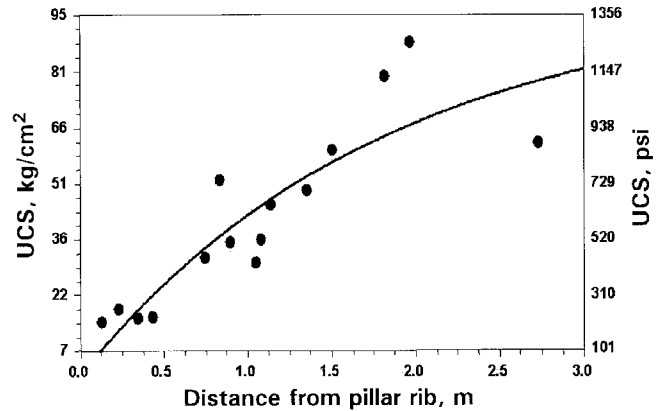


Figure 10.—Best-fit curve for 50-year-old parting.

the weathered zone is much less (from 0.2 to 1 m (0.7 to 3.2 ft)). These findings fit the conceptual model of the strength degradation for parting and coal over time described earlier.

Figures 8-13 also indicate that there is some borehole-to-borehole variability in the intact strength measured in the interior of the pillars for both the coal and the parting. This variability may be attributed to natural variability between the three different faces. In order to generalize the results, the data

from each borehole were normalized to the measured intact strength. The normalized strength curves are shown in figures 14 and 15.

FORMULATION OF TIME-DEPENDENT STRENGTH DETERIORATION

The BPT data can be used to derive a time-dependent strength formula for the pillars in the study. Using the best-fit equations shown in figures 14-15, data sets were generated for each material for all three ages. The data sets were generated for the depth ranges from 0.06 to 3 m (0.2 to 10 ft). No data could be generated right at the ribline because no BPT tests were conducted there. A nonlinear regression analysis was conducted on these data sets separately for the coal and for the parting with two independent variables (time and depth) and one dependent variable (strength). A freeware software called NLREG34 was used to perform the nonlinear regression. Equation 6 is the stress gradient for the parting, and equation 7 is the final equation for coal:

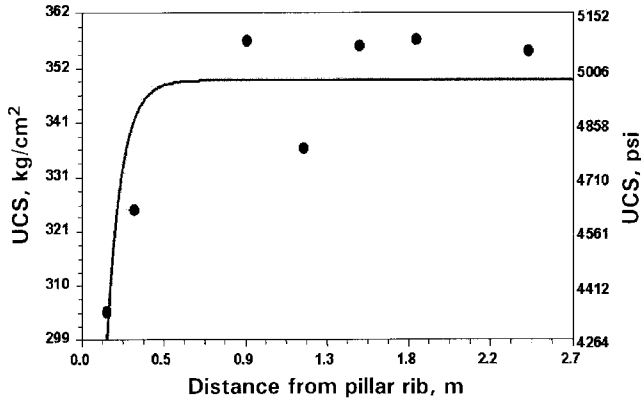


Figure 11.—Best-fit curve for 5-year-old coal.

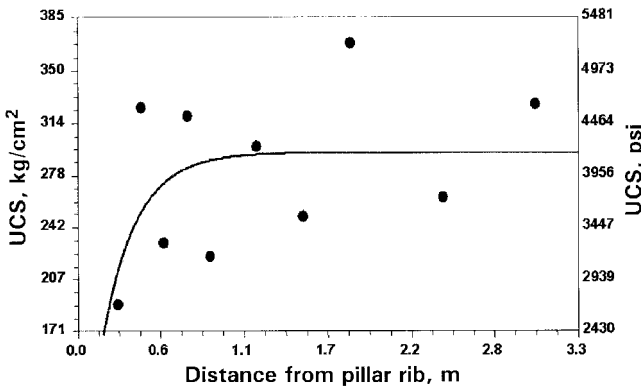


Figure 12.—Best-fit curve for 15-year-old coal.

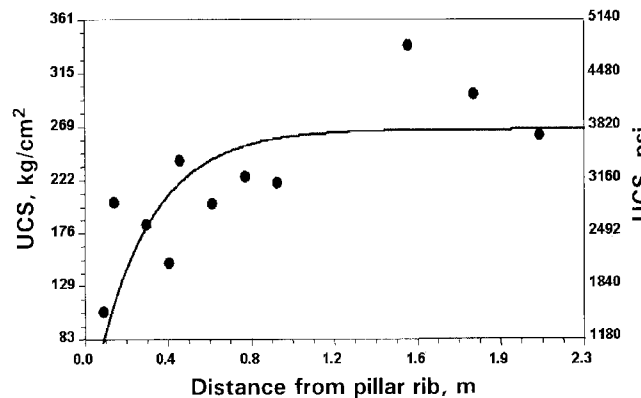


Figure 13.—Best-fit curve for 50-year-old coal.

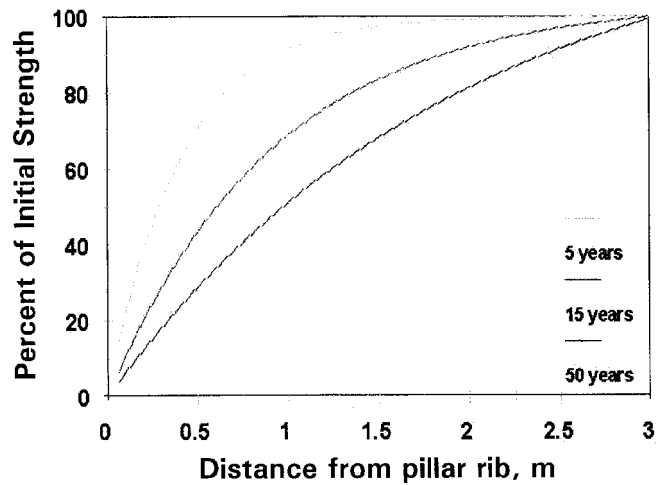


Figure 14.—Time-dependent strength deterioration for parting.

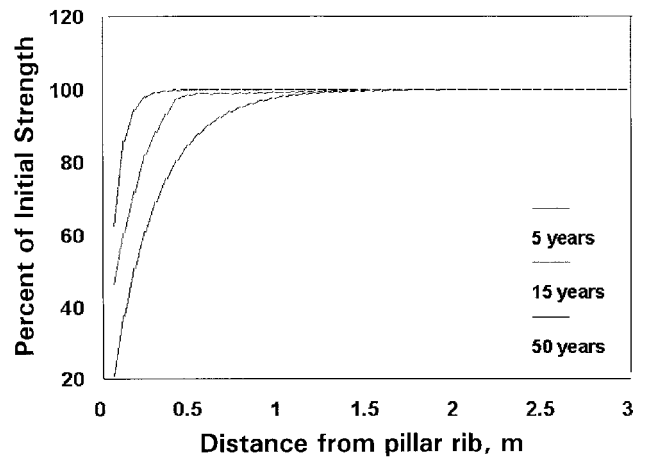


Figure 15.—Time-dependent strength deterioration for coal.

$$\% \text{ parting strength} = 100 (1.01 \cdot e^{80.5D}) \cdot 0.45t \quad (6)$$

$$\% \text{ coal strength} = 100 (1.01 \cdot e^{83.5D}) \cdot 0.13t \quad (7)$$

where D = depth into the rib, ft,

and t = time after mining, years.

In these equations, the strength is defined as a percent of the original intact compressive strength that is assumed to be constant in the core of the pillar. Near the rib, the strength is a function of the distance from the rib (depth) and the time after mining. The relationship between the strength and the depth is a negative exponential, but that between strength and time is linear.

Unfortunately, applying these time-dependent strength equations to predict the strength of full-scale pillars is not simple. Three issues are foremost:

1. *Effect of parting thickness:* If the parting is the pillar's weakest layer, as in this study, then a thicker parting would be expected to result in a weaker pillar.

2. *Effect of parting on confining stress within the pillar:* Most of the load-bearing capacity of a coal pillar is due to the development of confining stress within the pillar's core. Studies have shown that many pillars contain weak layers of clay or friable coal, but their effect on overall pillar strength is ambiguous [Mark and Barton 1996].

3. *Nonlinear effect of time:* In reality, the rate of strength degradation probably decreases with time, as suggested by van der Merwe [1998]. Because this study included only three pillars, it was difficult to quantify the nonlinear relationship between time and strength.

Nevertheless, if the limitations of the necessary assumptions are kept in mind, it is possible to use the strength gradient equations to shed light on the possible effects of time on coal pillar stability. The following example illustrates one possible approach. The key assumption is that *at any particular time, the distance from the actual pillar rib and the depth at which the strength is 60% of the intact strength will be considered as the width of the portion of the weathered zone that is not capable of carrying any load and thus transfers the load on the intact portion of the pillar.* The effect of this assumption is that the pillar's strength is decreased over time as the width-to-height ratio diminishes, whereas the applied stress increases as the pillar's load-bearing area is reduced.

To calculate the time-dependent stability factor, the following steps are followed:

1. Calculate the original stability factor using equations 1-3.
2. Determine the strength profile at a specified time using equation 3 or 4, and determine the depth of weathering (where the strength is 60% of the intact).
3. Calculate the resultant pillar width by subtracting the depth of weathering from the original pillar width.
4. Recalculate the applied stress using equation 1 and the new pillar dimensions.
5. Use equation 2 to determine the new pillar strength and equation 3 to calculate the reduced stability factor at the specified time.
6. Repeat this process to determine the approximate lifespan of the pillar.

For example, assume the following parameters:

- The overburden depth is 244 m (800 ft).
- The pillar is a square pillar with a 15.2-m (50-ft) dimension.
- The seam height is 1.8 m (6 ft).
- The entry width is 6.1 m (20 ft).
- The in situ seam strength is 6.2 MPa (900 psi).

Because the parting is the weakest layer of the seam in this case, to be on the conservative side, equation 6 (for the parting) is used to determine the strength profile and also the width of yielded zone due to the weathering process. From a statistical point of view, it is recommended that equations 6 and 7 be used within the same time range as the original field data used in their development, i.e., 5 to 50 years [Myers 1990].

Figure 16 illustrates the changes in strength and applied stress over time. Where the two curves meet, at time $t = 35$ years, the stability factor is 1.0, which means that the pillar has a 50% chance of failing before that time.

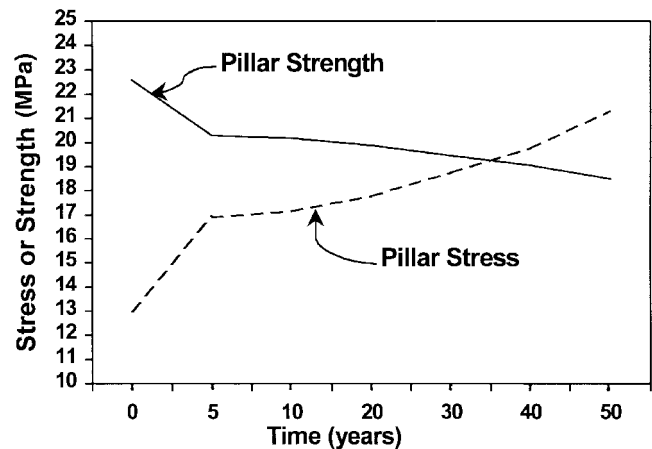


Figure 16.—Safety factor reduction over time.

CONCLUSIONS

The use of the BPT to measure the in situ time-dependent strength is the unique feature of this study. It generated a set of in situ strength data in a relatively simple field-testing program. The in situ data were used to develop time-dependent strength equations for coal and parting layers. An example case was used to demonstrate the use of these equations in predicting the change of stability factor over the years.

The parting material weathered much more rapidly than the coal. This implies that much of the observed between-seam variability in long-term pillar strength may be due to the presence or absence of partings in the coal. However, this study only addressed a single type of parting material within a single coal seam. Much work remains before the effect of time on coal pillar strength is fully understood.

ACKNOWLEDGMENTS

The authors are grateful for the opportunity to use the Safety Research Coal Mine at NIOSH's Pittsburgh Research Laboratory (PRL) for the in-mine studies. The expertise and

assistance of PRL employees David C. Oyler, mechanical engineer, and Craig S. Compton, engineering technician, were also invaluable.

REFERENCES

Bieniawski ZT [1992]. A method revisited: coal pillar strength formula based on field investigations. In: Proceedings of the Workshop on Coal Pillar Mechanics and Design. Pittsburgh, PA: U.S. Department of the Interior, Bureau of Mines, IC 9315, pp. 158-165.

Biswas K [1997]. Study of weathering actions on partings and their effects on long-term stability of coal pillar [Dissertation]. Morgantown, WV: West Virginia University, Department of Mining Engineering.

Craft JL, Crandall TM [1988]. Mine configuration and its relationship to surface subsidence. Paper in Proceedings, Mine Drainage and Surface Mine Reclamation, USBM IC 9184, Vol. 3, pp. 373-382.

Hladysz Z [1995]. Borehole rock strength tester manual. Rapid City, SD: Hladysz Rock Testers and Consulting.

Marino GG, Bauer RA [1989]. Behavior of abandoned room-and-pillar mines in Illinois. SME preprint 89-3. Littleton, CO: Society for Mining, Metallurgy, and Exploration, Inc.

Mark C, Barton TM [1996]. The uniaxial compressive strength of coal: should it be used to design pillars? In: Ozdemir L, Hanna K, Haramy KY, Peng S, eds. Proceedings of the 15th International Conference on Ground Control in Mining. Golden, CO: Colorado School of Mines, pp. 61-78.

Myers RH [1990]. Classical and modern regression with applications. Boston, MA: PWS-KENT Publishing Co., pp. 424-449.

Tsang P, Peng SS, Biswas K [1996]. Current practice of pillar design in U.S. coal mines. *Min Eng* 48(12):55-60.

van der Merwe JN [1998]. Practical coal mining strata control. Johannesburg, Republic of South Africa: Itasca Africa (Pty.) Ltd., 2nd ed., appendix B.

Zhang YJ, Unrug KF, Thompson ED [1996]. New approach to determine the in-situ strength of coal in mine pillars. *Min Eng* 48(10):49-53.

DEVELOPMENTS IN COAL PILLAR DESIGN AT SMOKY RIVER COAL LTD., ALBERTA, CANADA

By Peter Cain, Ph.D., P.Eng.¹

ABSTRACT

Smoky River Coal Ltd. mines low-volatile metallurgical coal by surface and underground methods in the foothills of the Rocky Mountains of Alberta, Canada. Current underground operations are confined to the 5B-4 Mine. Development of 5B-4 began in January 1998; production from depillaring sections commenced in July 1998.

This paper describes the history of underground mining on the Smoky River property in terms of extraction methods and pillar design. The development of the present pillar design guidelines is discussed in this context. Recent work to prepare a number of case histories for back-analysis using the Analysis of Retreat Mining Pillar Stability (ARMPS) method is described, along with the modifications developed for calculating the ARMPS stability factor for retreat extraction of thick seams. The design criteria are described, as well as the geotechnical program implemented in order to verify its applicability.

¹Senior ground control engineer, Smoky River Coal Ltd., Grande Cache, Alberta, Canada.

INTRODUCTION

The Smoky River Coalfield is located in west-central Alberta, Canada, within the inner foothills of the Rocky Mountains. The mine is approximately 20 km north of Grande Cache and 360 km west of Edmonton (figure 1). Most of the property is contained in a block approximately 29 km long by 19 km wide. The coal leases cover about 30,000 ha. The general mine layout is shown in figure 2. Underground mining is currently located in the 5 Mine area.

The coal seams and surrounding strata are within the Gates Formation (of the Lower Cretaceous Luscar Group) and outcrop near the mine. The Gates Formation is divided into three members: Torrens, Grande Cache, and Mountain Park (figure 3). The Torrens is a distinct marine sandstone and siltstone sequence about 30 m thick. It is overlain by the Grande Cache Member, which consists of approximately 158 m of nonmarine siltstones, sandstones, mudstones, and all of the significant coal seams in the area. The Grande Cache Member is overlain by the Mountain Park Member, which consists of 155 to 192 m of nonmarine sandstones, mudstones, siltstones, and minor coal seams.

The predominant structure of the coalfield strikes northwest to southeast and comprises thrust sheets containing folded layers of competent sandstone and siltstone units, incompetent mudstone, and coal. Dips vary considerably, from horizontal to overturned. Underground mining by room-and-pillar methods is restricted to areas where the strata dip less than 16°, which is the practical limit of continuous miner and shuttle car operation. The orientation of the underground mine workings in figure 2 gives a clear indication of the structural

environment; the workings are either faulted or steeply folded off on the northeast and southwest limits of mining.

The significant coal seams present are numbered from the lower (older) to the upper (younger) and comprise the 4, 8, 10, and 11 Seams. 4 Seam has been mined extensively (figure 2) using conventional room-and-pillar mining techniques. 8 and 11 Seams are not considered economical to mine because of thickness and low quality. Mining in 10 Seam has been attempted, including two longwall panels above 9G-4 Mine; however, a weak immediate roof comprising two 0.6-m coal seams in the first 2 m of strata has always presented stability problems.

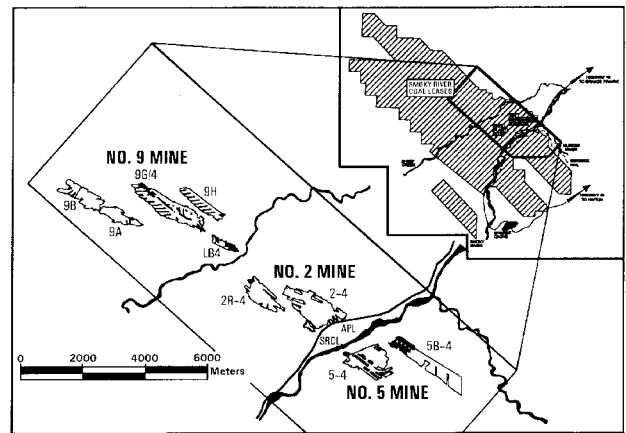


Figure 2.—Site layout.



Figure 1.—Location of Smoky River Coal Ltd.

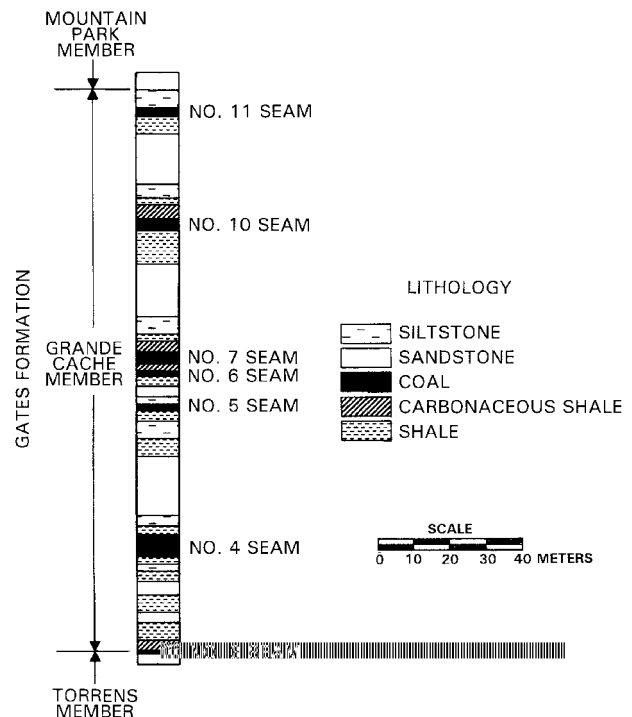


Figure 3.—Generalized stratigraphic column, Smoky River Coalfield.

HISTORICAL MINING METHODS AND PILLAR DESIGN

Underground mining at Smoky River Coal Ltd. (SRCL) commenced in 1969 in 5-4 and 2-4 Mines. The initial intent was to develop for longwall extraction; however, two early attempts at longwall mining failed and retreat room-and-pillar extraction became standard.

The original mining method was to develop three 6-m-wide entries on 30-m centers from the portal to the limit of mining, generally along strike, with crosscuts at 30-m centers. Parallel sets of entries were driven separated by 50-m barrier pillars (figure 4). On reaching the limit of mining, the road and barrier pillars were split along strike to form blocks approximately 12 m wide and mined using an open-ended "Christmas tree" method, taking 6-m passes each side with a conventional continuous miner. This method, described in more detail by Wright [1973], worked well in 2-4 Mine, but was unsuccessful in 5-4 Mine due to the weaker roof and pervasive thrust faulting in and above the coal seam.

In the early 1970s, a major geotechnical investigation program was launched to assist mine staff in planning pillar dimensions and support. Extensive load and deformation monitoring was conducted [Bielenstein et al. 1977]; concurrent testing by air injection investigated the development of yield and elastic zones within coal pillars [Barron et al. 1982].

In the early 1980s, the many disadvantages of the three-entry system were overcome by adopting a five-entry system (figure 4B) with short-life panels [Robson 1984]. Panels comprising five parallel entries were developed off of main development sections. This mining method depended for its success on the stability of pillars separating the panels and pillars that protected the main entries from the depillared areas. In fact, five types of pillars were recognized:

- Barrier pillars between mining panels;
- Entry pillars protecting the main entries;
- Panel pillars formed during the development of mining panels;
- Split pillars formed by splitting panel pillars prior to depillaring; and
- Remnant pillars, the diminishing remnants of split pillars formed during depillaring operations.

Tolerable probabilities of failure were estimated for each pillar type, and an empirical design criterion was developed that took into account this probability of failure [Barron et al. 1982]. Favorable trials of the five-entry system in A Mine (figure 2) resulted in its adoption in 9H and 9G Mines. Further refinement of pillar design methods, relying heavily on practical experience and a comprehensive review of pillar design methods from around the world, resulted in a design nomogram [Kulach 1989]. The method was based on the tributary area method of load calculation (considered to represent the best and safest estimate of the loads developed on pillars) and Bieniawski's [1983] method of determining pillar strength.

Mining continued in the late 1980s and 1990s in 9H and 9G Mines using this method of pillar design. The small resource block exploited by the LB-4 Mine necessitated a change in method, with entries developed to the farthest extent and retreated back, but all three mines were successful from a pillar stability standpoint.

In 1997, plans were developed to exploit a previously untouched parcel of coal to the north of the old 5-4 Mine. The shape of the resource block, 370 m wide by 2,500 m long, bounded by steeply dipping thrust zones to the northeast and southwest, largely dictated the mining layout, which is shown in figure 5.

During the planning stages of the mine, it was soon realized that conditions would be very different from the more recent underground operations, which were carried out at shallow to moderate depths under a competent sandstone roof. The proposed 5B-4 Mine would operate at depths of up to 550 m and beneath a roof affected by pervasive thrust faulting. Both pillar design and roof support requirements necessitated re-evaluation for the operation to be successful.

Although the SRCL pillar design criterion had been used successfully in a number of mines, it had some obvious disadvantages with respect to its application in 5B-4 Mine:

- The nomogram is restricted to 12-m-wide by 3.6-m-high pillars and 6-m-wide roadways.
- The method is based on a strength calculation for square pillars and severely underestimates the strength of rectangular pillars.
- The design criterion is based on U.S. methods that have undergone substantial modification in the past 10 years.

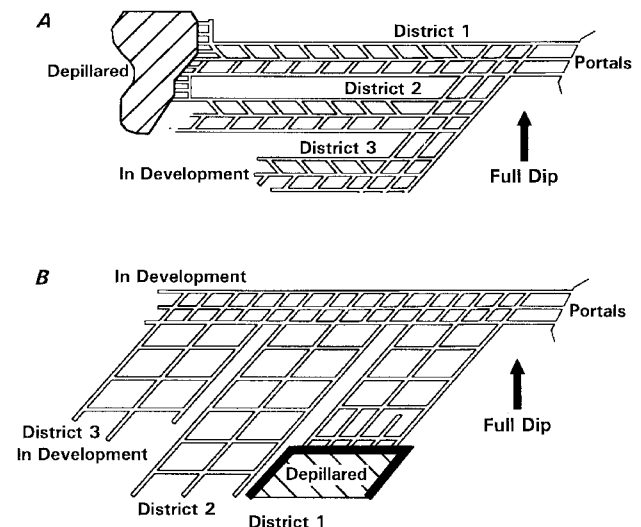


Figure 4.—Development of mining methods. A, three-entry system, long-life panels; B, five-entry system, short-life panels.

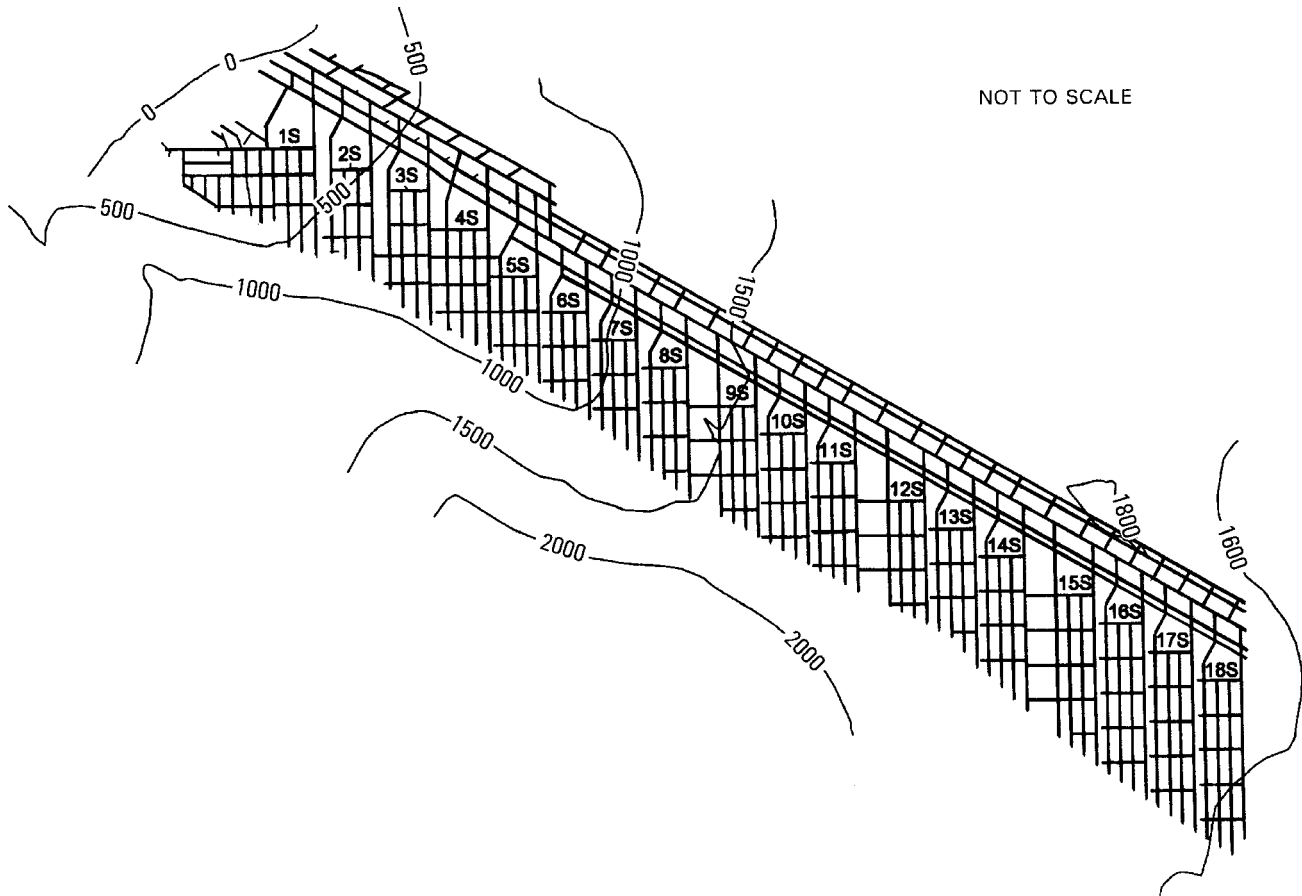


Figure 5.—Layout of 5B-4 Mine. (Elevation in feet.)

Mining plans for 5B-4 included rectangular pillars ranging from 15 m to 36 m wide and 3.6 m high, standing between 4.9-m-wide roadways, which lay outside the empirical basis of the design nomogram. Although a nomogram for 5B-4

parameters could have been developed, the availability of more recently developed design methods that specifically address the strength of rectangular pillars warranted consideration of a change in design approach.

ANALYSIS OF RETREAT MINING PILLAR STABILITY (ARMPS)

The most recent development in pillar design in the United States is the Analysis of Retreat Mining Pillar Stability (ARMPS). ARMPS was developed by the former U.S. Bureau of Mines [Mark and Chase 1997] based on extensive case history data. ARMPS is available as a Windows 95™ software package and has the following advantages over previous methods used by SRCL:

- The increased load-bearing capacity of rectangular pillars over that of square pillars of the same width is taken into consideration.
- The load-bearing capacity of diamond- or parallelogram-shaped pillars is taken into consideration.

- ARMPS allows for an analysis of the stability of pillars in the active mining zone (AMZ) during development, during retreat, and with gobbs on one or both sides.
 - The effect of depth on abutment loading, based on angles of caving, is considered.
 - The effect of slabbing the interpanel pillar on pillars in the AMZ is considered.

ARMPS is a very flexible method of analysis. The software allows the user to input all of the major parameters relating to layout, mining, and pillar dimensions and location of any worked-out, caved areas. It also allows analysis of changes in pillar stability as a result of mining progress, from development to the extraction of coal pillars alongside a gob or between

two gobbs. Mark and Chase [1997] present a full description of the methods used to calculate pillar loading and pillar strength

in the ARMPS program. The principal output of the program is the stability factor (SF), which is the product of the estimated

load-bearing capacity of pillars in the AMZ divided by the estimated load on those pillars.

The concept of the AMZ follows from a hypothesis by Mark and Chase [1997] that pillars close to the retreat extraction line behave together as a system, i.e., if an individual pillar is overloaded, load is transferred to adjacent pillars. If these are of adequate size, the system remains stable, otherwise the pillars fail in turn, resulting in a domino-type transfer of load and pillar failure.

The size of the AMZ is a function of depth, H , based on measurements of abutment zone widths conducted by Mark [1990], which showed that 90% of abutment loads fall within a distance $2.8/H$ from the gob edge.

U.S. case history data indicate that where the ARMPS SF is <0.75 , nearly all of the designs were unsatisfactory; where the SF is >1.5 , nearly all of the designs were satisfactory. For the deeper case histories, there was some evidence that stability factors can be lower and still ensure overall pillar stability. In

addition, case histories with less competent roof rock were more stable than those with stronger roof strata, as this promoted pillar squeeze or burst activity.

Despite its utility and comprehensive analytical method, ARMPS has several drawbacks when applied to SRCL conditions:

- Case histories were confined to U.S. mines. As with any empirically based design method, this presents problems in application outside the case history environment.
- The case history database extends only to depths of about 1,100 ft, and only a few case histories were obtained at this depth of cover.
- None of the case histories matched the seam thicknesses mined at SRCL (up to 6 m).

After discussions with the developers of ARMPS [Mark 1998], it was decided that in order to confirm the applicability of ARMPS to SRCL operations, a series of calibration analyses based on depillaring operations in the coalfield was required.

BACK-ANALYSIS OF CASE HISTORIES

Mine plans from 9G, 9H, and LB-4 Mines (figure 2) were reviewed, and relevant mining data were extracted to develop a series of case histories. Each case history was then analyzed using the ARMPS method, and safety factors were recorded and compared to the existing U.S. case history database.

In order to consider the extraction of thick seams as practiced at SRCL, the calculation of the SF was modified. ARMPS allows input of a single working thickness; in most SRCL depillaring operations, however, there are two mining heights. During development, the mining height is 3.7 m; during depillaring, the mining height is 6.1 m. This variation in mining height has a marked effect on pillar stability through the height/width ratio of the pillars. Rationally, load shed to the AMZ from the 6.1-m-high pillars in the mined-out area is more effectively controlled by the pillars of 3.7-m height in the AMZ.

In order to take into account this variation in mining height, ARMPS stability factors and details of pillar loading were calculated for extraction heights of both 3.7 m and 6.1 m. The SRCL stability factor was derived as follows:

(a) The pillar load transferred to pillars in the AMZ for a mining height of 6.1 m was determined using ARMPS.

(b) The load-bearing capacity of pillars in the AMZ for a mining height of 3.7 m was determined using ARMPS.

A stability factor was calculated as: (b) divided by (a).

Table 1 presents details of the mining parameters for each of the case histories considered, as well as the stability factors obtained. Figure 6 compares the SRCL stability factors with those obtained from the published U.S. database [Mark and Chase 1997] and indicates that SRCL stability factors representing satisfactory conditions range from 0.47 to 1.74, with the majority (66%) in the range of 0.5 to 1.0.

Local mining conditions provided some assurance that the low SF values were valid. Firstly, the lowest values occurred at the greatest depth; it has been recognized that acceptable stability factors appear to be lower at depth, perhaps due to the influence of horizontal stresses in reducing the pillar loading. Secondly, the SRCL case histories are characterized by a strong, competent roof; under such conditions in the United States, acceptable pillar stability was obtained at lower values of the calculated SF.

Table 1.—Summary of SRCL case histories analyzed using the ARMPS method

Mine	District	Depth, ft	ARMPS SF (6.1 m)	Load shed to AMZ, tons	ARMPS SF (3.7 m)	Capacity of AMZ, tons	SRCL SF	Load condition
LB-4	Mine	580	1.35	5.83E+6	1.99	1.16E+7	1.56	2
9H-4	SW2	390	1.23	1.18E+6	1.80	2.05E+6	1.74	3
9H-4	SW3	485	1.35	1.69E+6	0.92	1.63E+6	0.96	3
9H-4	SW4	575	0.73	2.44E+6	1.12	2.49E+6	1.02	3
9H-4	SW5	660	0.56	3.43E+6	0.89	2.69E+6	0.78	3
9H-4	SW6	715	0.49	4.05E+6	0.77	2.77E+6	0.68	3
9H-4	SW7	755	0.61	4.71E+6	1.04	4.14E+6	0.87	3
9H-4	SW8	832	0.50	6.11E+6	0.79	4.35E+6	0.71	3
9H-4	SW9	932	0.35	4.60E+6	0.53	2.30E+6	0.50	3
9G-4	SW2	560	0.85	2.05E+6	1.27	2.46E+6	1.20	3
9G-4	SW3	650	0.58	3.26E+6	0.94	2.65E+6	0.81	3
9G-4	SW4	730	0.49	4.10E+6	0.80	2.83E+6	0.69	3
9G-4	SW5	745	0.51	3.98E+6	0.85	2.83E+6	0.71	3
9G-4	SW6	780	0.51	4.01E+6	0.88	2.90E+6	0.72	3
9G-4	SW7	840	0.41	5.21E+6	0.69	2.97E+6	0.57	3
9G-4	SW8	885	0.37	5.84E+6	0.62	3.05E+6	0.52	3
9G-4	SW9	920	0.34	6.56E+6	0.51	3.11E+6	0.47	3
9G-4	SW10	915	0.34	6.49E+6	0.53	3.10E+6	0.47	3

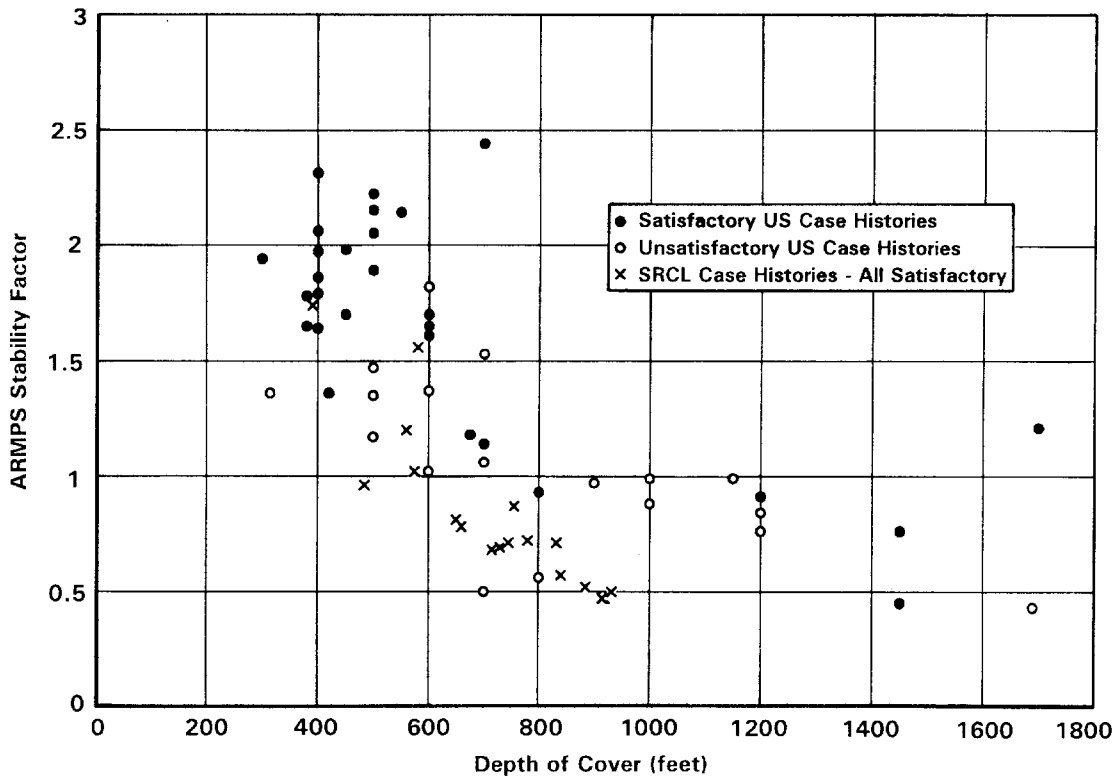


Figure 6.—Comparison of U.S. and SRCL stability factors.

DEVELOPMENT OF A DESIGN CRITERION

After considering the results of the case history analysis, it was decided to use the ARMPS method to assist in pillar design at 5B-4 Mine. Appropriate engineering practice in such cases is to design to the minimum SF that resulted in stable conditions. Evidence suggests that a pillar design resulting in an ARMPS SF of 0.5 would be stable in Smoky River Coalfield conditions. A more conservative SF of 0.7 was established.

A further limitation was imposed after an analysis of the pillar stresses on the gob corner pillar. This pillar, located adjacent to both the active retreat section gob and the barrier pillar between the active panel and the old gob, is subjected to the highest stresses and is therefore more prone to failure. The primary concern in this case is the threat of coal bumps or pillar burst, resulting in the transference of loads to adjacent pillars in the AMZ and possibly massive failure.

ARMPS analyses of SRCL case histories revealed that the maximum stress experienced on any gob corner pillar was about 41 MPa. At this stress level, the pillar proved to be stable.

A third criterion was adopted based on the size of pillars analyzed from the case histories. The minimum pillar size analyzed was 12 m wide between 6-m roadways. Maintaining this extraction ratio for the 4.9-m-wide roadways employed at 5B-4 Mine precluded the use of ARMPS for pillars <9.7 m wide.

Based on the ARMPS output from the case history data compiled from previous pillar retreat mining in the Smoky River Coalfield, the following design criterion for pillars is suggested:

- The ARMPS SF should be maintained above 0.7.
- The maximum stress on the corner pillar should not exceed 41 MPa (6,000 psi).
- Pillar widths must not be <9.7 m.

It was realized that the ARMPS-derived design criterion was also limited in application, specifically to the depths encountered in the case history analysis. With depths of cover projected to exceed those of the case histories by 50%, there was an element of uncertainty with respect to the applicability of the design criterion. This is currently being addressed by a geotechnical program that includes pillar stress monitoring, numerical modeling, and continuing assessment of the design criterion.

Vibrating wire stress cells, electronic convergence meters, and an I. S. Campbell data logger have already been deployed at three monitoring sites to collect data on the effects of mining on pillar stability. Two of the sites monitored stress changes while the site was being "mined by" during the development phase. It is hoped that these two sites will provide valuable information on the strength of the coal pillars monitored.

Results are still being evaluated; however, indications are that the design criterion is applicable. Further sites will be established as mining progresses, and the results will be incorporated into the design criterion.

SUMMARY

Development of pillar design methods at SRCL's underground operation has proceeded with developments in the mining method. The extension of mine workings to previously unencountered depths at the new 5B-4 Mine has resulted in a requirement to develop pillar design methods to match the new mining environment.

Pillar designs are currently being based on the results of a back-analysis of case histories using the recently developed

ARMPS method. As with any empirical method of design, prudent engineering practice dictates the collection and analysis of pillar behavior information for design verification. Monitoring results already obtained are being analyzed to improve the design criteria. Future sites will collect data from greater depth and adjacent to more extensive workings.

REFERENCES

- Barron K, Wright PL, Smales T [1982]. Guidelines for the design of coal pillars in the No. 4 seam at McIntyre Mines Ltd., Grande Cache, Alberta. Paper presented at the First International Conference on Stability in Underground Mining (Vancouver, British Columbia, Canada).
- Bielenstein HU, Wright PL, Mikalson D [1977]. Multi-seam mining at Smoky River. Paper presented at the Sixth International Strata Control Conference (Banff, Alberta, Canada).
- Bieniawski ZT [1983]. New design approach for room-and-pillar coal mines in the U.S.A. In: Proceedings of the Fifth ISRM Congress on Rock Mechanics. Balkema, pp. E27-E36.
- Kulach J [1989]. Smoky River Coal Ltd. pillar design criteria. SRCL internal report, May.
- Mark C [1990]. Pillar design methods for longwall mining. Pittsburgh, PA: U.S. Department of the Interior, Bureau of Mines, IC 9247.
- Mark C [1998]. Personal communication between C. Mark, Pittsburgh Research Laboratory, National Institute for Occupational Safety and Health, and P. Cain, Smoky River Coal Ltd.
- Mark C, Chase FE [1997]. Analysis of retreat mining pillar stability (ARMPS). In: Proceedings - New Technology for Ground Control in Retreat Mining. Pittsburgh, PA: U.S. Department of Health and Human Services, Public Health Service, Centers for Disease Control and Prevention, National Institute for Occupational Safety and Health, DHHS (NIOSH) Publication No. 97-122, IC 9446, pp. 17-34.
- Robson TA [1984]. The application of improved room-and-pillar techniques at Smoky River Coal's underground operations. SRCL internal report, August.
- Wright PL [1973]. Layout of continuous mining operations in the Smoky River Mines. CIM Bulletin, March.

COAL PILLAR DESIGN FOR LONGWALL GATE ENTRIES

By John W. Cassie,¹ Peter F. R. Altounyan, Ph.D.,² and Paul B. Cartwright³

ABSTRACT

This paper describes measured data on strata behavior obtained in recent years from sites in the United Kingdom and the implications for pillar design. The data include results from overcoring stress measurements adjacent to coal mine roadways and deformation monitoring related to longwall extraction. The stresses adjacent to mine roadways or entries have been measured at a number of coal mine sites in the United Kingdom. The results are analyzed with regard to the information they provide on pillar behavior and strength estimates.

A reduction in stress consistent with yielding of the strata adjacent to the roadways is evident. This is consistent with the confined core model for pillar behavior. The pillar strength is dependent on the rate at which vertical stress can increase with distance from the pillar edge and hence the confinement provided to the yielded material.

The measured data indicate a wide range in pillar strengths. Two groups of results are identified that show significantly different behavior corresponding to differing effective pillar strengths. Estimates of pillar strengths derived from the measured data for these two groups are compared with established equations used for pillar design.

The differing behaviors and strengths are attributed to variations in the amount of yielding and deformation in roof and floor strata and hence in the amount of confinement they provide to the coal seam. Numerical modeling is used to provide a comparison with the measured data and to indicate that this provides a feasible mechanism to account for the measured data.

As the depth of mining increases, pillars tend to become increasingly wide and squat. In such cases, it is possible for the surrounding roadways to become badly deformed and damaged while the pillars remain stable. The criteria of comparing pillar strengths and loads to establish pillar stability become less applicable in these circumstances; rather, considerations of roadway stability may be the limiting factor in determining suitable pillar dimensions.

This is the case for pillar dimensions typically employed around longwall panels in the United Kingdom. Depending on the properties of the site and what are deemed to be satisfactory roadway conditions, this can lead to wide variations in required pillar dimensions. Measured data for deformations in roadways influenced by adjoining longwall workings are presented. These show that in some circumstances the influence of longwall extraction can be transmitted over large distances and confirm the variability in required pillar sizes depending on site properties.

¹Senior engineer.

²General manager.

³Engineer.

Rock Mechanics Technology Ltd., Burton-on-Trent, United Kingdom.

INTRODUCTION

There are many equations and methods for designing coal pillars; these include back-analyses of failed and successful case histories, extrapolation from strength tests on small-scale coal samples to full-size pillars, and analytical consideration of the limiting stress distribution across the pillar. The latter approach would nowadays normally involve the use of numerical modeling. In many instances, a combination of these approaches is adopted.

The range of methods developed can be accounted for by the wide range of geological conditions encountered underground and the different functions that coal pillars must fulfill in different mining methods. It would be remarkable if a single design equation were applicable to the entire range of coal pillar types and conditions. The design approach employed should be relevant to both the geological conditions at the site and the function of the coal pillar being considered.

Stress measurements provide a tool that can assist in the study of pillars. Comparison of the results from different sites shows a wide range of potential strata conditions and resulting pillar characteristics. For pillars of moderate widths sufficient to allow the development of confinement within the coal, the stress measurements can be used to obtain estimates of the available pillar strengths or load-bearing capacities.

For wider pillars employed in deeper mines and with long-wall layouts, characterizing pillars simply by their strength is less applicable. Such pillars are unlikely to fail in the sense of collapsing. However, the size of pillar employed can have a major influence on conditions in the surrounding entries. In this case, the distribution of stress within the pillars becomes more relevant, and the performance of pillars can be assessed by its impact on deformations and support requirements in the surrounding entries.

STRESS MEASUREMENT DATA

Measurement of stresses provides another tool for studying pillar behavior. During recent years, the stresses adjacent to mine roadways or entries have been measured at a number of coal mine sites in the United Kingdom. The results have been analyzed, and estimates of pillar strengths derived from them were compared with established pillar design equations [Cassie et al., in press]. The data and main points of the analysis are discussed here.

The general form of the results obtained was consistent with the confined core concept—the stresses are reduced immediately adjacent to the ribside and increase deeper into the strata. They provide a measure of the rate of increase of vertical stress actually obtained underground and can be studied with regard to their implications for the potential strength and behavior of pillars at sites where the confined core concept is considered valid.

Twenty sites have been included in this analysis where there were sufficient reliable results to allow the stresses to be characterized. At these sites, 63 stress measurements were

available; they were carried out by overcoring hollow inclusion stress cells. Relevant data on the 20 sites are presented in table 1; individual test results are listed in table 2. Although only the vertical stress component has been used in this analysis and listed in the table, the measurement technique employed provides all six stress components. Knowledge of these can be invaluable in assessing the reliability of individual tests and interpreting overall behavior at a site.

The results were collated from several field investigations that have been previously reported and analyzed on a site-by-site basis [Hendon et al. 1995; ECSC 1997a, 1997b, 1998]. In several instances, the primary objective of the measurements was to investigate mine entry, rather than pillar behavior. The extraction geometries varied widely, including individual entries unaffected by other mine openings, twin-entry developments, room-and-pillar panels, and yield pillars. Working depths at the sites ranged from <200 m to >1,000 m. Site T was located at Jim Walter Resources, Inc.'s No. 7 Mine in Alabama; all other sites were in the United Kingdom.

Table 1.—Measurement sites

Site	Depth, m	Seam height, m	Roadway height, m	Mining geometry	Deformation level
A	620	7.5	3.5	Single-entry gate road	High.
B	500	3.0	2.9	20-m pillar	High.
C	500	3.0	2.9	30-m pillar	High.
D	480	2.5	2.7	30-m pillar	High.
E	950	2.2	2.8	20-m pillar	High.
F	950	2.2	2.8	Single-entry gate road	High.
G	900	2.2	3.0	Single-entry gate road	High.
H	800	1.5	3.0	Irregular pillar	High.
I	950	2.4	3.0	60-m pillar	High.
J	840	2.2	2.8	Single-entry gate road	Low.
K	840	2.2	2.8	Yield pillar trial	Low.
L	320	2.8	2.9	Single-entry gate road	Low.
M	400	3.0	3.7	Trunk roadway	Low.
N	480	2.7	2.6	Single-entry gate road	Low.
O	560	2.5	2.9	Single-entry gate road	Low.
P	700	2.0	4.0	Trunk roadway	Low.
R	1,060	2.6	3.0	Trunk roadway	Low.
S	1,085	2.6	4.1	40-m pillar	Low.
T	560	2.5	2.5	Multientry gate road	Low.
U	180	1.2	1.2	11-m pillar	Low.

Table 2.—Measurement data

Site	Height above roof, m	Distance into ribs, m	Vertical stress, MPa	Site	Height above roof, m	Distance into ribs, m	Vertical stress, MPa
A . . .	3.2	4.0	5.9	L	1.8	1.7	6.3
A . . .	4.5	5.7	8.2	L	1.6	3.4	¹ 7.6
A . . .	5.0	9.4	14.1	L	2.1	6.4	¹ 7.8
B . . .	4.6	3.9	7.4	L	2.0	10.0	¹ 8.0
B . . .	4.6	6.2	10.5	M	3.1	1.1	10.0
B . . .	4.6	6.4	15.2	M	3.2	2.6	14.8
B . . .	4.6	8.1	17.5	M	3.0	4.3	¹ 15.5
C . . .	4.6	4.2	9.0	M	6.6	10.7	¹ 13.8
C . . .	4.6	6.9	8.7	N	3.5	1.5	9.0
C . . .	4.6	8.6	15.0	N	3.5	3.0	16.9
C . . .	4.6	11.7	¹ 15.7	N	3.6	7.0	¹ 11.4
D . . .	1.4	2.5	6.0	N	3.6	7.5	¹ 10.8
D . . .	1.2	4.1	10.3	O	4.8	2.9	13.3
E . . .	4.8	4.6	8.8	O	5.0	5.4	¹ 19.8
E . . .	5.2	7.2	10.6	O	5.0	7.4	¹ 15.6
E . . .	3.9	9.6	20.0	P	3.8	1.9	10.0
F . . .	1.5	2.2	4.6	P	3.6	3.0	14.7
F . . .	2.9	4.2	11.3	P	3.3	4.8	19.5
F . . .	4.0	5.9	13.7	P	6.5	8.1	¹ 18.5
G . . .	5.3	2.8	5.0	R	0.6	0.8	2.6
G . . .	4.2	3.7	9.5	R	1.7	2.4	12.0
G . . .	6.3	6.1	15.2	R	1.8	3.2	17.1
G . . .	6.8	10.9	24.5	R	3.5	4.7	21.6
H . . .	3.0	3.0	5.5	S	1.7	1.1	15.4
H . . .	5.9	5.2	8.9	S	1.5	3.0	26.7
H . . .	4.2	7.3	14.1	S	1.5	6.1	30.0
I	1.0	1.5	1.1	T	1.0	2.5	16.5
I	2.2	3.0	8.5	T	1.0	5.0	19.4
I	3.5	3.9	18.2	T	1.0	10.0	¹ 21.0
J . . .	2.2	5.6	26.0	U	1.6	1.0	8.4
K . . .	2.6	4.1	11.7	U	1.8	3.3	22.3
				U	1.7	5.2	¹ 23.5

¹Postpeak.

ANALYSES OF DATA

For consistency and ease of interpretation, it would have been preferable to conduct the tests in the coal seam. However, because of the need for sufficiently competent strata in which to conduct the overcore tests, they were conducted above, rather than within, the coal seam, with the height above the roof dependent on the strength and condition of the roof at the site. At each site, several tests were conducted at varying distances from the mine entry (figure 1). Those tests deeper into the strata and judged to be beyond the sector of increasing stress (i.e., postpeak) were omitted from the analyses (figure 2). A tendency for the data to form two groups with different rates of stress increase was evident (figure 3). It was also observed that the sites where the rate of stress increase was lower were characterized by large and deep-seated strata deformations. These sites were all at depths >480 m. The stress gradients measured were lower than for similar data from sites in the United States [Mark and Iannacchione 1992].

The lower rate of stress increase observed at sites where the strata deformations around roadways were large was not unexpected. The rate at which the vertical stress can increase will be related to the degree of confinement that the roof and floor provide to the coal seam. If the roof and floor provide a high degree of confinement to the coal in the ribside, the stress it can sustain will increase rapidly with distance from the ribside. The frictional properties of the coal and its bounding strata will influence this. The amount of failed or yielding ground surrounding a roadway will also have a large influence. If the roof and/or floor are themselves deforming, the confinement that they can provide to the coal ribside will reduce, as will the rate at which the vertical stress can increase. This is consistent with the correspondence observed between the measured stresses and entry deformations.

The nonzero stresses at the ribside indicated by the results in figure 3 are worth noting here. They may be a consequence of the stresses being measured above, rather than within, the seam. Very low stresses in the immediate yielded coal ribside, which increase rapidly with distance into the ribside, would be expected to result in nonzero stresses in the roof immediately above the coal rib. Measuring the stresses in the roof may therefore average out the stress variations in the seam.

ESTIMATES OF PILLAR STRENGTHS

Pillar load-bearing capacities were estimated from the measured stress data with the assumption that the stress is related linearly to distance from the ribside normalized with respect to roadway height. Utilizing the measured stress data in this manner could underestimate pillar strengths. They provide an estimate of stresses that can be sustained in the ribside, but not necessarily of the maximum stresses. Given that the stress distribution in the ribside may be expected to be nonlinear (with the gradient increasing deeper into the pillar), assuming a linear distribution will also tend to underestimate pillar strengths when extrapolated to greater pillar widths. The linear estimates of pillar strength have been obtained not because it is proposed

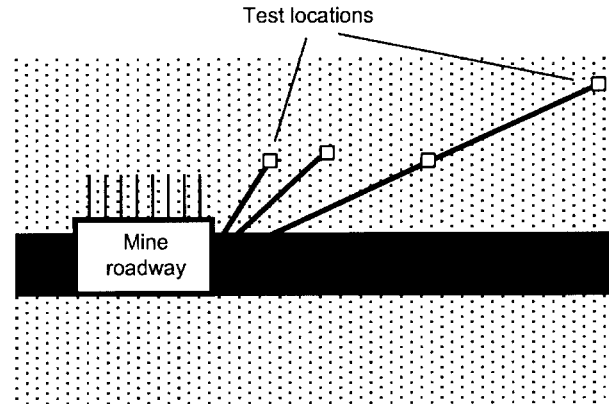


Figure 1.—Typical measurement site.

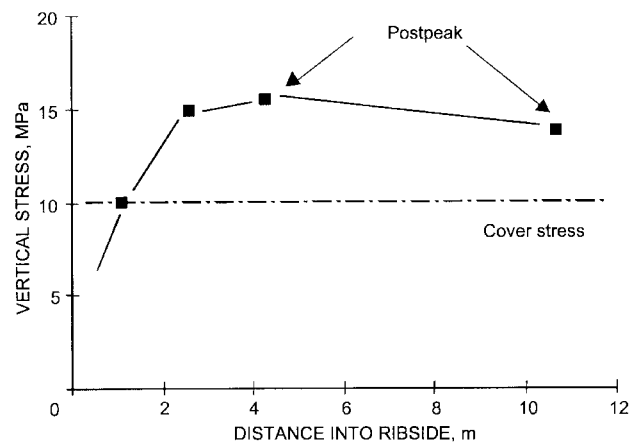


Figure 2.—Interpretation of test results.

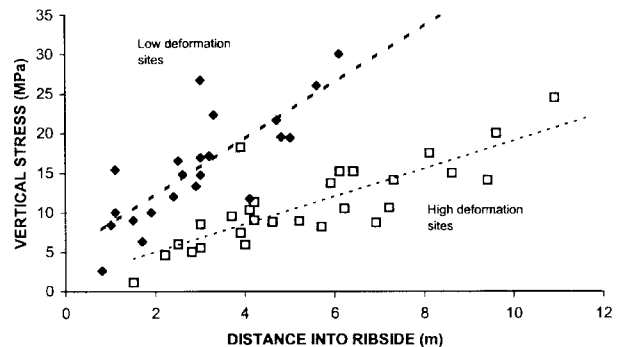


Figure 3.—Measured data from high and low deformation sites.

that they be adopted as a design equation, but rather to enable a comparison with the values given by recognized equations.

The formulas used as a basis for comparison were those presented by Bieniawski [1984], Wilson [1983], and the Salamon squat pillar equation with the parameters described by Wagner [1992]. An in situ coal compressive strength of 6 MPa was used in the Bieniawski formula.

Using results from sites typified by low deformations, the strengths were similar to those obtained using the Bieniawski equation and the Salamon squat pillar formulas (figure 4). This

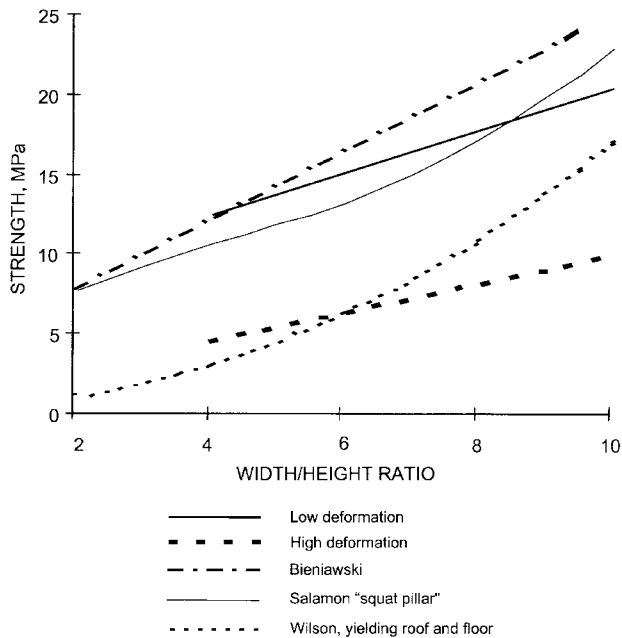


Figure 4.—Comparison of pillar strength estimates.

was making use of the average or regressed stress distribution. Estimates obtained for single sites within this group would imply strengths significantly in excess of or below these values. The Bieniawski and Salamon formulas were derived from back-analysis of failed and unfailed pillars or from testing of rock and coal specimens with different sizes and shapes; they have been widely recognized and applied to room-and-pillar layouts. In the case of the formulas, the strength at low width-to-height (w/h) ratios is associated with the in situ coal strength. For the estimates derived from the stress measurements, it is associated with the nonzero intercept obtained from linear regressions of the data. Despite this conceptual difference, the correspondence with the strength estimates for the low deformation sites is striking.

The pillar strengths implied using results from sites typified by high deformations were considerably lower. They indicate that, in these cases, strengths obtained using the same formulas and parameters could represent an overestimate. Significantly lower in situ coal strengths would be required to obtain a match with the measured data. Given that these equations are rooted in experience and the degree of acceptance that they have

gained, in the mining environments where they are applied the strata conditions giving rise to the lower pillar strengths cannot be widely encountered. This could largely be accounted for by the observation that all of the stress measurement sites categorized as high deformation were at depths of 480 m or more; room-and-pillar mining operations are mostly at depths less than this. Not all of the deeper sites fell into the category of high deformation with weaker pillars. At one of the deepest sites (>1,000 m), analysis of the measured results and experience indicated pillar strengths significantly greater than the estimates provided by the equations used in figure 4. The weaker pillar strengths are in closer agreement with those estimated using Wilson's equations.

The measured stress data imply a wide range of possible pillar strengths depending on whether a site falls into the high or low deformation categories used here. Using a set of case histories that includes some of the sites listed here, two types of behavior were similarly identified by Gale [1996]. He noted that the identification of two groups is somewhat arbitrary and it may be expected that the full range of behaviors between these extremes could be encountered.

It is possible that part of the apparent variation in pillar strength inferred from the measured stresses was associated with variations in the in situ uniaxial compressive strength (UCS) of the coal. However, the form of behavior assumed in interpreting the measured stress data implies that the coal in the ribside had already yielded (with a reduction in cohesion) and that its strength was due to its frictional properties and confinement rather than cohesion. This would suggest that variations in the coal's UCS were unlikely to have a major influence. A study by Mark and Barton [1996] suggested that variations in laboratory test values for coal UCS were poorly correlated with pillar strengths determined by back-analyses of failed and unfailed cases.

It appears that for the sites considered here the degree of confinement provided to the coal seam was a major factor in determining the pillar strength. If the roof and/or floor are themselves yielding and deforming, the confinement that they can provide to the coal ribside will reduce, as will the rate at which the vertical stress can increase, thus leading to a weaker pillar. This is consistent with the marked correlation between the measured stresses and roadway deformations and is largely equivalent to the distinction between the cases of rigid or yielding roof and floor made by Wilson.

COMPARISON WITH NUMERICAL MODELING

Computer modeling has been used to investigate pillar or entry behavior at the various sites in conjunction with the field measurements. The model parameters used and results presented here were not intended to represent any individual site;

rather, they illustrate the strata behavior and properties that may explain the measured data, in particular, the influence of the strata bounding the coal pillar.

The main parameters are summarized in table 3. Plane strain was assumed with two-dimensional cross sections of pillars being represented and boundary conditions set to define vertical axis of symmetry through the center of both the pillar and adjoining roadway. Initial stresses were applied and the roadway excavated to form the pillar. The loading on the pillar was then increased in several stages by displacing the upper and lower boundaries of the model grid. Results obtained for two cases are included. In the first, a uniformly strong host rock has been used; in the second, 3.0 m of weaker strata have been included above and below the seam. In other respects, the properties were identical. A cohesion equivalent to an in situ UCS of 6 MPa was used for the coal.

Table 3.—Modeling parameters

Modeling code	FLAC (version 3.3).		
Initial stresses, MPa	5 (sxx, syy, and szz).		
Dimensions:			
Seam height, m	2.4		
Roadway height, m	2.4		
Roadway width, m	4.8		
Pillar width, m	20.0		
Strata sequence:			
Case 1	Host rock and seam only.		
Case 2	3.0 m of weak strata in roof and floor.		
	Coal	Host rock	Weak strata
Density, kg/m ³	1,500	2,500	2,500
Bulk modulus, GPa	1.5	12.0	6.0
Shear modulus, GPa	1.0	7.0	3.5
Cohesion, MPa	1.6	12.0	4.0
Friction angle, °	35	40	30
Tensile strength, MPa	0.8	6.0	2.0
Residual cohesion, MPa	0.1	0.1	0.1
Residual friction angle, °	35	40	30
Dilation angle, °	0	0	0

In the case of the stronger strata, yielding was effectively confined within the coal seam. The vertical stresses in the ribside increased progressively, and large stresses developed as loading proceeded (figure 5). Examining the stresses at a horizon 3 m above the seam, the results were compared with the measured data that were also obtained from above the the seam, although not at a constant horizon. The model results show the rate of stress buildup increasing as the pillar was loaded. For average stresses across the pillar corresponding to the range likely to be encountered in practice, they lay through the measured data from low deformation sites. Given sufficiently strong roof and floor strata, very high pillar strengths can be developed.

With weaker strata introduced in the immediate roof and floor, the behavior was similar for the initial load stages (figure 6). As the loading was increased, the roof and floor started to yield and the rate of stress buildup in the ribside reduced. For the final load stages, yielding of the roof and floor

had fully developed, spread across the width of the pillar being modeled, and the stresses settled to an approximately constant residual distribution. For these latter stages, the stress distribution was irregular due to the development of bands of strata that were actively shearing with the stresses at yield; between these bands, the stresses are below yield. The trend of model results matched those of the measured data at high deformation sites.

For the strata properties and loading path used in this example, the weaker strata model exhibits a postpeak reduction in strength to a residual value (figure 7). The loss of pillar strength was associated with the reducing confinement as the strata bounding the coal seam yielded, rather than a reduction in coal strength. Should the initial stresses be sufficient to cause the roof and floor to yield and deform as the entries and pillar were formed, there would be no apparent loss in pillar strength by this mechanism and the postpeak strength would be applicable from the outset. In this way, the initial stresses, in addition to the strata properties, may influence pillar behavior.

Numerical modeling allows an improved interpretation of measured data. The influence of more factors can be taken into account, and it provides a better means of extrapolating to

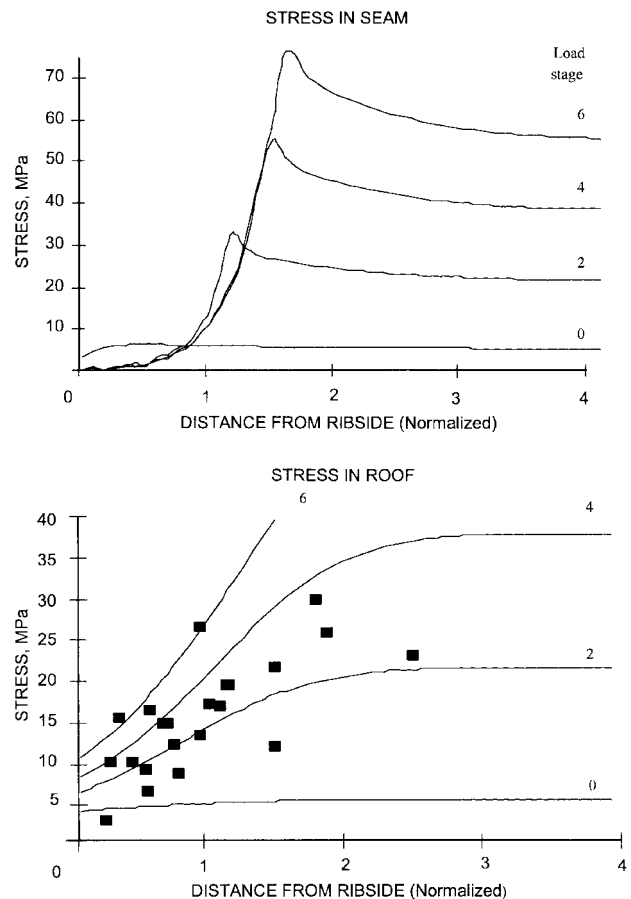


Figure 5.—Strong roof and floor strata.

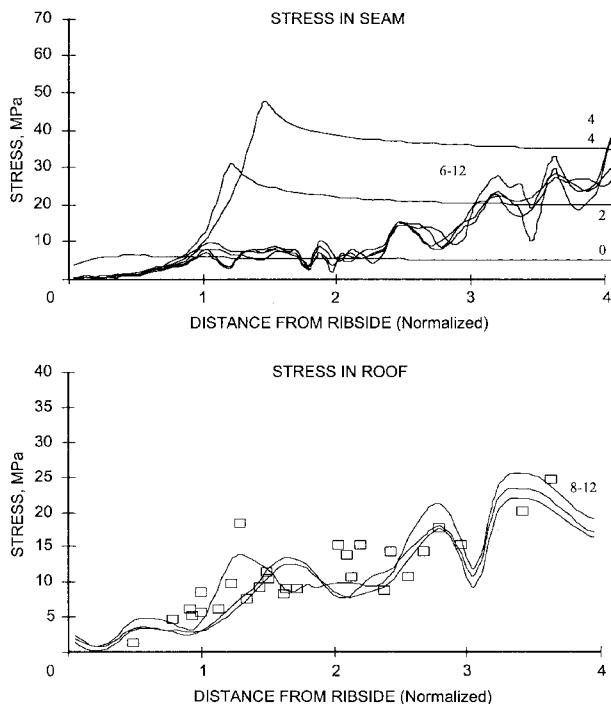


Figure 6.—Weak roof and floor strata.

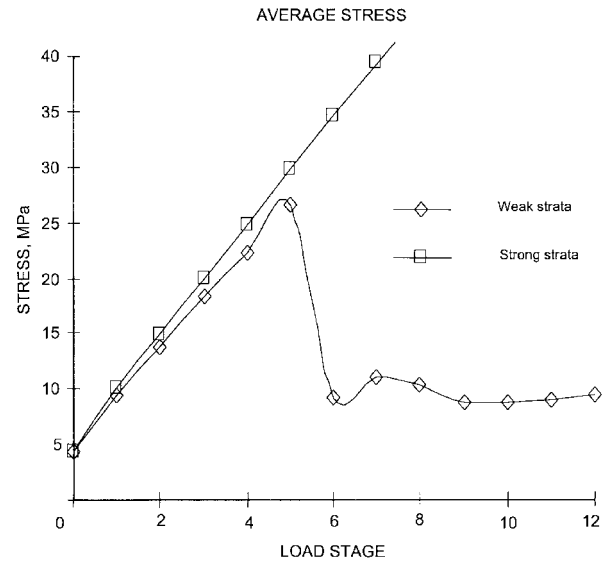


Figure 7.—Modeled pillar loads.

different geometries or loading. In addition, the interaction between pillars and the surrounding entries can be assessed and taken into account. In many circumstances, particularly with wider pillars, considerations of entry rather than pillar stability may be the limiting factor.

WIDE PILLARS

With large w/h ratios, it is widely accepted that the probability of pillar failure and loss of strength decreases. Nevertheless, excessive loading of the pillars may result in damage to the surrounding mine entries. For deeper mines and those using longwall mining methods, pillar w/h ratios frequently exceed those for which the most widely known strength equations were derived. In these circumstances, it is likely that pillar dimensions will be limited by considerations of the stability of the surrounding mine entries, rather than that of the pillars.

Design of pillars or pillar systems to maintain acceptable conditions in the surrounding entries is likely to lead to consideration of the nonuniform stress distribution across pillars, rather than simply the average stress or total load acting through a pillar. Although a simplification, one possible approach is to limit the maximum stress or the stress at a particular location expected within a pillar. This approach was adopted by Wilson with his "entry stability" as opposed to "ultimate stability" criteria for pillar strength [Carr and Wilson 1982].

The choice of a suitable limiting value for the stress is fundamental to this approach. Wilson related the maximum

allowable stress to the triaxial strength of the strata and the in situ vertical stress. Other estimates are possible, although it is likely to depend in some degree on the surrounding strata strength. In some regards, the choice of this value is analogous to the problem of determining the appropriate value for the in situ coal strength for use in pillar strength equations such as Bieniawski's.

The wide range of entry conditions encountered at sites subject to similar stress levels, but with different strata properties, suggests that appropriate values for the maximum stress to allow in a pillar may vary widely from site to site. The variation may be greater than that apparent in effective in situ coal strengths.

An advantage for using numerical modeling in investigating pillar behavior is that it enables consideration of the interaction between pillars and the surrounding entries. Mine entry conditions are, of course, influenced by factors other than surrounding pillars. This should be taken into account if adopting an approach of using favorable mine entry conditions as an objective of pillar design.

PROTECTION PILLARS BETWEEN LONGWALL PANELS

The pillars left between longwall panels are a particular case of wide pillars as described above. The method of longwall retreat typically employed in U.K. coal mines uses a single gate at each side of the panel, with adjacent panels separated by wide protection pillars (figure 8). The tailgate for the next in a sequence of longwall panels is driven during or subsequent to retreat of the previous panel. As a result, the tailgate may be driven in a stress regime that is subsequently altered by extraction of the previous panel, one that has already been altered, or a combination of these.

Pillar widths that have been adopted for recent layouts of this type in the United Kingdom are shown in figure 9. They clearly come into the category of wider pillars (the w/h ratios range up to 40:1). Coal pillars of these dimensions do not fail in the normally accepted sense. Despite this, the use of inadequate pillars may result in difficult mining conditions.

The choice of pillar dimensions may influence—

1. The stress change due to extraction of the previous panel and hence conditions in the tailgate while or after it is driven;
2. The concentration of stress and hence conditions at the tailgate-faceline junction during retreat; and
3. The surface subsidence profile across the sequence of panels.

The first and second of the above will almost certainly be considered in determining the pillar size. The third may be considered if the surface is subject to subsidence limitations.

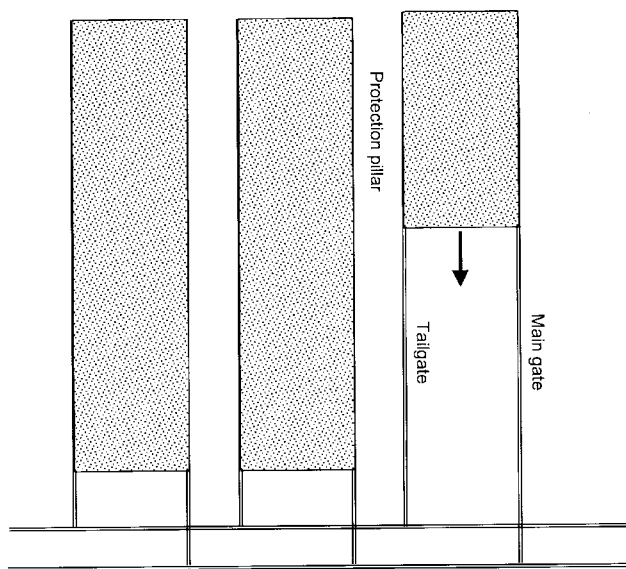


Figure 8.—Typical longwall retreat layout in U.K. coal mines.

Wilson's pillar equations were originally developed as a method for determining dimensions for this kind of pillar. The method estimates the distribution of stresses transferred onto the pillar due to extraction of the panels. It effectively limits the stress at the location of the tailgate with the first panel extracted and the maximum stress across the pillar with both panels extracted. Numerical modeling can now be used to provide a more sophisticated estimate of how the stresses will be distributed across the pillar. It will, however, be strongly dependent on the caving behavior of the longwall and the reconsolidation of the waste that remains subject to considerable uncertainty. Suitable limits to place on the stress levels must also be determined for the site, as described earlier.

Roof displacements showing the influence on gate conditions of stresses distributed over substantial pillars such as these are shown in figures 10-12. The data are from telltale devices used to measure roof deformations [Altounyan and Hurt 1998]. Their purpose is to provide a routine assessment of roof condition, rather than acting as field measurement stations for research purposes. However, the data obtained can be used to enable a comparison between different entries and sites.

In figure 10, a histogram compares data from the tailgate and main gate for a panel at an average depth of 590 m with a 50-m pillar. At this depth, the pillar width is at the lower range in figure 9. For the main gate, none of the instruments showed

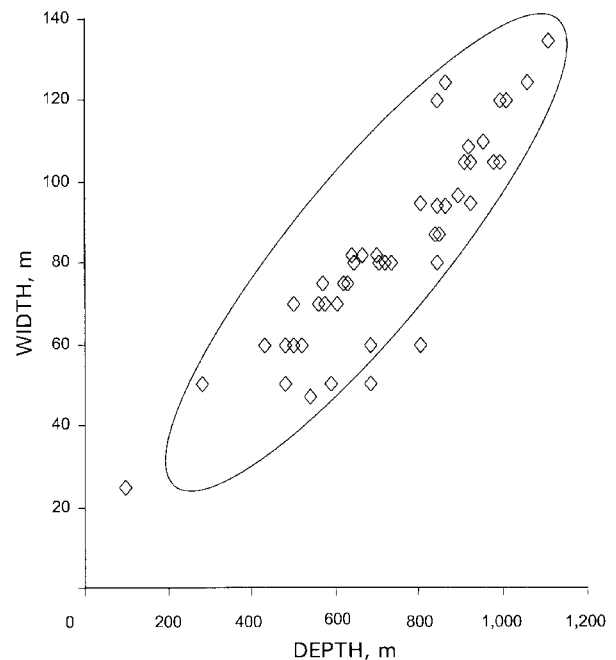


Figure 9.—Pillar widths between retreat longwall panels.

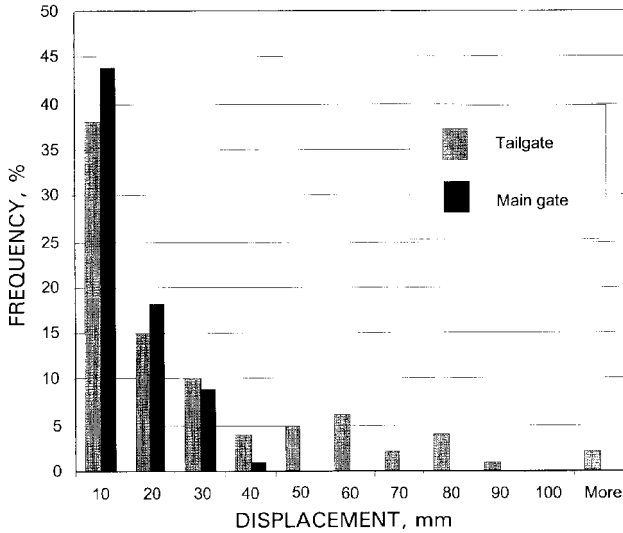


Figure 10.—Comparison of roof displacements in main gate and tailgate during development.

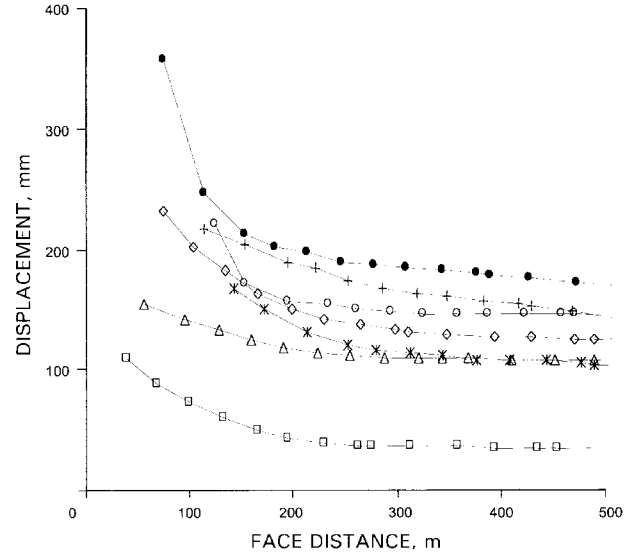


Figure 12.—Roof displacements in tailgate during retreat.

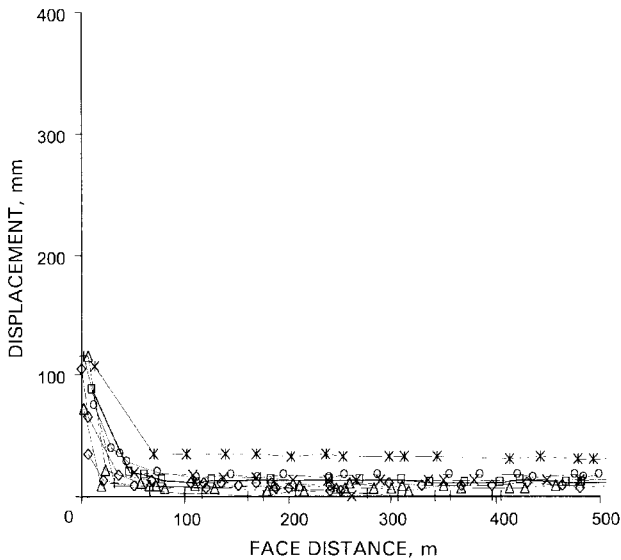


Figure 11.—Roof displacements in main gate during retreat.

displacements in excess of 40 mm; in the tailgate, 20% exceeded this value. There was considerable spread in the roof deformations along the length of each gate; this can be expected due to geological variations. The form of the distributions suggests that in zones of weaker geology the increased stress levels experienced by the tailgate resulted in increased roof displacements. The displacements plotted were those recorded up to 50 days after drivage of the gate; the difference between the gates increased with time and during retreat of the panel.

Increasing roof displacements as the retreating panel approaches are plotted in figures 11 and 12. For the main gate (figure 11), its influence only becomes apparent within the final 50 m. The displacements in the tailgate (figure 12) are larger and start to accelerate at an earlier stage than for the main gate. In fact, tailgate conditions for this panel were poor with large amounts of convergence and roof softening. A considerable amount of extra support had to be installed in the tailgate to maintain stability up to the junction with the faceline. The different amount of support employed in the gates needs to be taken into account in comparing figures 11 and 12.

Variability in conditions such as that evident in figures 10-12 may provide a guide in determining suitable pillar dimensions. If the difference between main gate and tailgate attributable to increased stress is small compared to the spread due to geological variability along the length of each gate, there is little point in increasing pillar widths in order to improve conditions in subsequent tailgates.

Although pillar dimensions are usually described with regard to consideration of vertical stresses and their effects, many other factors can also affect longwall gate conditions and influence the choice of suitable pillar dimensions. These include—

- Horizontal stresses and their orientation relative to the panel;
- Timing of gate drivage relative to the previous panel; and
- Interaction with workings in other seams.

If significant interaction is expected, this may be the dominant consideration in determining the position of the tailgate and thus the pillar size. These are technical factors and are not the sole determinants of pillar size. The choice of pillar size will also be strongly influenced by the priorities of the

mine management or operator. If the priority is to maximize extraction, smaller pillars are likely to be adopted, with adverse conditions in the tailgate giving rise to increased repair and support costs being accepted. If the priority is to minimize production costs, larger pillars are likely to be adopted.

SUMMARY

Comparison of stress measurement results from different sites, mostly in U.K. mines, shows a wide range of potential strata conditions and resulting pillar characteristics. The range can be accounted for by variations in the degree of confinement provided to the coal by the roof and floor strata. The lower pillar strengths inferred from measured stress data were encountered at deeper sites with weak roof or floor strata and characterized by large deformations. Such sites are likely to employ mining methods other than room- and-pillar and use wide pillars. Although the wider pillars employed between longwall panels may not fail in the usual sense, their

dimensions can have a critical impact on conditions in the surrounding entries or gates.

For wide pillars, it is likely that pillar dimensions will be limited by considerations of the stability of the surrounding mine entries rather than of the pillars. This requires that factors other than pillar strengths and load be taken into account. A possible general approach is to establish stress levels that are acceptable for a site and dimension pillars so that these stress levels are not exceeded and to consider the pillar in context with the stability of the entries.

REFERENCES

- Altounyan P, Hurt K [1998]. Advanced rockbolting technology. *World Coal* May:30-36.
- Bieniawski ZT [1984]. *Rock mechanics design in mining and tunnelling*. Rotterdam: A. A. Balkema.
- Carr F, Wilson AH [1982]. A new approach to the design of multi-entry developments for retreat longwall mining. In: *Proceedings of the Second Conference on Ground Control in Mining*. Morgantown, WV: West Virginia University, pp. 1-21.
- Cassie JW, Cartwright PB, Altounyan PFR [in press]. Coal pillar behavior from underground stress measurements. In: *Proceedings of the 9th International Congress on Rock Mechanics* (Paris, France, August 25-28, 1999).
- ECSC (European Coal and Steel Research) [1997a]. Application of rock reinforcement techniques to difficult mining conditions. Report on ECSC Research Project 7220-AB/836.
- ECSC (European Coal and Steel Research) [1997b]. Lateral stress relief for longwall access and trunk roadways. Report on ECSC Research Project 7220-AB/834.
- ECSC (European Coal and Steel Research) [1998]. Coal pillar design. Report on ECSC Project 720-AF/861.
- Gale WJ [1996]. Geological issues relating to coal pillar design. In: *Symposium of Geology in Longwall Mining*, pp. 185-191.
- Hendon G, Carr F, Lewis A, Cassie J [1995]. A cooperative study of gate entry designs, Welbeck Colliery (UK) and Jim Walter Resources (USA). In: *Proceedings of the 14th International Conference on Ground Control in Mining*. Morgantown, WV: West Virginia University, pp. 94-103.
- Mark C, Barton TM [1996]. The uniaxial compressive strength of coal: should it be used to design pillars? In: Ozdemir L, Hanna K, Haramy KY, Peng S, eds. *Proceedings of the 15th International Conference on Ground Control in Mining*. Golden, CO: Colorado School of Mines, pp. 61-78.
- Mark C, Iannacchione AT [1992]. Coal pillar mechanics: theoretical models and field measurements compared. In: *Proceedings of the Workshop on Coal Pillar Mechanics and Design*. Pittsburgh, PA: U.S. Department of the Interior, Bureau of Mines, IC 9315, pp. 78-93.
- Wagner H [1992]. Pillar design in South African collieries. In: *Proceedings of the Workshop on Coal Pillar Mechanics and Design*. Pittsburgh, PA: U.S. Department of the Interior, Bureau of Mines, IC 9315, pp. 283-301.
- Wilson AH [1983]. The stability of underground workings in the soft rocks of the coal measures. *Int J Min Eng* 1:91-187.

ANALYSIS OF LONGWALL TAILGATE SERVICEABILITY (ALTS): A CHAIN PILLAR DESIGN METHODOLOGY FOR AUSTRALIAN CONDITIONS

By Mark Colwell,¹ Russel Frith, Ph.D.,² and Christopher Mark, Ph.D.³

ABSTRACT

This paper summarizes the results of a research project whose goal was to provide the Australian coal industry with a chain pillar design methodology readily usable by colliery staff. The project was primarily funded by the Australian Coal Association Research Program and further supported by several Australian longwall operations.

The starting point or basis of the project was the Analysis of Longwall Pillar Stability (ALPS) methodology. ALPS was chosen because of its operational focus; it uses tailgate performance as the determining chain pillar design criterion rather than simply pillar stability. Furthermore, ALPS recognizes that several geotechnical and design factors, including (but not limited to) chain pillar stability, affect that performance.

There are some geotechnical and mine layout differences between United States and Australian coalfields that required investigation and, therefore, calibration before the full benefits offered by the ALPS methodology could be realized in Australia.

Ultimately, case history data were collected from 19 longwall mines representing approximately 60% of all Australian longwall operations. In addition, six monitoring sites incorporated an array of hydraulic stress cells to measure the change in vertical stress throughout the various phases of the longwall extraction cycle. The sites also incorporated extensometers to monitor roof and rib performance in response to the retreating longwall face.

The study found strong relationships between the tailgate stability factor, the Coal Mine Roof Rating, and the installed level of primary support. The final outcome of the project is a chain pillar design methodology called Analysis of Longwall Tailgate Serviceability (ALTS). Guidelines for using ALTS are provided.

¹Principal, Colwell Geotechnical Services, Caloundra, Queensland, Australia.

²Principal, Strata Engineering, Teralba, New South Wales, Australia.

³Supervisory physical scientist, Pittsburgh Research Laboratory, National Institute for Occupational Safety and Health, Pittsburgh, PA.

INTRODUCTION

In many cases, chain pillars in Australia have been designed solely with regard to pillar stability using a process similar to that used for pillars within bord-and-pillar operations. The bord-and-pillar approach is based on analysis of collapsed pillar cases from Australia and the Republic of South Africa [Salamon et al. 1996] and applies a factor of safety in relation to pillar collapse. This approach is inappropriate for a number of reasons when designing chain pillars.

Australian chain pillars typically have minimum width-to-height (w/h) ratios >8 , which is approximately 4.5 standard deviations away from the mean of the pillar collapse case histories. In addition, the chain pillar loading cycle and active life are significantly different from those experienced by pillars within a bord-and-pillar operation. Finally, the goal of maintaining gate road stability is very different from that of avoiding a pillar collapse.

The need for a design method uniquely developed for Australian longwall chain pillars was clear. The original submission for funding by the Australian Coal Association Research Program (ACARP) stated that the calibration (to Australian conditions) of a proven chain pillar design methodology offered the least risk for a successful and timely outcome. It was assessed that the most comprehensive chain pillar design tool then available was the Analysis of Longwall Pillar Stability (ALPS) [Mark 1990; Mark et al. 1994]. The primary consideration in selecting ALPS is that it uses gate road (i.e., tailgate) performance as the determining chain pillar design criterion. Secondly, ALPS is an empirical design tool based on a U.S. coal mine database; thus, it provided a ready framework for calibration to Australian conditions.

The aim of the project was to provide the Australian coal industry with a chain pillar design methodology and computer-based design tool readily usable by colliery staff. A further objective was to ensure that the methodology developed by the project had the widest possible application to all Australian coalfields by identifying where local adjustments and limitations may apply.

In formulating the design methodology, the primary goal was to optimize pillar size (specifically pillar width) so as to—

- Maintain serviceable gate roads such that both safety and longwall productivity are unaffected;
- Minimize roadway drivage requirements so as to have a positive impact on continuity between successive longwall panel extraction; and
- Maximize coal recovery.

In designing chain pillars, specifically with regard to satisfactory gate road performance, the following design criteria were proposed:

- The chain pillar must provide adequate separation between the main gate travel road and belt road, such that the travel road (tailgate of the subsequent longwall panel) will be satisfactorily protected from the reorientation and intensification of the stress field caused by the extraction of the first longwall panel.
- The tailgate (with a focus on the tailgate intersection with the longwall face) will be sufficiently serviceable for ventilation and any other requirements (setting of secondary support, second egress, etc).

BACKGROUND

ALPS was originally developed by Mark and Bieniawski [1986] at The Pennsylvania State University. It was further refined [Mark 1990, 1992; Mark et al. 1994] under the auspices of the former U.S. Bureau of Mines (USBM).⁴ The initial ALPS research involved field measurements of longwall abutment loads at 16 longwall panels at 5 mines. These measurements were used to calibrate a simple conceptualization of the side abutment, similar to models proposed by Wilson [1981] and Whittaker and Frith [1987]. The side abutment (A) equates to the wedge of overburden defined by the *abutment angle* (ϕ) (see figure 1). The tailgate loading condition is considered to be some percentage of the side abutment, called the *tailgate abutment factor* (F_t). The U.S. field measurements found a range of abutment angles, from $\phi = 10.7^\circ$ to $\phi = 25.2^\circ$. A value of $\phi = 21^\circ$ and $F_t = 1.7$ was selected for use in design.

⁴The safety and health research functions of the former U.S. Bureau of Mines were transferred to the National Institute for Occupational Safety and Health in October 1996.

Because of the encouraging results obtained from the initial

study, the USBM commissioned further research directed toward quantifying the relative importance of roof and floor quality and artificial support on gate road performance. The approach was to analyze actual longwall mining experience. Case histories from 44 U.S. longwall mines were characterized using 5 descriptive parameters. Pillar design was described by the ALPS stability factor (ALPS SF = pillar strength \div pillar load); roof quality was described by the Coal Mine Roof Rating (CMRR) [Molinda and Mark 1994; Mark and Molinda 1996]. Other rating scales were developed for primary support, secondary support, and entry width.

Mark et al. [1994] reported that statistical analyses indicated that in 84% of the case histories the tailgate performance (satisfactory or unsatisfactory) could be predicted correctly using only the ALPS SF and the CMRR. It was further stated that most of the misclassified cases fell within a very narrow borderline region. The analyses also confirmed that primary

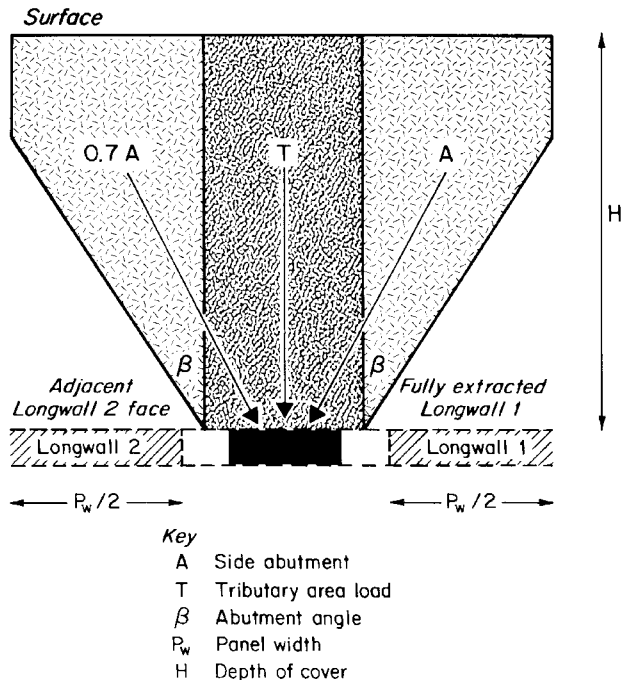


Figure 1.—Conceptual model of the side abutment load.

roof support and gate entry width are essential elements in successful gate entry design. The relative importance of the floor and of secondary support installed during extraction could not be determined from the data.

NEED FOR CALIBRATION

Conventional longwall mines in the United States generally use a three-heading gate road system; Australian longwall panel design typically employs a two-heading gate road system with rectangular chain pillars separating these gate roads. A typical Australian longwall panel layout is presented in figure 2. Figure 2 also details the stages of the chain pillar loading cycle:

1. Development loading (calculated using tributary area concepts);
2. Front abutment loading, which occurs when the first longwall face is parallel with the pillar;
3. Main gate (side) abutment loading, when the load has stabilized after the passage of the first face;
4. Tailgate loading, when the second face is parallel with the pillar; and
5. Double goafing, when the pillar is isolated between two gobbs.

It is during tailgate loading that the chain pillar (or cross section thereof adjacent to the tailgate intersection) experiences the greatest vertical loading during its "active life," i.e., the period where the chain pillar is playing its role in helping to maintain satisfactory gate road conditions. This project focused on tailgate performance (at the T-junction) as the design condi-

The following equation (relating the ALPS SF and CMRR) was presented to assist in chain pillar and gate entry design:

$$\text{ALPS SF}_R = 1.76 + 0.014 \text{ CMRR}, \quad (1)$$

where the ALPS SF_R is the ALPS SF suggested for design.

The Primary Support Rating (PSUP) used in ALPS was developed as an estimate of roof bolt density and is calculated as follows:

$$\text{PSUP} = \frac{L_b (N_b (D_b)}{S_b (w_e (84)}, \quad (2)$$

where L_b = length of bolt, m,

N_b = number of bolts per row,

D_b = diameter of the bolts, mm,

S_b = spacing between rows of bolts, m,

and w_e = entry (or roadway) width, m.

PSUP treats all bolts equally and does not account for load transfer properties, pretensioning effects, etc.

tion. The pillar stability factor in relation to the tailgate loading condition is designated as the "tailgate stability factor" (TG SF).

The project found that Australian chain pillars have an average length-to-width ratio of 3.2; crosscut centers on average are spaced at 100 m. The pronounced rectangular shape of Australian chain pillars may add strength to the pillar compared to a square pillar of the same minimum width. Mark et al. [1998b] reanalyzed the U.S. database using the Mark-Bieniawski rectangular pillar strength formula and found a slightly better correlation (in relation to the predictive success rate) than using the Bieniawski equation. In addition to the Bieniawski equation, this project assessed both the Mark-Bieniawski rectangular pillar formula [Mark and Chase 1997] and the squat pillar formula [Madden 1988] in relation to the correlation between the pillar stability factor and the CMRR.

In Australia, the significant impact of horizontal stress on coal mine roof stability is well documented [Frith and Thomas 1995; Gale and Matthews 1992]. The in situ horizontal stresses should not have a significant direct influence on tailgate roof stability due to the presence of an adjacent goaf. However, there is an indirect influence in terms of the degree of damage done to the roof during the initial roadway development and

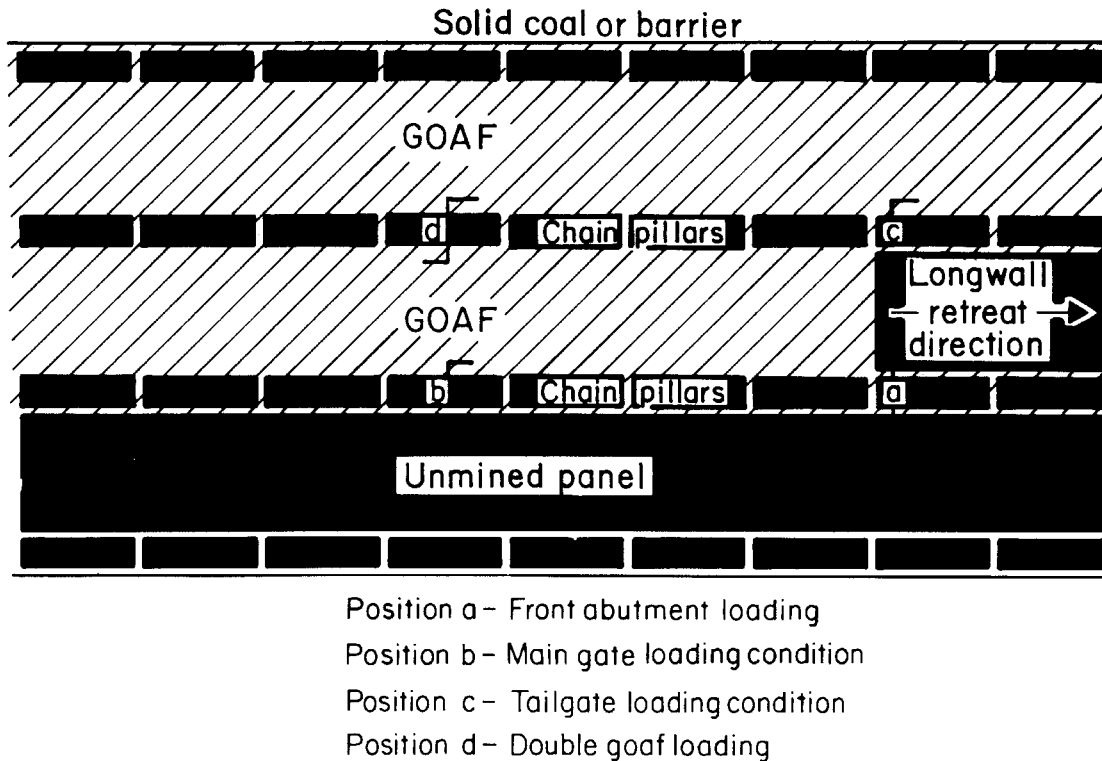


Figure 2.—Stages in the dynamic loading cycle of longwall chain pillars.

then to the main gate travel road and cut-throughs during longwall retreat. The effect of the in situ horizontal stress field on gate road serviceability (particularly on roof stability) is not taken into account directly by the ALPS methodology and was considered in more detail by the ACARP project.

Finally, the project aimed to verify the applicability of the ALPS loading parameters to Australian conditions. The ALPS methodology uses an abutment angle of 21° in all cases, and it assumes that the tailgate load is 1.7 times the side abutment load.

MEASUREMENTS OF AUSTRALIAN ABUTMENT LOADS

The project measured changes in vertical stress across (and within) chain pillars at six collieries to determine whether the ALPS approximations should be refined. Three sites were located in the Bowen Basin Coalfield in Queensland (Central, Crinum, and Kenmare Collieries), two were in the Newcastle Coalfield (Newstan and West Wallsend Collieries), and one was at West Cliff Colliery in the Southern Coalfield. Each monitoring site included an array of hydraulic stress cells (HSCs) generally located at midseam height to measure the changes in vertical stress. Most sites also included extensometers to monitor roof and rib performance. A general instrumentation layout is shown in figure 3.

The HSC used in this project is a modification of the borehole-platened flatjack developed by the former USBM. The HSC was developed, calibrated, and tested by Mincad Systems Pty. Ltd. [1997]. The HSC consists of a stainless steel bladder into which hydraulic fluid is pumped via tubing extending along the borehole. The bladder is encased between two steel platens that are forced against the borehole wall as the

bladder is pumped up.

As with every stress measurement instrument, proper calibration is important. Mincad Systems provided two calibration formulas based on its research with the HSC. The formula used in this project employs a calibration factor $K' = 1.0$ for a stress increase of $\#5$ MPa and $K' = 1.3$ for that portion of an increase above 5 MPa. Because ALPS is a comparative chain pillar design tool, it is not critical which calibration method is used as long as the method is consistent from site to site.

The six sites add considerably to the ALPS abutment load database. They include a much wider range of cover depths and width-to-depth ratios than the original U.S. data. There is also much more variety in the geologic environments. In addition, because the stress readings could be made remotely, monitoring was possible subsequent to the passing of the second longwall

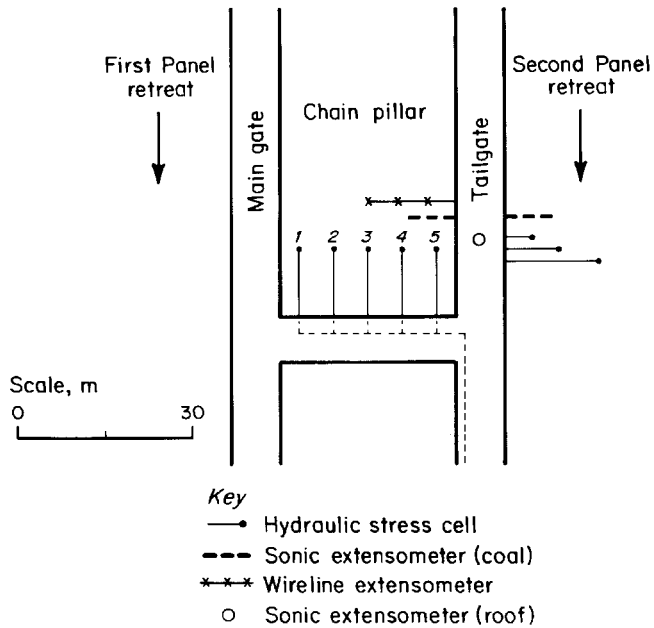


Figure 3.—Instrumentation layout at a typical stress measurement site.

face. Of the 16 original U.S. panels, there were sufficient data to characterize the side abutment load in only 6, and only one panel provided data on the tailgate abutment factor. In contrast, data on both the side and tailgate loads were obtained from all six Australian monitoring sites.

At the Australian sites, entry width and height ranged from 4.8 to 5.2 m and 2.5 to 3.6 m, respectively. Pillar width and length (rib to rib) ranged from 26 to 40 m and 95 to 125 m, respectively; cover depths varied from 130 to 475 m. Due to the relatively high length-to-width ratio of Australian chain pillars (i.e., extracted crosscut coal <5%), a plane strain or two-dimensional loading analysis is common in Australia and was considered appropriate by the Australian researchers. Furthermore, the Australian researchers recognized that the location of the stress cells within the pillar would in all probability affect the measured vertical stress changes. In placing the cells near a cut-through rather than across the longitudinal center of the chain pillar, the monitoring exercises were viewed as recording the loading behavior of a thin, two-dimensional slice of the pillar near a critical location during its "active life."

The ALPS loading parameters account for the extracted coal within the cut-throughs. Therefore, the abutment angles reported by the ACARP project [Colwell 1998] would be slightly different if the load had been addressed in the same manner as the U.S. field measurements in back-calculating the abutment angles. However, the end effect on the design chain pillar width is negligible.

Measurements of the main gate side abutment loading are used to calculate the abutment angle; measurements of the tailgate abutment (when longwall 2 is parallel with the instruments) are used to calculate the tailgate abutment factors. Examples of the data obtained from two of the sites are shown

in figure 4. The results from all six monitoring sites are summarized in table 1 and figure 5 (along with the U.S. data).

The measurements of the abutment angle from the three Queensland mines and from Newstan Colliery clearly fall within the range of the U.S. data. However, the abutment angles calculated for the two deepest mines, West Wallsend and West Cliff, are the smallest of any in the database. The overburden at these two mines (and at Newstan Colliery) also contains the massive sandstone and sandstone/conglomerate strata commonly associated with the Newcastle and Southern Coalfields. The low width-to-depth ratio, along with the strong overburden, may be affecting the caving characteristics of the gob.

Table 1 also shows two sets of tailgate abutment factors. The first set was obtained by dividing the measured tailgate loading by the measured main gate (side abutment) loading. The second set, which is the one used in the U.S. version of ALPS, is obtained by dividing the measured tailgate load (adjacent to the T-junction) by the *calculated* side abutment load using an abutment angle of 21° . The one U.S. measurement found this second tailgate abutment factor to be 1.7. The Australian data in table 1 show a high variability, with the mean at 1.3 in relation to an ALPS-style analysis.

Figure 6 plots the development of the change in load during tailgate loading (as a multiple of the side abutment) against face position. It clearly indicates that the nature of the loading behavior at Central, Crinum, and Kenmare Collieries closely approximates that proposed by ALPS. However, the tailgate loading behavior at Newstan Colliery and particularly at West Wallsend Colliery reveals that the *double goaf load* is significantly greater than twice the measured main gate side abutment load. It is likely that West Cliff would have behaved in a manner similar to Newstan if the cabling and/or cells had not become inoperable with the second longwall face only 5 m past the instrumentation site.

The field data associated with Newstan, West Wallsend, and West Cliff Collieries clearly suggest that a *much* greater portion of the main gate abutment load is distributed onto the adjacent unmined longwall panel than calculated on theoretical grounds (see figure 2).

Although the double goaf loading condition could not be measured at West Wallsend Colliery, it would seem that the bulk of the tailgate load manifests itself within that distance 100 m outby of the face. There are distinct increases in the rate of loading at approximately 70 m and again at 20 m outby of the face. This correlates well with the observed tailgate condition and strata behavior.

In contrast to West Wallsend Colliery, the bulk of the tailgate load at Newstan Colliery manifests itself after the passage of the longwall face. Both Newstan and West Wallsend Collieries have experienced greater difficulties with regard to both gate road and face control issues when massive sandstone/conglomerate channels are within 0 to 30 m of the mining horizon. Face width optimization has played a critical role in alleviating the face control difficulties.

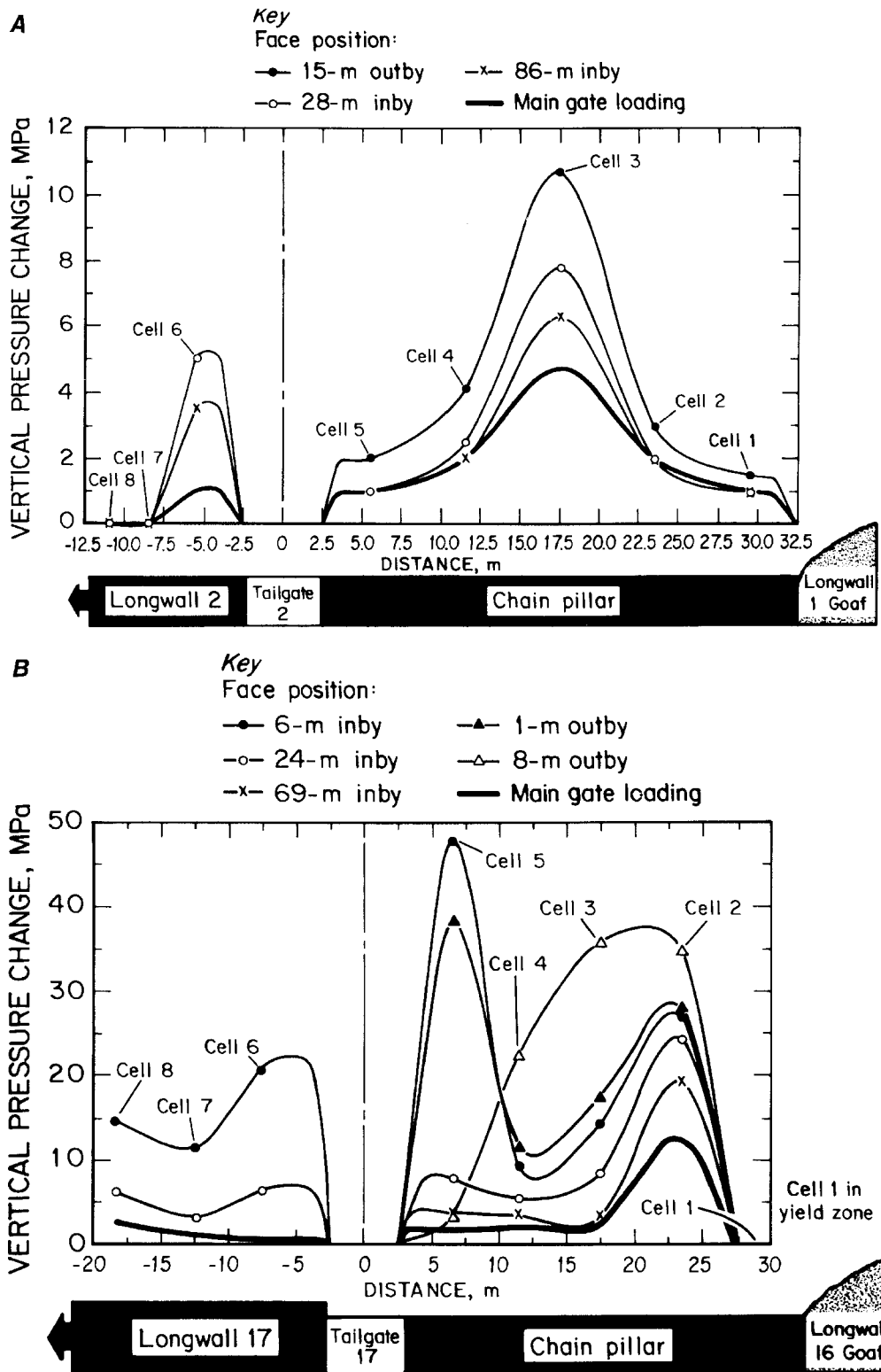


Figure 4.—A, Abutment load profiles at different locations of the longwall face (Crinum Colliery) with highly cleated coal. B, Abutment load profiles at different locations of the longwall face (West Wallsend Colliery), where the tailgate load is extremely aggressive.

Table 1.—Results of stress measurements

Monitoring site	H, m	w, m	w _p , m	P _w , m	β, °	F _t (Meas)	F _t (Calc)
Central	265	39.9	5.1	230	24.7	1.77	2.05
Crinum	125	30.2	4.8	275	19.1	1.52	1.35
Kenmare	130	24.8	5.2	200	19.2	1.49	1.22
Newstan	180	26.0	5.0	130	15.3	1.48	1.04
West Cliff	475	37.2	4.8	200	5.9	1.81	0.60
West Wallsend	240	30.1	4.9	145	8.5	3.79	1.52

NOTE.—β and F_t (Meas) are based on two-dimensional analyses (C = 0.25 MN/m³; Kenmare (C = 0.23 MN/m³). F_t (Meas) is based on ALPS loading parameters (β = 21° and C = 0.255 MN/m³).

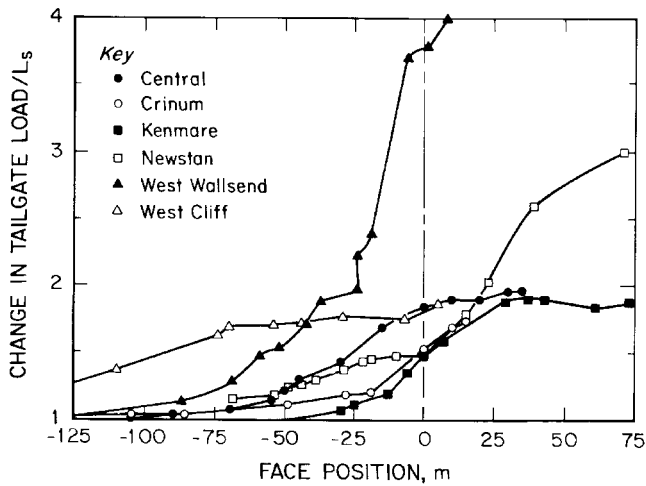


Figure 5.—Development of abutment load at the six monitoring sites.

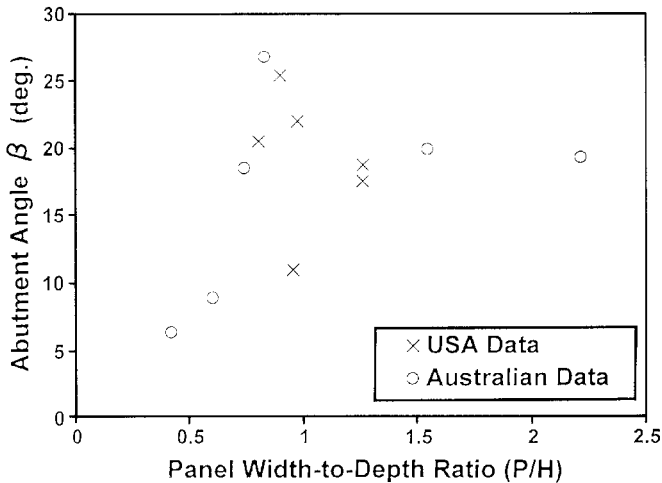


Figure 6.—Abutment angles determined from stress measurements.

A possible explanation for the variation in the manifestation of the tailgate load (in relation to face position) is that while a near-seam conglomerate channel exists in relation to the monitoring site at West Wallsend Colliery, it is absent at the Newstan Colliery site. The anecdotal evidence suggesting the near-seam channel as a possible cause of this variation in load manifestation is strong (i.e., secondary support requirements,

seismic monitoring [Frith and Creech 1997]; however, the mechanics are not yet fully understood.

The stress measurements collected by the project were supplemented by data from similar investigations previously conducted by other collieries, which were gratefully made available to the project. The supplementary field data were obtained using nearly all of the different types of stress cells that have been used in Australia (CSIRO HI, IRAD, Geokon, and HSC). The variety of instruments hinders comparison between studies, yet some trends emerge.

In general, the supplementary field data support the observations made from the project data. In Bowen Basin collieries, the loading behavior closely approximates that proposed within ALPS. In contrast, there are some significant departures in New South Wales for collieries that have strong, spanning overburden and a low width-to-depth ratio. Table 2 indicates that at Angus Place, South Bulli, West Cliff, West Wallsend, and Wye the measured side abutment angles are significantly less than 21°.

In summary, it seems that an abutment factor of 1.5, in conjunction with an abutment angle of β = 21°, is a reasonable and generally conservative approximation of the actual tailgate load for most Australian mines. The exceptions are two collieries and one locality (containing three collieries) within the Australian database, where there is sufficient evidence to suggest that site-specific loading parameters are more applicable. These are the Central and West Wallsend Collieries, and the deepest collieries within the Southern Coalfield (South Bulli, Tower, and West Cliff Collieries). For Central Colliery, the appropriate loading parameters seem to be β = 26° and F_t = 1.6. With regard to the three Southern Coalfield collieries, the recommended loading parameters are β = 10° and F_t = 1.5, which also apply to areas associated with West Wallsend Colliery that are unaffected by the near-seam sandstone/conglomerate channels. In areas where thickening of the channel occurs, it is assessed that the abutment angle of β = 10° should be maintained, while F_t should be increased to 3.5.

Two other variables can influence the calculation of pillar stability factors: *in situ coal strength* (S₁) and the *overburden density* (C). A comprehensive study in the United States recently concluded that uniaxial compressive strength tests on small coal samples do not correlate with *in situ* pillar strength [Mark and Barton 1996]. That study and others in Australia and the Republic of South Africa [Salamon et al. 1996] found that using a constant seam strength works well for empirical pillar design methods. Accordingly, the *in situ* coal strength is taken to be 6.2 MPa, as used in ALPS.

In some Australian mines, there is so much coal in the overburden that the overburden density is significantly reduced below the C = 0.25 MN/m³ that is typical for sedimentary rock. Dartbrook and Kenmare Collieries have undertaken satisfactory analyses of their overburden and have determined that C = 0.22 MN/m³ and 0.23 MN/m³, respectively.

Table 2.—Supplemental stress measurements from other Australian mines

Site details	Reference	Cell type	Cell position	Remarks	N, °	F _t (Meas)
Angus Place longwall 12	Clough [1989]	CSIRO HI	In roof	Author indicates vertical stress increase small; may be affected by clay bands within roof strata.	5.5	—
Central longwalls 301-302	Wardle and Klenowski [1988]	IRAD	In seam	Satisfactory results from which to interpret main gate and tailgate loading.	26.8	1.48
Cook longwalls 5-6	Gale and Matthews [1992]	CSIRO HI	In roof	Satisfactory results from which to interpret main gate and tailgate loading.	38.0	1.31
Ellalong longwall 1	Wold and Pala [1986]	IRAD	In seam	Satisfactory results from which to interpret main gate loading for barrier and adjacent development pillars.	17.2	—
Ellalong longwall 1	Wold and Pala [1986]	IRAD	In seam	Satisfactory results so as to interpret main gate loading for chain pillar.	9.8	—
Kenmare longwall 1B ¹	Gordon [1998]	CSIRO HI	In roof	Satisfactory results from which to interpret main gate loading condition.	54.2	—
North Goonyella longwalls 3-4	Nemcik and Fabjanczyk [1997]	CSIRO HI	In roof	Only 2 of 4 cells functioned reliably such that a subjective assessment of the stress profiles was required.	31.5	1.2
South Bulli longwalls 504-505	Mincad Systems Pty. Ltd. [1997]	IRAD and hydraulic.	In seam	Satisfactory results from which to interpret main gate and tailgate loading.	8.8	1.47
Ulan longwalls A and B	Mills [1993]	CSIRO HI	In roof	Satisfactory results from which to interpret main gate and tailgate loading.	35.3	1.09
West Cliff longwall 1	Skybey [1984]	IRAD	In seam	3-heading with large/small pillar combination; subjective assessment of main gate stress profile was required.	4.9	—
West Cliff longwalls 12-13	Gale and Matthews [1992]	CSIRO HI	In roof	3-heading with large/small pillar combination, interpretation of main gate and tailgate loading.	0.9	1.52
West Wallsend longwall 12	Stewart [1996]	Hydraulic	In seam	Satisfactory results from which to interpret main gate loading condition.	5.2	
Wyee longwall 5	Seedsman and Gordon [1991]	Geokon	In seam	Satisfactory results from which to interpret main gate loading condition.	6.2-8.8	

¹SCT operations stress monitoring exercise with HI Cells located in roof above this project's hydraulic stress cell site.

INDUSTRY REVIEW

The aim of the industry review was to construct a historical database of gate road and chain pillar performance. During the course of the project, 19 longwall mines (a cross section from the 5 major Australian coalfields) were visited. Underground inspections were conducted at each that incorporated a subjective assessment of gate road performance while documenting the relevant details in relation to panel and pillar geometry, roof and floor geology, artificial support, and in situ stress regime. Brief summary reports were then forwarded to each mine to confirm the accuracy of the recorded data. Table 3 summarizes the Australian case histories.

The U.S. database included the Secondary Support Rating (SSUP), which is described as a rough measure of the volume of wood installed per unit length of the tailgate [Mark et al. 1994]. It should be noted that 59 of the 62 cases (i.e., 95%) within the U.S. database used standing secondary support (predominantly in the form of timber cribbing) along the tailgate. In the Australian database, less than 50% (9 out of 19) mines routinely installed standing secondary support along the tailgate. In the context of this study, standing secondary support refers to timber cribbing, the Tin Can system, Big Bags, etc., and does not include tendon support (cable bolts or Flexibolts) installed within the roof. Because of the variety of secondary supports used, no Australian SSUP was attempted. Instead, a yes/no outcome is provided in table 3.

An additional geotechnical parameter included within the Australian database, but not considered during the development of ALPS in the United States, is the presence of adverse horizontal stress conditions (HORST) (see table 3). Horizontal stress can damage roadways when they are first driven, and stress concentrations associated with longwall retreat can cause further roof deterioration. The following criteria were used to categorize the operations visited on a yes/no basis:

- $30^\circ < \alpha < 135^\circ$ (see figure 7); and
- The magnitude of the major horizontal stress (F_H) is >10 MPa.

STATISTICAL ANALYSES

The same statistical technique used with the U.S. ALPS database, that of discriminant analysis, was used with the Australian data. Discriminant analysis is a regression technique that classifies observations into two (or more) populations. In the case of the ALPS data, the classified populations are tailgates with satisfactory and unsatisfactory tailgate conditions.

An initial change that was made with the Australian data was to include "borderline" tailgates with the unsatisfactory cases. This modification is consistent with the Australian underground coal industry's desire to have in place strata management plans that design against both borderline and unsatisfactory gate road conditions. It also adds to the otherwise small pool of un-

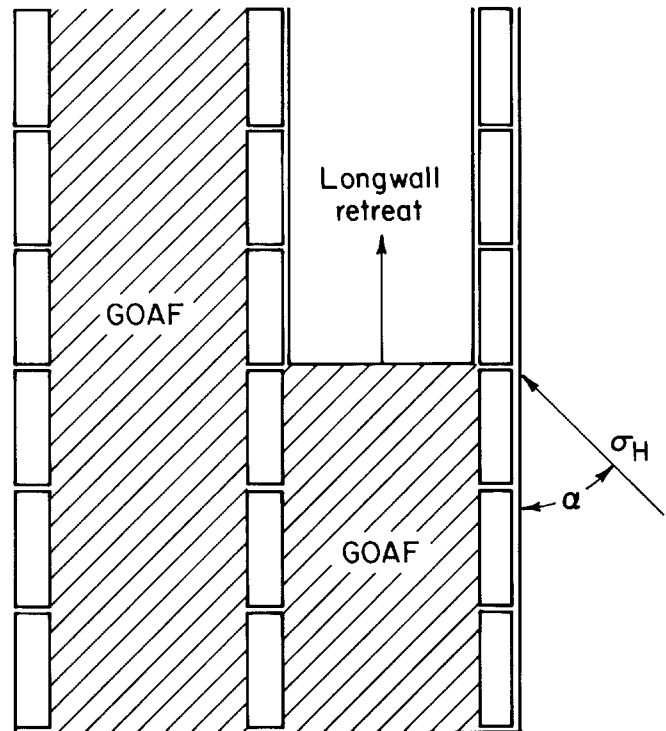


Figure 7.—The angle α used to determine the value of HORST.

Actual stress measurements were available from all except three mines in the database. The major horizontal stress is characteristically twice the vertical stress within Queensland and New South Wales coalfields. Therefore, at a depth of cover equal to 200 m, F_H is approximately 10 MPa.

It is recognized that geological structure can result in an adverse reorientation and/or magnification of the general in situ stress regime. However, there are insufficient data, within the context of this study, to include such an assessment within HORST.

satisfactory cases available for analysis.

In their analysis, Mark et al. [1994] were not able to quantify the effect of standing secondary support on tailgate conditions. However, because nearly every U.S. case used some standing support, SSUP is basically *intrinsic* to the design equation (see equation 1). Because less than 50% of Australian mines use secondary support, it seems reasonable to assume that tailgates that presently incorporate standing secondary support would become unsatisfactory if it were removed. A major modification was to include all collieries utilizing standing secondary support in the modified-unsatisfactory category of tailgate conditions.

Table 3.—Australian tailgate performance case history database

Mine	Location	Pillar width, m	Pillar length, m	Seam height, m	Depth, m	Panel width, m	CMRR	TG SF	PSUP	SSUP, Yes/No	HORST, Yes/No	Tailgate condition
Angus Place	Tailgate 21	40	95.5	3.0	340	256	35	0.84	0.84	Yes	No	S
Angus Place	Tailgate 18	40	94.5	3.0	280	206	35	1.11	0.84	Yes	No	B
Angus Place	Tailgate 22	40	95.5	3.0	360	256	35	0.76	0.84	Yes	Yes	U
Central (200)	Tailgate 202	25	94.9	2.5	165	200	55	1.33	0.27	No	No	S
Central (200)	Tailgate 203	25	94.9	2.5	190	206	55	1.05	0.27	No	No	S
Central (200)	Tailgate 204	30	94.9	2.5	210	206	55	1.26	0.27	No	No	S
Central (200)	Tailgate 205	35	94.9	2.5	225	206	55	1.50	0.27	No	No	S
Central (200)	Tailgate 206	45	94.9	2.5	240	206	55	2.14	0.27	No	Yes	S
Central (200)	Tailgate 207	45	94.9	2.5	265	206	55	1.87	0.27	No	Yes	S
Central (200)	Significant jointing		94.9	2.5			48	1.05	0.50	No	No	S
Central (300)	Tailgate 302	30	94.9	2.8	140	200	50	2.00	0.27	No	No	S
Central (300)	Tailgate 303	30	94.9	2.8	170	206	50	1.63	0.27	No	No	S
Central (300)	Tailgate 304	35	94.9	2.8	190	206	50	1.80	0.27	No	No	S
Central (300)	Tailgate 305	40	94.9	2.8	210	206	50	1.95	0.27	No	No	S
Central (300)	Tailgate 306	45	94.9	2.8	230	206	50	2.07	0.27	No	No	S
Central (300)	Tailgate 307 - 18 cut-through	45	94.9	2.8	285	206	31	1.45	0.50	No	No	U
Clarence	Tailgate 2	45	54.5	4.1	260	178	59	1.20	0.23	No	No	S
Clarence	Tailgate 3	43	54.5	4.1	260	200	59	1.10	0.23	No	No	S
Clarence	Tailgate 5	45	54.5	4.1	260	158	59	1.21	0.23	No	No	S
Clarence	Tailgate 6	45	39.5	4.1	260	200	59	1.22	0.23	No	No	S
Crinum	Tailgate 2	35	125.2	3.6	135	275	40	2.57	0.69	Yes	No	S
Dartbrook	Tailgate 2	35	94.8	3.9	250	200	51	0.86	0.42	No	No	S
Elouera	Tailgate 2 - 4 lower stress	45	12.5	3.3	350	155	40	1.02	0.85	Yes	No	S
Elouera	Tailgate 4 - 19.5 cut-through	45	125.0	3.3	350	155	40	1.00	0.85	Yes	Yes	B
Gordonstone	Tailgate 102	40	94.8	3.2	230	200	30	1.49	0.79	Yes	No	B
Gordonstone	Tailgate 202	40	94.8	3.2	230	255	35	1.49	0.79	Yes	No	S
Kenmare	Tailgate 2 - 13 cut-through	30	119.8	3.1	172	200	65	1.46	0.53	No	No	S
Kenmare	Tailgate 3 - stronger roof	25	119.8	3.1	160	200	65	1.17	0.28	No	No	S
Kenmare	Tailgate 3 - weaker roof	25	119.8	3.1	130	200	46	1.65	0.42	No	No	S
Newstan	Tailgate 10	31	97.0	3.3	180	130	39	1.39	0.66	Yes	Yes	B
North Goonyella	Tailgate 4	30	94.8	3.4	180	255	38	1.26	0.77	No	No	S
Oaky Creek	Tailgate 7 - normal roof	30	94.8	3.2	180	200	57	1.32	0.40	No	No	S
Oaky Creek	Tailgate 7 - weaker roof	30	94.8	3.2		200	48	1.32	0.57	No	No	S
South Bulli (200)	Tailgate 203	24	84.0	2.7	465	138	57	0.23	0.44	Yes	Yes	U
South Bulli (200)	Tailgate 204	31	94.0	2.7	470	183	57	0.36	0.44	Yes	Yes	U
South Bulli (200)	Tailgates 205-208, 210	40	96.0	2.7	460	183	57	0.66	0.44	Yes	Yes	B
South Bulli (200)	Tailgates 209, 211-212	38	97.0	2.7	460	183	57	0.59	0.44	Yes	Yes	B
South Bulli (300)	Tailgate 303	40	96.0	2.7	450	138	65	0.68	0.44	Yes	No	S
South Bulli (300)	Tailgates 304-305	55	74.0	2.7	450	183	65	1.15	0.44	Yes	No	S

See explanatory notes at end of table.

Table 3.—Australian tailgate performance case history database—Continued

Mine	Location	Pillar width, m	Pillar length, m	Seam height, m	Depth, m	Panel width, m	CMRR	TG SF	PSUP	SSUP, Yes/No	HORST, Yes/No	Tailgate condition
South Bulli (300)	Tailgates 308-309	38	97.0	2.7	410	185	65	0.68	0.44	Yes	No	S
Southern (600)	Tailgate 606	30	94.8	2.8	170	200	60	1.62	0.26	No	No	S
Southern (600)	Tailgates 607-608	35	94.8	2.8	190	200	60	1.79	0.26	No	No	S
Southern (700)	Tailgate 702	30	94.8	2.8	160	250	60	1.79	0.26	No	No	S
Springvale	Tailgate 402	45	95.2	2.7	325	250	35	1.22	0.63	Yes	Yes	B
Tower	Tailgate 14	45	66.0	3.2	500	203	40	0.59	1.26	No	No	S
Ulan	Tailgate 11	30	94.8	3.1	145	255	50	1.65	0.28	No	No	S
West Cliff	Tailgate 22	42	97.2	2.5	480	200	48	0.69	0.49	Yes	No	S
West Wallsend	Tailgate 13 - 4.5 cut-through	35	97.1	2.9	240	145	40	1.24	0.75	Yes	Yes	U
West Wallsend	Tailgate 13 - 7 cut-through	35	97.1	2.9	255	233	40	1.11	0.75	No	Yes	S
West Wallsend	Tailgates 14-16	32	110.1	2.9	250	145	40	0.99	0.75	Yes	Yes	U
West Wallsend	Tailgate 17 - 6 cut-through	35	110.1	3.2	250	145	40	1.08	0.75	Yes	Yes	B
Wyee	Tailgate 13	35	102.0	2.8	220	163	45	1.43	0.52	No	Yes	B
Mean		31.2	94.5	3.0	266	200	49.52	1.27	0.49			
Standard deviation		7.2	16.9	0.4	106	33	10.04	0.47	0.24			

S Satisfactory. B Borderline. U Unsatisfactory.

Two cases posed additional complications. Tower Colliery does not incorporate standing secondary support, yet its PSUP (1.26) is 3.2 standard deviations above the Australian mean. Therefore, Tower Colliery was also included within the modified-unsatisfactory tailgate category. Crinum uses standing secondary support, but it is a relatively new operation, and it seems that there has been an understandable, but nonetheless highly conservative approach to its geotechnical design. To include Crinum within the modified-unsatisfactory group would have been overly conservative, so it was excluded from the database entirely.

Therefore, the final database includes 50 case histories with 29 modified satisfactory and 21 modified-unsatisfactory cases. Numerous analyses were conducted to determine the best design equation. Ultimately, the most successful design equation relates the required TG SF to the CMRR, as shown in figure 8:

$$TG\ SF \ ' \ 2.67 \ \& \ 0.029 \ CMRR \ \quad (3)$$

Equation 3 correctly predicted the outcome of all except seven case histories, for a success rate of 86%. Comparing equation 3 to the U.S. design equation (equation 1), it may be seen that the TG SF is generally more conservative than the ALPS SF for weaker roof, but the TG SF decreases more rapidly than the ALPS SF as the roof becomes stronger.

Another strong relationship that was evident in the case histories was between the primary support and the roof quality. Figure 9 plots the PSUP against the CMRR, and the best-fit regression is of the following form:

$$PSUP \ ' \ 1.35 \ \& \ 0.0175 \ CMRR \ \quad (4a)$$

It seems that Australian mine operators have intrinsically adapted their primary support patterns to the roof conditions and operational requirements. Mark et al. [1994] reached a similar conclusion for the United States.

Upper- and lower-boundary equations (4b and 4c, respectively) relating CMRR to PSUP have also been proposed and are illustrated in figure 8:

$$PSUP_U \ ' \ 1.45 \ \& \ 0.0175 \ CMRR \ \quad (4b)$$

$$PSUP_L \ ' \ 1.24 \ \& \ 0.0175 \ CMRR \ \quad (4c)$$

Equation 4c may be applicable, for example, when the mining layout is not subject to adverse horizontal stress conditions and/or standing secondary support is planned as part of the colliery's strata management plan.

Mark et al. [1994] also found a strong correlation between the CMRR and the entry width. No such correlation was seen here.

It is interesting to note some similarities and differences between the U.S. and Australian databases. For example, overall roof quality seems to be reasonably similar in the two countries. The mean CMRR in the United States is 53.7 with a standard deviation (SD) of 13.9; this compares with an Australian mean of 49.5 and SD ' 10.0. However, the mean Australian PSUP is 0.49 (SD ' 0.23), which is approximately twice that of the U.S. database.

Studies by Mark [1998] and Mark et al. [1998a] suggest that the horizontal stress levels in the two countries are comparable. It seems that philosophical differences are more likely responsible for the different levels of primary support. Most

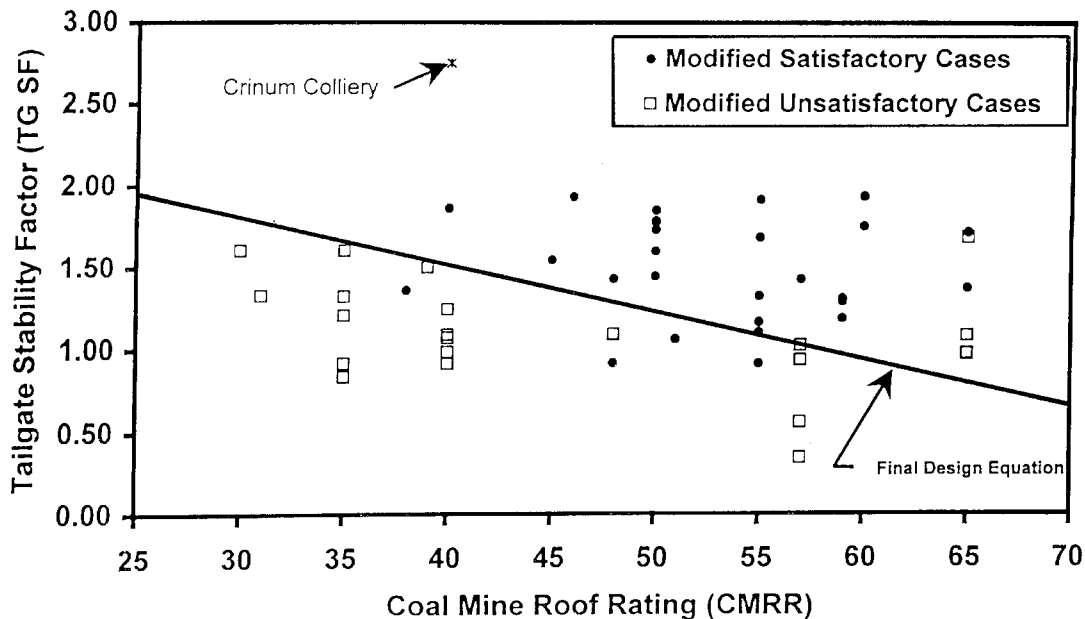


Figure 8.—The final design equation relating the CMRR to the TG SF.

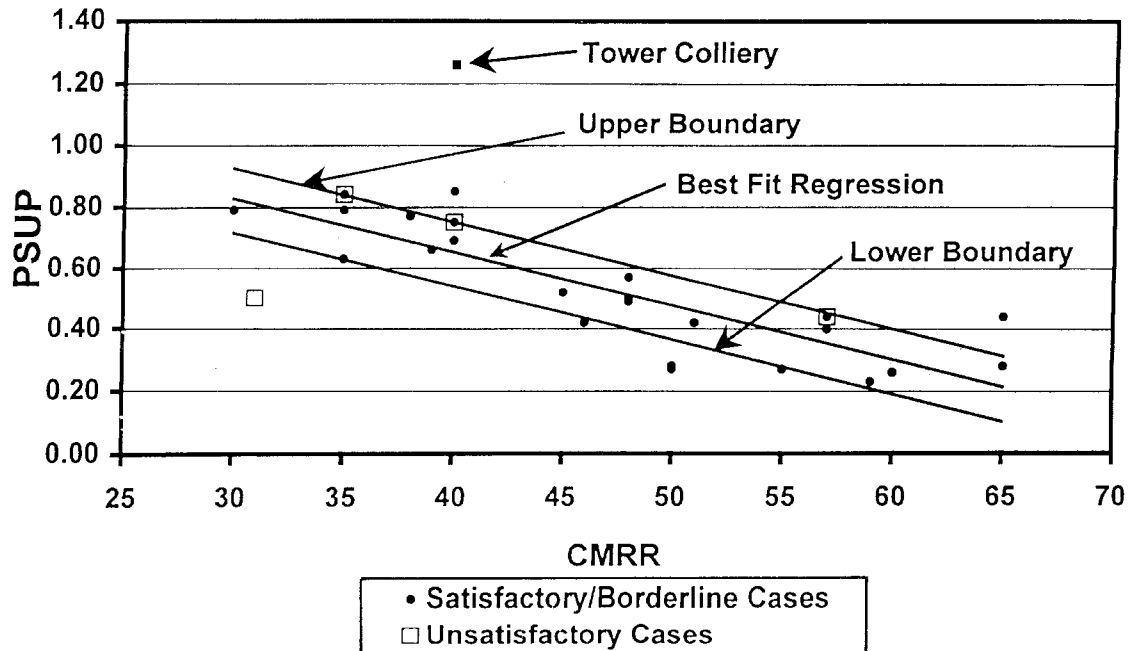


Figure 9.—Design equations for primary support based on the CMRR.

Australian coal mines have an unwritten (sometimes written) policy of no roof falls; U.S. multientry mining systems seem more tolerant of roof falls. Also, most Australian coal mines have an antipathy toward standing secondary support for reasons associated with a two-entry gate road system. It seems that the main way in which Australian operations prevent poor tailgate conditions is to install substantial primary support on development. Therefore, in Australia one would expect a strong relationship between the level of primary support and a reliable roof rating system. This is exactly what transpires, which adds to the credibility of the CMRR.

Additional statistical analyses tested whether the accuracy of ALPS could be improved by replacing the original Bieniawski formula with another pillar strength formula. Two formulas were trialed—the Mark-Bieniawski formula [Mark and Chase 1997] and Salamon's squat pillar formula [Madden 1988]. The Mark-Bieniawski formula had virtually no impact on the classification success rate. However, incorporating the squat pillar formula resulted in a significant decrease in the classification success rate. The conclusion was to remain with the original Bieniawski formula used in the "classic" ALPS.

ANALYSIS OF TAILGATE SERVICEABILITY (ALTS)

The chain pillar design methodology proposed by the project is referred to as "Analysis of Longwall Tailgate Serviceability" (ALTS). The design methodology recognizes the impact of ground support on tailgate serviceability and incorporates guidelines in relation to the installed level of primary support and the influence of standing secondary support on the design process.

A design flowchart (figure 10), Microsoft® Excel Workbook, and user manual have been developed. The spreadsheet workbook (*ALTS Protected.xls*) was formulated to facilitate the computational components of the design methodology.

The ALTS design process should only be employed in designing chain pillars that are subject to second-pass longwall extraction. If the chain pillars under consideration are not to be subject to second-pass longwall extraction, then an alternative pillar design method should be employed based on pillar stability and outer gate road serviceability requirements. The

monitored chain pillar loading behavior (conducted as a part of the project) will assist in estimating the main gate load for design purposes.

The recommended chain pillar width (rib to rib) is contingent upon an appropriate level of primary support. That level of primary support (i.e., $PSUP_L$ to $PSUP_U$) is dependent on (1) the orientation of longwall retreat in relation to the magnitude and direction of the major horizontal stress and (2) the use of standing secondary support along the length of the gate road.

The database is able to identify situations where it is likely that standing secondary support may be required. However, there are insufficient data at this stage to make numerical recommendations for the SSUP similar to those made for the TG SF and PSUP. Appropriately qualified personnel should assess the type, level, and timing of SSUP installation.

CONCLUSIONS

The following main goals of the project were achieved:

- To establish a chain pillar design methodology that has widespread application to Australian longwall operations; and
- To quantify the probable variance in the chain pillar loading environment between collieries and mining localities and to incorporate this variance within the design methodology.

In addition, the study has been able to propose definitive guidelines with regard to the installed level of primary support and to conduct a subjective analysis regarding the impact of standing secondary support on the design process. This provides the Australian coal industry with a truly integrated design methodology with regard to tailgate serviceability that has been able to address the main factors controlled by the mine operator.

The initial benefit from this project is that mine managers and strata control engineers will be able to identify where chain pillars can be reduced in size and where increases may be necessary. They can make these decisions with the confidence that a credible Australian database is the foundation for the design methodology.

This project has identified that there is an opportunity for some mines that do not currently incorporate the routine installation of secondary support along their tailgate to make significant reductions in chain pillar width. It is an operational decision whether a reduction in pillar width is more or less beneficial to production output and costs than the introduction of secondary support along the length of the tailgate. This project simply highlighted that the opportunity exists.

The chain pillar monitoring exercises conducted at collieries under deep cover or with strong roof have found that the abutment load may be overestimated by using a generic abutment angle of $\delta = 21^\circ$. However, the aggressive tailgate loading behavior monitored at West Wallsend Colliery (see figure 5) provided a warning, which emphasized the need to use great caution before making any sweeping changes to a proven chain pillar design tool. Although the way in which the load manifested itself at West Wallsend was significantly different from that proposed by ALPS, the resultant tailgate load was quite similar.

REFERENCES

- Clough AJ [1989]. Monitoring of chain pillar behavior at Angus Place Colliery. Strata Control Technology Pty. Ltd. report No. SCT9005 to Newcom Collieries Pty. Ltd, November.
- Colwell MG [1998]. Chain pillar design - calibration of ALPS. Australian Coal Association Research Program, final report—ACARP project C6036.
- Frith RC, Creech M [1997]. Face width optimization in both longwall and shortwall caving environments. Australian Coal Association Research Program, final report—ACARP project C5015.
- Frith RC, Thomas RG [1995]. Roadway roof stability and its attainment through pretensioned bolting. Australian Coal Association Research Program, ACARP project report 3032.
- Gale WJ, Matthews SM [1992]. Stress control methods for optimized development and extraction methods. National Energy Research, Development and Demonstration Program, final report C1301.
- Gordon N [1998]. Geological and geotechnical aspects of the development and extraction of Aries Seam Longwalls 1A and 1B, Kenmare Colliery. Internal report for South Blackwater Coal Ltd.
- Madden BJ [1988]. Squat pillar design. *Coal Int Jan*:6-9.
- Mark C [1990]. Pillar design methods for longwall mining. Pittsburgh, PA: U.S. Department of the Interior, Bureau of Mines, IC 9247.
- Mark C [1992]. Analysis of longwall pillar stability (ALPS): an update. In: Proceedings of the Workshop on Coal Pillar Mechanics and Design. Pittsburgh, PA: U.S. Department of the Interior, Bureau of Mines, IC 9315, pp. 238-249.
- Mark C [1998]. Comparison of ground conditions and ground control practices in the United States and Australia. In: Peng SS, ed. Proceedings of the 17th International Conference on Ground Control in Mining. Morgantown, WV: University of West Virginia, pp. 63-71.
- Mark C, Barton TM [1996]. The uniaxial compressive strength of coal: should it be used to design pillars? In: Ozdemir L, Hanna K, Haramy KY, Peng S, eds. Proceedings of the 15th International Conference on Ground Control in Mining. Golden, CO: Colorado School of Mines, pp. 61-78.
- Mark C, Bieniawski ZT [1986]. An empirical method for the design of chain pillars in longwall mining. In: Proceedings of the 27th U.S. Symposium on Rock Mechanics. New York, NY: American Institute of Mining, Metallurgical, and Petroleum Engineers, pp. 415-422.
- Mark C, Chase FE [1997]. Analysis of retreat mining pillar stability (ARMPS). In: Proceedings - New Technology for Ground Control in Retreat Mining. Pittsburgh, PA: U.S. Department of Health and Human Services, Public Health Service, Centers for Disease Control and Prevention, National Institute for Occupational Safety and Health, DHHS (NIOSH) Publication No. 97-122, IC 9446, pp. 17-34.
- Mark C, Molinda GM [1996]. Rating coal mine roof strength from exploratory drill core. In: Ozdemir L, Hanna K, Haramy KY, Peng S, eds. Proceedings of the 15th International Conference on Ground Control in Mining. Golden, CO: Colorado School of Mines, pp. 415-428.
- Mark C, Chase FE, Molinda GM [1994]. Design of longwall gate entry systems using roof classification. In: New Technology for Longwall Ground Control - Proceedings: U.S. Bureau of Mines Technology Transfer Seminar. Pittsburgh, PA: U.S. Department of the Interior, Bureau of Mines, SP 01-94, pp. 5-17.
- Mark C, Mucho TP, Dolinar D [1998a]. Horizontal stress and longwall headgate ground control. *Min Eng* 50(1):61-68.
- Mark C, Su D, Heasley KA [1998b]. Recent developments in coal pillar design in the United States. In: Aziz NI, Indraratna B, eds. Proceedings of the International Conference on Geomechanics/Ground Control in Mining and Underground Construction. Wollongong, New South Wales, Australia: University of Wollongong, Vol. 2, pp. 309-324.
- Mills KW [1993]. AMIRA pillar strength measurements. Strata Control Technology Pty. Ltd. report No. ULA0290B to Ulan Coal Mines, October.
- Molinda GM, Mark C [1994]. Coal mine roof rating (CMRR): a practical rock mass classification for coal mines. Pittsburgh, PA: U.S. Department of the
- Mincad Systems Pty. Ltd. [1997]. AMIRA Project P396 - Hydraulic stressmeter, final report.

Interior, Bureau of Mines, IC 9387.

Nemcik J, Fabjanczyk M [1997]. Virgin stress and stress change measurements in maingate 3, North Goonyella underground mine. Strata Control Technology Pty. Ltd. report No. NGY1069 to White Mining Ltd., January.

Salamon MDG, Galvin J, Hocking G, Anderson I [1996]. Coal pillar strength from back-calculation. Part of a New South Wales Joint Coal Board Research Project - Strata Control for Coal Mine Design. Sydney, Australia: University of New South Wales, School of Mines.

Seedsman RW, Gordon N [1991]. Methods to optimise mining operations affected by weak claystone materials. NERDCC end-of-grant report - project No. 1336.

Skybey G [1984]. Evaluation of the stability of longwall chain pillars at West Cliff Colliery. Australian Coal Association Research Program, published report 84-19.

Stewart A [1996]. Chain pillar monitoring - West Wallsend Colliery, LW 12 cut-through 11. Coffey Partners International Pty. Ltd. report No. Z267/4-AB to Oceanic Coal Australia Ltd., November.

Wardle LJ, Klenowski G [1988]. Rational longwall layout design based on numerical stress analysis. In: Proceedings of AusIMM - 21st Century Higher Production Coal Mining Systems—Their Implications, pp. 115-121.

Whittaker B, Frith RC [1987]. Aspects of chain pillar design in relation to longwall mining. Proceedings of the Sixth International Conference on Ground Control in Mining. Morgantown, WV: West Virginia University, pp. 172-182.

Wilson AH [1981]. Stress and stability in coal ribsides and pillars. In: Peng SS, ed. Proceedings of the First International Conference on Ground Control in Mining. Morgantown, WV: West Virginia University, pp. 1-12.

Wold MB, Pala J [1986]. Three-dimensional stress changes in pillars during longwall retreat at Ellalong Colliery. Commonwealth Scientific and Industrial Research Organisation (CSIRO) Australia, Division of Geomechanics, coal mining report No. 65.

EXPERIENCE OF FIELD MEASUREMENT AND COMPUTER SIMULATION METHODS FOR PILLAR DESIGN

By Winton J. Gale, Ph.D.¹

ABSTRACT

Coal pillar design has been based on generalized formulas of the strength of the coal in a pillar and experience in localized situations. Stress measurements above and in coal pillars indicate that the actual strength and deformation of pillars vary much more than predicted by formulas. This variation is due to failure of strata surrounding coal. The pillar strength and deformation of the adjacent roadways is a function of failure in the coal and the strata about the coal. When the pillar is viewed as a system in which failure also occurs in the strata rather than the coal only, the wide range of pillar strength characteristics found in the United Kingdom, United States, Republic of South Africa, Australia, People's Republic of China, Japan, and other countries are simply variations due to different strata-coal combinations, not different coal strengths.

This paper presents the measured range of pillar strength characteristics and explains the reasons. Methods to design pillar layouts with regard to the potential strength variations due to the strata strength characteristics surrounding the seam are also presented.

¹Managing director, Strata Control Technology, Wollongong East, New South Wales, Australia.

INTRODUCTION

The strength characteristics of coal pillars have been studied by many, and the subject is well discussed in the literature (Salamon and Munro [1967]; Wilson [1972]; Hustrulid [1976]; Mark and Iannacchione [1992]; Gale [1996]). In general, a range of strength relationships has been derived from four main sources:

- (1) Laboratory strength measurements on different-sized coal block specimens;
- (2) Empirical relationships from observations of failed and unfailed pillars;
- (3) A theoretical fit of statistical data and observations; and
- (4) Theoretical extrapolation of the vertical stress buildup from the ribside toward the pillar center to define the load capacity of a pillar.

These relationships provide a relatively wide range of potential strengths for the same pillar geometry. In practice, it has been found that various formulas are favored (or modified) by users, depending on past experience in their application to certain mining districts or countries.

In general, the application of empirically and statistically based formulas has been restricted to the mining method and geological environment for which they were developed, and they often relate to specific pillar geometries. In general, these

methods were developed for shallow, extensive bord-and-pillar operations for which the pillar was designed to hold the weight of overburden. The wider application of longwall mining methods and increasing depth has required a greater understanding of factors influencing pillar strength and their role in the control of ground deformation about the mining operations. The development of stress measurement and detailed rock deformation recording tools over the last 10-15 years has allowed much more quantification of actual pillar stresses and deformations. Few data were available when many of the pillar strength relationships were originally defined. Similarly, the development of computer simulation methods has allowed detailed back-analysis of the mechanics of strata-coal interaction in formed-up pillars.

The author and his colleagues have conducted numerous monitoring and stress measurement programs to assess roadway stability and pillar design requirements in Australia, the United Kingdom, Japan, the United States, Indonesia, and Mexico. The results of these investigations and others reported in the literature have demonstrated that the mechanical response of the coal and surrounding strata defines the pillar strength, which can vary widely depending on geology and stress environment. The application of a pillar strength formula to assess the strength of a system that is controlled by the interaction of geology, stress, and associated rock failure is commonly an oversimplification.

MECHANICS OF THE PILLAR-COAL SYSTEM

The strength of a pillar is determined by the magnitude of vertical stress that can be sustained within the strata-coal sequence forming and bounding it. The vertical stress developed through this sequence can be limited by failure of one or more of the units that comprise the pillar system. This failure may occur in the coal, roof, or floor strata forming the system, but usually involves the coal in some manner. The failure modes include shear fracture of intact material, lateral shear along bedding or tectonic structures, and buckling of cleat-bounded ribsides.

In pillar systems with strong roof and floor, the pillar coal is the limiting factor. In coal seams surrounded by weak beds, a complex interaction of strata and coal failure will occur; this will determine the pillar strength. The strength achievable in various elements largely depends on the confining stresses developed, as illustrated in figure 1. This indicates that as confinement is developed in a pillar, the axial strength of the material increases significantly, thereby increasing the actual strength of the pillar well above its unconfined value.

The strength of the coal is enhanced as confining stress increases toward the pillar center. This increased strength is often related to the width-to-height (w/h) ratio; the larger the ratio, the greater the confinement generated within the pillar. Hence, squat pillars (high w/h) have greater strength potential than slender ones (low w/h).

The basic concepts related to confinement within coal pillars were developed by Wilson [1972]; with the growing availability of measurement data, these general mechanics are widely accepted. However, confining stress can be reduced by roadway deformations such as floor heave, bedding plane slip, and other failure mechanisms. These mechanisms are described below.

ROADWAY DEVELOPMENT PHASE

Prior to mining, the rock and coal units will have in situ horizontal and vertical stresses that form a balanced initial stress state in the ground. As an opening (roadway) is created in a coal seam, there is a natural tendency for the coal and rock to move laterally and vertically into the roadway. In this situation, the horizontal stress acting across the pillar will form the confining stress within that pillar. If this lateral displacement is resisted by sufficient friction, cohesion, and shear stiffness of the immediate roof and floor layers, then most of the lateral confining stress is maintained within the pillar. Consequently, the depth of "failure" (yield) into the pillar ribside is small. If the coal and rock layers are free to move into the roadways by slippage along bedding planes or shear deformation of soft bands, this confining stress will be reduced.

Hence, the depth of failure into the pillar ribside may be significantly greater.

The geometry of failure in the system and the residual strength properties of the failure planes will therefore determine the nature of confining stress adjacent to the ribsides and extending across the pillars. This mechanism determines the depth of failure into the pillar and the extent of ribside displacement during roadway drivage.

PILLAR LOADING BY ABUTMENT STRESSES

Roadways are subjected to an additional phase of loading during longwall panel extraction, as front and then side abutment pressures are added to the previous (and generally much smaller) stress changes induced by roadway excavation. These abutment stresses typically considered are predominantly vertical in orientation, but can generate additional horizontal (confining) stresses (by the Poisson's ratio effect) if there is sufficient lateral restraint from the surrounding roof and floor. Conversely, if the ground is free to move into the roadway, this increased horizontal stress is not well developed and increased rib squeeze is manifest instead.

This concept is presented in figure 2; with strong cohesive coal-rock interfaces the confining stress in the pillar increases rapidly inward from the ribsides, allowing high vertical stresses to be sustained by the pillar. The opposite case of low shear strength coal-rock contact surfaces is presented in figure 3. In this situation, confinement cannot be maintained sufficiently; hence, the allowable vertical stress would be significantly less than that in figure 2. The diagram shows that the pillar has failed because of its inability to sustain the imposed vertical abutment stresses. In addition, lateral movement has caused floor heave and severe immediate roof shearing.

The implications of this for the strength of an isolated pillar are presented in figure 4, where the load carried by the pillar is the mean of the vertical stress across it. If this mean stress is equal to the average "applied load" to be carried by the pillar, then the pillar is stable (figure 4A). If the applied load is greater, then the pillar is said to fail (figure 4B) and the deficit stress must be redistributed onto nearby pillars.

Conceptually, pillar strength behavior should fall between the two end members of:

- (1) Lateral slip occurring totally unresisted, so that pillar strength is limited to the unconfined value of the coal; and
- (2) Lateral slip being resisted by system cohesion and stiffness, such that pillar strength is significantly above its unconfined value due to confinement.

A range of potential pillar strengths associated with these two end members relative to the w/h ratio is presented after Gale [1996] in figure 5. It is assumed that the rock mass strength of the coal is 6.5 MPa and that the coal is significantly involved in the failure process. This range of pillar strengths is representative of most rock failure combinations, except in rare cases where small stiff pillars may punch into soft clay-rich

strata at loading levels below the field uniaxial compressive strength of the coal. In the punching situations, pillar strength may be lower than that depicted, but the variation would generally be confined to pillars having small w/h ratios.

A comparison of these "end member" situations with a range of pillar strengths determined from actual measurement programs conducted in Australia and the United Kingdom by Strata Control Technology and from the United States [Mark

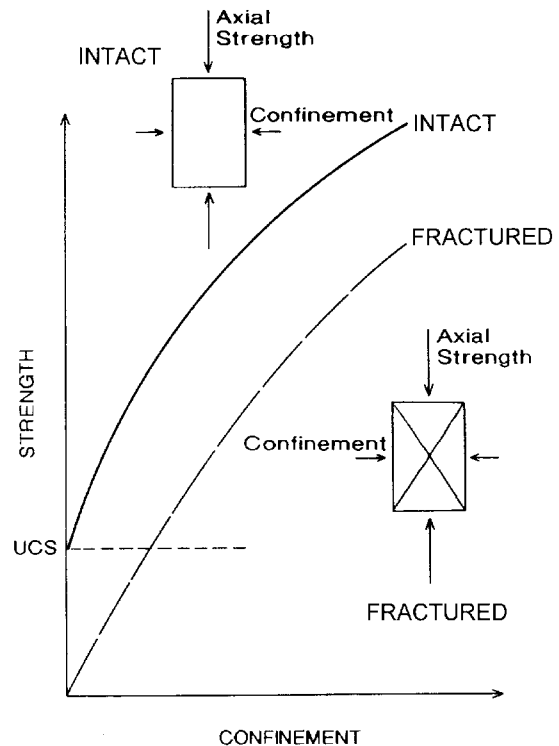


Figure 1.—Effect of confining stress on compressive strengths of intact and fractured rocks.

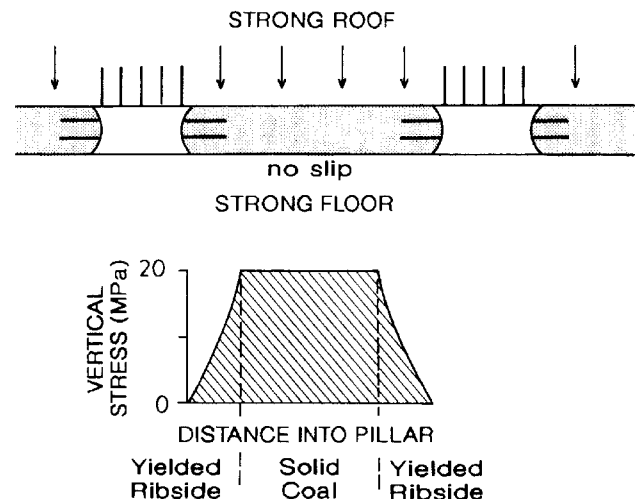


Figure 2.—Rapid buildup of vertical stress into the pillar where high confining stresses are maintained.

et al. 1988] is presented in figure 6. The comparison indicates that a wide range of pillar strengths have been measured for the same geometry (in terms of w/h) and that the data appear to span the full interval between the end members. However, two groupings can be discerned and are shaded in figure 7:

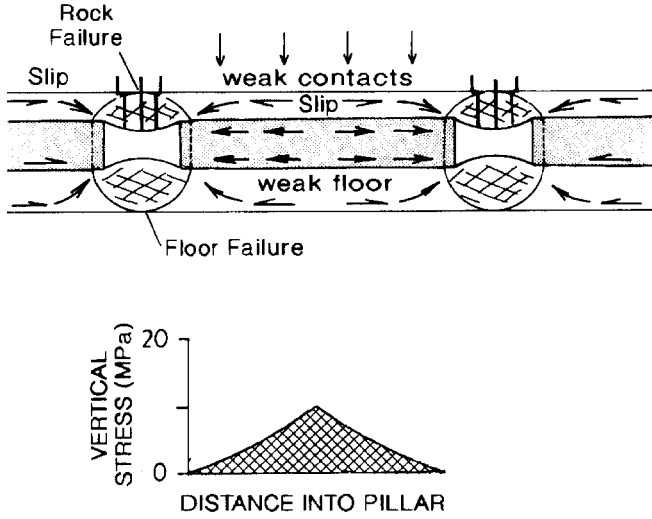


Figure 3.—Slow buildup of vertical stress in the pillar where slip occurs and confinement is reduced.

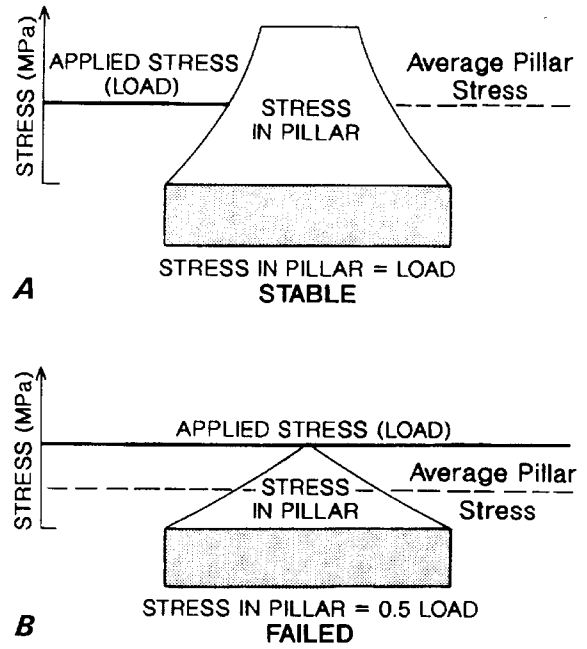


Figure 4.—Pillar strength cases for strong and weak geologies. A, strong system; B, weak system.

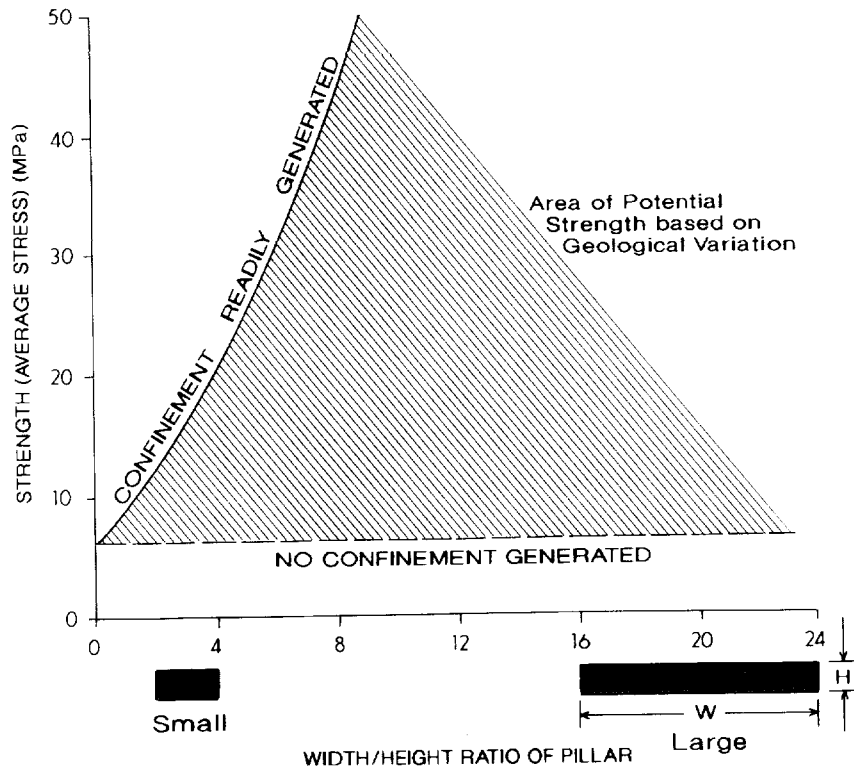


Figure 5.—Range of potential pillar strengths relative to w/h based on confinement variation (after Gale [1996]).

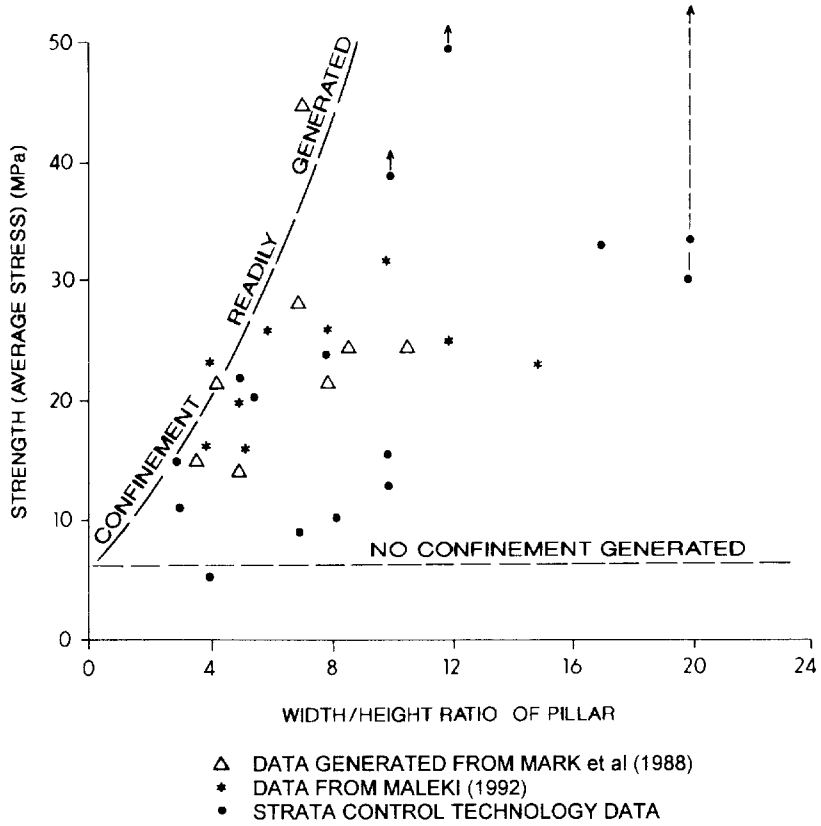


Figure 6.—Pillar strength information relative to changes (after Gale [1996]).

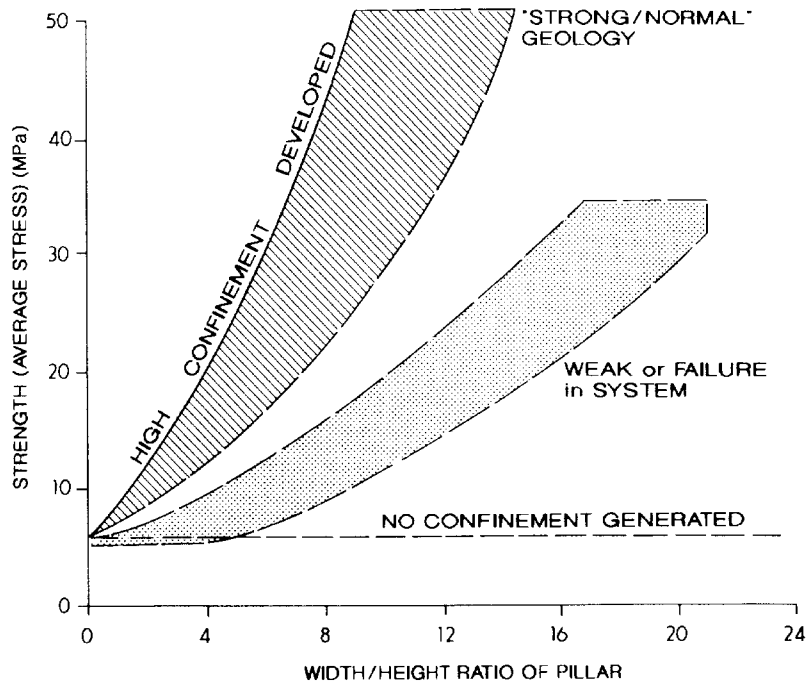


Figure 7.—Generalized groupings of strong/normal and weak geology (after Gale [1996]).

(1) The "strong/normal" geologies, where pillar strength appears to be close to the upper bound.

(2) The structured or weak geologies, where the strength is closer to the lower bound and it is apparent that the strength of the system is significantly limited.

It should be noted that these two groupings are arbitrary and are possibly due to limited data. With more data points, the grouping may become less obvious.

EFFECT OF GEOLOGY

It is clear that a wide range of pillar strengths is possible and that these are not only related to coal strength and w/h ratio. Geological factors have a major impact on the strength achievable under the various pillar geometries.

EFFECT OF GEOLOGY ON PILLAR STRENGTH

The effect of various strata types in the roof-coal-floor pillar systems has been investigated further by computational

methods. Computer models of four pillar systems were loaded to determine their strength characteristics (figure 8). These are—

- Massive sandstone-coal-massive sandstone
- Laminite-coal-sandstone
- Weak siltstone-coal-weak siltstone
- Laminite-clayband-coal-clayband-laminite

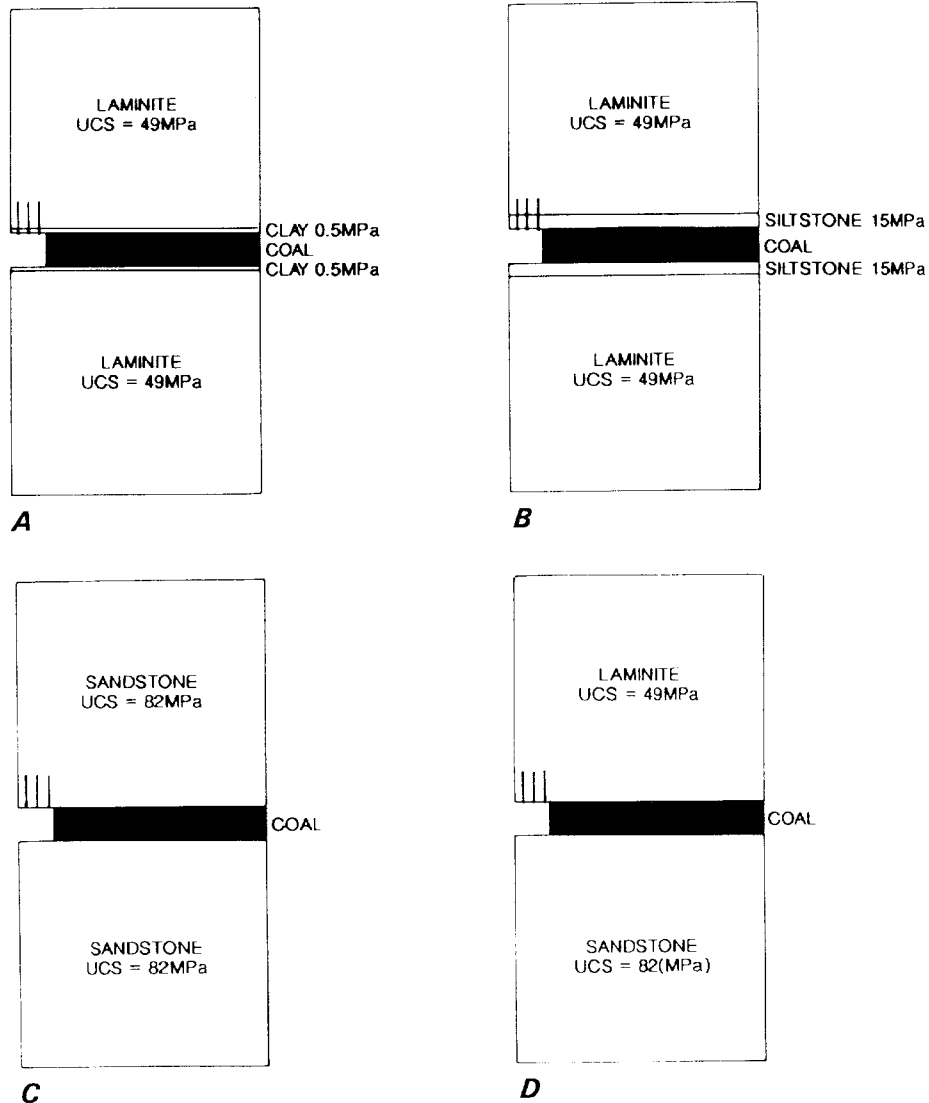


Figure 8.—Geological sections modeled to assess load deformation characteristics. A, coal-clay-laminite; B, coal-siltstone-laminite; C, coal-sandstone; D, coal-laminite-sandstone.

The results of the pillar strength characteristics relative to w/h are presented in figure 9. The results closely relate to the field measurement data and confirm that the strata types surrounding the coal have a major impact on strength and also provide insight into the geological factors affecting strength. The results indicate that—

(1) Strong immediate roof and floor layers and good coal-to-rock contacts provide a general relationship similar to the upper bound pillar strength in figure 5.

(2) Weak, clay-rich, and sheared contacts adjacent to the mining section reduce pillar strength to the lower bound areas.

(3) Soft strata in the immediate roof and floor, which fail under the mining-induced stresses, will weaken pillars to the lower bound areas.

(4) Tectonic deformation of coal in disturbed geological environments will reduce pillar strength, although the extent depends on geometry and strength of the discontinuities.

Obviously, combinations of these various factors will have a compounding effect. For example, structurally disturbed, weak, and wet roof strata may greatly reduce pillar confinement and, consequently, pillar-bearing capacity.

EFFECT OF GEOLOGY ON POSTPEAK PILLAR STRENGTH

The postpeak pillar strength characteristics for some of the pillars modeled are presented in figure 10. The pillar strength is presented as a stress/strain plot for various width/height pillars. The results presented in figure 10A show that in strong sandstone geology, high strengths are achievable in small pillars (w/h \leq 5) and the pillar maintains a high load-carrying capability. In the example modeled, "short-term" load losses were noted to occur in association with sudden rib failure. These instances are present in figure 10A as "rib bumps." In sections of laminite roof, these pillars may lose strength if the laminite fails at a very high load above the pillar. For pillars with a w/h less than 4/5, a loss in strength is expected at a high load due to failure of the coal.

In pillar systems with weak strata surrounding the coal, the pillars typically exhibit a strength loss after peak load is achieved. Large width/height pillars are required to develop a high load-carrying capacity after failure in the weak pillar systems modeled. Two examples are presented in figure 10B, which shows the postpeak strength characteristics of pillars with weak mudstone or clay surrounding the coal. In these

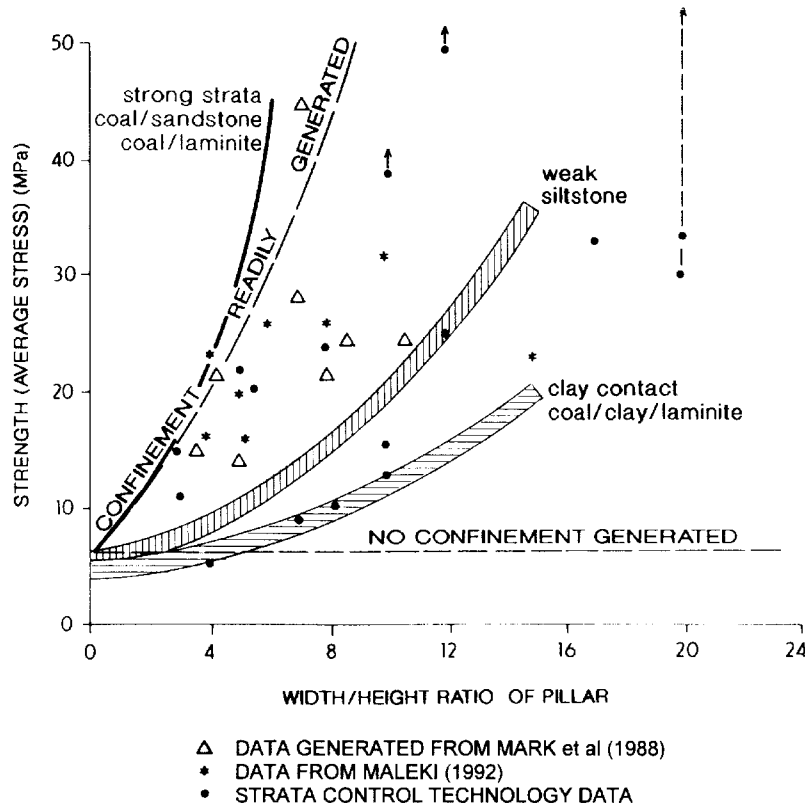


Figure 9.—Strength and w/h for models.

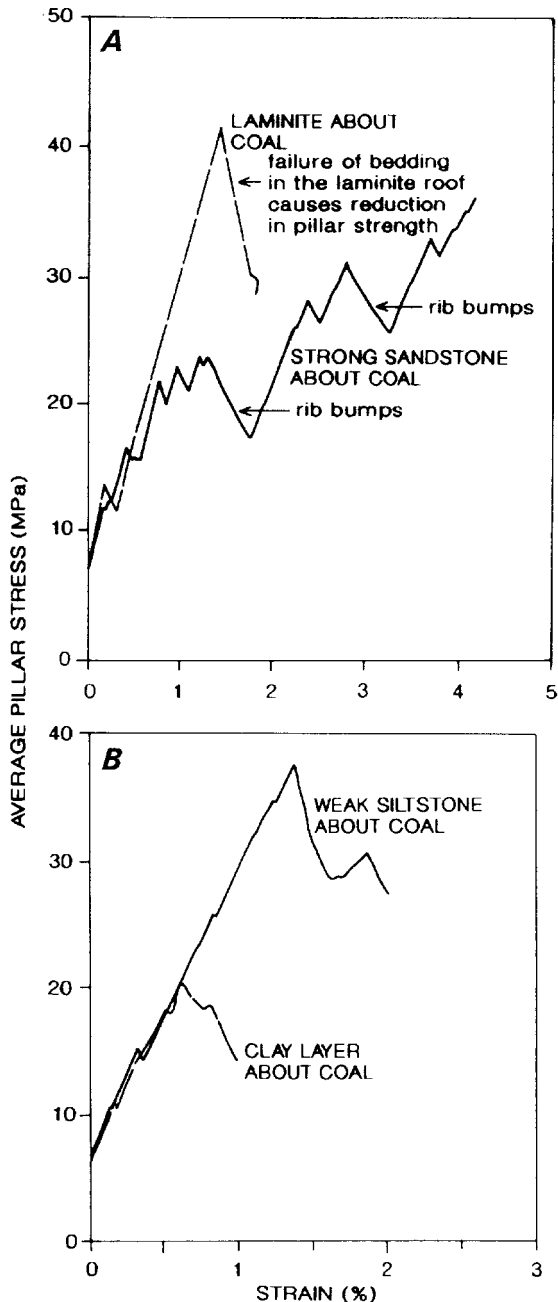


Figure 10.—Postpeak strength of models. A, $w/h = 5$; B, $w/h = 15$.

examples, the strength loss is greater in the situation of weak clay surrounding the coal.

The implications of this are significant for the design of barrier and chain pillars where high loads are anticipated. If excessive loads are placed on development pillars in this environment, pillar creep phenomena are possible due to the load shedding of failed pillars sequentially overloading adjacent pillars. The effect of load shedding in chain pillars when isolated in the goaf is to redistribute load onto the tailgate area and to potentially display increased subsidence over the pillar

area. The typical result is to have major tailgate deformation, requiring significant secondary support to maintain access and ventilation.

AN APPROACH TO PILLAR DESIGN

Field studies suggest that a range of strengths is possible extending within upper and lower bounds. If we make use of these relationships as "first-pass estimates" to be reviewed by more detailed analysis later, then a number of options are available. In known or suspected weak geologies, the initial design may utilize the lower bound curve of the weak geology band in figure 7. In good or normal geologies, the Bieniawski or squat pillar formulas may be suitable for initial estimates. Two obvious problems with this approach are:

- (1) Estimates of pillar size can vary greatly, depending on the geological environment assumed; and
- (2) The pillar size versus strength data set used (figure 6) is limited.

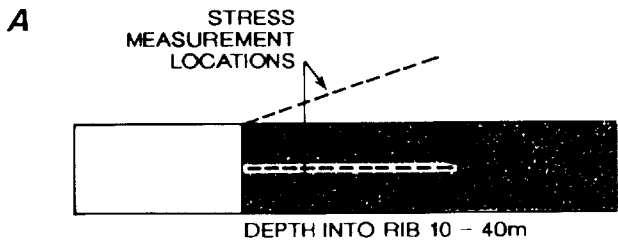
This is why such formulas or relationships are considered as first-pass estimates only, to be significantly improved later by more rigorous site-specific design studies utilizing field measurements and computer simulation.

Design based on measurement requires that the vertical stress distribution within pillars be determined and the potential strength for various sized pillars be calculated. It is most useful to measure the vertical stress rise into the pillar under a high loading condition or for the expected "working loads." The stress measurement profiles are used to determine the potential load distributions in pillars of varying dimension and hence to develop a pillar strength relationship suitable for that geological site. An example of stress measurements over a pillar is presented in figure 11; however, the method is limited to determining the potential stress distribution in different pillar widths under the measured loading condition.

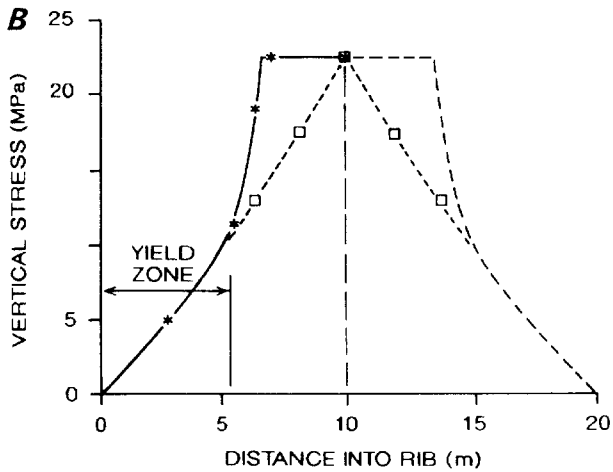
Extrapolation of increased loading is more problematic. In weak ground, an approach is to extrapolate the vertical stress buildup from the rib toward the pillar center. This may be possible where the vertical stress buildup approximates a line in the yield zone. This often provides a low estimate of the peak pillar strength and should be considered a working estimate only. An example of this is presented in figure 11B. Experience suggests that this is more likely in weak ground; however, in stronger ground the stress buildup is often more exponential and, as such, difficult to extrapolate.

To assess the potential strength under higher loading conditions, a method to redistribute the stress within the pillar associated with an increased average load, or the ability to monitor the effect of additional loading, is required.

Monitoring of stress distributions within pillars during mining can provide elevated loading conditions for analysis. An example is presented in figure 12, whereby small pillars were



NOT TO SCALE

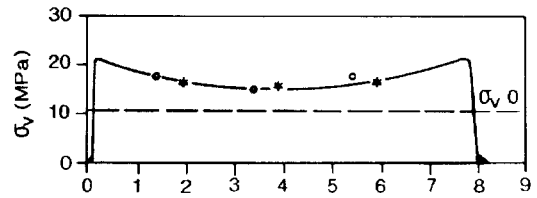


- * — * MEASURED
- - - - - EXTRAPOLATED STRESS DISTRIBUTION IN A 20m PILLAR
- - - - - □ EXTRAPOLATED STRESS DISTRIBUTION AT 'FAILURE'

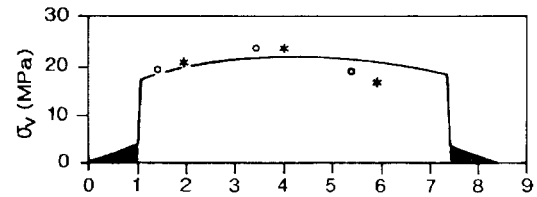
Figure 11.—Stress measurements over ribsides for strength assessment. A, typical stress measurement locations; B, stress distribution in pillar from measurements.

instrumented with CSIRO HI Cells and monitored until well isolated in the goaf after the passage of a longwall panel.

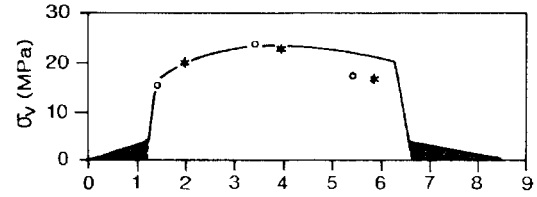
Computer modeling methods have been developed to simulate the behavior of the strata sections under various stress fields and mining geometries. For mine design, such simulations must be validated against actual ground behavior and stress measurements. This provides confidence that sufficient geological investigation has been undertaken and that the strength properties and deformation mechanisms are being simulated accurately. The computer software developed by Strata Control Technology has been verified in a number of field investigations where computer predictions of stress distributions and rock failure zones have been compared. An example is presented in figure 13, which compares the measured and modeled stress distribution over a yield pillar and solid coal in a deep mine. Another example of computer



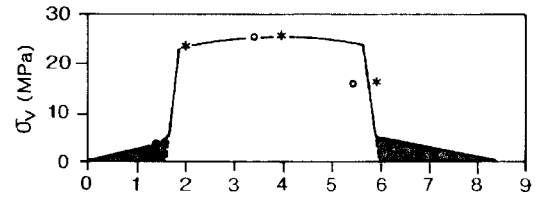
Development



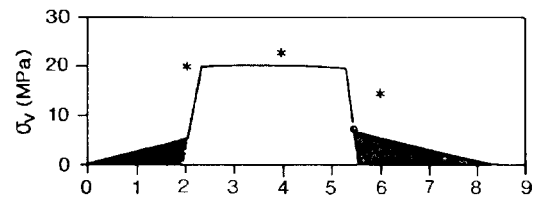
+30m to longwall face



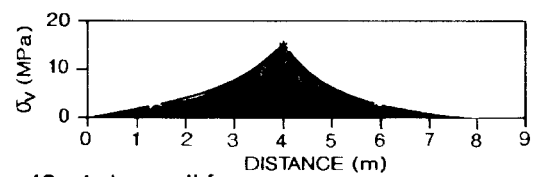
+20m to longwall face



+10m to longwall face



0m to longwall face



-40m to longwall face

- DEPTH OF YIELD INDICATED BY RIB EXTENSOMETER
- o STRESS RELIEF PILLAR 'A'
- * STRESS RELIEF PILLAR 'B'
- $\sigma_v 0$ COVER LOAD

Figure 12.—Example of small pillar monitoring studies indicating pillar stress history.

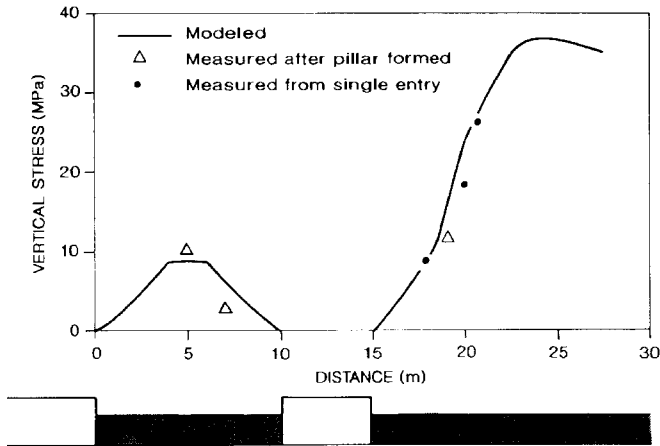


Figure 13.—Stress over yield pillar and adjacent to longwall.

modeling capabilities is presented in figure 14 for weak ground adjacent to a longwall panel. A series of stress measurements was conducted to define the abutment geometry and compared to computer simulations based on the geological section and goaf geometry. The results indicate a very close correlation and that rigorous computer simulation methods can provide a good estimation of the actual stresses and ground failure zones.

One major benefit of computer modeling is that the behavior of roadways adjacent to the pillars can be simulated. In this way, the design of a pillar will reflect not only the stress distribution within it, but also its impact on roadway stability. An example is presented in figure 15 in which the anticipated deformation of a roadway adjacent to a longwall panel under elevated abutment loading was evaluated. The effect of various reinforcement, support, and mining sections was simulated to determine the appropriate mining approach.

In mining situations where there are large areas of solid ground about the working area, the potential for regional collapse of pillars is typically low. Design in these areas usually relates to optimizing roadway conditions and controlling ground movements rather than the nominal pillar strength. Yield pillars and chain pillars are obvious examples of this application. Design must assess the geometry of other pillars

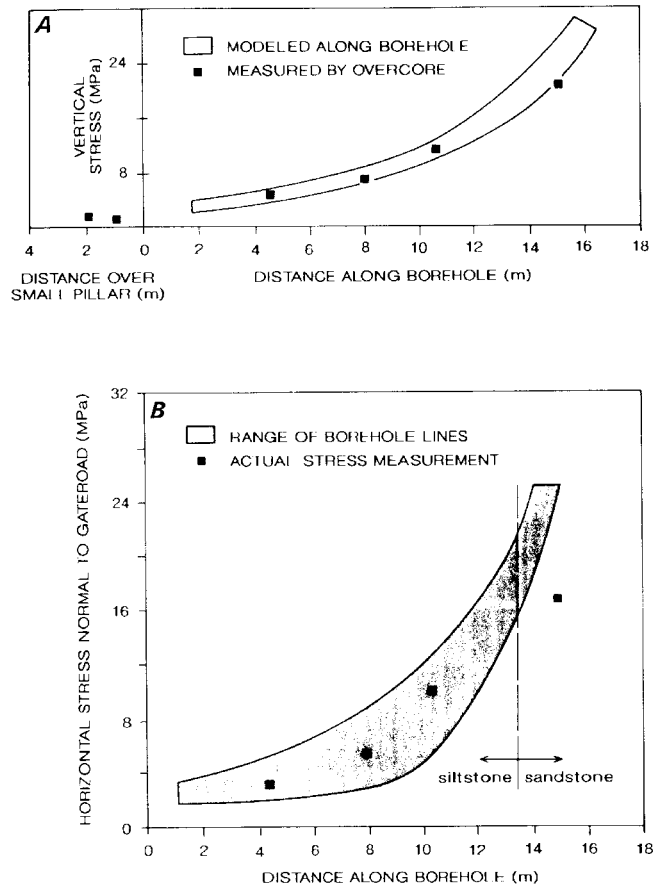


Figure 14.—Comparison of modeled and measured (A) vertical and (B) horizontal stress over a longwall side abutment. Stress measurements were made in a borehole drilled from an adjacent roadway.

and virgin coal areas in determining the impact of a particular stress distribution within a pillar and the ability of the overburden to span over a yielded pillar and safely redistribute the excess stress to adjacent ground. Figure 13 shows an example of this process for a failed ("yield") pillar adjacent to solid ground.

CHAIN PILLAR DESIGN ISSUES

It has become increasingly apparent from field monitoring and computer simulations of longwall caving that the design of chain pillars requires a larger scale review of ground behavior rather than "small-scale" pillar strength criteria. Microseismic monitoring [Kelly et al. 1998] has demonstrated significant rock fracture above and below chain pillars. Computer modeling of caving [Gale 1998] has also demonstrated rock fracture above and below pillars. Rock failure above and below chain pillars occurs as a result of gross scale stress changes and fluid pressure redistributions.

The strength and loading conditions of chain pillars can reflect the larger scale fracture geometries that may develop.

An example of an abutment stress within a pillar at shallow depth (250 m) is presented in figure 16. In this case, rock failure extends over the ribside and shifts the abutment distribution within the pillar.

Modification of the vertical abutment stress distribution has been noted in field monitoring and computer simulations under conditions of high lateral stress. It has been found that the abutment distribution tends to have a lower peak stress, but it spreads over a longer lateral extent. An example is presented in figure 17.

In both of these examples, computer modeling of the caving process within the geological section closely correlates

with the measured data. The use of generalized empirical methods to determine the abutment profile is also presented and indicates that their application is best utilized as initial estimates to be reassessed by site-specific investigations for key design areas.

Rock failure above and below chain pillars does not necessarily occur at all sites; however, experience suggests that this is common. The gross scale rock failure about longwall

panels, therefore, requires design for ground control issues rather than pillar design, as traditionally conceived. Field measurement, computer modeling, and microseismic investigations play a key role in defining the design criteria. Empirical databases are also useful; however, the user should be aware of the ground deformation mechanics in order to assess the applicability of the data being used relative to the site conditions to which it would be applied.

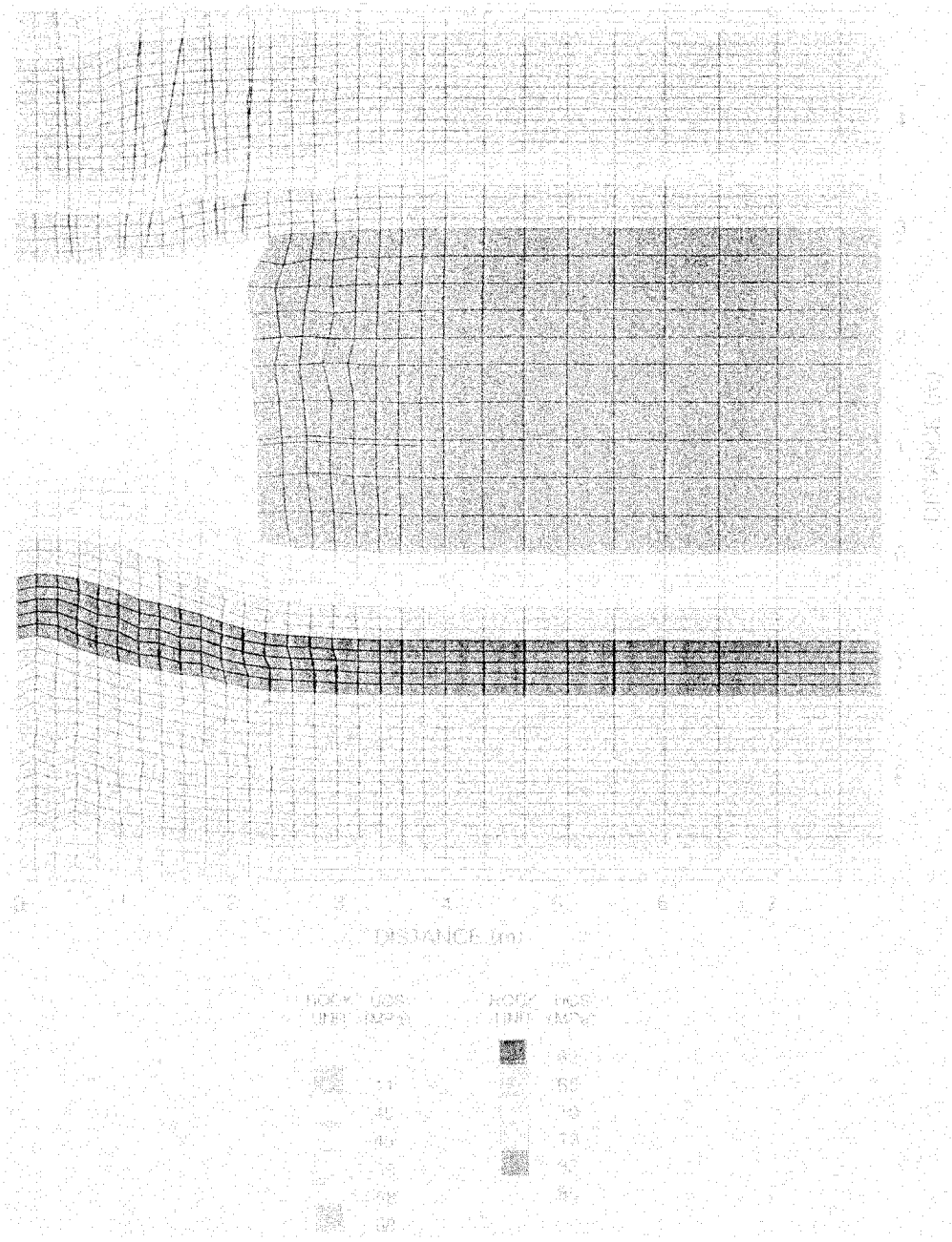


Figure 15.—Simulation of roadway conditions under abutment stress.

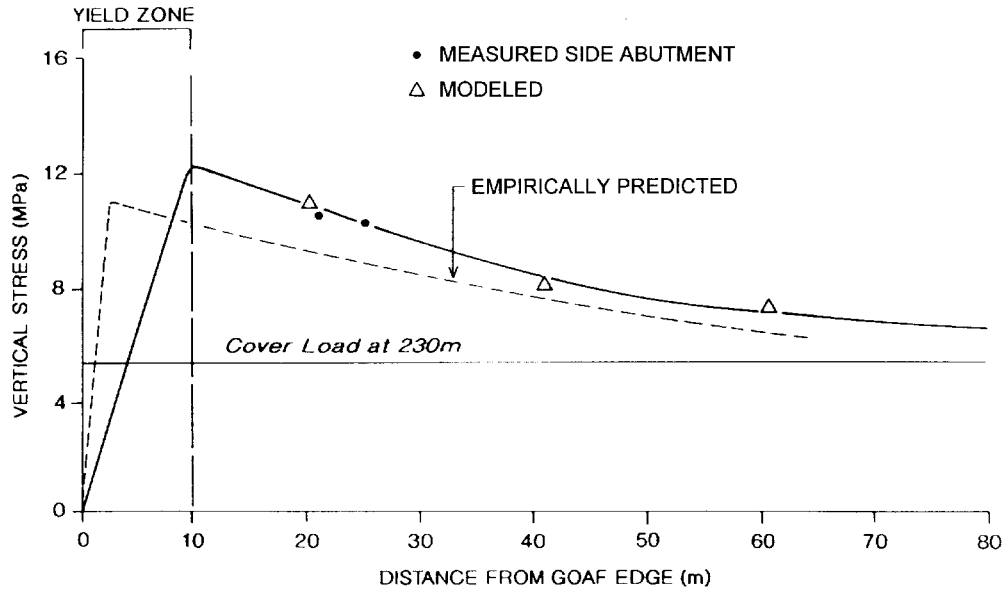


Figure 16.—Longwall side abutment profiles for modeled, measured, and empirical approaches. In this example, rock failure occurred about the pillar, forming a more extensive yield zone.

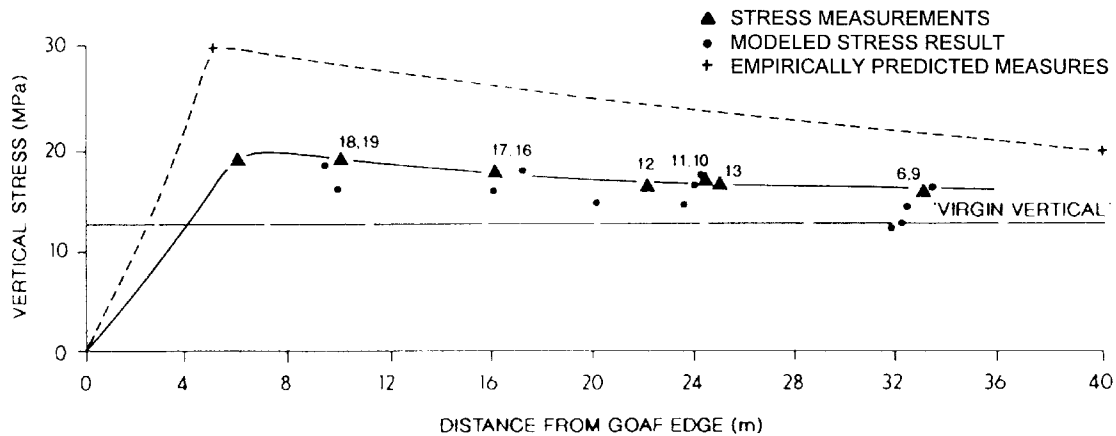


Figure 17.—Longwall side abutment profiles for modeled, measured, and empirical approaches in a high stress mining area.

CONCLUSIONS

The strength characteristics of pillars depend on the strength properties of the strata surrounding the coal.

It is important to consider the postfailure strength of pillars in design, particularly in areas of weak strata where a post-failure strength loss in moderate to large width/height pillars is possible.

Computer simulation methods in association with site measurements are recommended for the design of key layouts that require an assessment of geological variations, pillar size,

and stress field changes to optimize the mining operation. This approach also assesses the expected roadway conditions or pillar response for various mine layouts; these can be monitored to determine if the ground is behaving as expected.

Design of pillars adjacent to large extraction areas needs to include the large-scale fracture distributions and, in general, needs to be based on a ground control criterion rather than on a pillar strength criterion only.

REFERENCES

- Gale WJ [1996]. Geological issues relating to coal pillar design. In: McNally GH, Ward CR, eds. Symposium of Geology in Longwall Mining, pp. 185-191.
- Gale WJ [1998]. Experience in computer simulation of caving, rock fracture and fluid flow in longwall panels. In: Proceedings of the International Conference on Geomechanics/Ground Control Mining and Underground Construction, pp. 997-1007.
- Hustrulid WA [1976]. A review of coal strength formulas. *Rock Mech* 8:43-50.
- Kelly M, Gale WJ, Luo X, Hatherly P, Balusu R, LeBlanc Smith G [1998]. Longwall caving process in different geological environments; better understanding through the combination of modern assessment methods. In: Proceedings of the International Conference on Geomechanics/Ground Control Mining and Underground Construction, pp. 573-589.
- Maleki H [1992]. In situ pillar strength and failure mechanisms for U.S. coal seams. In: Proceedings of the Workshop on Coal Pillar Mechanics and Design. Pittsburgh, PA: U.S. Department of the Interior, Bureau of Mines, IC 9315, pp. 73-77.
- Mark C, Iannacchione AT [1992]. Coal pillar mechanics: theoretical models and field measurements compared. In: Proceedings of the Workshop on Coal Pillar Mechanics and Design. Pittsburgh, PA: U.S. Department of the Interior, Bureau of Mines, IC 9315, pp. 78-93.
- Mark C, Listak JM, Bieniawski ZT [1988]. Yielding coal pillars: field measurements and analysis of design methods. In: Proceedings of the 29th U.S. Symposium on Rock Mechanics. New York, NY: American Institute of Mining, Metallurgical, and Petroleum Engineers, pp. 261-270.
- Salamon MDG, Munro AH [1967]. A study of the strength of coal pillars. *J S Afr Inst Min Metall*, pp. 55-67.
- Wilson AH [1972]. An hypothesis concerning pillar stability. *Min Eng (London)* 131(141):409-417.

UNIVERSITY OF NEW SOUTH WALES COAL PILLAR STRENGTH DETERMINATIONS FOR AUSTRALIAN AND SOUTH AFRICAN MINING CONDITIONS

By Jim M. Galvin, Ph.D.,¹ Bruce K. Hebblewhite, Ph.D.,²
and Miklos D. G. Salamon, Ph.D.³

ABSTRACT

A series of mine design accidents in the late 1980s resulted in a major research program at the University of New South Wales, Australia, aimed at developing pillar and mine design guidelines. A database of both failed and unfailed Australian underground coal mine pillar case studies was compiled. A procedure was developed to enable the effective width of rectangular pillars to be taken into account. The database was analyzed statistically using the maximum likelihood method, both independently and as a combined data set with the more extensive South African database. Probabilities of failure were correlated to factors of safety. It was found that there was less than a 4% variance in pillar design extraction ratios resulting from each of these approaches. There is a remarkable consistency between the design formulas developed from back-analysis of the two separate national pillar databases containing many different coal seams and geological environments.

¹Professor and Head, School of Mining Engineering, University of New South Wales, Sydney, Australia.

²Professor, School of Mining Engineering, University of New South Wales, Sydney, Australia.

³Distinguished professor, School of Mining Engineering, Colorado School of Mines, Golden, CO.

INTRODUCTION

In the 3-year period to 1992, 60 continuous miners were trapped by falls of strata for more than 7 hr in collieries in New South Wales, Australia. In the preceding 2 years, eight coal miners were killed in pillar extraction operations in New South Wales. In the New South Wales and Queensland coalfields, at least 15 extensive collapses of bord-and-pillar workings occurred unexpectedly in the 15-year period to 1992. Six of these collapses occurred in working panels; fortuitously, five occurred during shutdown periods and the sixth occurred while the continuous miner was being flitted to the surface for repairs.

One contributor to these events was the lack of a comprehensive pillar design procedure. Legislation in New South

Wales at the time simply required coal pillars to have a minimum width of one-tenth depth or 10 m, whichever was greater. The influence of pillar height on strength received no recognition.

This set of circumstances led to funding by the New South Wales Joint Coal Board of a major research project on pillar design and behavior. The research was undertaken by the School of Mining Engineering at the University of New South Wales (UNSW). The primary objectives of the research were to improve the understanding of coal pillars and associated floor and roof strata behavior under various loading conditions and to incorporate these outcomes into the mine design knowledge base.

RESEARCH METHODOLOGY

The approach adopted to pillar design was based on that developed for square pillars by Salamon and Munro [1966, 1967]. However, the extensive use of rectangular and diamond-shaped pillars in Australia required more detailed consideration of the *effective width* of parallelepiped pillars and the effect of this width on pillar strength.

Firstly, an adequate Australian database of failed and unfailed pillar case histories was established. A relationship was then developed to factor in the influence of rectangular and diamond-shaped pillars, which comprised just over 50% of the database. This database was then subjected to rigorous statistical analysis using a range of techniques in order to quantify

parameters associated with each of two generally accepted empirical formulas for describing pillar strength. This facilitated the establishment of correlation, for all strength expressions, between the probability that a formula would yield a successful design versus the respective design factor of safety.

The Australian database was also combined with the much larger and long-established South African database, and the analysis was repeated to determine if the two population bases could be considered as one. A close correlation was obtained, leading to an increased level of confidence in this methodology and to a number of more universal conclusions concerning pillar design.

EMPIRICAL COAL PILLAR STRENGTH ESTIMATIONS

The development of computer and numerical technologies in recent decades has facilitated, at least in principle, the analysis of stresses in pillars and their foundations, i.e., the roof and floor strata. Unfortunately, physical experimentation has not advanced equally rapidly. Hence, the understanding of the intrinsic constitutive laws controlling the behavior of yielding rocks is still unsatisfactory. More immediate problems include the significant discrepancies between the physical properties exhibited by rocks in situ and those measured in the laboratory by testing small specimens. These problems relate to the effects of size and shape on rock strength.

Many investigators have proposed simple empirical formulas to describe the strength of coal pillars. The most common feature of most of these empirical relationships is that they define strength ostensibly only in terms of the linear dimensions of the pillars and a multiplying constant, representing the

strength of the unit volume of coal. Investigators over the years have proposed formulas that belong to one of two types. One type defines pillar strength simply as a linear function of the width-to-height (w/h) ratio:

$$F_{s1} = K_1 \left[r \% (1 + r) \frac{w}{h} \right], \quad (1)$$

where K_1 is the compressive strength of a cube and r is a dimensionless constant. The quantities of w and h are the width and height of the pillar, respectively.

If the notation

$$R = w/h \quad (2)$$

is introduced, then equation 1 becomes

$$F_{s1} = K_1 [r \% (1 + r)R]. \quad (3)$$

According to this formula, geometrically similar pillars have the same strength regardless of their actual dimensions.

A second commonly used pillar strength formula takes the form

$$F_{s2} = K_2 \left(\frac{w}{w_0} \right)^n \left(\frac{h}{h_0} \right)^s, \quad (4)$$

EFFECTIVE WIDTH OF PARALLELEPIPED PILLARS

The development of statistically based pillar design formulas rests minimally upon the premise that a fairly large and tolerably reliable database of unfailed and failed pillar panels can be compiled. Salamon et al. [1996] have identified a number of strict criteria that must be satisfied before a case can be included in the database. One of these that must be appreciated when applying the outcomes of this pillar design research is that these outcomes apply only to competent roof and floor environments, i.e., the database relates only to failures of the coal pillar element of the pillar system, not to the roof or floor elements.

Against this background, an Australian database of 19 failed and 16 unfailed cases was assembled. Rectangular pillars comprised eight of the failed and nine of the unfailed cases. Diamond-shaped pillars comprised one failed case. In order to preserve in these circumstances the availability of the strength formulas derived for square pillars, many researchers have proposed the introduction of an *effective* width.

One of the most basic approaches is to define the effective width, w_e , as

$$w_e = \sqrt{w_1 w_2}, \quad (5)$$

where w_1 = minimum pillar width (measured along roadway)

and w_2 = maximum pillar width (measured along roadway).

In situations where w_2 is not extremely different to w_1 , this approach has merit. However, when $w_2 \gg w_1$, the equation produces an unrealistic effective pillar width (table 1).

which is expressed in a dimensionally correct form. n and s are dimensionless parameters; w and h are the linear dimensions of the pillar. Multiplier K_2 is the strength of a reference body of coal of height h_0 and a square cross section with side length w_0 .

In most instances, the reference body is taken to be cube of unit volume for convenience's sake, in which case h_0 and w_0 are both unity and can be omitted from the formula. Expressions belonging to this family are referred to as *power law* strength formulas. In contrast to formulas of the form of equation 1, these formulas are also volume-sensitive.

Table 1.—Application of various effective pillar width formulas
(Width and height in meters)

w_1	w_2	h	$/w_1 w_2$	$4A_p/C_p$	w_1
100	100	3	100.0	100	100
80	100	3	89.4	88.9	88.9
50	100	3	70.7	66.7	66.7
30	100	3	54.7	46.2	46.2
20	100	3	44.7	33.3	33.3
15	100	3	38.7	26.1	21.7
10	100	3	31.6	18.2	10.7
1	100	3	10.0	2.0	1

The most promising recommendation has come from Wagner [1974, 1980], who, making use of the concept of hydraulic radius, suggested that the effective width be defined as

$$w_e = 4 \frac{A_p}{C_p}, \quad (6)$$

where A_p and C_p are the cross-sectional area and the circumference of the pillar, respectively.

Application of equation 6 produces effective pillar width similar to that of equation 5 when w_1 is greater than about $0.5w_2$ (table 1). At moderate to low values of w_1 ($0.4w_2 \leq w_1 \leq 0.2w_2$), equation 6 predicts a smaller effective width, which is more sensible from a mechanistic viewpoint. However, at very low values of w_1 ($w_1 < 0.2w_2$), the equation is still considered to overestimate the effective pillar width. This is because when a pillar is narrow, failure is likely to occur across the narrow dimension before sufficient confinement is generated in the longitudinal direction to be of benefit.

This leads to the concept that rectangular and irregular pillars need to be of a critical minimum width before benefit is gained from confinement generated in the longitudinal direction. This benefit can be expected to ramp up to a plateau level as the minimum width increases. Furthermore, it is reasonable to expect that this minimum critical width will be a function of mining height, increasing with increasing mining height.

The need to nominate a minimum critical pillar width has been incorporated into the analysis by modifying equation 6 on the basis that almost all pillars can be regarded as parallelepipeds, i.e., their bases are parallelograms (figure 1). Pillars therefore have side lengths w_1 and w_2 ($w_1 \neq w_2$) and an internal angle $2 \neq 90^\circ$. Equation 6 then becomes

$$w_{e_o} = 1_o w, \tag{7}$$

where w is the minimum width of the pillar, i.e.,

$$w = w_1 \sin 2 \tag{8}$$

and the dimensionless factor 1_o is defined by

$$1_o = \frac{2w_2}{w_1 + w_2} \tag{9}$$

The range of this factor is $1 \leq 1_o < 2$, which is encountered as the aspect ratio moves from unity toward infinity. Experience indicates that much before the complete failure of a pillar, its edges are already yielding. Thus, if the w/h ratio in one direction of a rectangular pillar is low, one of the principal stresses confining its core will remain small, and this stress, together with the maximum stress, will control failure.

Hence, the extra confinement that may arise from the aspect ratio will have little or no effect. It is suggested that such apprehension may be catered for by postulating that the effective width is the minimum width, i.e., $w_e = w$ as long as $R < R_1$, and it becomes $w_e = w_{e_o}$ when $R > R_u$.

In the intermediate range, i.e., when $R_1 \neq R \neq R_u$, the effective width changes smoothly in accordance with

$$w_e = w 1_o^{\frac{R \& R_1}{R_u \& R_1}} \tag{10}$$

Here, the choice of the limiting w/h ratios is open to judgment. It appears reasonable, however, to use the following values:

$$R_1 = 3 \quad R_u = 6 \tag{11}$$

Table 1 and figure 2 show the effects of the various approaches when applied to calculating the effective width of a 100-m-long, 3-m-high rectangular pillar.

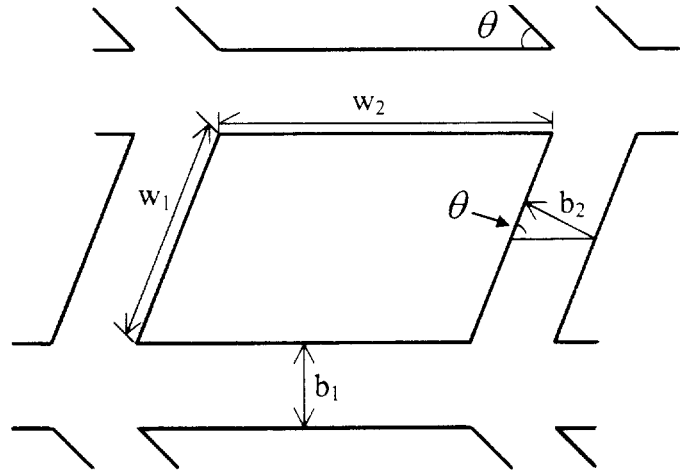


Figure 1.—Definition of mining variables associated with a parallelepiped pillar.

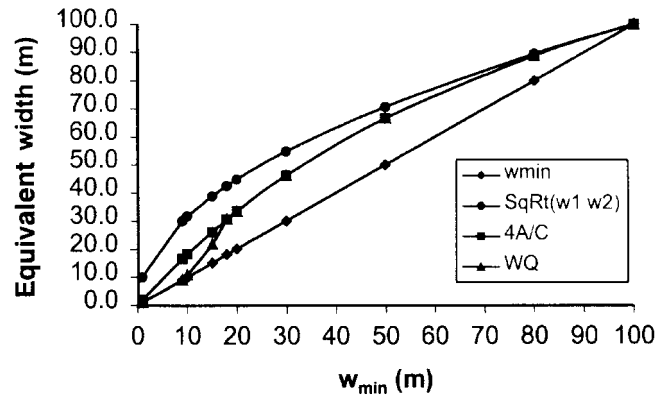


Figure 2.—Comparison of the various proposals for calculating the effective width of a 100-m-long, 3-m-high rectangular pillar.

Using the concept of effective width, the power law in equation 4 can be rewritten for pillars with a general parallelepiped shape:

$$F_{s2} = K_2 w^a h^b 1^n \tag{12}$$

An alternative form of this formula expresses the strength as the function of the pillar volume V and the w/h ratio R :

$$F_{s2} = K_2 V^a R^b 1^n, \tag{13}$$

where the volume refers to a dummy square pillar of width w and height h , and the w/h ratio is calculated from the minimum pillar width:

$$V = w^2 h \quad R = \frac{w_1 \sin 2}{h} = \frac{w}{h} \tag{14}$$

The new constants a and b can be defined in terms of constants " and \$:

$$a = \frac{1}{3}(" \% \$) \quad b = \frac{1}{3}(" \& 2\$) \quad (15)$$

Experience has shown that the original power law formula (equation 4) tends to underestimate the strength of squat pillars, i.e., pillars with a w/h ratio in excess of about 5. To cater for this problem, Salomon and Wagner [1985] suggested an extension of equation 4 into the range of higher w/h ratios. This extension, after adaptation to pillars of parallelepiped shape, is

$$F_{s2} = K_2 V^a R_o^b 1^n \left\{ \frac{b}{g} \left[\left(\frac{R}{R_o} \right)^g \& 1 \right] \% 1 \right\}, \quad (16)$$

which is valid if $R > R_o$ and where 1 is defined in equation 10. This particular form was chosen to ensure that there is a smooth transition between this and equation 13 at $R = R_o$ [Salomon and Wagner 1985]. Here, R_o and g are appropriately chosen constants. The expression is often referred to as the *squat pillar strength* formula. Since its inception, it has been applied

widely in the Republic of South Africa using the following pair of constants:

$$R_o = 5 \quad g = 2.5 \quad (17)$$

In critical situations, the judgment exercised in deriving the effective pillar width relationship may be regarded as too speculative. This concern can be addressed by either choosing an elevated design factor of safety to account for this level of uncertainty or reverting to the use of the minimum pillar width in pillar strength calculations.

Another aspect to the use of rectangular pillars is the calculation of pillar load. In calculating the tributary load, the true dimensions need to be employed. Thus, the pillar load assumes the following form:

$$q_m = (H^* \frac{(w \% b_1) (w_2 \% b_2 / \sin 2)}{ww_2}) \quad (18)$$

In this relationship, * is a modifier. It is unity in all cases where the pillar burden is the conventional tributary load. If, however, due to secondary extraction the pillar load is believed to differ from this value, the load can be adjusted by applying this factor. Moreover, to remain consistent with earlier calculations, C is taken to be: (1.1 psi/ft 24.8827 kN/m³ 24.8827 kPa/m.

UNSW INITIAL DESIGN FORMULAS

In 1992, following a number of serious incidents related to the lack of restriction on pillar height, the Chief Inspector of Coal Mines in New South Wales required operators to obtain approval to mine at heights exceeding 4 m. To address the need for a pillar design methodology, the UNSW research team undertook in 1995 a preliminary analysis of its database [Hocking et al. 1995]. At the time, the database comprised 14 collapsed cases and 16 stable cases that satisfied the selection criteria. The database was analyzed statistically using the full maximum likelihood method. Galvin and Hebblewhite [1995] subsequently published the following pillar design formulas, which find current application in Australia:

$$F_{s2} = 7.4 \frac{w^{0.46}}{h^{0.66}} \quad (\text{MPa}) \quad (19a)$$

and its squat pillar version ($R > 5$):

$$F_{s2} = \frac{19.24}{w^{0.133} h^{0.067}} \left\{ 0.237 \left[\left(\frac{w}{5h} \right)^{2.5} \& 1 \right] \% 1 \right\} \quad (\text{MPa}) \quad (19b)$$

A conservative approach was adopted, and the minimum pillar width was proposed as the effective width. It follows, therefore, that 1 = 1 in these expressions. There was little difference in the pillar strength obtained by allowing all parameters to float in the statistical analysis as opposed to allowing only the K values to float and fixing the other parameters to be the same as those used for many years in the Republic of South Africa. To avoid confusion and to facilitate the introduction of the formulas, therefore, only those formulas derived by allowing the K values to float were presented to operators. The formula for strength based on the linear relationship took the following form:

$$F_{s1} = 5.36(0.64 \% 0.36R) \quad (\text{MPa}) \quad (20)$$

UNSW REFINED (RECTANGULAR) FORMULAS

In 1996, a more comprehensive statistical analysis of the expanded Australian database was completed that incorporated the effective width of rectangular pillars as defined earlier [Salamon et al. 1996]. Statistical methods included least squares, limited maximum likelihood, and full maximum likelihood. Both power law models and linear law models were evaluated, and all parameters were allowed to float. In all instances, the power law model gave better correlations.

The following strength formulas were found to best describe the observed behavior of pillars in New South Wales and Queensland:

$$F_{s2} \approx 8.60 \frac{(w1)^{0.51}}{h^{0.84}} \text{ (MPa)} \quad (21a)$$

The corresponding expression for squat pillars is given by

$$F_{s2} \approx \frac{27.63 \cdot 1^{0.51}}{w^{0.220} h^{0.110}} \left\{ 0.290 \left[\left(\frac{w}{5h} \right)^{2.5} + 1 \right] \% 1 \right\} \text{ (MPa)} \quad (21b)$$

In these expressions, $w \approx w_1 \sin 2$, and the effective width factor 1 is as defined in equation 10.

The relationship between pillar strength and pillar load produced by these equations for each point in the database is shown in figure 3. Design factors of safety associated with the probability of achieving a stable design are shown in table 2.

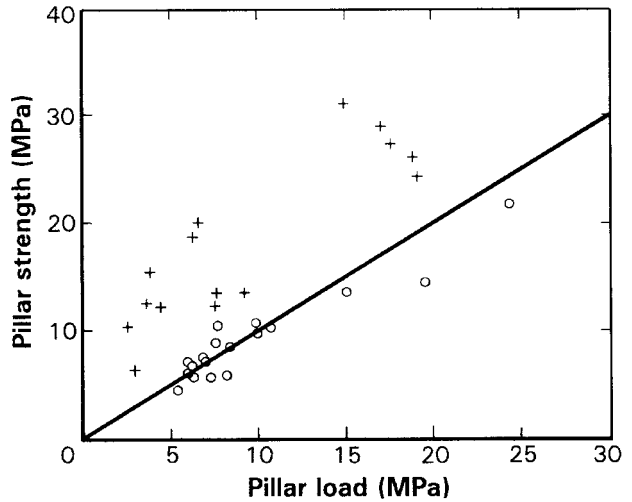


Figure 3.—Pillar strength and pillar load relationship for both the failed (o) and unfailed (+) Australian cases.

Table 2.—Probability of failure versus factor of safety

Probability of failure	Factor of safety
8 in 10	0.87
5 in 10	1.00
1 in 10	1.22
5 in 100	1.30
2 in 100	1.38
1 in 100	1.44
1 in 1,000	1.63
1 in 10,000	1.79
1 in 100,000	1.95
1 in 1,000,000	2.11

REANALYSIS OF THE SOUTH AFRICAN DATABASE

The original extensive South African coal pillar database used by Salamon and Munro in 1966 has since been updated and supplemented by Madden and Hardman [1992]. This combined South African database comprises 44 failed and 98 unfailed cases. It has also been reanalyzed using the same statistical techniques used for the Australian database. Two failed cases were later omitted from the data set [Salamon et al. 1996].

This analysis has produced the following strength formulas:

$$F_{s2} \approx 6.88 \frac{(w1)^{0.42}}{h^{0.60}} \text{ (MPa)} \quad (22a)$$

The corresponding expression for squat pillars ($R > 5$) is given by

$$F_{s2} \approx \frac{16.36 \cdot 1^{0.42}}{w^{0.116} h^{0.058}} \left\{ 0.215 \left[\left(\frac{w}{5h} \right)^{2.5} + 1 \right] \% 1 \right\} \text{ (MPa)} \quad (22b)$$

The linear version of the strength estimator is simply

$$F_{s1} \approx 5.60(0.69 \% 0.31R) \text{ (MPa)} \quad (23)$$

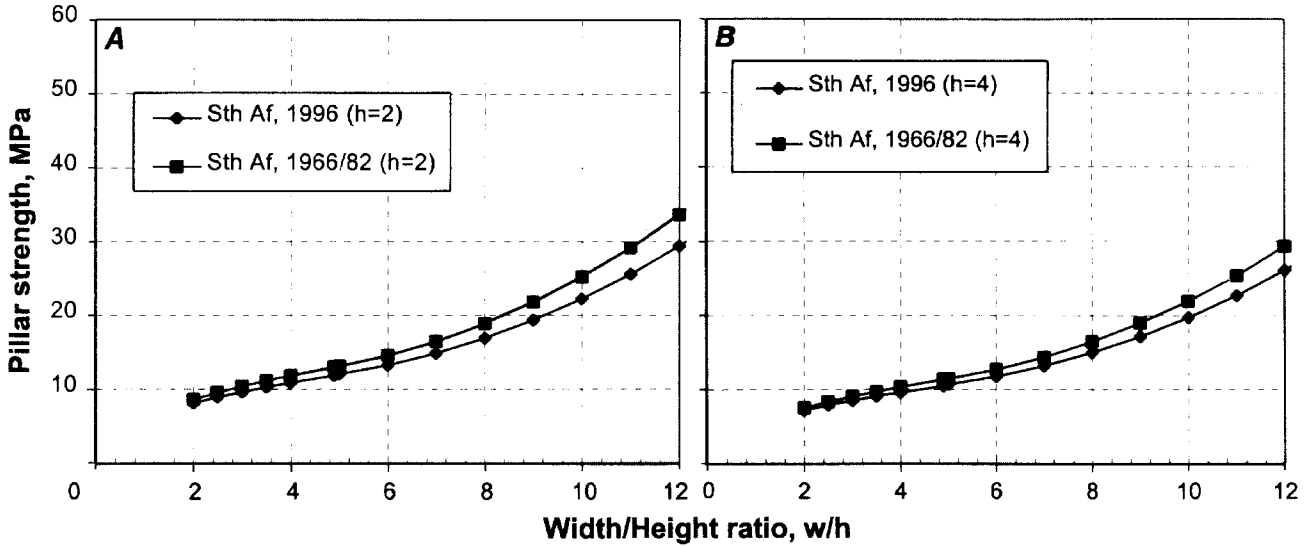


Figure 4.—Comparison between South African power formulas, 1966/82 and 1996. A, h = 2 m; B, h = 4 m.

Figure 4 shows the comparison between the pillar strength produced by equations 22a and 22b and that predicted by the original Salamon and Munro formula and its modified squat pillar form. In the case of a mining height of 2 m, the figure shows that for a given pillar strength, pillars designed with the

updated formulas may need to be about 2 m wider. For a bord width of 6 m at a w/h ratio of 10, this results in about 3% less resource recovery. For similar circumstances in a 4-m mining height, the increase in pillar size is on the order of 3.2 m.

COMBINED AUSTRALIAN AND SOUTH AFRICAN DATABASES

A further step in the research program was to combine the South African and Australian databases and to analyze them as a combined population, then compare and contrast them with the two independent data populations for each country. This combined database comprised 177 cases of pillar systems, including 61 collapsed cases. This produced the following formulas:

$$F_{s2} = 6.88 \frac{\sqrt{w}}{h^{0.7}} \text{ (MPa)} \quad (24a)$$

For $R > 5$, the squat version of this expression takes the following form:

$$F_{s2} = \frac{19.05\sqrt{1}}{w^{0.133} h^{0.066}} \left\{ 0.253 \left[\left(\frac{w}{5h} \right)^{2.5} + 1 \right] \% 1 \right\} \text{ (MPa)} \quad (24b)$$

The corresponding linear formula is simply

$$F_{s1} = 5.41(0.63 \% 0.37R) \text{ (MPa)} \quad (25)$$

Figure 5 shows failed and unfailed cases in the load plane. The figure illustrates a fairly good discrimination between the two sets of points. Only one unfailed point occurs on the wrong side of the $s = 1$ line, and the median failed cases is 1.039.

Figure 6 shows a comparison between pillar strengths using power law estimators derived from the Australian, South

African, and combined Australian-South African databases. The closeness of the predictions is remarkable considering the geographical separation of the Australian and South African coalfields.

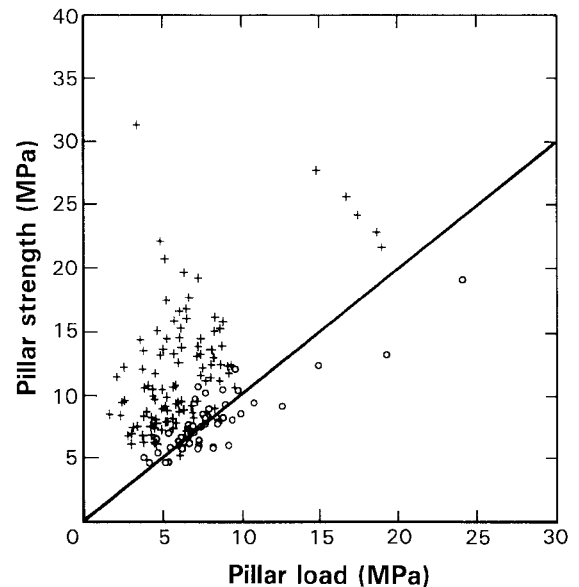


Figure 5.—The failed (o) and unfailed (+) cases in a pillar strength versus pillar load plot using the combined Australian-South African database.

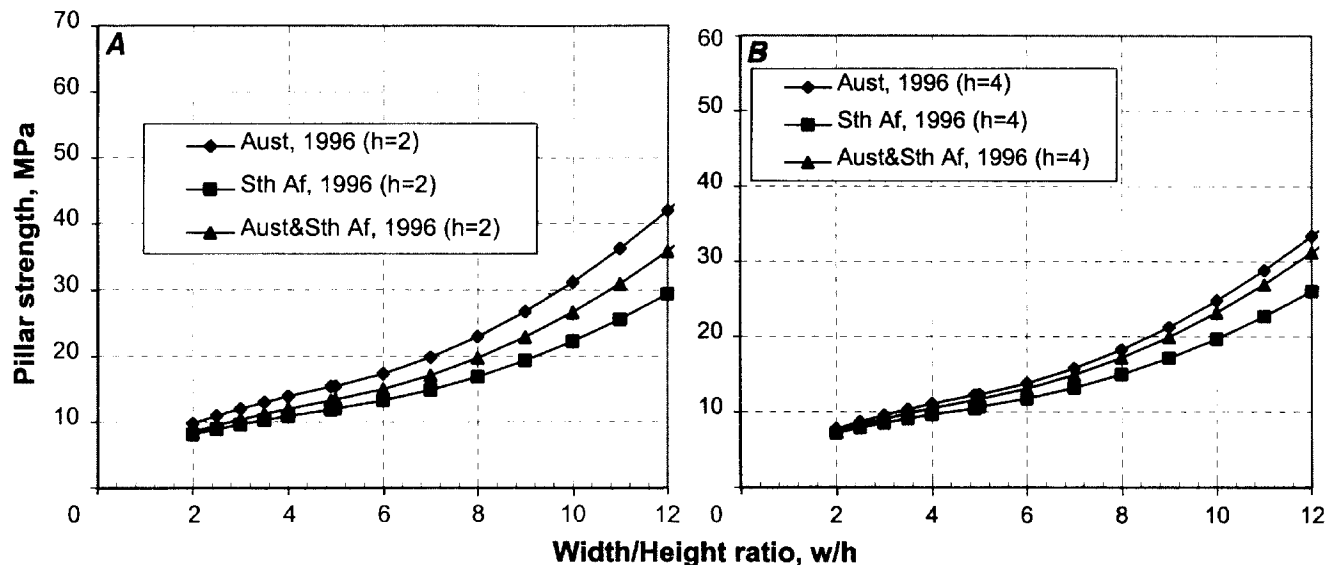


Figure 6.—Comparison between power law strength formulas derived for the Australian, South African, and combined databases. A, $h = 2$ m; B, $h = 4$ m.

CONCLUSIONS

The statistical analysis of the Australian database indicates that the method proposed for calculating the effective width of parallelepiped pillars produced sensible outcomes. However, it must be remembered that, although of sufficient size to be statistically significant, the parallelepiped database is small. The method should therefore be used with caution.

In order to enhance confidence in the pillar design procedure, including the use of the effective pillar width method, additional research was undertaken. It was noted that the formula derived from the initial Australian database closely resembled the original Salamon-Munro expression. This somewhat surprising resemblance prompted further research and enlargement of the database. The larger database yielded pillar strengths that again were similar to those obtained from the initial UNSW research and by Salamon and Munro. The combination of the Australian and South African databases reinforced the original impression, namely, that the underlying pillar strengths in these countries resembled each other closely.

The outcome of the investigation lends support to the view expressed by Mark and Barton [1996]. They suggested that strength values obtained in the laboratory cannot be utilized in

a meaningful way in pillar design and that the variation in the strength of pillars of the same size can be disregarded in many instances. Mark and Barton [1996] emphasize that they do not claim that the in situ strength of all U.S. coal is the same. Their study merely showed that a uniform strength is a better approximation than one based on laboratory testing. Although the UNSW research conclusions are encouraging, complacency is not justified. The formulas are based on competent roof and floor conditions. Significantly different pillar strengths may be associated with abnormal strata behavior mechanisms. Because pillars with w/h ratios greater than 10 have not been tested to destruction, it must also be recognized that neither linear nor power law formulas have been validated at w/h ratios greater than about 8.

It cannot be overemphasized that, because the design formulas have been developed on a probabilistic basis, they need to be reviewed periodically as the database expands and the understanding of pillar mechanics advances. A fundamental rule of empirical research is that the results should be used within the range of data used in their derivation. Extrapolation with empirical formulas is always fraught with danger.

REFERENCES

- Galvin JM, Hebblewhite BK [1995]. UNSW pillar design methodology. Sydney, Australia: University of New South Wales, School of Mining Engineering, Research Release No. 1.
- Hocking G, Anderson I, Salamon MDG [1995]. Coal pillar strength formulae and stability criteria. Sydney, Australia: University of New South Wales, School of Mining Engineering, Research Report 1/95.
- Madden BJ, Hardman DR [1992]. Long-term stability of bord-and-pillar workings. In: Proceedings of the Symposium on Construction Over Mined Areas. Pretoria, Republic of South Africa.
- Mark C, Barton TM [1996]. The uniaxial compressive strength of coal: should it be used to design pillars? In: Ozdemir L, Hanna K, Haramy KY, Peng S, eds. Proceedings of the 15th International Conference on Ground Control in Mining. Golden, CO: Colorado School of Mines, pp. 61-78.
- Salamon MDG, Munro AH [1966]. A study of the strength of coal pillars. Transvaal and Orange Free State Chamber of Mines, Research Report No. 71/66.
- Salamon MDG, Munro AH [1967]. A study of the strength of coal pillars. J S Afr Inst Min Metall, pp. 55-67.

Salamon MDG, Wagner H [1985]. Practical experiences in the design of coal pillars. In: Green AR, ed. Proceedings of the 21st International Conference of Safety in Mines Research Institutes (Sydney, Australia). Balkema, pp. 3-9.

Salamon MDG, Galvin JM, Hocking G, Anderson I [1996]. Coal pillar strength from back calculation. Sydney, Australia: University of New South Wales, School of Mining Engineering, Research Report 1/96.

Wagner H [1974]. Determination of the complete load deformation characteristics of coal pillars. In: Proceedings of the Third International Congress on Rock Mechanics. International Society for Rock Mechanics, pp. 1076-81.

Wagner H [1980]. Pillar design in coal mines. J S Afr Inst Min Metall, pp. 37-45.

PRACTICAL BOUNDARY-ELEMENT MODELING FOR MINE PLANNING

By Keith A. Heasley, Ph.D.,¹ and Gregory J. Chekan²

ABSTRACT

As part of the initial investigation and validation of a new boundary-element formulation for stress modeling in coal mines, the underground stresses and displacements at two multiple-seam coal mines with unique stress problems were modeled and predicted. The new program, LAMODEL, calculates stresses and displacements at the seam level and at requested locations in the overburden or at the surface. Both linear elastic and nonlinear seam materials can be used, and surface effects, multiple seams, and multiple mining steps can be simulated. In order to most efficiently use LAMODEL for accurate stress prediction, the program is first calibrated to the site-specific geomechanics based on previously observed stress conditions at the mine. For this calibration process, a previously mined area is "stress mapped" by quantifying the observed pillar and strata behavior using a numerical rating system. Then, the site-specific mechanical properties in the model are adjusted to provide the best correlation between the predicted stresses and the observed underground stress rating. Once calibrated, the model is then used to predict future stress problems ahead of mining. At the two case study mines, the calibrated models showed good correlation with the observed stresses and also accurately predicted upcoming high stress areas for preventive action by the mines.

¹Supervisory physical scientist.

²Mining engineer.

Pittsburgh Research Laboratory, National Institute for Occupational Safety and Health, Pittsburgh, PA.

INTRODUCTION

Mine planners have a variety of modeling methods, both empirical and numerical, for analyzing pillar stresses and determining safe pillar sizes for various mine geometries and geologic structures. Empirical methods emphasize the collection and interpretation of case histories of pillar performance. The Analysis of Longwall Pillar Stability (ALPS) and Analysis of Retreat Mining Pillar Stability (ARMPS) programs are two such empirical programs that are derived from large databases of real-world pillar studies and can be used for determining pillar sizes for single-seam longwall and retreat room-and-pillar mining, respectively [Mark 1992; Mark and Chase 1997]. The Virginia Polytechnic Institute and State University, Blacksburg, VA, recently developed a comparable empirical program called Multi-Seam Analysis Package (MSAP) for sizing pillars for multiple-seam situations [Kanniganti 1993]. These empirical programs are closely linked to reality and very user-friendly; for many typical mining geometries, they work extremely well.

However, it is difficult to apply these empirical programs to mining situations beyond the scope of the original empirical database. Therefore, when complicated stress conditions arise from complex single- or multiple-seam mining geometries, numerical modeling techniques such as finite-element, boundary-element, discrete-element, or finite-difference are usually applied. In general, these numerical, or analytical, design methods are derived from the fundamental laws of force, stress, and elasticity. Their primary advantage is that they are very flexible and can quickly analyze the effect of numerous geometric and geologic variables on mine design. Their primary disadvantage is that they require difficult-to-obtain and/or controversial information about material properties, failure criteria, and postfailure mechanics. In this paper, the solid foundation of empirical pillar design and in-mine observation is combined with the flexibility of numerical modeling to provide a practical technique for mine planning in difficult situations.

LAMODEL

In order to analyze the displacements and stresses associated with the extraction of large tabular deposits such as coal, potash, and other thin vein-type deposits, the displacement-discontinuity variation of the boundary-element technique is frequently the method of choice. In the displacement-discontinuity approach, the mining horizon is treated mathematically as a discontinuity in the displacement of the surrounding media. Using this technique, only the planar area of the seam needs to be discretized, or gridded, in order to obtain the stress and displacement solution on the seam. Often, this limited analysis is sufficient, because in many applications only the distributions of stress and convergence on the seam horizon are of interest. Also, by limiting the detailed analysis to only the seam, the displacement-discontinuity method provides considerable computational savings over other techniques that discretize the entire body (such as finite-element, discrete-element, or finite-difference). It is a direct result of this computational efficiency that the displacement-discontinuity method is able to handle large areas of tabular excavations, which is needed in many practical coal mining problems.

A displacement-discontinuity program incorporating a laminated medium was recently developed by the National Institute for Occupational Safety and Health, Pittsburgh

Research Laboratory; this new program is called LAMODEL. Traditional displacement-discontinuity programs use a homogeneous isotropic elastic formulation that simulates the overburden as one solid material. In contrast, the LAMODEL program simulates the geologic overburden stratifications as a stack of layers with frictionless interfaces. Specifically, each layer is homogeneous isotropic elastic and has the same elastic modulus, Poisson's ratio, and thickness. This "homogeneous layering" formulation does not require specifying the material properties for each individual layer, yet it still provides a realistic suppleness to the mining overburden that is not possible with the classic homogeneous isotropic elastic overburden model. From our experience, this suppleness provides a more accurate strata response for modeling local deformations, interseam interactions, and/or surface subsidence. The LAMODEL program calculates stresses and displacements at the seam level and at requested locations in the overburden or at the surface. Both linear elastic and nonlinear seam materials can be used. The program also has the ability to analyze (1) the interseam stresses resulting from multiple-seam mining, (2) the effects of topographic relief on pillar stress and gob loading, (3) the stress changes during mining through multiple mining steps, and (4) the surface subsidence.

INITIAL MATERIAL PROPERTY GENERATION

As mentioned earlier, one of the most difficult aspects of using a numerical model is determining the correct (most accurate) material properties for input. After developing numerous displacement-discontinuity models and then

comparing their results with field measurements and observations, a fairly streamlined, systematic technique for developing initial material properties was developed. Initially, the critical material properties (coal, gob, and rock mass) are

determined using a combination of laboratory research, empirical formulas, and experience. Then, in the calibration process, these initial material properties are systematically adjusted in subsequent runs of the model until the results correspond as closely as possible to field observations. This technique for determining material properties has many similarities to the procedure used by Karabin and Evanto [1999].

First, to address the problem of determining the input coal behavior, the basic coal strengths are derived from the empirical pillar strength formulas, which are solidly based on observed pillar behavior. Specifically, the peak strength of a model coal element is directly determined based on an in situ coal strength and its distance from the edge of the pillar [Heasley 1998] using the stress gradient implied by the Bieniawski pillar strength formula [Mark and Chase 1997]. This peak strength is then implemented using an elastic, perfectly plastic material model [Zipf 1992]. For an initial estimate, an in situ coal strength of 6.2 MPa (900 psi) [Mark and Barton 1997] and an elastic modulus of 2 GPa (300,000 psi) is typically used.

This general procedure for generating the initial coal properties for elements in LAMODEL fulfills a number of practical requirements. It provides LAMODEL pillars with peak strengths that closely follow the empirically proven Mark-Bieniawski pillar strength formula and with stress profiles that closely follow the Bieniawski stress profile. As opposed to a simple elastic material model with no load limit, this procedure using elastic-plastic material allows the pillars to reach a maximum load-carrying capacity and then realistically shed additional load to surrounding areas. Table 1 presents typical elastic-plastic material input values for 3-m (10-ft) coal elements in a 1.8-m (6-ft) seam with a 6.2-MPa (900-psi) in situ coal strength. (Note that the peak stress for the coal elements decreases from the core to the rib of the pillar, which gives the pillar the proper stress profile.)

Second, to address the gob loading and compaction behavior, a combination of laboratory research and modeling experience is used. In the laboratory, Pappas and Mark [1993] found that an exponentially strain-hardening material with a tangent modulus that increases linearly with stress provided a reasonable representation of simulated gob material. This

material model is implemented in LAMODEL [Heasley 1998] and is used for the gob modeling. The necessary input for this material is initial modulus, final modulus, and final vertical stress. From experience, these three values are initially set at 6.2 MPa (900 psi), 110 MPa (16,000 psi) and 27.6 MPa (4,000 psi), respectively (see table 1).

Table 1.—Typical elastic-plastic coal and strain-hardening gob parameters

COAL ELEMENTS: UPPER MINE		
Element	Peak stress, MPa	Peak strain
A (core)	85.9	0.04152
B	56.1	0.02712
C	38.3	0.01992
D (rib)	11.4	0.00552
GOB ELEMENTS		
Initial modulus, MPa	Final modulus, MPa	Final stress, MPa
6.2	110	27.6

The third critical set of material inputs in LAMODEL is for the overburden and consists of a lamination thickness and an elastic modulus. In LAMODEL, the lamination thickness has a major influence on the stress and displacement distribution at the seam and throughout the overburden. Prior research [Heasley 1998] comparing LAMODEL results with empirical relationships and measured field data shows that for large-scale stress distributions (such as longwall abutments) lamination thicknesses ranging from 15 to 100 m (50 to 300 ft) provide the best match to field measurements. However, when small-scale stress distributions (such as interseam stresses) or overburden displacements (such as subsidence) are of primary concern, then lamination thicknesses ranging from 3 to 15 m (10 to 50 ft) provide the best match to field observations [Karabin and Evanto 1999; Pappas and Mark 1993]. A lamination thickness of 15 m (50 ft) was used for case study 1, and a thickness of 5 m (15 ft) was used for case study 2. In both case studies, an elastic modulus of 20 GPa (3,000,000 psi) was used for the overburden.

STRESS MAPPING

In order to optimally use LAMODEL for accurate stress prediction at a given mine, the program should first be calibrated to the site-specific geomechanics based on previously observed stress conditions at that mine. One of the simplest and easiest methods to "quantify" the stress at a particular mine is to use "stress mapping." The pillar-centric stress mapping technique used here to quantify the observed stress conditions is a slight modification of the stress mapping technique originally developed for mapping areas of high horizontal stress

[Mucho and Mark 1994]. For LAMODEL calibration in these case studies, the primary interest is the stress in the pillars; therefore, the primary stress indicator is the pillar rib damage, although other stress-related features, such as roof cracks or floor heave, are also noted during the stress mapping process because they can be useful indicators of stress reactions.

Stress mapping a mine area essentially consists of traveling the rooms and crosscuts in that area and carefully observing the conditions of the pillars, roof, and floor. The observed

conditions are assigned a numerical rating and indicated on a map. For the rib damage stress mapping used here, the following numerical rating criteria were applied:

- 0: Rib still intact with no sloughed coal, original rock dust still in place.
- 1: Very slight pillar sloughage, some broken coal at base of rib.
- 2: Slight pillar sloughage, broken coal covers one-third of rib.
- 3: Significant pillar sloughage, broken coal piled halfway up rib.
- 4: Severe pillar sloughage, broken coal piled almost to roof.
- 5: Rib is composed of completely broken coal at the angle of repose, pillar may be failed.

MODEL CALIBRATION

In the model calibration process, the initial material properties are systematically adjusted in subsequent runs of the model until the results correspond as closely as possible to field observations and/or empirical formulas. For the coal properties, the in situ coal strength is adjusted until the pillar stress/failure in the model matches the observed pillar behavior as represented by the stress mapping/rib rating. For the gob properties, the final modulus value is typically adjusted up or down in LAMODEL to increase or decrease the gob stress until the model gob stress matches empirical abutment angle formulas [Mark and Chase 1997] and/or field measurements and observations. For the overburden properties, the lamination thickness is typically adjusted up to provide wider abutment stresses and smaller interseam stresses or adjusted down to provide narrower abutment stresses and greater interseam stresses as dictated by the observed stress mapping.

Once the model is reasonably calibrated and realistic pillar strengths and load distributions have been established, the

mechanics-based overburden behavior in the LAMODEL program can be effectively used to accurately analyze the complicated stresses and displacements associated with future complex mining scenarios. The above technique of combining empirical pillar strength and abutment load formulas with in-mine stress mapping and the analytical mechanics of a displacement-discontinuity model capitalizes on the strengths of both the empirical and analytical approaches to pillar design. The empirical formulas and observational calibration base the model on realistic behavior; the analytical mechanics allow the model to accurately consider and analyze the effects of numerous geometric and geologic variables. Using this technique, a displacement-discontinuity model can be the most practical approach for stress analysis and pillar design in complex mining situations such as multiple seams, random pillar layouts, and/or variable topography.

CASE STUDY 1

The first case study location was a multiple-seam, room-and-pillar coal mining situation in eastern Kentucky. At this location, the lower mine had been adversely affected by mining in the upper seam (see figure 1). In particular, the lower mine experienced serious ground control problems when it mined under a barrier pillar between two upper seam gobs ("Model Area" shown in figure 1). At this multiple-seam interaction site, in-mine stress mapping was used to quantify the severity of the multiseam interactions. This stress mapping was also used to calibrate a LAMODEL simulation of the area. The results of this numerical simulation provided predicted stress levels to avoid in future multiple-seam or high-cover mining.

The geology at this location is fairly typical of the southern Appalachian coal basin, with various sedimentary layers of sandstones, siltstones, shales, and numerous coal seams. The topography is very rugged, with various steep ridges and valleys that have a topographic relief of over 600 m (2,000 ft) (see figure 1). The overburden in the study area ranged from 150 to 450 m (500 to 1,500 ft), with an average of about 300 m (1,000 ft). Because of the highly variable topography at this mine, it was critical to include the topographic stress effects in LAMODEL in order to obtain accurate results.

The overlying, or upper, mine operates in the Upper Darby Seam, which typically averages about 2.0 m (6.0 ft) thick. The lower mine operates in the Kellioka Seam, which averages about 1.5 m (4.5 ft) thick in the study area. The interburden between the two seams averages about 14 m (45 ft) and consists of interbedded sandstones and shales. The core logs nearest to the study site indicate about 3.5 to 5 m (10 to 15 ft) of shale directly over the Kellioka Seam. This is then overlain by 7.5 to 10.5 m (25 to 35 ft) of interbedded sandstones and shales, with shale primarily forming the floor of the Upper Darby Seam. Both mines are room-and-pillar drift mines and use continuous miners for coal extraction. In some production sections, depending on local mining conditions, the mines remove the pillars on retreat for full extraction.

In the study area, the lower mine was forced to dogleg around an abandoned, flooded mine in the upper seam (not shown in figure 1). This dogleg forced the lower mine to develop entries under a barrier pillar between two previously mined, upper seam gobs, as shown in the detail of figure 2. Mine management anticipated increased multiple-seam stresses in this area. In an effort to safely control these higher stress levels, the mine located the critical travelway and belt entries

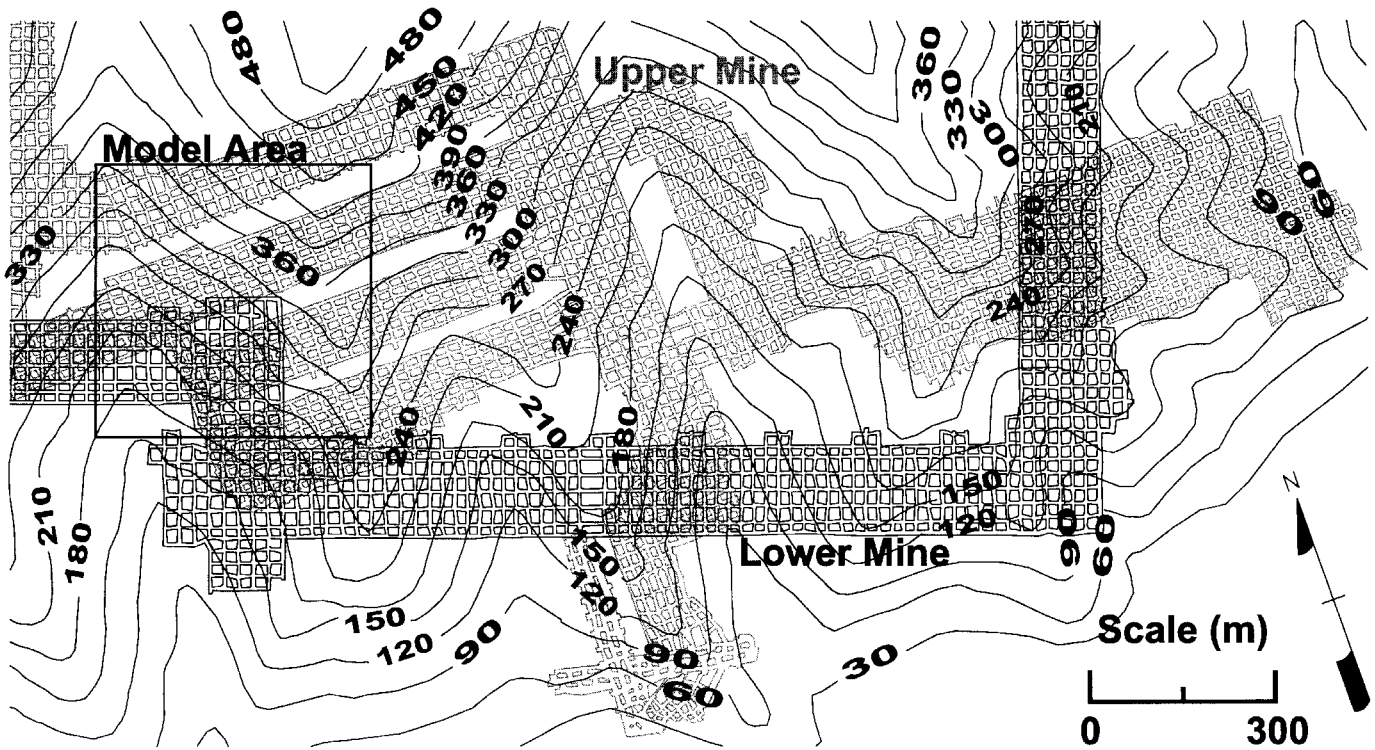


Figure 1.—Mine map for case study 1.

away from the influence of the barrier pillar and used a double row of supplemental cable bolts on 0.6-m (2-ft) centers throughout most of the travel entry under the upper seam mining. With these precautions, the mine was able to safely and efficiently mine the entries under the barrier pillar and surrounding gob. However, throughout the section, the stress effects of the overlying barrier and gob were abundantly visible, and on two occasions (in the northeast corner of the section), the mine was unable to complete crosscuts because of roof instability and poor pillar conditions.

STRESS MAPPING

In order to quantify the stress effects of the barrier pillar and gob zones on the lower seam, a detailed stress mapping of a large portion of overmined area was performed. As previously described, the amount of rib sloughing was noted on a scale of 0 to 5, and any stress-related features such as roof cracking, potting, cutting, or floor heave were also noted. The results of this stress mapping exercise are shown in figure 3A. In this figure, the observed condition of the pillar ribs is shown in gray scale by degree of damage; the darker shades signify increased sloughing (or stress). Also, the observed roof cracking, potting, cutting, and floor heave are indicated on the map.

Several useful observations can be made from the detailed stress mapping shown in figure 3A. First, the transfer of the abutment stresses from the overlying mine to the area under the barrier pillar and to the area at the ends of the pillared sections can clearly be inferred in the rib conditions of the lower mine pillars. Also, as a corollary to the interseam transfer of the

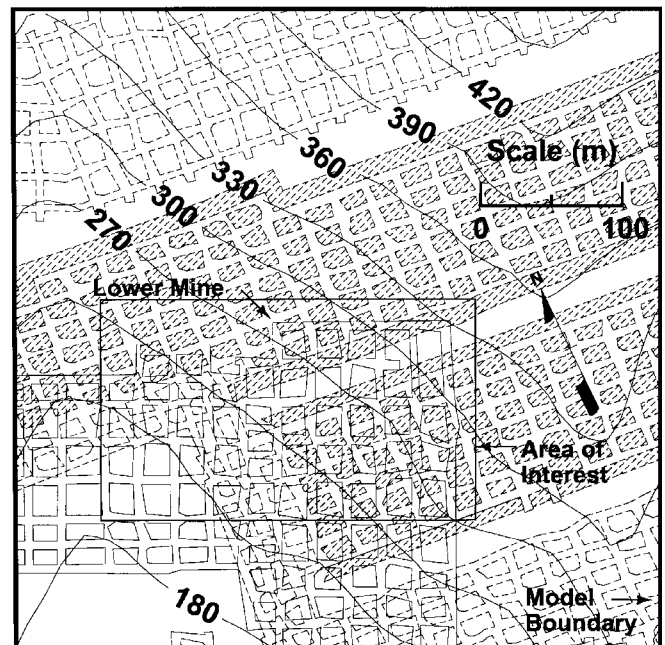


Figure 2.—Enlargement of model area for case study 1.

barrier pillar abutment stresses, the lower seam pillars under the gob areas in the upper seam show considerable stress relief. The next major observation pertains to the location and orientation of the roof tension cracks and guttering. Clearly, the tension cracks in the roof of the northeast corner of the section are situated directly under the overlying barrier pillar and are oriented parallel to the axis of this pillar. Also, the observed

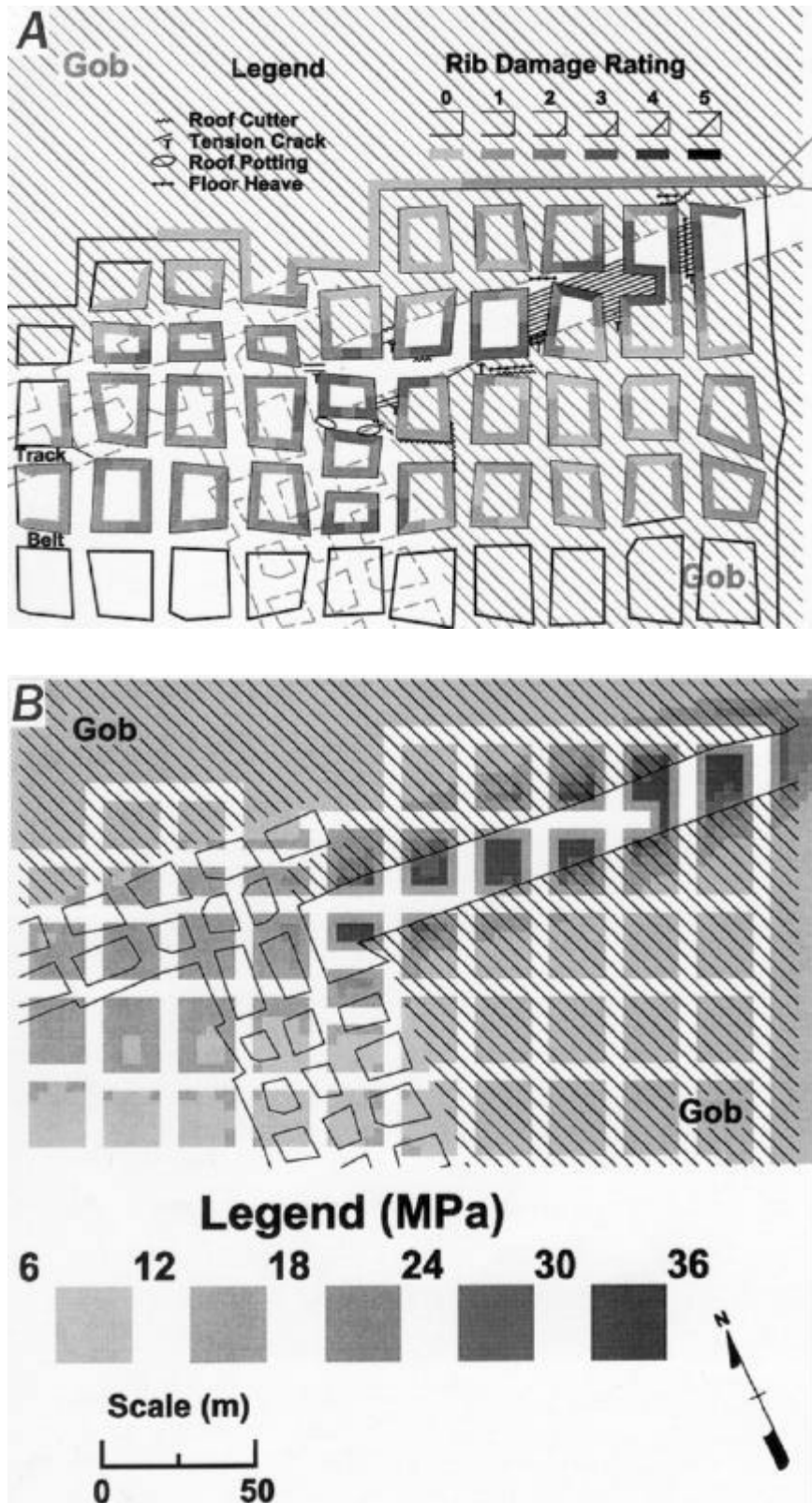


Figure 3.—Comparison between (A) in-mine stress mapping and (B) LAMODEL calculated stresses for mine 1.

compressional roof cutters are located at the edge of, or adjacent to, the overlying abutment zones and oriented parallel to these zones. This location and orientation of the tension and compression suggest that the lower mine roof is behaving like a beam that is bending into the relatively soft coal seam under the load of the barrier pillar in the upper seam. This beam scenario correctly accounts for the tension directly under the applied load and the compression adjacent to the applied load.

MODEL DESIGN

For the LAMODEL simulation of this area, the seams were discretized with 3-m (10-ft) elements in a 150-by-150 grid with the model boundary, as shown in figure 2. Symmetrical seam boundary conditions were set on all four sides, and no free-surface effects were included. The interburden was set at 14 m (45 ft), and the rock mass was simulated with a modulus of 20 GPa (3,000,000 psi) and 15-m (50-ft) thick laminations. An elastic, perfectly-plastic material was used for the coal in both seams, and the peak strength of the coal was determined from the Mark-Bieniawski pillar strength formula, as in appendix C of Heasley [1998]. Table 2 presents the coal and gob input values used in LAMODEL for this particular case study.

Also, because of the high topographic relief at the site, the topography was discretized with 15-m (50-ft) elements for an area extending 300 m (1,000 ft) beyond the limits of the displacement-discontinuity grids. The importance of including the topographic stress effects in the model is evident in figure 4, which shows the topographic stress at the level of the lower mine. It is interesting to note in this figure the amount to which the topographic stress is "smoothed" with depth compared to the original topography. Also, it is evident that the overburden stress changes about 3 MPa (450 psi) in traversing from the southwest to the northeast corner of the pillars in the study area. This difference in overburden stress could very well account for the increased mining difficulties at the northeast corner of the section.

MODEL CALIBRATION AND ANALYSIS

Very little work was required for calibrating the LAMODEL simulation to the observed stress mapping. In both seams, the original Mark-Bieniawski pillars strengths and the initial overburden modulus and lamination thickness provided a good fit to the observed pillar behavior (see figure 3). The only parameter that was ultimately manipulated was the modulus of the gob material (see table 2). This modulus was adjusted to provide a peak gob stress in the range of 40% to 60% of in situ stress, a reasonable range for a 90-m (300-ft) wide gob in 300 m (1,000 ft) of cover [Mark and Chase 1997]. A number of variations in pillar strength, overburden modulus, and lamination thickness were investigated, and the simulation results varied a little. However, the initial parameter values with the adjusted gob modulus provided a reasonably optimum fit to the observational stress mapping.

Table 2.—Coal and gob parameters for case study 1

COAL ELEMENTS: UPPER MINE		
Element	Peak stress, MPa	Peak strain
A (core)	85.9	0.04152
B	56.1	0.02712
C	38.3	0.01992
D (rib)	11.4	0.00552
COAL ELEMENTS: LOWER MINE		
Element	Peak stress, MPa	Peak strain
A (core)	113.2	0.05472
B	73.5	0.03552
C	53.6	0.02592
D (rib)	13.9	0.00672
GOB ELEMENTS		
Initial modulus, MPa	Final modulus, MPa	Final stress, MPa
6.2	110	27.6

The calculated pillar stresses from the final calibrated LAMODEL run are shown in figure 3B. These modeled stresses correlate extremely well with the stress mapping in figure 3A. The high stresses under the barrier pillar are evident in the model results; the area of stress relief under the gob is also shown. Even the intermediate stress levels under the overlying pillars and solid coal in the southwest corner of the model closely match the observed pillar stress mapping. A few more details of the modeled stress output are shown in figure 5, where the isolated single-seam stress and just the interseam stress are displayed. In this figure, the effect of the overlying barrier pillar can be clearly seen. In particular, the maximum single-seam stress on the pillars (figure 5A) of around 15 MPa (2,200 psi) is seen to increase to over 36 MPa (5,200 psi) with the addition of the barrier pillar stress (figures 5B and 5C). Also, it is interesting to note the increased abutment stress in the northeast corner of the section (figure 5C), presumably due to the increasing overburden and the increasing distance from the upper panel boundaries. A stress relief of about 7 MPa (1,000 psi) under the gob areas is also shown in figure 5C.

For the mine management, this stress modeling using LAMODEL, in conjunction with good in-seam correlations with stress mapping, provided valuable background information for future multiple-seam mine planning. In this case study, a calculated multiseam stress concentration of about 15 MPa (2,200 psi) with pillar stresses of 35 MPa (5,200 psi) at this site caused sufficient roof instability to prohibit the mine from driving two crosscuts. Therefore, it seems that the 15-MPa stress concentration (35-MPa pillar stress) is close to an upper limit for successful entry development at this mine. The mine can use this calculated limit in conjunction with future modeling in order to lay out future room-and-pillar panels influenced by overlying workings.

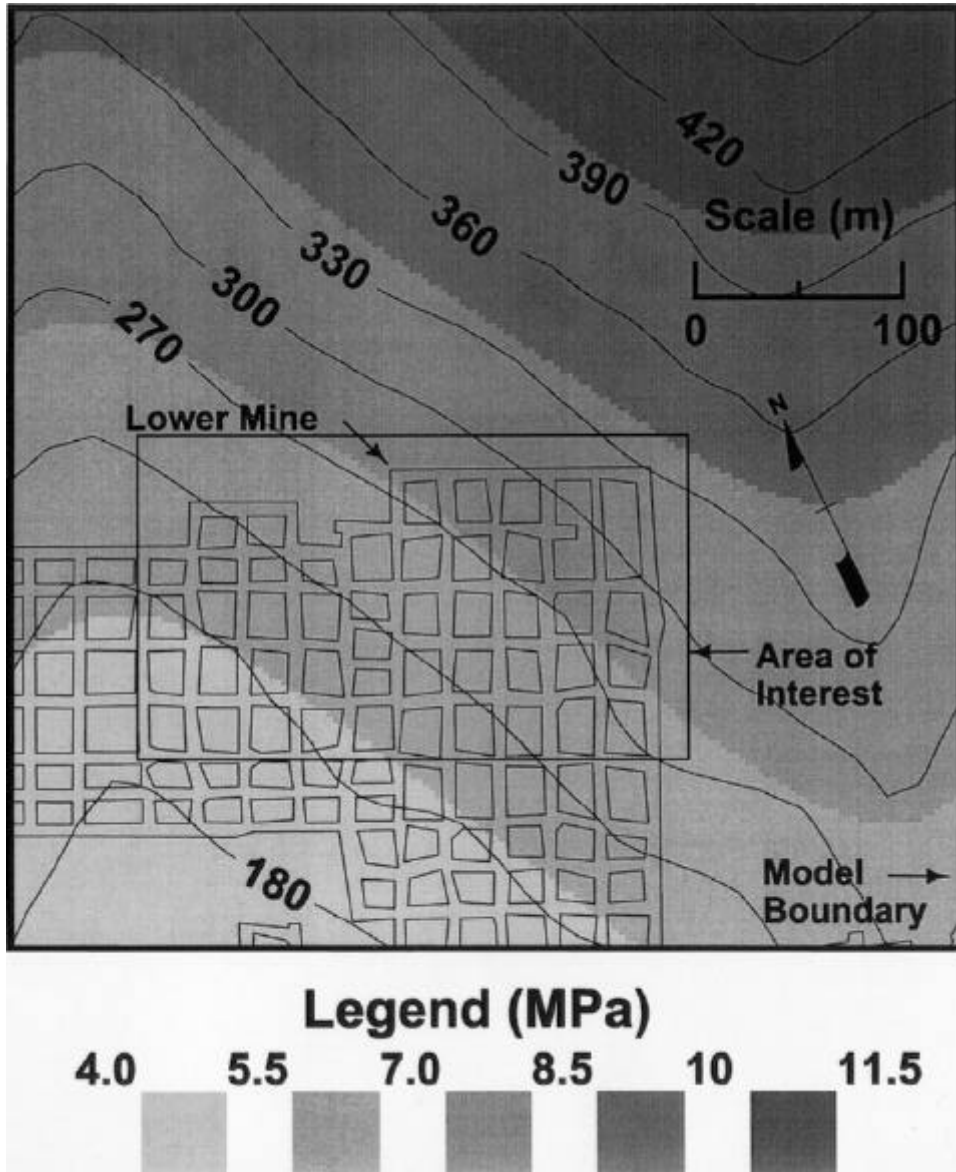


Figure 4.—Calculated topographic stress for case study 1.

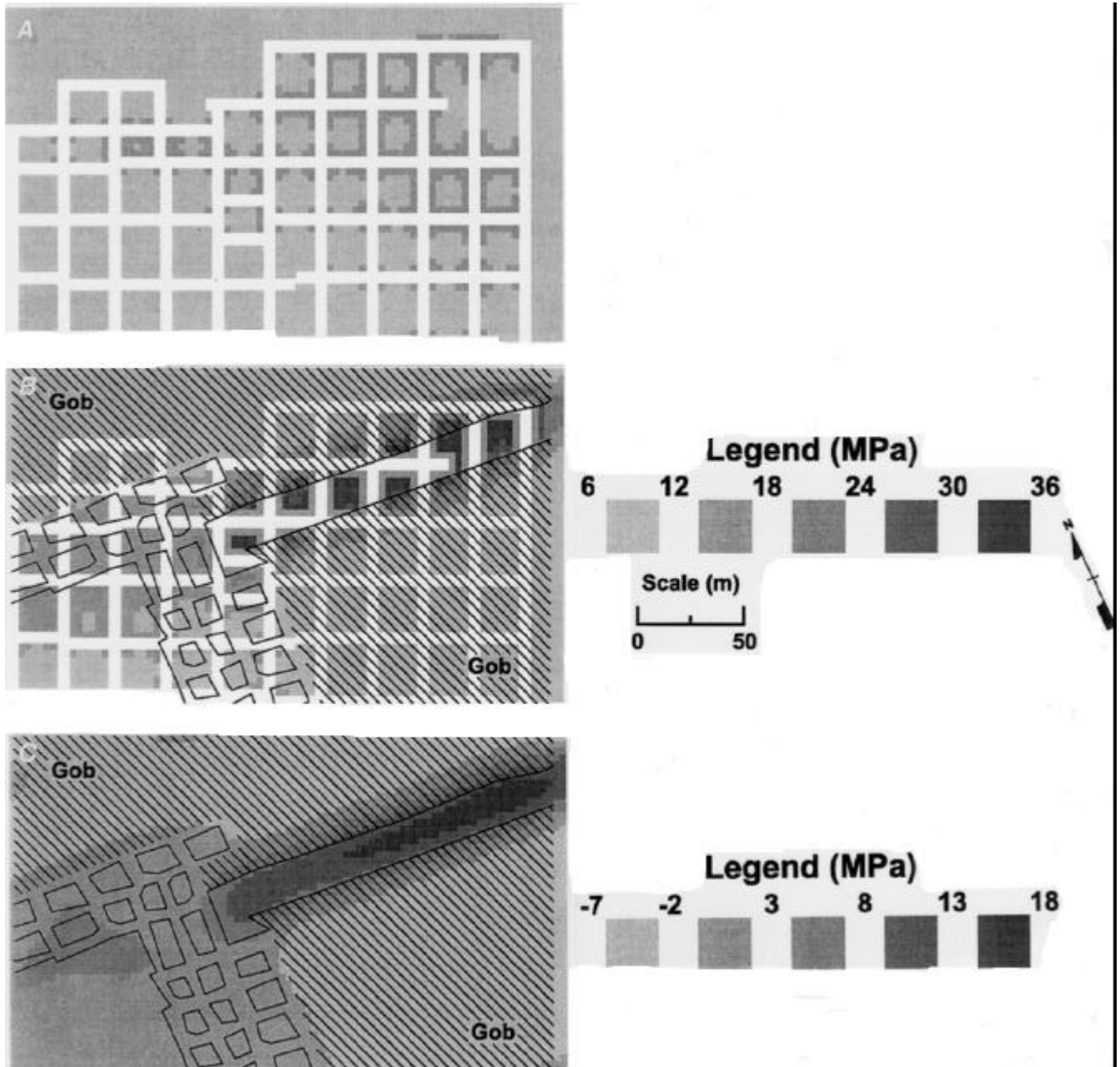


Figure 5.—The LAMODEL stress output for case study 1. A, Single-seam stress; B, multiple-seam stress; C, additional stress from upper seam.

CASE STUDY 2

The second study site was a longwall mine located in Greene County, PA, and operating in the Sewickley Seam. This mine is underlain by an abandoned room-and-pillar operation in the Pittsburgh Seam. The primary problem at this site was the transfer of multiple-seam stress from the lower mine. Yielding of smaller pillars and the subsequent transfer of their load to larger pillars in the lower seam apparently caused increases in vertical stress in the upper seam that were noticed during development of the headgate entries (see figure 6). Severe pillar spalling and poor roof conditions were experienced when mining the headgate over these large pillars in the lower seam (figure 7). Mine management was concerned that these underlying abutment pillar stresses would continue to be a problem farther in by in the headgate and also in the longwall panel because there were several areas in the lower seam where similar pillar conditions seemed to exist.

In the study area, the overburden above the Sewickley Seam ranges from 150 to 280 m (500 to 910 ft) and consists predominantly of interbedded shales and sandstones. The interburden between the Sewickley and Pittsburgh Seams ranges from 27 to 30 m (90 to 100 ft) thick and consists of interbedded shales and limestones. The average mining heights of the Sewickley and Pittsburgh Seams are 1.5 m (5 ft) and 1.8 m (6 ft), respectively. The immediate roof of the Sewickley Seam is composed of a jointed dark sandy shale that ranges from 3 to 4.5 m (10 to 15 ft) thick and is overlain by a competent limey shale. The immediate floor of the Sewickley Seam is composed of a 1.2-m (4-ft) thick dark limey shale underlain by a competent limestone unit.

STRESS MAPPING

Figure 6 shows the overlay of the lower seam workings on the upper seam longwall panel and the area of the headgate where the stress mapping and model calibration were conducted. As described earlier, the process of calibration involved the use of stress mapping to assign a rating from 0 to 5 based on the observed pillar rib conditions. The first 600 m (2,000 ft) of the headgate entries, where problems first occurred (see figure 6), were traversed and assigned rating numbers based on the observed conditions. Figure 7A shows the rib damage rating assigned to each rib in this area of the headgate.

MODEL DESIGN AND CALIBRATION

Once the stress mapping was complete, LAMODEL calibration was initiated. For calibration purposes, the "Stress Mapped Area" shown in figure 6 was discretized with 3-m (10-ft) elements with a 90-by-200 grid. Symmetrical boundary conditions were set on all four sides, and no free-surface effects were included. The interburden was set at 27 m (90 ft), and the rock mass was simulated with a modulus of 20 GPa (3,000,000 psi) and 5-m (15-ft) thick laminations. The overburden above the lower mine in this area ranged from 180 to 300 m (600 to

1,000 ft). Due to this variable topography, the topographic stress effects were included in LAMODEL in order to obtain accurate overburden stress results.

Based on the observed stress mapping, model calibration was conducted under the assumption that the smaller pillars (<10.5 m (<35 ft) wide) in the lower mine had essentially yielded and transferred their load to nearby larger pillars. Therefore, in the first step of the calibration process, the coal strength in the lower mine model was adjusted until the pillars showed this observed behavior. Initially, using the elastic-plastic implementation of the Bieniawski formula, as previously explained, an in situ coal strength of 6.2 MPa (900 psi) was used to calculate peak stress and strain values for each coal element, and the initial calibration model was run. In this initial model, the coal in the lower mine was too strong and did not show the desired yielding in the smaller pillars. Therefore, in order to obtain the desired small pillar yielding and subsequent stress transfer to the larger pillars, the in situ coal strength in the lower seam was gradually decreased to 4.2 MPa (600 psi).

With the in situ coal strength of 4.2 MPa (600 psi) in the lower seam and the original coal strength of 6.2 MPa (900 psi) in the upper seam, the model correlated very well with the rib damage rating from the stress mapping. The rib damage rating is in gray scale in figure 7A; the results from the model are in a comparative gray-scale plot in figure 7B. Clearly, the model pillars with high rib stress correlate well with the pillars with high damage ratings. It can be observed in figure 6 that these high rib stresses occur over the large pillars located in the lower mine in conjunction with overburden that exceeds 250 m (870 ft). The final coal and gob properties used in LAMODEL for the upper and the lower mine are presented in table 3.

Table 3.—Coal and gob parameters for case study 2

COAL ELEMENTS: UPPER MINE		
Element	Peak stress, MPa	Peak strain
A (core)	102.3	0.04944
B	66.5	0.03216
C	48.7	0.02352
D (rib)	12.9	0.00624
COAL ELEMENTS: LOWER MINE		
Element	Peak stress, MPa	Peak strain
A (core)	56.8	0.02747
B	36.9	0.01787
C	27.0	0.01307
D (rib)	7.2	0.00347
GOB ELEMENTS		
Initial modulus, MPa	Final modulus, MPa	Final stress, MPa
6.2	138	27.6

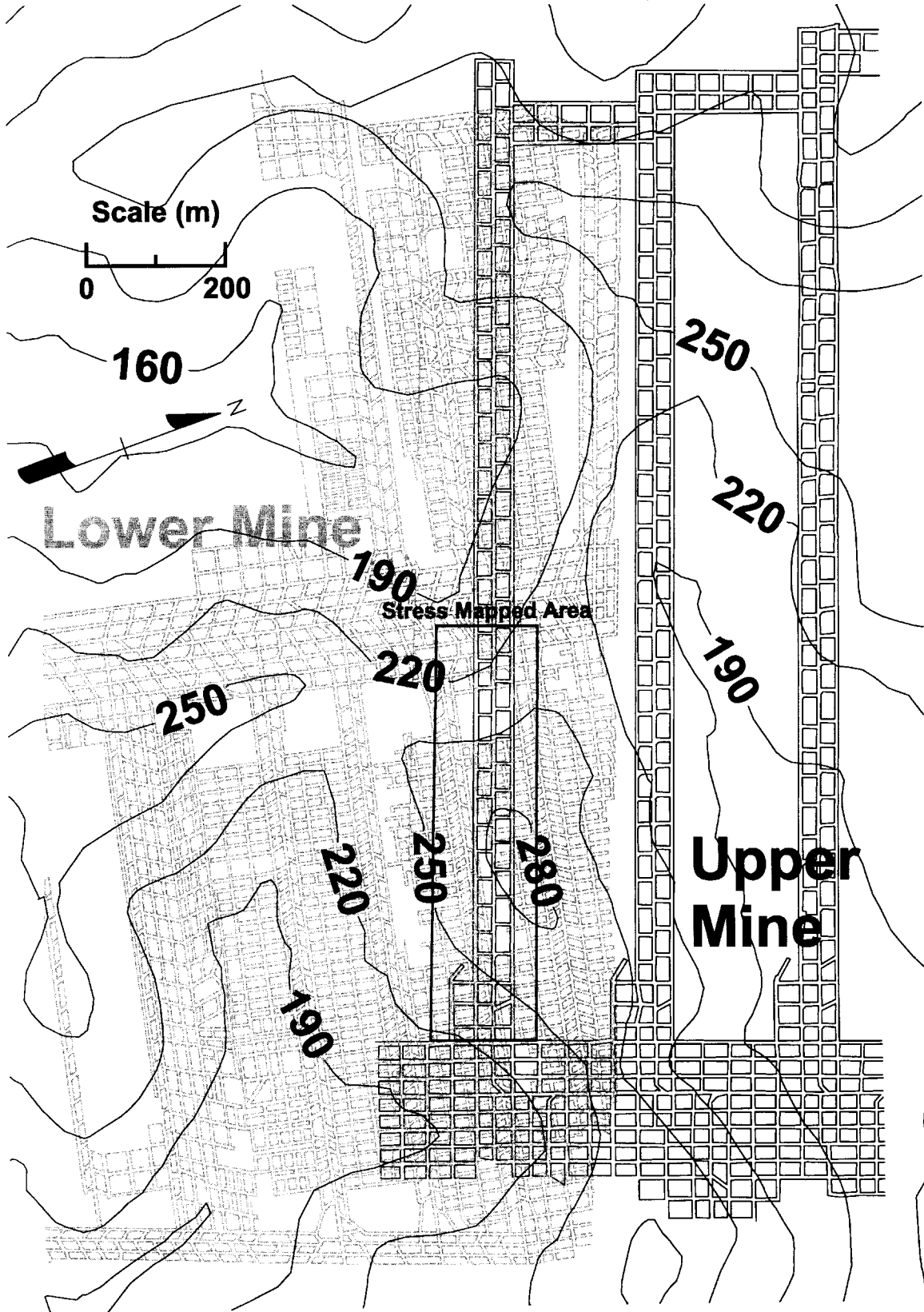


Figure 6.—Mine map for case study 2.

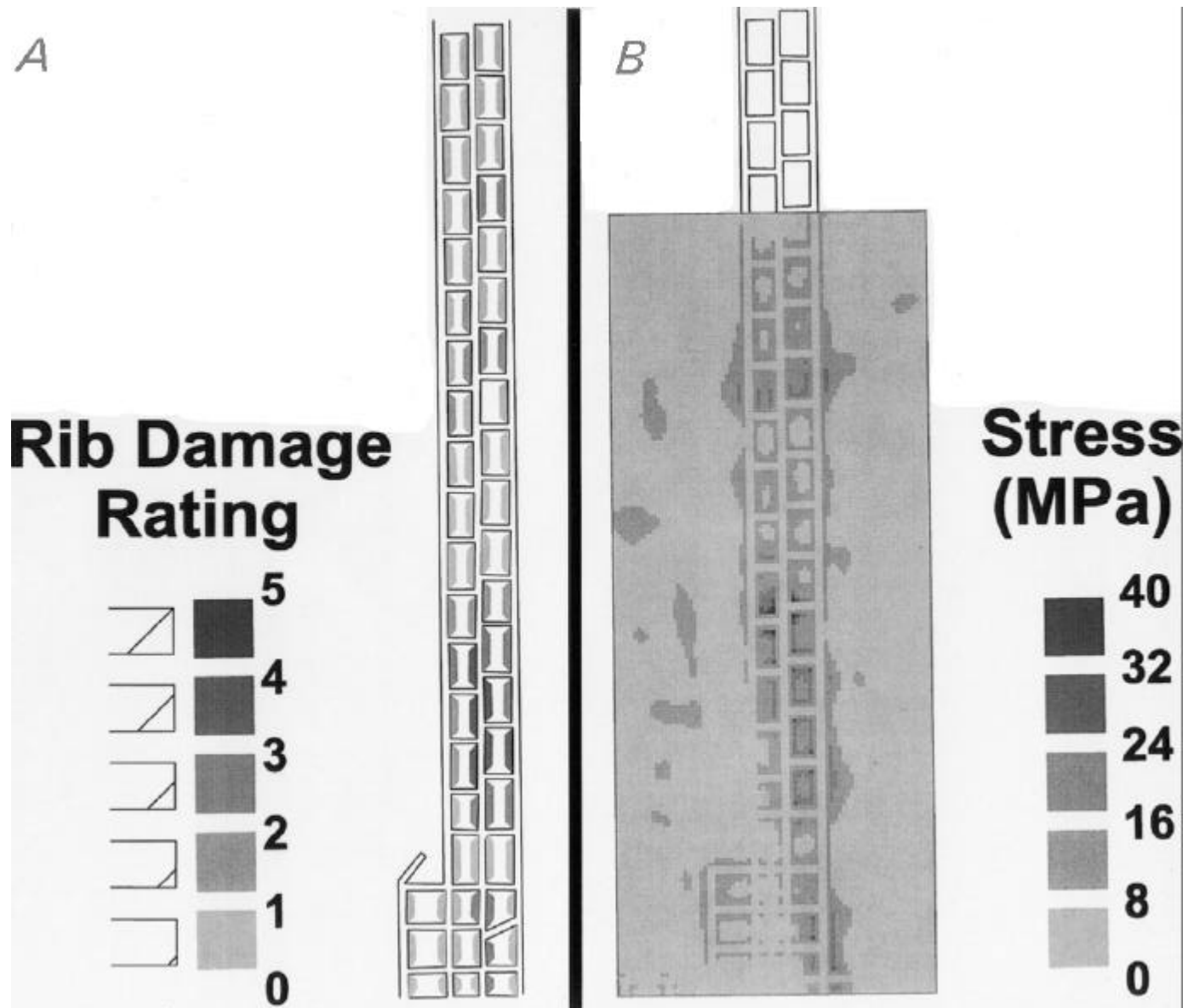


Figure 7.—Comparison between in-mine stress mapping and LAMODEL calculated stresses. *A*, rib damage rating; *B*, stress (MPa).

STRESS PREDICTION FOR MINE PLANNING

With material properties calibrated from observed stress conditions in the mine, additional LAMODEL analyses were created and run in order to predict areas of potential problems within the remaining headgate and the future longwall panel. Figure 8 shows two areas of the headgate and longwall panel that were modeled using optimized properties from the calibration process. These gray-scale plots show the interseam stress, which is the additional stress on the upper mine due to the lower seam mining. In this figure, zone 1 covers the upper (inby) part of the headgate panel and the first 365 m (1,200 ft) of the longwall panel; zone 2 covers the lower part of the headgate (where the stress problems were first noticed) and the last (outby) 330 m (1,100 ft) of the longwall panel. In these

two zones, the lower mine pillar conditions and the overburden depths appeared similar; therefore, the poor pillar conditions encountered in zone 2 were expected in zone 1.

However, when comparing the interseam stress between these two zones as shown in figure 8, it is obvious that the stress in zone 2 is considerably greater than that in zone 1. Closer investigation reveals two primary reasons for this. First, the maximum depth over the gate roads and panel in zone 2 is over 280 m (920 ft); in zone 1, the maximum depth is just over 250 m (870 ft). Second, when examining the model output for the lower mine, there seems to be less pillar yielding in zone 1 than in zone 2. In figure 6, it can be seen that the smaller pillars in zone 1 are dispersed among larger pillars and have widths >12 m (>40 ft), whereas in zone 2, there is a large area of pillars with widths <10.5 m (<35 ft). The larger, more dispersed small

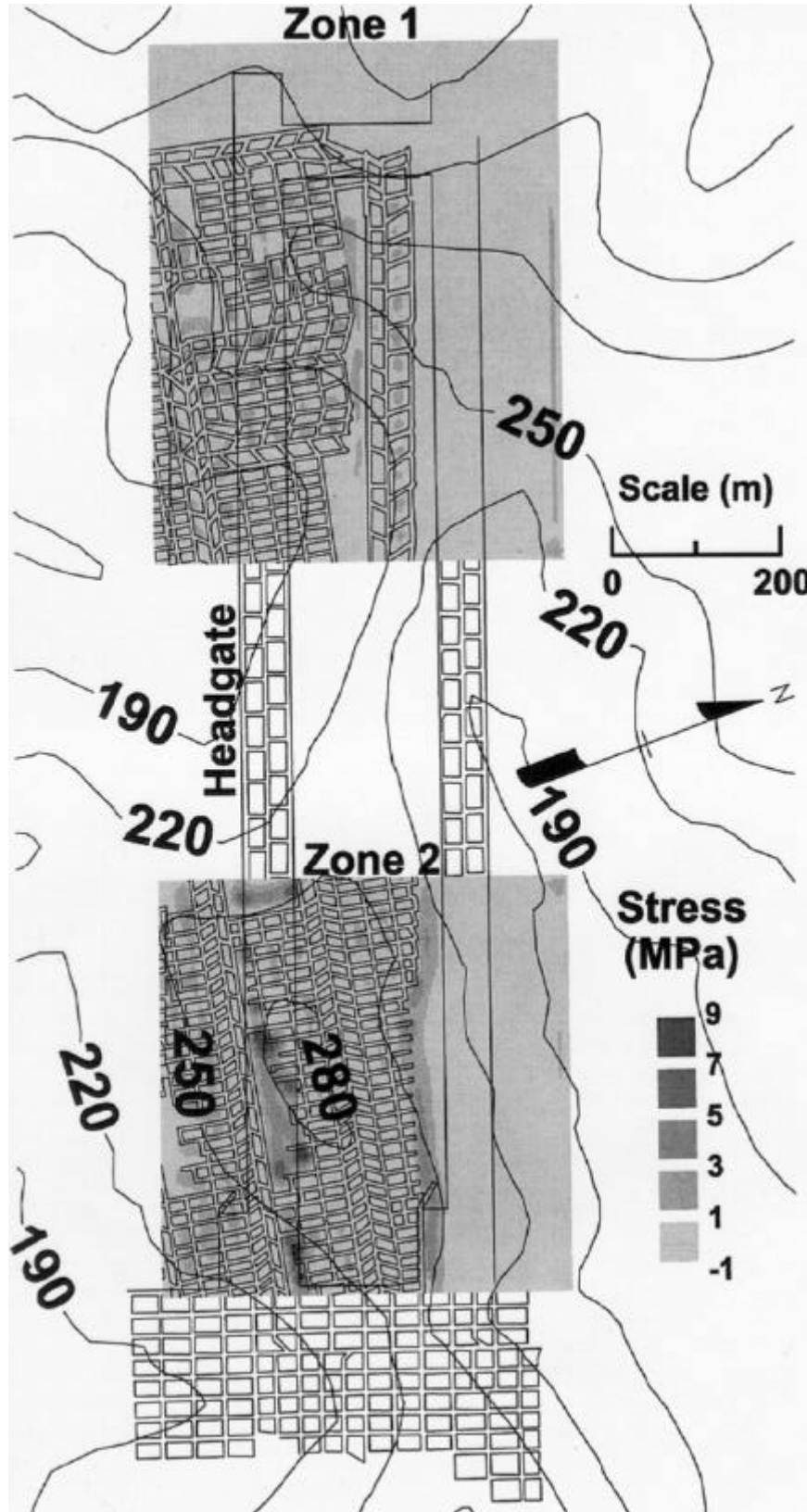


Figure 8.—Interseam stress for zones 1 and 2.

pillars in zone 1 suffer less pillar yielding and therefore cause less load transfer (or interseam stress) on the upper mine (see figure 8). During headgate development in zone 1, no pillar problems were encountered. Thus, the calibrated model successfully predicted the reduced stress conditions in the headgate of zone 1.

The mine management was also concerned about the multiple-seam stresses adversely affecting the retreating longwall panel. In particular, a large, irregularly shaped barrier pillar in the lower mine is superimposed under the center line of the initial half of the longwall panel in zone 1 (see figure 8). However, the interseam stress calculated by the model from this barrier pillar reaches only about 3 MPa (450 psi). When the panel was mined, this slightly increased face stress presented very little problem. Some slight spalling was present on the face during the extraction, but overall face conditions were generally good and no severe ground control problems were evident.

However, in the lower part of the panel near the headgate location where poor ground conditions were first encountered (see zone 2, figure 8), an area of interseam stress up to 9 MPa (1,300 psi) is evident in the panel. Because of the underlying barrier pillar, the mine anticipated difficult face conditions in

this area. Indeed, when the longwall face reached this area, ground control problems that included severe face spalling and poor roof condition in the headgate entries were encountered. In fact, the stress interaction with the lower seam was severe enough to stop the longwall face about 15 m (50 ft) short of the longwall recovery chute and make recovery of the supports difficult.

When comparing conditions in zone 1 with those of zone 2, there seems to be a very fine line in the occurrence of ground control problems in the upper seam depending on the overburden depth and the pillar size in the lower seam. Problems were more likely to occur when the depth of cover over the Sewickley Seam exceeded 250 m (820 ft) and when large areas of narrow pillars (<10.5 m (<35 ft) wide) in the lower seam were located adjacent to a larger barrier pillar. These conditions caused yielding of the narrow pillars and the shedding of their load to the adjacent larger pillar. This concentrated abutment stress was then transferred to the upper mine, resulting in poor ground conditions in areas of the headgate entry and longwall panel. Throughout this case study, the calibrated LAMODEL program successfully predicted the high stress areas in advance of mining.

CONCLUSIONS

The primary purpose of the case studies presented in this paper was to validate the new LAMODEL boundary-element program and investigate its utility for stress modeling in mine planning. Based on the comparisons between the stress mapping and the model results for the two case studies, it seems that the LAMODEL program can be calibrated to produce good correlations with the observed stresses. In addition, once realistic pillar strengths and load distributions were established by calibration, the mechanics-based overburden behavior in LAMODEL effectively analyzed the complicated stresses and displacements associated with the complex multiple-seam mining scenarios and successfully predicted upcoming high stress conditions in advance of mining for preventive action by mine management. In case study 1, a calculated multiseam stress concentration of around 15 MPa (2,200 psi) with pillar stresses of 35 MPa (5,200 psi) seemed to be an upper limit for successful entry development at this mine. Similarly, in case study 2, a calculated multiple-seam stress concentration of 9 MPa (1,300 psi) produced severe face spalling and poor roof conditions in the headgate entries, whereas a 3-MPa (450-psi) stress concentration was barely noticeable.

A secondary goal was to present a fairly streamlined, systematic methodology for developing initial material properties and then calibrating these properties to field observations. Initially, the critical material properties (coal, gob, and rock mass) are developed using a combination of laboratory research, empirical formulas, and experience. Then, in the calibration process, a previously mined area is "stress mapped" by quantifying the observed pillar and strata behavior using a simple numerical rating system. Finally, the initial material properties are systematically adjusted in subsequent runs of the model until the results provide the best correlation between the predicted stresses and the observed underground stress rating. This methodology of combining empirical pillar strength and abutment load formulas with in-mine stress mapping and the analytical mechanics of a displacement-discontinuity model capitalizes on the strengths of both the empirical and analytical approaches to pillar design to provide a practical technique for mine planning in difficult situations.

REFERENCES

Heasley KA [1998]. Numerical modeling of coal mines with a laminated displacement-discontinuity code [Dissertation]. Golden, CO: Colorado School of Mines, Department of Mining and Earth Systems Engineering.

Kanniganti RS [1993]. Interactive prediction software for underlying multi-seam design [Thesis]. Blacksburg, VA: Virginia Polytechnic Institute and State University, Department of Mining and Minerals Engineering.

Karabin GJ, Evanto MA [1999]. Experience with the boundary-element method of numerical modeling to resolve complex ground control problems. In: Proceedings of the Second International Workshop on Coal Pillar Mechanics and Design. Pittsburgh, PA: U.S. Department of Health and Human Services, Public Health Service, Centers for Disease Control and Prevention, National Institute for Occupational Safety and Health, DHHS (NIOSH) Publication No. 99-114, IC 9448.

Mark C [1992]. Analysis of longwall pillar stability (ALPS): an update. In: Proceedings of the Workshop on Coal Pillar Mechanics and Design. Pittsburgh, PA: U.S. Department of the Interior, Bureau of Mines, IC 9315, pp. 238-249.

Mark C, Barton TM [1997]. Pillar design and coal strength. In: Proceedings - New Technology for Ground Control in Retreat Mining.

Pittsburgh, PA: U.S. Department of Health and Human Services, Public Health Service, Centers for Disease Control and Prevention, National Institute for Occupational Safety and Health, DHHS (NIOSH) Publication No. 97-122, IC 9446, pp. 49-59.

Mark C, Chase FE [1997]. Analysis of retreat mining pillar stability (ARMPS). In: Proceedings - New Technology for Ground Control in Retreat Mining. Pittsburgh, PA: U.S. Department of Health and Human Services, Public Health Service, Centers for Disease Control and Prevention, National Institute for Occupational Safety and Health, DHHS (NIOSH) Publication No. 97-122, IC 9446, pp. 17-34.

Mucho TP, Mark C [1994]. Determining horizontal stress direction using the stress mapping technique. In: Peng SS, ed. Proceedings of the 13th International Conference on Ground Control in Mining. Morgantown, WV: West Virginia University, pp. 277-289.

Pappas DM, Mark C [1993]. Behavior of simulated longwall gob material. Pittsburgh, PA: U.S. Department of the Interior, Bureau of Mines, RI 9458.

Zipf RK Jr. [1992]. MULSIM/NL theoretical and programmer's manual. Pittsburgh, PA: U.S. Department of the Interior, Bureau of Mines, IC 9321.

EXPERIENCE WITH THE BOUNDARY-ELEMENT METHOD OF NUMERICAL MODELING TO RESOLVE COMPLEX GROUND CONTROL PROBLEMS

By George J. Karabin, P.E.,¹ and Michael A. Evanto, P.G.²

ABSTRACT

The Mine Safety and Health Administration, Pittsburgh Safety and Health Technology Center, Roof Control Division, is routinely involved in the evaluation of ground conditions in underground coal mines. Assessing the stability of mined areas and the compatibility of mining plans with existing conditions is essential to ensuring a safe working environment for mine workers at a given site. Since 1985, the Roof Control Division has successfully used the boundary-element method of numerical modeling to aid in the resolution of complex ground control problems. This paper presents an overview of the modeling methodology and details of techniques currently used to generate coal seam, rock mass, and gob backfill input data. A summary of coal and rock properties used in numerous successful evaluations throughout the United States is included, and a set of deterioration indices that can aid in the quantification of in-mine ground conditions and verification of model accuracy is introduced. Finally, a case study is detailed that typifies the complexity of mining situations analyzed and illustrates various techniques that can be used to evaluate prospective design alternatives.

¹Supervisory civil engineer.

²Geologist.

Mine Safety and Health Administration, Pittsburgh Safety and Health Technology Center, Roof Control Division, Pittsburgh, PA.

INTRODUCTION

Effective mine design has long been recognized as an essential element in establishing safe and productive mining operations. Numerous investigators have developed techniques to analyze pillar stability and maximize mining efficiency. The work of Holland and Gaddy [1964], Obert and Duvall [1967], and Bieniawski [1984], to name a few, served as a staple for mining engineers for many years. With the advent of longwall mining, new techniques were developed by Carr and Wilson [1982], Hsuing and Peng [1985], Choi and McCain [1980], and Mark [1990] to address design considerations for that technology. Most recently, the development of the Analysis of Retreat Mining Pillar Stability (ARMPS) methodology [Mark and Chase 1997] for the evaluation of retreat mining operations added an additional tool for engineers to design and evaluate full pillaring techniques.

Each of these methods can provide a reasonable estimate of pillar strength and stability under specific conditions and relatively simple mining geometries. In practice, however, situations often arise where areas of concern contain a number of pillar configurations with varying entry and crosscut widths, spacings, and orientations. Additional factors, such as non-uniform pillar lines, remanent stumps scattered throughout irregularly shaped gobs, and multiple-seam mining, can further complicate an analysis. In such instances, application of the previously mentioned empirical and analytical methods to accurately evaluate ground stability is difficult, if not totally impossible.

A primary function of the Roof Control Division, Pittsburgh Safety and Health Technology Center, is to provide technical assistance to the Mine Safety and Health Administration (MSHA) and the mining industry in the resolution of complex

roof control problems. In order to evaluate mining systems not easily treated by simplified empirical or analytical methods, boundary-element numerical modeling was initiated in 1984 and expanded in 1987 with acquisition of the BESOL system from Crouch Research, Inc., St. Paul, MN. The ability of the three-dimensional (3-D) boundary-element method to model large mine areas with complex geometries has enabled the Roof Control Division to successfully simulate conditions and identify potential solutions to ground control problems in mines throughout the United States. The technique has been applied to a variety of mining scenarios, including longwall and room-and-pillar operations using both conventional and yield pillar configurations. The influence of vertical and horizontal stress has been modeled to simulate underground conditions ranging from deteriorating roof and persistent falls to areas of squeezing ground and complete pillar failure.

In the process of developing numerical models for the various mining operations analyzed during the last 10 years, a systematic simulation methodology has evolved. Techniques to estimate the necessary coal, rock, and gob backfill properties have been established, and a deterioration index was developed to quantify in-mine roof, floor, and pillar behavior to assist in calibrating model parameters and evaluating potential mine design alternatives. This paper presents a brief description of the BESOL system, an overview of the simulation process used, and details of methods used to construct models and estimate rock mechanics parameters. A discussion of the deterioration index system and details of a case study typifying an actual mine simulation and techniques used to evaluate conditions and proposed mining options is also included.

BESOL SYSTEM DESCRIPTION

BESOL is a system of computer programs for solving rock mechanics problems based on the boundary-element displacement discontinuity method of analysis. The 3-D MS221 version (yielding and multiple-seam capability) was acquired from Crouch Research, Inc., and has been used by the Roof Control Division to evaluate complex mining systems since 1987. The BESOL system is complete with graphic pre- and postprocessors that greatly simplify model construction and output data interpretation.

Figure 1 presents a generalized BESOL boundary-element model that illustrates a tabular seam or ore body surrounded by

a homogenous, isotropic, linearly elastic rock mass. Input data include elastic rock mass properties and rock strength criteria, seam properties, and backfill or artificial support characteristics. A definition of the seam plane(s), detailed geometry of the excavation, mining depth, seam height, and a complete 3-D in situ stress state of the model are also required. Output capabilities include stress, strain, and displacement calculations within user-selected areas (both on and off the seam plane), failure index (Mohr-Coulomb or Hoek-Brown roof and floor safety factors) calculations at variable locations in the rock mass, and energy release estimates in yielding areas.

BESOL was selected by the Roof Control Division because it offered a number of features considered essential in simulating complex mining situations. These include:

- 3-D capability
- Large fine-mesh grid (180 by 270 elements)
- Yielding seam option (user-defined)
- Multiple-seam capability
- Backfill and artificial support materials

Other features that made the package attractive were:

- PC-based operation
- Off-seam stress/strain capability
- Failure index calculation (Mohr-Coulomb/Hoek-Brown)
- Graphic pre- and postprocessors
- Multiform hard-copy output capability

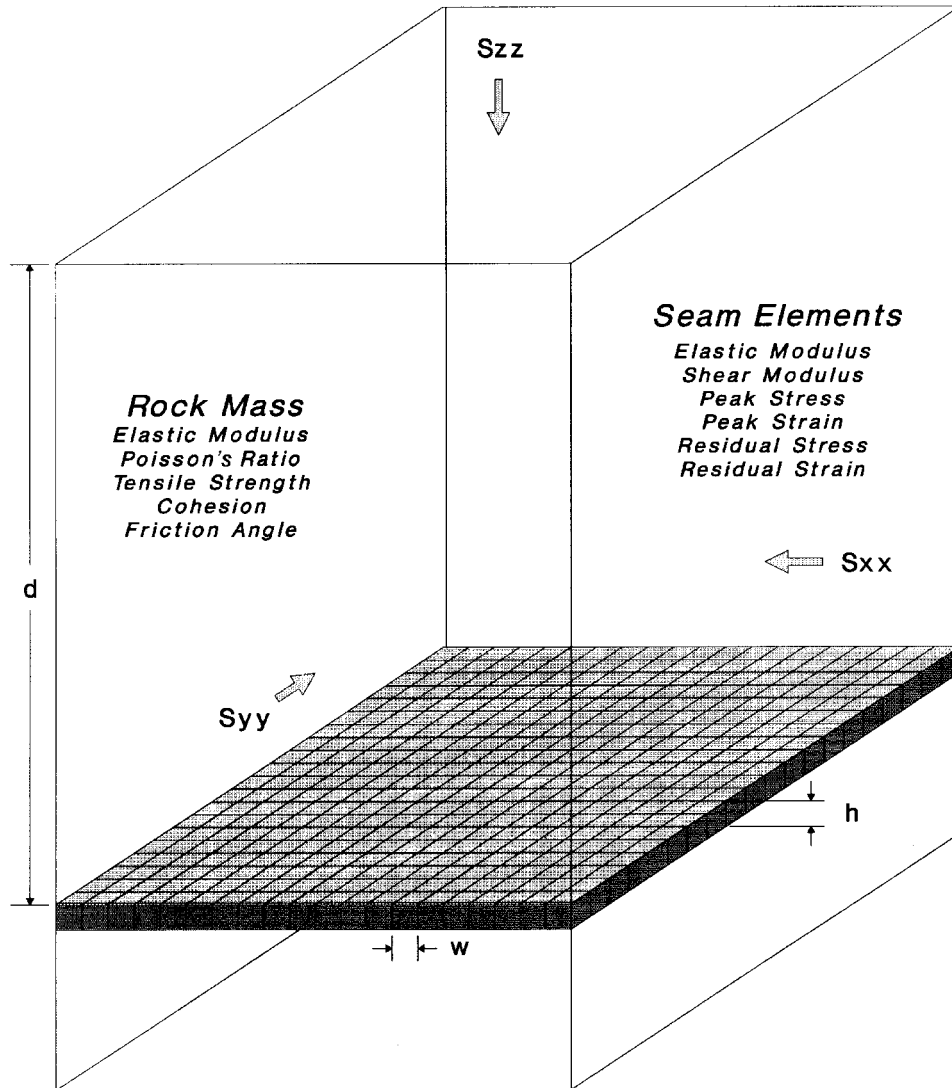


Figure 1.—Generalized BESOL boundary-element model.

SIMULATION PROCESS

Figure 2 presents an eight-step process used by the Roof Control Division during the simulation of underground mining systems. Although it is specifically directed to numerical modeling applications, it can also be used in conjunction with empirical or analytical methods.

1. *Observe Underground Areas:* This is an essential first step in solving ground control problems regardless of the methodology employed. Mine conditions should be categorized

in a number of areas where differing pillar sizes, panel configurations, and overburden levels are found. The deterioration index system, which will be discussed later in this paper, can aid in the description of in-mine ground conditions.

2. *Estimate Model Parameters:* Coal, rock, and gob properties must be established consistent with the requirements of a particular numerical method. Ideally, these properties will be based on coal and rock tests of the specific mine site. In the absence of these data, published properties of adjacent or same seam mines can be used. When no site-related data are available, general coal and mine roof rock properties can be used. Regardless of the source of data, it cannot be over-emphasized that they represent only a *first estimate* of mine roof and rock properties that must be validated.

3. *Model Observed Areas:* The third step of the process involves modeling each of the areas observed underground. The properties estimated above are tested under various geometric and overburden conditions to determine their usability. Successfully modeling many areas under a variety of different conditions increases confidence in the properties used.

4. *Verify Model Accuracy:* This is the most critical step in the entire simulation process. Each of the areas modeled must be closely examined to ensure that the results correlate with observed conditions. If reasonable correlations cannot be made, the model must be recalibrated (material properties adjusted) and the process repeated. It should be noted that relating the output of numerical models (stress, convergence, etc.) to observed conditions (pillar sloughing and roof or floor deterioration) is often difficult given the complexities of the underground environment. The use of regression techniques to define actual conditions as a function of model output parameters (using the deterioration index rating system) can simplify that task.

5. *Establish Threshold Limits:* Once the accuracy of the model is verified, threshold limits delineating acceptable and unacceptable mining conditions must be established in order to evaluate the effectiveness of proposed design alternatives. Stress or convergence levels corresponding to deteriorating ground conditions can be identified. Other factors such as the extent of pillar yielding or predicted pillar, roof, and floor conditions from a more comprehensive regression analysis can also be used.

6. *Model New Configurations:* Having established an effective model and a means of evaluating the results of analyses, new mining techniques can be simulated. Generally, several alternatives are modeled under the conditions expected at the mine location where the design will be implemented.

7. *Evaluate New Configurations:* The various alternatives can be evaluated relative to the threshold limits established. For instance, if specific stress and convergence values were found to correspond to deteriorating ground conditions, an alternative

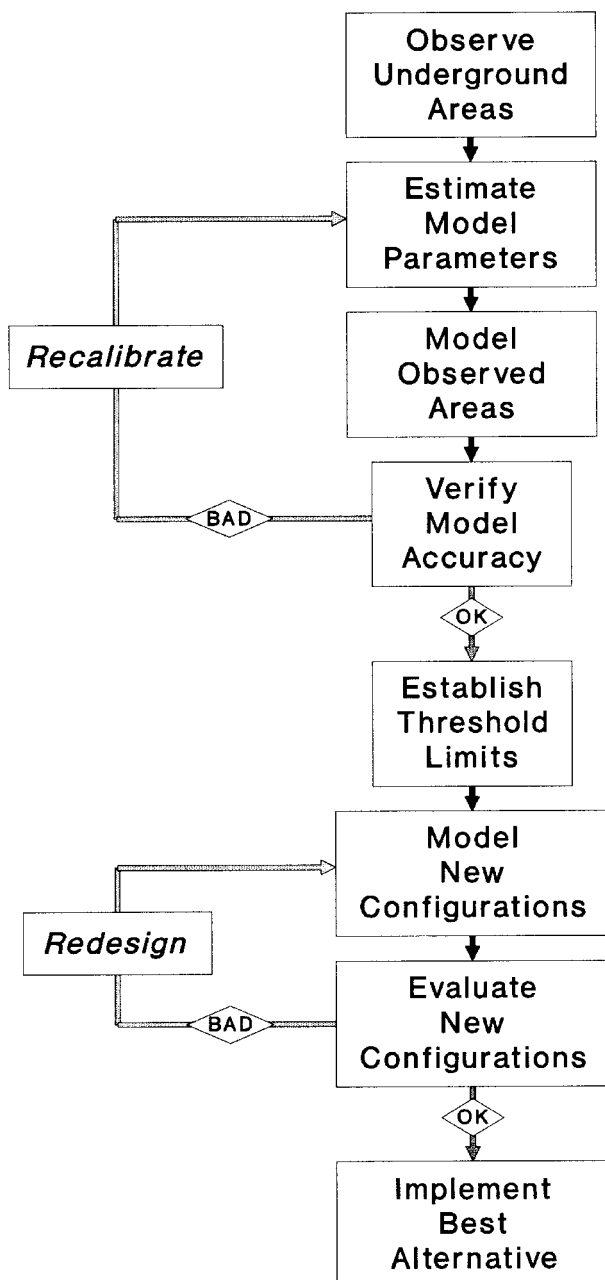


Figure 2.—Simulation process.

that produces levels lower than those values would be desired. However, if none of the configurations evaluated meet the threshold requirement for stable conditions, new alternatives must be developed and analyzed.

8. *Implement Best Alternative:* Once the best alternative is identified (either meeting the threshold criteria or providing the most favorable conditions), it can be *cautiously* implemented.

The level of confidence in achieving a successful design is directly proportional to the breadth of the evaluation and the degree of correlation noted in the model verification process. In any event, conditions should be closely monitored as the design is implemented; any deviations from the expected behavior warrants recalibration of the model.

MINING GEOMETRY AND INITIAL STRESS

An essential element in the simulation process is creating a model grid that duplicates the in-mine geometry. The seam must be broken into elements of a size that allows the entry, crosscut, and pillar dimensions to be accurately reproduced. Seam elements must be small enough to model details of the mine geometry and produce discernable differences in performance, yet large enough to allow broad areas of the mine to be included in the simulation.

Generally, setting the element size at 1/2 the entry width (figure 3) has provided acceptable results in most coal mining

applications. A 10-ft element width (for a 20-ft-wide entry/crosscut configuration) enables a large area (1,800 by 2,700 ft) to be modeled, yet provides the stress and convergence detail needed to effectively evaluate conditions. Both larger (one-entry width) and smaller (1/4-entry width) element sizes have been used out of necessity in specific applications, but are limited in application to scenarios where detail (large elements) or influence area (small elements) are not critical.

A number of other geometric guidelines have been identified that can aid in creating an effective boundary-element model:

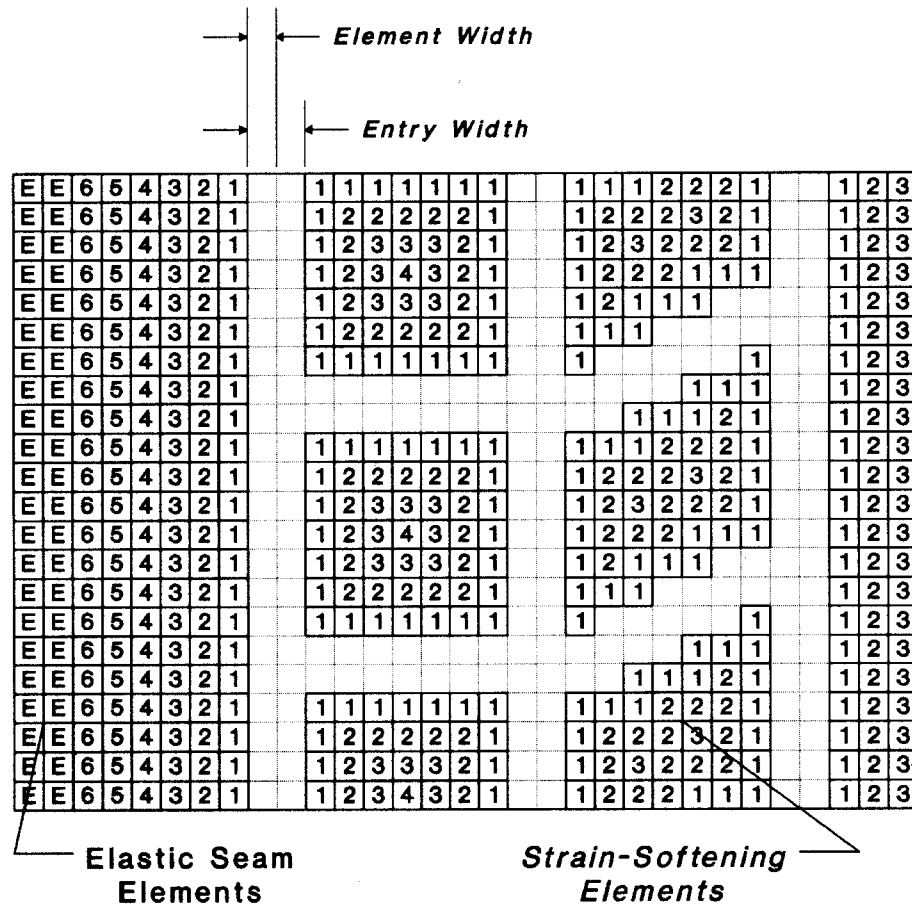


Figure 3.—Model elements and strain-softening locations.

- To the extent possible, locate model boundaries over solid coal or known stable areas to reduce the likelihood of erroneous loading conditions (resulting from the exclusion of transferred stress from adjacent yielded areas in the zone of interest).
- Orient the model such that the primary areas of interest are positioned away from the boundaries to minimize end effects.
- Known or potential yielding pillars should not contain linear-elastic elements that could erroneously affect the stress transfer to adjacent areas.
- Known or potential yielding pillars should contain an odd number of elements across the minimum dimension to ensure accurate pillar strength and peak core stress calculations.
- Care should be taken when entries or crosscuts are not oriented at 90° angles (see figure 3) to ensure that the effective widths and percent extraction match the actual mine geometry.

Initial stress conditions on the rock mass, in the absence of known high horizontal stress fields, have generally been as follows:

S_{zz} (vertical) ' 1.1 psi per foot of depth

S_{xx} (x-horizontal) ' 50% of the vertical stress

S_{yy} (y-horizontal) ' 50% of the vertical stress

These values have resulted in effective simulations of in-mine conditions in the vast majority of cases modeled, even when the influence of horizontal stress was suspected. High horizontal stress was rarely found to actually control mine conditions, and high horizontal stress values are only used when clear evidence of their existence and magnitude is available.

ROCK PROPERTIES

The rock mass properties needed for boundary-element models are minimal because the assumption of a linearly elastic material is inherent. The BESOL system requires only estimates of the modulus of elasticity and Poisson's ratio of the rock mass. Initially, it may seem that treating a complex rock structure in such a simplistic manner is not appropriate. However, considering that seam stresses are generated through massive main roof loading (generally remaining in elastic compression), it is not unreasonable to expect that an effective representation of pillar loading (the crux of a boundary-element model) would result.

The Roof Control Division uses a weighted-average technique to calculate the rock mass modulus of elasticity. As many borehole logs as possible located over areas to be modeled are examined, and the percentages of the various rock types (e.g., shale, sandstone, coal) in each core are identified (table 1). These values are averaged, multiplied by the modulus of elasticity of each rock type to calculate composite portions,

then summed to estimate the rock mass modulus of elasticity. Ideally, individual strata moduli are established by site-specific tests. If those data are not available, then published data for local mine roof strata or typical rock properties must be used. It should be noted that published data for particular rock types vary widely, and some judgment is needed in selecting appropriate values. The specific rock moduli listed in table 1 have been used successfully in a number of instances when on-site data were not available.

A similar weighted-average process is recommended for the calculation of Poisson's ratio. Again, the use of site-specific data would be ideal, but estimates based on published data are generally used. Poisson's ratios ranging from 0.20 to 0.25 have been acceptable in the analyses made to date.

The properties used to define the rock mass can have a significant effect on the accuracy of a simulation. Overestimating the rock modulus results in lower pillar stresses within a panel or mined area (gob) and higher loads over the

Table 1.—Composite rock modulus calculation

Rock type	Percent in borehole					Rock modulus, psi	Composite portion, psi
	Hole No. 1	Hole No. 2	Hole No. 3	Hole No. 4	Average		
Dirt	10.84	8.07	11.51	15.64	11.52	50,000	5,750
Coal	1.52	1.60	1.34	0.96	1.36	473,000	6,409
Shale	51.15	26.86	21.79	48.22	37.01	900,000	333,090
Slate	1.18	0.78	2.54	0	1.13	1,250,000	14,125
Sandstone	22.28	28.63	23.70	26.31	25.23	2,200,000	555,060
Limestone	0	0	0	0	0	3,200,000	0
Sandy shale	11.47	31.70	36.01	7.78	21.74	1,500,000	326,100
Fireclay	1.57	2.35	3.11	1.08	2.03	900,000	18,270
TOTAL							1,258,804

E ' 1,260,000 psi

adjacent abutments due to the enhanced bridging action (less

deformation) of the rock strata. Conversely, underestimating

the rock modulus leads to higher panel pillar stress or gob loading in mined areas and lower stresses on the adjacent abutments.

As noted previously, the BESOL system contains a failure index (safety factor) calculation to evaluate the rock strength/stress ratios using either a Mohr-Coulomb or Hoek-Brown failure criterion. Essentially, the state of stress of a point in the rock mass is calculated in terms of 3-D principal stresses, and the "available strength" of the rock (as influenced by confinement) is compared to the existing stress level. To date, only the Mohr-Coulomb technique has been used, which requires input of cohesion, friction angle, and tensile strength of the rock (roof or floor) material. Because the analysis of the rock structure is completely elastic, exact properties (although desirable) are not required. The failure index analysis is treated

in a relative manner (higher failure indices indicate a more stable condition), and the following parameters have provided reasonable results:

Tensile strength - 1,000 psi
Cohesion - 800 psi
Friction angle - 25°

The failure index has been successfully used to indicate high stress locations and the effect of mining changes to relieve those stresses. Although they can be calculated anywhere in the rock mass, failure index calculations made at the immediate roof or floor lines have been most useful. Coupling them with stress and convergence data provides a more complete picture of mine stability that can be correlated to observed or expected conditions.

COAL PROPERTIES

Establishing representative coal properties for a boundary-element analysis is the most critical step in model formulation. The need for yielding seam capability is clear to accurately simulate the complex underground environment where localized coal failure results in the redistribution and concentration of stress in adjacent areas. The strain-softening approach [Crouch and Fairhurst 1973] has been identified as a reasonable method of describing coal seam behavior. Although that concept has been widely discussed, little specific information is available concerning the actual construction of a strain-softening model.

The Roof Control Division has established a technique to make a *first approximation* of the stress and strain values needed to describe the strain-softening characteristics of a specific coal seam. As generalized in figure 4, peak and residual (postpeak) stress and strain levels are required for seam elements located at various distances from a mined area. BESOL allows up to six user-defined elements (each characterized by three stress-strain values), and model elements located farther away from a free face are treated as linearly elastic (figure 3).

Peak coal strength values are estimated at the center of each of the six yielding seam elements by the following equation:

$$S_p(i) = S_1 (0.78 + 1.74 x/h), \quad (1)$$

where $S_p(i)$ = peak strength of element (i), psi,

S_1 = in situ coal strength, psi,

x = distance from element (i) center to free face, ft,

and h = seam height, ft.

Equation 1 was based on the derivations of Mark and

Iannacchione [1992] for estimating the stress gradient in the yield zone of several empirical pillar design formulas and represents an average of the Bieniawski and Obert-Duvall methods. The in situ coal strength is usually based on uniaxial compression tests of samples acquired from the mine, although published data have also been used when site-specific data were not available. Strength reduction factors of 1/5 for 2-in cubes and 1/4 for 3-in cubes have been used to estimate in situ strength from test data and have generally provided acceptable results. Figure 5 presents a summary of peak strengths measured (with borehole pressure cells) at various depths into coal pillars at three mines where pillar yielding was evident. Data are shown as a ratio of the measured peak stress to that estimated by equation 1; the majority fall within 10% of the predicted stress level. Because the seam is considered to behave elastically until peak stress is reached, the total strain at that level is simply

$$e_p(i) = S_p(i)/E, \quad (2)$$

where $e_p(i)$ = strain at peak strength of element (i), in/in,

$S_p(i)$ = peak strength of element (i), psi,

and E = coal seam modulus of elasticity, psi.

Residual (postpeak) seam stress and strain values are approximated by the following relationship:

$$S_{R1}(i) = (0.1385 (\ln(x) + 0.413)) (S_p(i)) \quad (3)$$

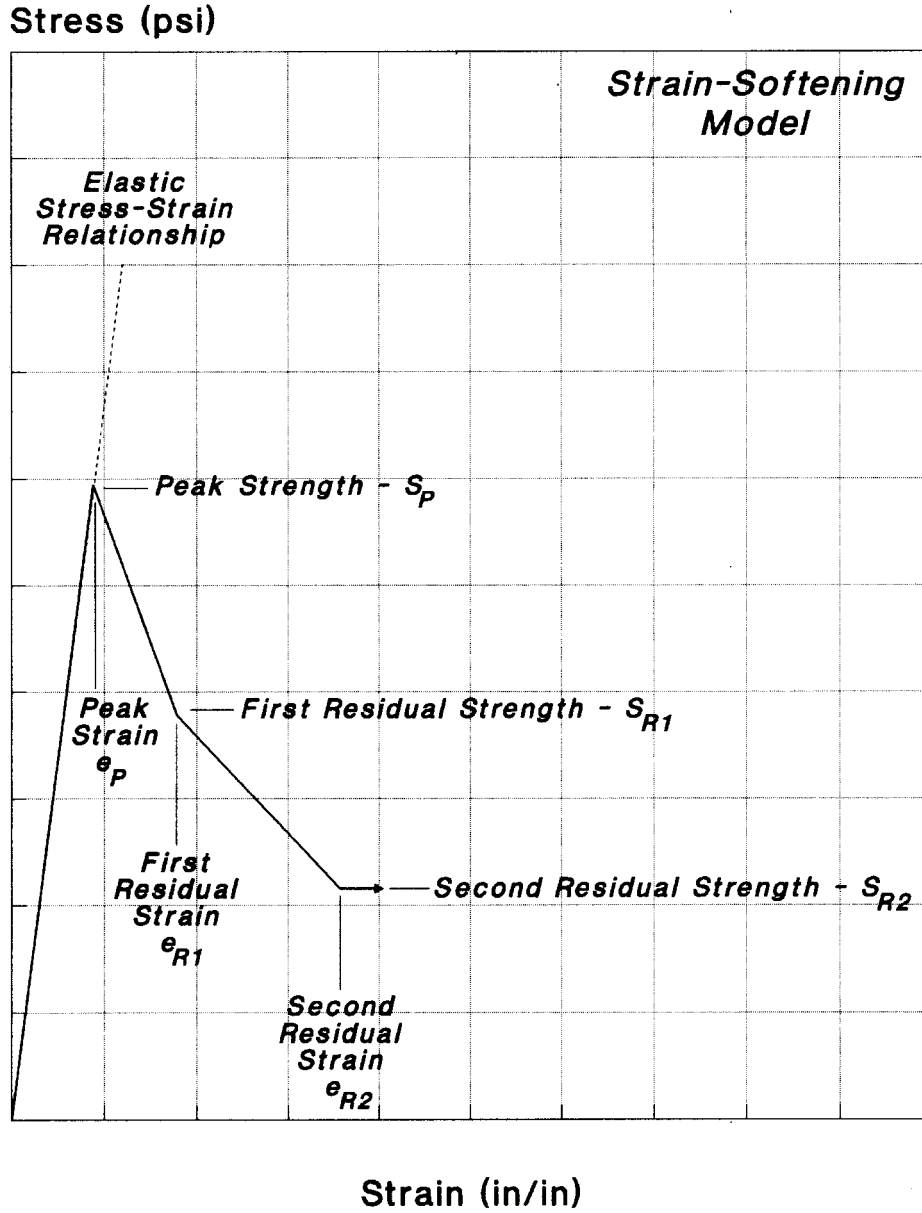


Figure 4.—General strain-softening element characteristics.

$$e_{R1}(i) = 2 (e_p(i)) \tag{4}$$

$$SR2(i) = (0.2254 (\ln (x)) (S_p(i)) \tag{5}$$

$$e_{R2}(i) = 4 (e_p(i)) \tag{6}$$

$e_{R2}(i)$ ' strain of element (i) at second residual stress level, in/in,

and x ' distance from element (i) center to free face, ft.

where $S_{R1}(i)$ ' first residual stress level of element (i), psi,

$e_{R1}(i)$ ' strain of element (i) at first residual stress level, in/in,

$S_{R2}(i)$ ' second residual stress level of element (i), psi,

These relationships were patterned after the load/deflection response of coal samples under uniaxial testing, yield pillar stress and entry convergence measurements made at one mine site, and the assumption that at increasing depth into the pillar core a higher residual strength would be maintained.

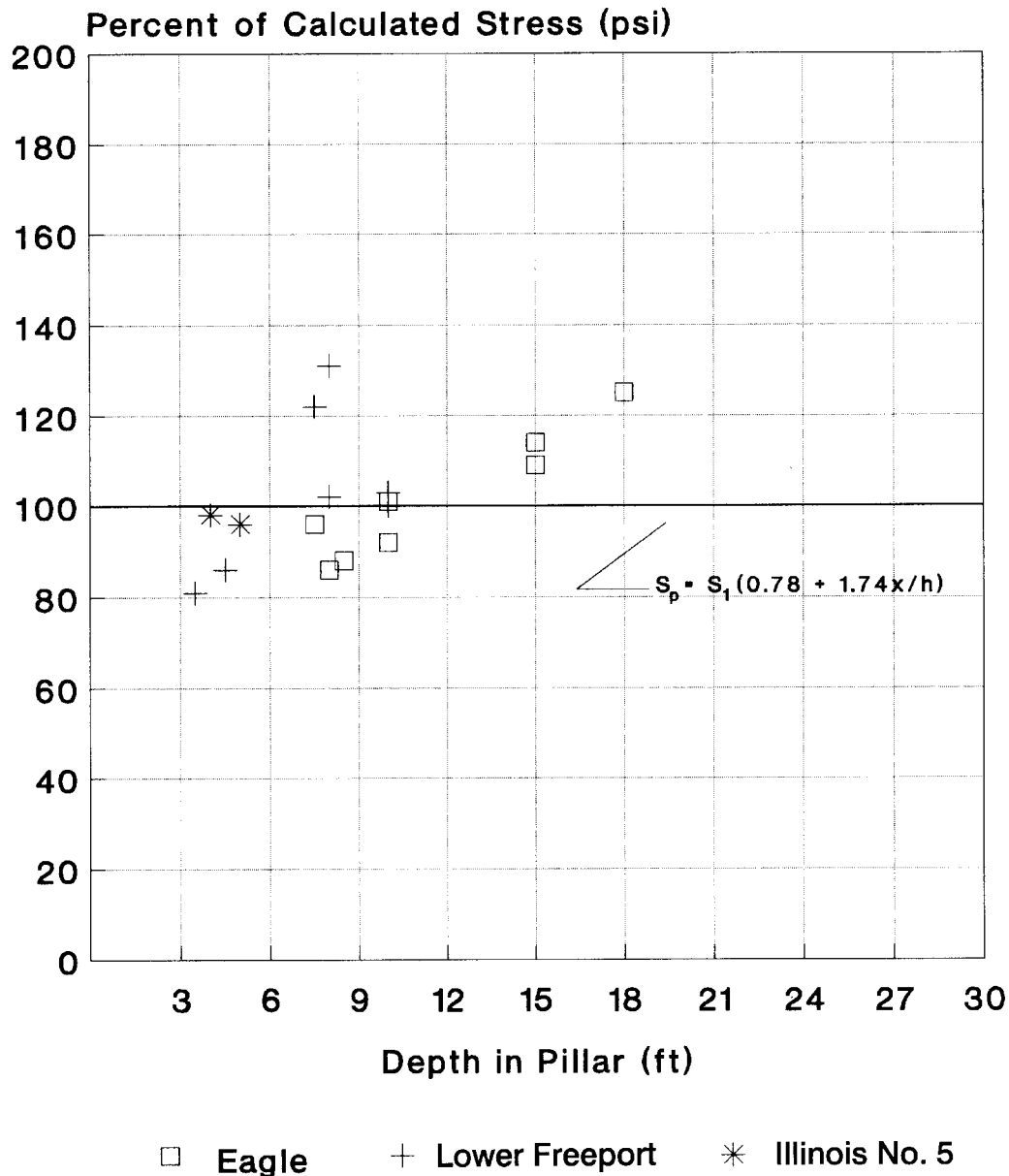
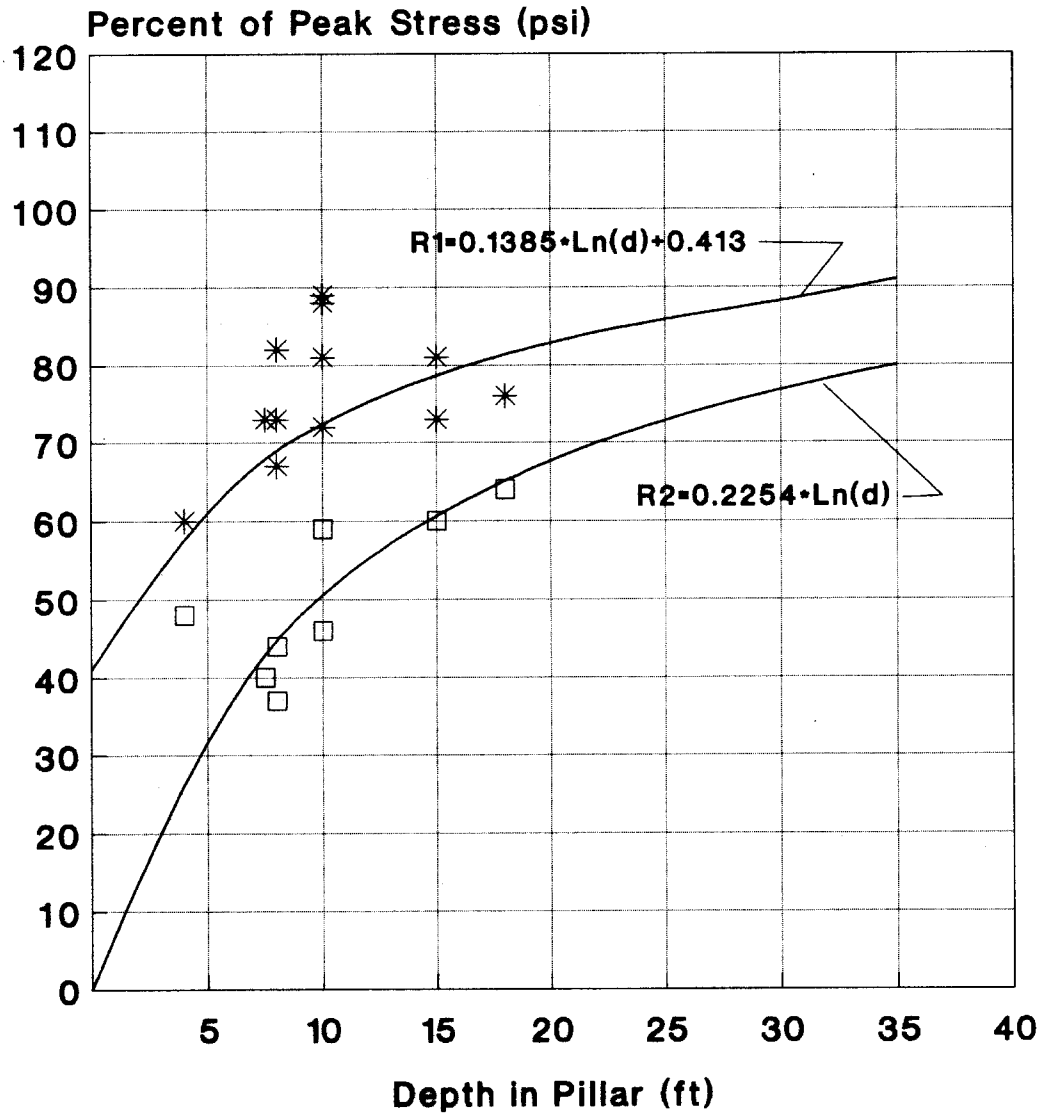


Figure 5.—Measured versus calculated peak coal strength.

Figure 6 presents a summary of residual stress levels measured at various depths at four mines where pillar yielding was monitored. The data are illustrated as a percentage of measured peak stress and compared to levels predicted by the above equations. The R1 levels represent the initial drop in stress once the peak has been reached; the R2 values indicate the final magnitude after substantial convergence. Both are difficult to identify because deformation plays a significant role in the unloading process; however, figure 6 represents a best estimate of those stress levels for the pillars monitored.

Figure 7 illustrates a family of six curves representing a strain-softening model with an element size of 10 ft, a seam height of 2.8 ft, an elastic modulus of 500,000 psi, and an in situ coal strength of 967 psi. Curve No. 1 represents the behavior of free-face or pillar perimeter elements; the remaining curves represent the stress-strain relationship of elements located successively deeper into the pillar core.

The BESOL system also requires estimates of the seam shear modulus (G) and similar shear stress-strain characteristics for the six yieldable elements described above. These geotechnical



* Actual R1 Data □ Actual R2 Data

Figure 6.—Measured versus calculated residual strength.

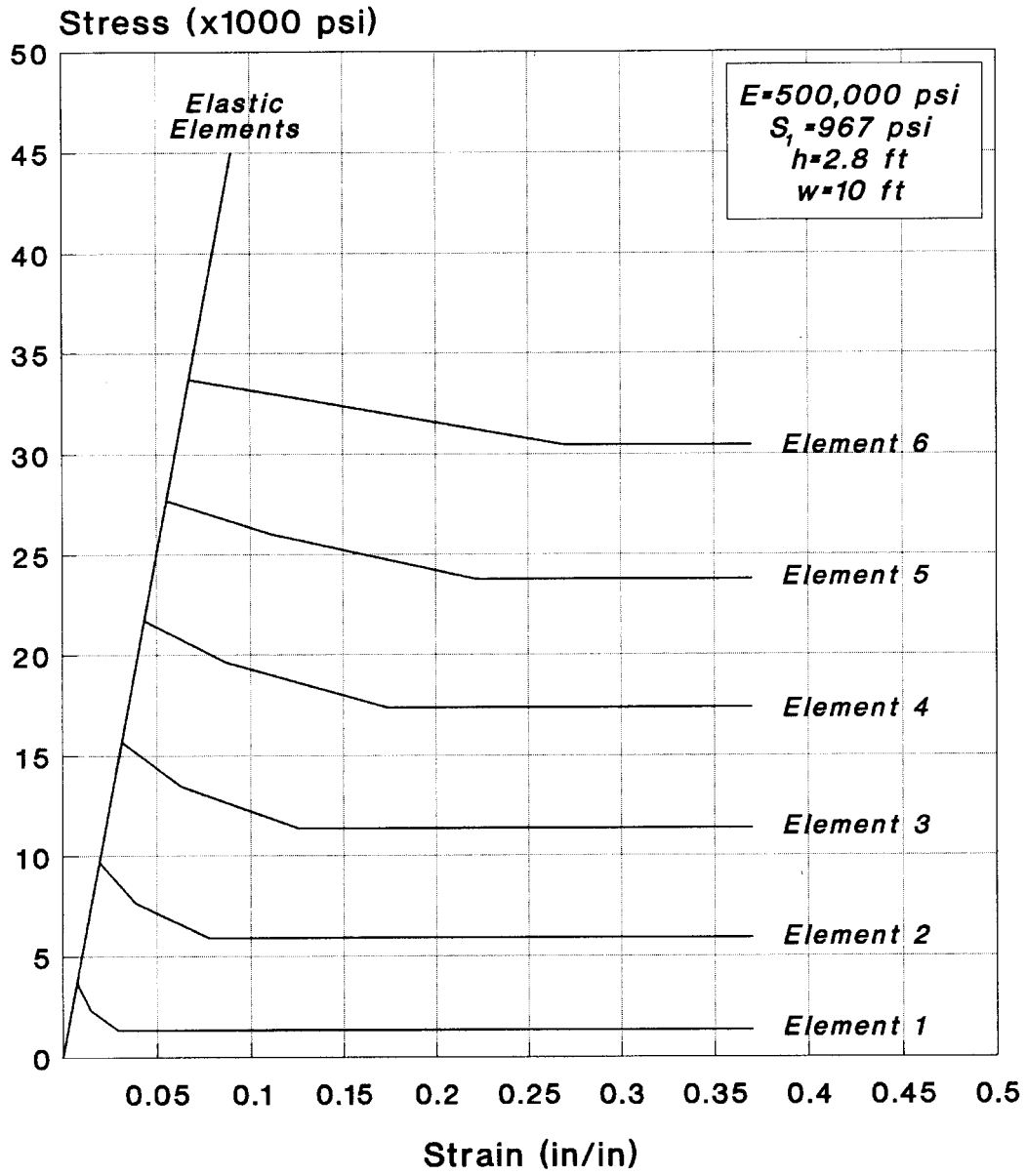


Figure 7.—Typical strain-softening seam behavior.

data are rarely available, and estimates (using the previously described procedure) based on a shear modulus equal to 1/2 to 1/3 of the elastic modulus and shear strengths of 1/2 to 1/3 of the strain softening values have been used.

It must again be emphasized that, although the methodology described above has been successfully used to estimate coal strain-softening properties, the properties generated are only a *first approximation* that must be verified for accuracy. Although in situ measurements have generally validated properties assigned to near-excavation locations, peak and residual stress levels deeper than 20 ft into a pillar or solid coal (where yielding rarely occurs) are largely unverified. Further, the procedure has been applied only to a limited number of coal seams, none of which experienced bump problems. The application of this technique to bump coal is not recommended because the strength increase due to confinement would likely exceed that predicted by the peak stress equations.

The suitability of assigned coal properties can be assessed by comparing the simulation output to observed pillar conditions. Test models should include underground areas (varying depths and pillar sizes) where definite observed pillar behavior can be isolated. For instance, if a model with 8-ft-wide elements predicts corner yielding, significant sloughing and crushing for

a length of 8 ft from the pillar corner should be obvious. A similar condition would be expected along the sides of pillars if perimeter yielding were projected. In general, more observed pillar deterioration than that projected by the model suggests that the coal strength has been overestimated; less sloughing than predicted indicates that it has been underestimated. There are occasions, however, where the element size itself can contribute to erroneous interpretations. A model using 10-ft elements may indicate elevated stress at the pillar corners, but no yielding. Underground observations of 4-ft crushed zones at the pillar corners may suggest that the model coal strength has been overestimated. Remodeling the area using 4-ft elements (with corresponding recalculation of element properties) may in fact result in the prediction of corner yielding that would match the in-mine conditions.

When constructing calibration models to verify coal strength, it is essential that:

- The element size selected is appropriate to illustrate phenomena (yielding) observed underground; and
- Element properties are recalculated when element sizes are changed; smaller elements have lower strength values than larger ones because of their proximity to the free face.

GOB PROPERTIES

When numerical models contain large mined areas, such as longwall or pillar line gobs, some mechanism must be employed to simulate caving and stress relief associated with those areas. Without it, the full weight of the overburden would be transferred to adjacent areas and result in a significant overestimation of abutment loads. The stress relief process is complex and comprises caving, bulking, and subsequent compaction of the gob material. Although a number of investigators, including Pappas and Mark [1993], have evaluated the behavior of gob material, little published data exist regarding the simulation of caving in 3-D boundary-element numerical models.

The BESOL system provides a fill material that has been used to absorb a portion of the gob loads and provides a measure of stress relief associated with caving. The stress-strain relationship for the fill material is based on the work of M. D. G. Salamon and is of the form [Crouch Research, Inc. 1988]:

$$F_n = a (e_n / (b + e_n)), \quad (7)$$

where F_n = normal stress on the fill element,

e_n = normal strain of the fill element,

b = limiting value of normal strain (total compaction),

and a = stress to compress fill 1/2 of b .

For a first approximation, values for the necessary constants have been estimated as:

$$\begin{aligned} a &= 100 \text{ psi} \\ b &= 0.50 \text{ in/in} \end{aligned}$$

Figure 8 illustrates the relatively soft stress-strain response of backfill using these parameters. That material was tested in a number of general scenarios; resultant abutment loads were compared with those predicted by the inverse square decay function used by Mark [1990] in the Analysis of Longwall Pillar Stability (ALPS) methodology. As typified by figure 9, a reasonable agreement in resultant abutment stress distributions was found. The peak stress of the BESOL model exceeds that of the inverse square decay function; the average stress over the first 150 ft of the abutment (usually the zone of concern) is nearly identical. It appears that the use of a relatively soft backfill compensates for the tendency of boundary-element models to distribute abutment loads over a wide area and results in a reasonable approximation of near-gob stresses. Fill material of this type has been placed in gob areas during the BESOL simulation of nine mines (starting 20-30 ft from solid coal to allow an area of hanging roof) that have been successfully evaluated.

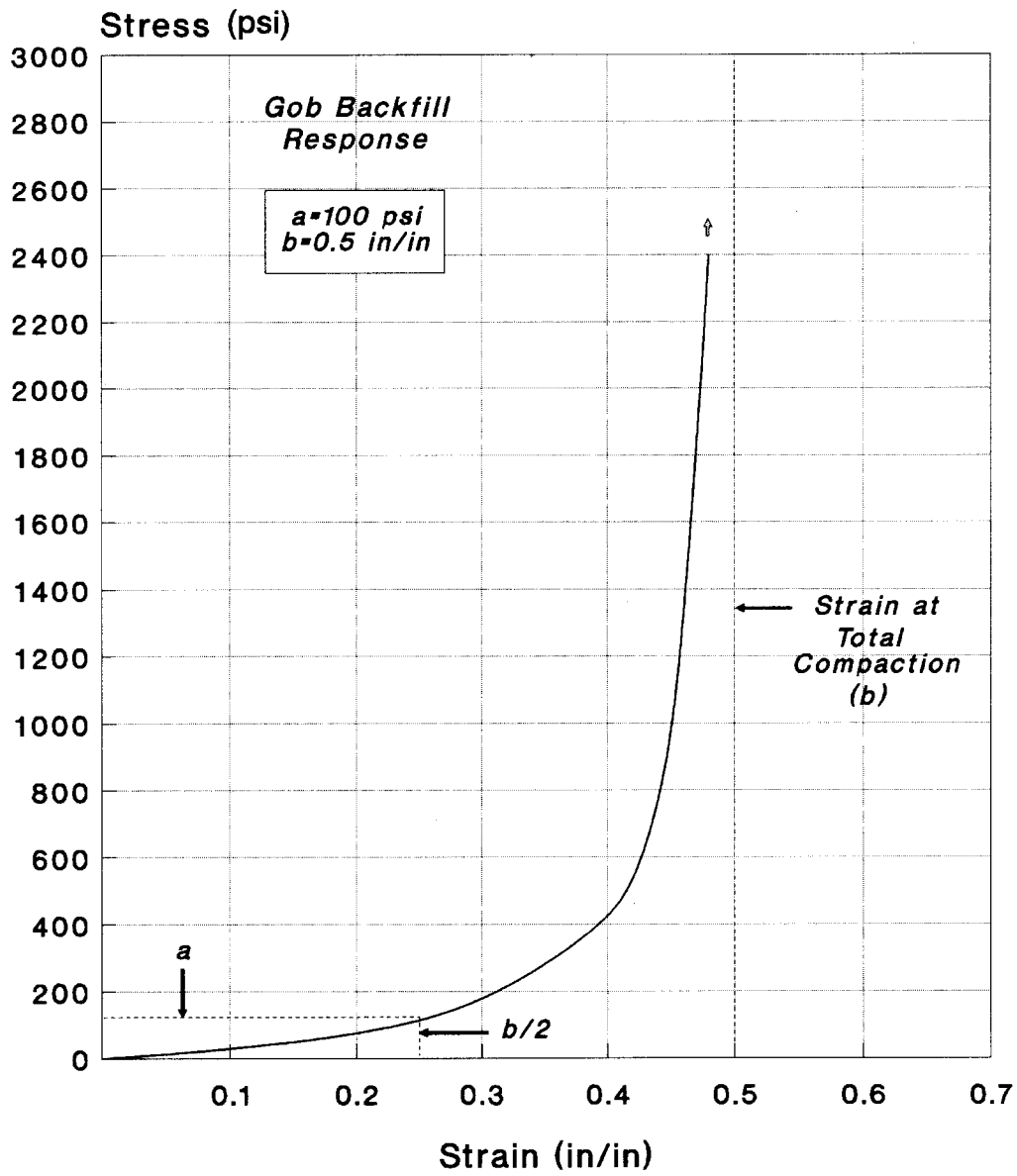


Figure 8.—BESOL strain-hardening backfill behavior.

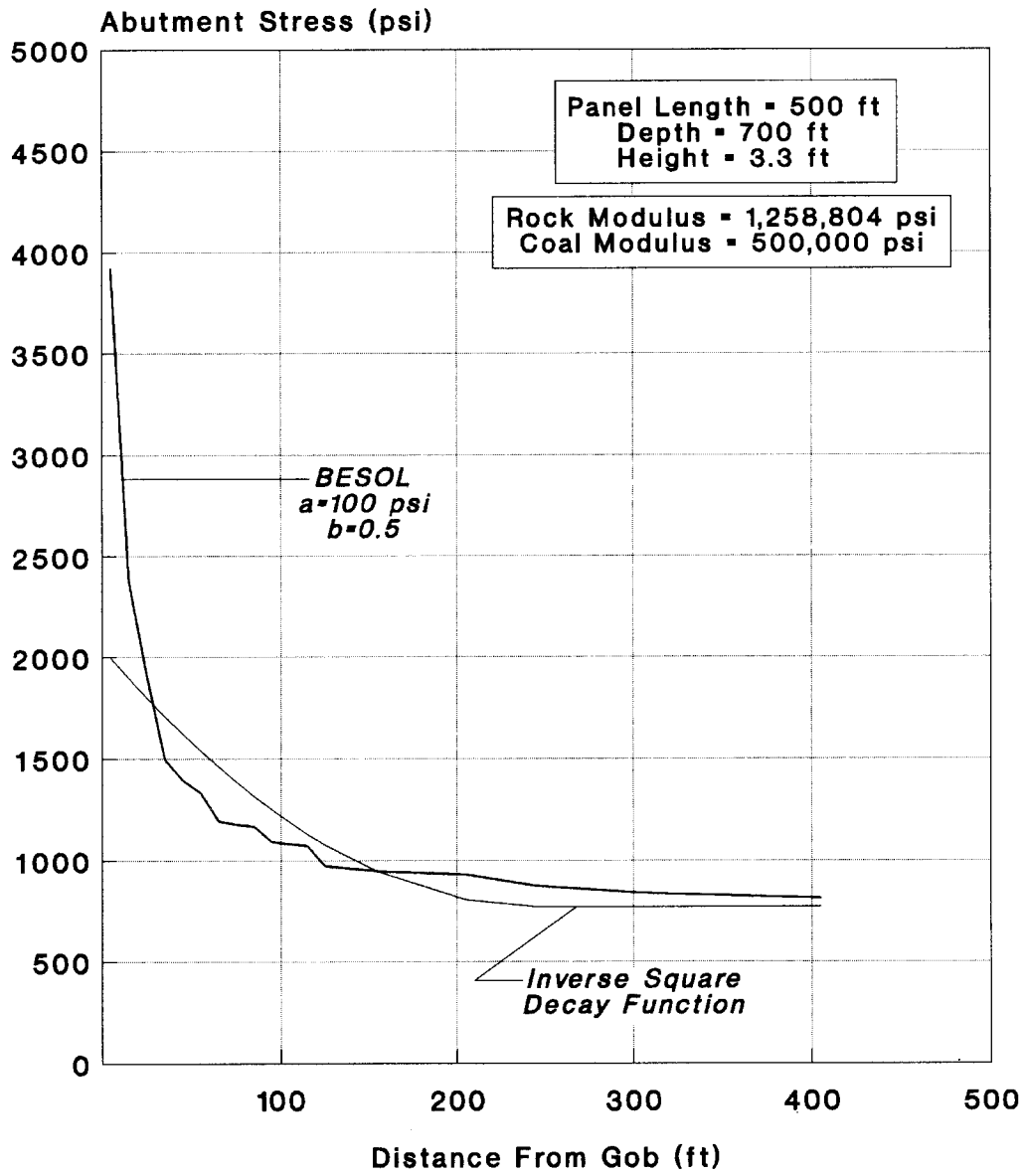


Figure 9.—BESOL versus inverse square decay function.

As with the other material properties discussed in this paper, the suitability of gob backfill based on the above or any other parameters must be verified. Obviously, the use of backfill that is too stiff will result in excessive gob loading and reduced abutment loads. Conversely, a gob material that is too soft will generate excessive abutment loads and low-gob stress. The

modulus of elasticity of the rock mass and other geometric parameters (depth, panel width, etc.) can have a significant impact on backfill loading and must be considered. Examining backfill stress in gob areas can indicate the amount of relief simulated by the model and can be compared to known or anticipated cave heights associated with those areas.

SUMMARY OF PROPERTIES

In the process of simulating ground conditions at mines throughout the United States (12 coal seams in 5 States), a host of coal and rock properties have been generated. Table 2 summarizes the in situ coal strength, coal modulus of elasticity,

and rock moduli of elasticity used in 18 successful evaluations. The mining depth of each simulation is also shown in the table. The data are presented for reference purposes and illustrate the variation in properties that can be expected at different sites.

Table 2.—Successfully applied coal and rock properties

State and coal seam	Mining depth, ft	In situ coal strength, psi	Coal modulus of elasticity, psi	Rock modulus of elasticity, psi
PA:				
Lower Freeport	420	¹ 462	¹ 550,000	² 1,000,000
Upper Freeport	700	¹ 405	¹ 200,000	¹ 590,000
Upper Freeport	360	¹ 775	¹ 200,000	¹ 740,000
Pittsburgh	950	² 790	² 350,000	² 2,100,000
Pittsburgh	650	² 900	² 500,000	² 3,280,000
Pittsburgh	575	² 790	² 350,000	² 2,140,000
Lower Kittanning	375	² 679	² 300,000	² 1,850,000
WV:				
Cedar Grove	900	¹ 705	² 500,000	² 1,800,000
Dorothy	150	¹ 290	¹ 121,000	² 910,000
Eagle	950	¹ 712	¹ 490,000	¹ 880,000
Eagle	850	¹ 850	¹ 500,000	¹ 810,000
Lower Lewiston	260	¹ 583	¹ 200,000	² 2,400,000
Sewell	470	¹ 312	¹ 250,000	² 1,400,000
KY:				
Elkhorn No. 3	420	¹ 951	¹ 548,000	² 1,750,000
Hazard No. 4	900	¹ 967	² 500,000	² 1,260,000
Hazard No. 4	950	² 967	² 500,000	² 1,260,000
IL:				
Illinois No. 5	700	² 620	² 330,000	² 1,000,000
AL:				
Blue Creek	1,200	² 750	² 580,000	² 1,440,000

¹Based on site-specific tests.

²Estimated from published data provided by the mine or found in literature reviews.

DETERIORATION INDICES AND ANALYSIS

As mentioned previously, the most critical phase of the simulation process is verifying the accuracy of a model through correlation with actual underground conditions. To aid in that exercise, a set of deterioration indices was established to quantify pillar, roof, and floor behavior. Observed sites are assigned a numerical rating on a scale of 0 to 5 (0 is the best condition; 5 is the most severe) in each of the three categories. The deterioration index levels are reasonably well defined to minimize subjectivity of observations and promote consistency in ratings from site to site.

The pillar deterioration index (PDI) establishes observable sloughing levels that can be directly related to numerical model projections. A rating of 1 indicates corner crushing for a distance equal to one element width (usually 1/2-entry width) in the boundary-element model. A rating of 2 indicates some perimeter sloughing, but to a depth of less than one element width. This corresponding model would indicate yielding of some, but not all, of the perimeter seam elements. At the 2.5 level, sloughing is severe enough to cause concern over the stability of the area. A PDI of 3.5 represents a situation where

sloughing caused widening of the entry to a point that supplemental support (cribs or posts) was required to narrow the roadway. A corresponding model would indicate yielding of all perimeter elements and elevated pillar core stresses. PDIs of 4 and 5 represent progressively more severe conditions. A model response equivalent to a level 4 would indicate deeper pillar yielding and core stresses approaching the maximum capacity; a level of 5 indicates total pillar yielding and elevated convergence.

Pillar deterioration index (PDI)

0	Virtually no sloughing
1.0	Corner sloughing
2.0	Light perimeter sloughing
2.5	Onset of pillar stability concerns
3.0	Significant perimeter sloughing
3.5	Supplemental support required
4.0	Severe perimeter sloughing
5.0	Complete pillar failure

The roof deterioration index (RDI) defines a rating scale to quantify the condition of the roof strata in observed areas. Unlike the PDI, however, roof deterioration cannot be directly correlated to model output. The levels were established to correspond to progressively more significant observable phenomena ranging from roof flaking or sloughing (level 1) to widespread and massive roof falls (level 5). The severity of each feature can be identified within a one-point band. For instance, areas with only a hint of roof cutters would be rated at 1.6; those containing many severe cutters (a situation causing roof stability concerns) would receive a 2.5 rating. A roof deterioration index of 3.5 corresponds to conditions where supplemental support was required to maintain stability.

Roof deterioration index (RDI)

0	Virtually no deterioration
1.0	Flaking or spalling
2.0	Cutter roof
2.5	Onset of roof stability concerns
3.0	Broken roof
3.5	Supplemental support required
4.0	Significant roof falls
5.0	Widespread and massive roof falls

The floor deterioration index (FDI) provides a measure of mine floor stability relative to fracturing and the level of heave experienced. Like the RDI, this index cannot be directly

correlated to the model output, and the established levels represent progressively more serious floor conditions. An FDI of 2.5 represents the occurrence of heave that causes concern over floor stability; a level of 3.5 indicates a condition that impedes passage and requires grading to maintain an active travelway.

Floor deterioration index (FDI)

0	Virtually no deterioration
1.0	Sporadic cracks
2.0	Consistent localized cracks
2.5	Onset of floor stability concerns
3.0	Widespread cracks and obvious heave
3.5	Travel impeded; grading required
4.0	Significant floor displacement
5.0	Complete entry closure

The deterioration indices have been effectively used to describe in-mine ground conditions and to correlate BESOL output data to those observations. While simulation output such as stress and convergence can often be directly related to in-mine conditions, many instances arise where the combined influence of a number of factors affects ground behavior. To better establish those relationships and provide an effective means of evaluating potential design alternatives, a multiple linear regression can be used to relate model output to observed (deterioration index) conditions.

Table 3 presents a partial listing of BESOL output (stress, convergence, and failure index (FI) at the immediate roof line) and deterioration indices for a number of areas modeled and observed during an actual mine analysis. Other BESOL output (i.e., horizontal stress or displacement) could be included if applicable to a particular situation, but the three parameters listed are those routinely used. After model and observation data for all of the evaluated areas are compiled, multiple linear regression analyses are performed to define each deterioration index as a function of model output. In the sample instance in table 3, the various deterioration indices were related to maximum stress, maximum convergence, and minimum failure index at the roof line, and the resultant regression equations and correlation coefficients are listed.

Once the model accuracy is verified by comparing predicted to observed pillar yielding, examining the regression correlation coefficients, and using the regression equations to back-calculate deterioration indices for the observed (modeled) areas, design alternatives can be modeled and expected conditions predicted. Table 4 contains projected deterioration indices at a critical pillar line location for various pillar sizes and depths of

cover as predicted by BESOL output and the verified regression equations. The difference in expected conditions with each design alternative is clear.

The deterioration index/regression equation technique has proved to be a viable method of verifying numerical model accuracy and evaluating the potential of design alternatives *provided that* relatively consistent mining conditions exist. When changing roof, pillar, or floor strengths are encountered, the usability of the regression technique may be greatly reduced. Further, the relationships established are based on strata reaction at a particular mine, and only those observed (which are limited by current mine design and environment) can be included in the database. This is a particular concern when the use of yield

pillars as an alternative configuration is considered, but no complete pillar yielding is evident at the mine.

The Roof Control Division is currently exploring the use of normalizing parameters in the regression analysis to alleviate these difficulties. Factors such as in situ coal strength and seam height (for the PDI), a roof rock rating such as the Coal Mine Roof Rating (CMRR) [Molinda and Mark 1993] for the RDI, and a floor characterization number (for the FDI) are being evaluated to determine their usefulness in the regression analysis to buffer the variations found within a given mine and also between mines. If successful, the resultant technique could enhance individual mine analyses and allow the experience of many mines to be used.

Table 3.—Partial BESOL/deterioration index listing and regression equations

Location and entry	BESOL output			Deterioration indices					
	Maximum stress, psi	Maximum convergence, ft	Minimum failure index (FI)	Observed			Back-calculated		
				PDI	RDI	FDI	PDI	RDI	FDI
Face area:									
1	4,000	0.113	1.04	1.5	1.5	0.0	1.5	1.2	0.2
2	6,800	0.195	1.09	2.0	1.8	0.3	2.5	2.4	1.2
3	8,100	0.251	0.96	3.5	3.0	1.0	3.0	2.9	1.7
4	8,800	0.289	0.89	4.0	4.2	2.5	3.3	3.3	2.0
5	8,800	0.307	0.87	4.0	3.5	4.0	3.3	3.4	2.1
1 crosscut outby:									
1	3,100	0.083	1.11	1.2	1.5	0.0	1.1	0.9	0.0
2	5,400	0.161	1.16	1.5	1.5	0.0	2.0	1.9	0.8
3	7,000	0.207	1.11	2.0	2.0	0.5	2.6	2.5	1.3
4	7,500	0.230	1.02	3.0	3.0	1.0	2.8	2.7	1.5
5	7,500	0.223	0.94	3.0	3.0	3.0	2.7	2.6	1.4
3 crosscuts outby:									
1	2,710	0.063	1.25	1.0	0.5	0.0	1.0	0.7	0.0
2	3,900	0.089	0.93	1.5	0.8	0.0	1.3	1.1	0.0
3	6,000	0.150	1.16	1.5	1.5	0.2	2.2	2.0	0.9
4	7,000	0.182	1.13	2.0	2.0	1.0	2.5	2.4	1.2
5	7,300	0.204	1.21	3.0	2.5	2.0	2.7	2.6	1.4
3-Right:									
2	2,240	0.059	1.53	1.0	0.5	0.0	1.0	0.7	0.0
4	2,560	0.070	1.41	1.4	1.0	0.0	1.1	0.8	0.0
5	2,820	0.072	1.45	1.5	1.4	0.1	1.2	0.9	0.0
1-Right:									
2	1,530	0.040	2.13	1.0	0.2	0.0	1.0	0.6	0.0
4	1,700	0.047	1.91	1.0	1.0	0.0	1.0	0.6	0.0
5	1,780	0.047	2.00	1.0	1.0	0.0	1.0	0.7	0.0
PDI ' 0.000268 (STR % 3.259622 (CONV % 0.379665 (FI & 0.383740				r^2 ' 0.79					
RDI ' 0.000263 (STR % 4.603502 (CONV % 0.309200 (FI & 0.643870				r^2 ' 0.80					
FDI ' 0.000170 (STR % 6.094244 (CONV % 0.600442 (FI & 1.82412				r^2 ' 0.60					

Table 4.—Full pillaring BESOL output and predicted deterioration index

Pillar size (ft), depth, and location	Maximum stress, psi	Maximum convergence, ft	PDI	RDI	FDI
50 by 50 (900-ft depth):					
1	¹ 8,300	¹ 0.291	² 3.0	² 3.1	³ 1.7
2	¹ 8,200	² 0.247	² 3.1	² 3.1	³ 1.9
3	³ 5,900	² 0.185	³ 2.1	³ 2.0	³ 0.8
4	³ 5,600	³ 0.161	³ 2.2	³ 2.0	³ 1.0
40 by 40 (900-ft depth):					
1	¹ 9,690	¹ 0.385	¹ 3.8	¹ 4.0	² 2.7
2	¹ 9,690	¹ 0.343	¹ 3.8	¹ 3.9	² 2.6
3	¹ 8,700	² 0.245	² 3.0	² 3.0	³ 1.6
4	¹ 8,300	² 0.230	² 3.1	² 3.0	³ 1.7
40 by 40 (800-ft depth):					
1	¹ 9,690	¹ 0.305	¹ 3.5	¹ 3.6	³ 2.2
2	¹ 9,690	¹ 0.269	¹ 3.6	¹ 3.5	³ 2.2
3	² 6,800	² 0.198	³ 2.4	³ 2.3	³ 1.0
4	² 6,600	² 0.182	² 2.5	³ 2.4	³ 1.3
40 by 40 (600-ft depth):					
1	² 7,300	² 0.204	² 2.6	² 2.5	³ 1.2
2	² 7,150	³ 0.171	² 2.7	² 2.5	³ 1.4
3	³ 3,500	³ 0.095	³ 1.2	³ 1.0	³ 0.0
4	³ 3,400	³ 0.087	³ 1.3	³ 1.0	³ 0.1
40 by 30 (400-ft depth):					
1	³ 4,400	³ 0.116	³ 1.5	³ 1.3	³ 0.2
2	³ 4,200	³ 0.098	³ 1.4	³ 1.2	³ 0.1
3	³ 2,660	³ 0.063	³ 1.0	³ 0.7	³ 0.0
4	³ 2,320	³ 0.060	³ 1.1	³ 0.8	³ 0.0

¹Severe conditions.²Borderline conditions.³Desirable mining conditions.

CASE STUDY

An investigation was conducted at a coal mine in eastern Kentucky to determine the cause of a roof fall and deteriorating ground conditions that were encountered on a full pillaring section. The mine is located in the Hazard No. 4 Seam and has a mining height of 32-40 in. Figure 10 presents an illustration of the 1-Left Mains in the vicinity of the roof fall. These mains were developed as a five-entry system on 50- by 60-ft centers with 20-ft-wide entries and crosscuts. Panels were driven to the right and retreated as the mains were advanced (13 panels total). Following development of the mains (and panels) to the property boundary, retreating of those pillars was initiated. As figure 10 illustrates, a roof fall occurred one crosscut outby the pillar line as the 18th row of blocks was being extracted. Cover at the face was about 800 ft, but ranged from 480 ft near the mouth of the section (about 2,400 ft outby) to over 950 ft several hundred feet inby and to the right of the fall. The immediate roof strata were composed of a 15-ft-thick laminated shale and were overlain by a 20-ft-thick sandstone layer. Roof support was provided by 4-ft-long fully grouted bolts installed in a 4- by 4-ft pattern throughout the mains.

Observations were made throughout the 1-Left Mains to characterize ground conditions under various depths of cover and degrees of gob influence. Significant deterioration (heavy pillar sloughing, cutters, and broken roof zones) was noted in the face area; conditions were most severe in the immediate vicinity of the roof fall. Outby the face, conditions gradually improved, although the right side of the mains consistently showed heavier deterioration than the left side. The most significant conditions noted in the outby area corresponded to zones of heavier cover, suggesting that overburden depth and the adjacent gob areas contributed to the deteriorating conditions. Detailed deterioration index ratings were made throughout the observed areas to quantify the roof, floor, and pillar behavior. The data presented in table 3 represent a partial listing of these ratings in a number of entry locations (crosscut conditions were also quantified and used in the analysis). Higher PDI, RDI, and FDI levels correspond to more severe deterioration, which were observed in the face area and along the right side of the mains. Cover at the face was about 800 ft and about 650 ft and 480 ft over the 3-Right and 1-Right outby

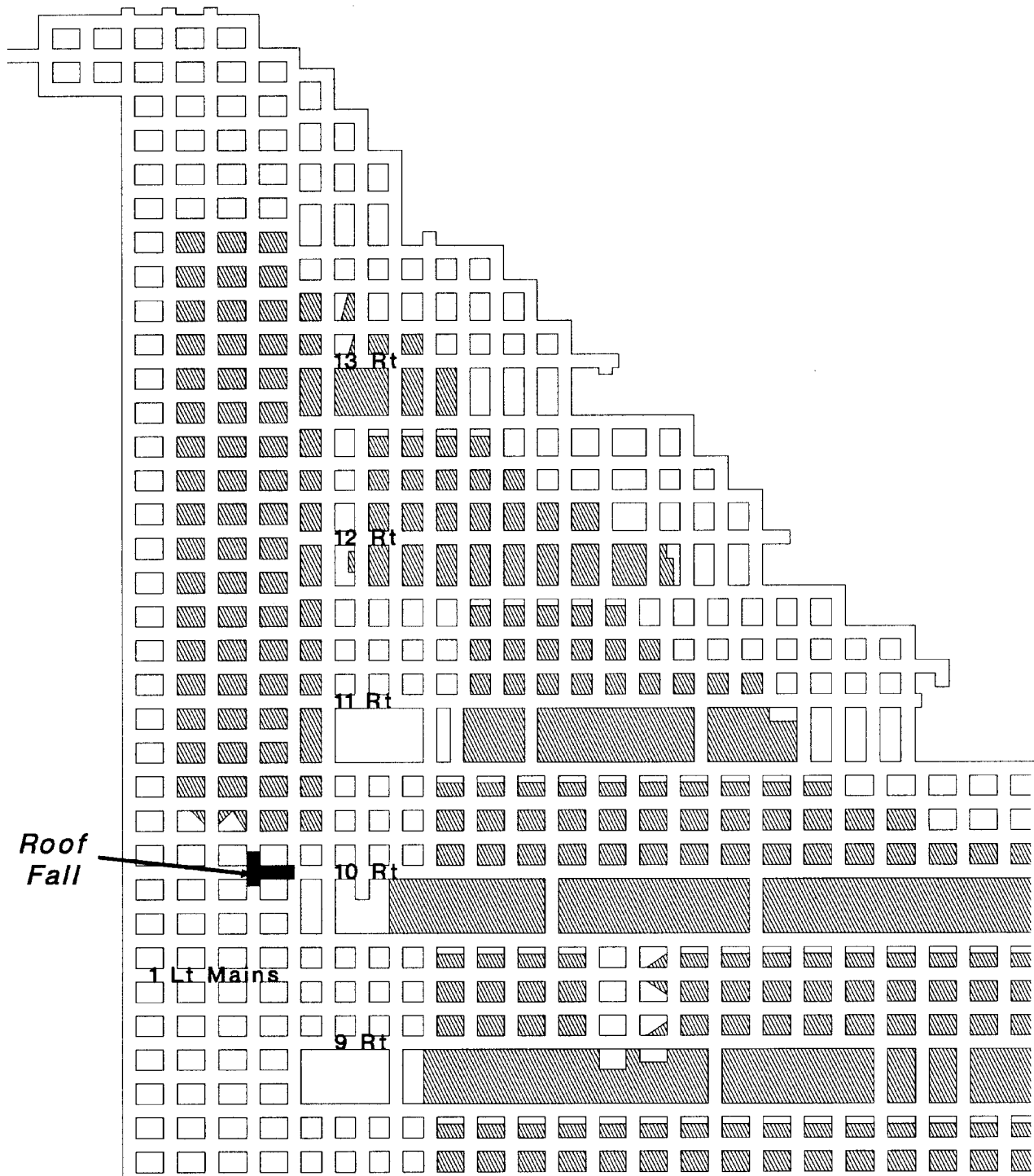
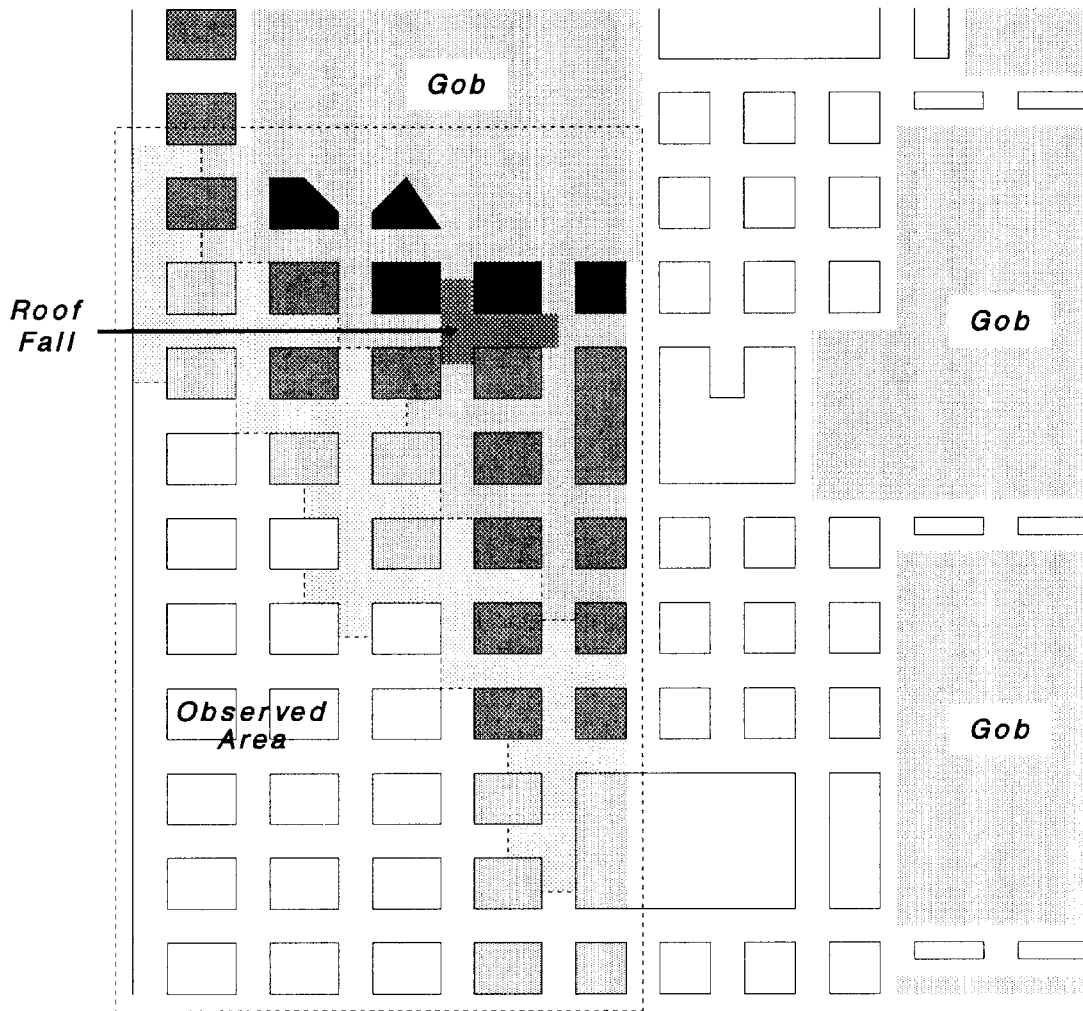


Figure 10.—Case study: partial mine map of pillaring section - roof fall area.

areas, respectively, where conditions were much improved. Figure 11 presents a composite deterioration index drawing of conditions observed at and just outby the face, illustrating the concentration of deterioration in the vicinity of the roof fall and along the right side of the section.

A series of three BESOL models was subsequently created to simulate conditions in the areas observed during the underground investigation. The first model (covering the area shown in figure 10) was used to simulate mining at the time of the roof fall and also at inby and proposed outby face positions



Pillar Deterioration	
	Severe (3.5-4.5)
	Significant (2.5-3.5)
	Moderate (1.5-2.5)
	Light (<1.5)

Roof/Floor Deterioration	
	Severe (2.75-4.0)
	Moderate (1.5-2.75)
	Light (<1.5)

Figure 11.—Case study: observations on pillaring section - roof fall area.

where cover was approximately 800 ft. Additional models were constructed of the outby areas (3-Right (650-ft cover) and 1-Right (480-ft cover)) to provide model verification under significantly differing conditions. Vertical stress applied to the models equaled 1.1 psi per foot of depth, and a horizontal stress of 1/2 the vertical stress was assumed in both the x and y directions. The element size used in the simulations was 10 ft, or 1/2 the 20-ft-entry width.

A composite rock modulus of 1,260,000 psi was based on data obtained from four boreholes in the vicinity, as shown in table 1. The individual rock moduli were estimated from published data for the specific strata contained in each borehole. A Poisson's ratio of 0.21 and the default Mohr-Coulomb properties (cohesion = 800 psi, friction angle = 25°, and tensile strength = 1,000 psi) were used because no site-specific data were available.

Coal properties were based on an in situ strength of 967 psi (site-specific coal strength data were provided by the mine); the peak and residual strength levels were calculated as outlined previously in this paper. A seam height of 2.8 ft was used, and a coal modulus of elasticity of 500,000 psi was assumed. The stress-strain curves of figure 7 represent the strain-softening model used in the analysis. Shear stress-strain properties were based on a shear modulus of 200,000 psi (0.4E).

Gob caving was simulated using the Salamon backfill discussed earlier with the constants $a = 100$ psi and $b = 0.50$. The comparison of abutment loading between BESOL and the inverse square decay function of figure 9 was based on the rock mechanics parameters used in this simulation.

Maximum pillar stress, maximum roof/floor convergence, and minimum failure index values were determined from the 3 models for 37 locations (entries and crosscuts) corresponding to the observed areas. The stress and convergence data compiled indicate the highest levels found in or adjacent to the 37 locations; the failure index values represent the lowest levels detected at the roof line in each area. A portion of these data (entry locations) is listed in table 3. A series of multiple linear regression analyses was made to relate the deterioration indices observed to the BESOL data and resulted in the equations also listed in table 3. The R-squared values for the PDI (0.79) and the RDI (0.80) were very good, but marginal for the FDI (0.60). It should be noted that the characterization of floor conditions was not a primary concern during the investigation, but sketchy data acquired were used to illustrate the process. The BESOL output was then inputted into the regression equations to predict (back-calculate) deterioration indices for the observed locations; these values describing entry conditions are also listed in table 3. Most of the predicted PDI and RDI levels match the observed data fairly well, and the trend of higher deterioration indices in areas of more severe conditions was evident, even with the FDI.

Figure 12 presents a composite of maximum pillar stress and convergence levels predicted by the BESOL model of the roof fall site. Note the correlation of BESOL stress and convergence

with the degree of deterioration observed underground. The zone of high convergence (>0.25 ft) and stress (>9,500 psi) encompasses the area of deteriorating conditions at the pillar line, including the roof fall. Lower stress and convergence levels also correspond to zones of lesser deterioration, and the more severe conditions predicted on the right side of the mains (indicating the influence of the adjacent gob) also match the conditions observed underground. These correlations, coupled with the good fit of the regression analysis (deterioration indices), confirmed the accuracy of the model (and properties used) to simulate conditions at the mine. Confidence was further enhanced by an evaluation of the BESOL model with a face position several crosscuts inby the roof fall. The results showed significantly lower stress and convergence levels in the face area that correlated to the better mining conditions actually encountered.

It was concluded that the roof fall (and deteriorating conditions) resulted from a combination of stresses from the active and adjacent gobs overriding the pillar line (yielding) and focusing outby the face. The small pillar size employed (30 by 40 ft) on the mains, the lack of protection provided by the combination of chain and barrier pillars from the adjacent gob, and the depth of cover (>800 ft) contributed to the problems encountered.

A series of additional models was created to evaluate the performance of various pillar sizes at different mining depths that would be encountered. Figure 13 illustrates the pillaring plan to be implemented using a 200-ft barrier between adjacent panels that would be roomed and retreated along with the panel being extracted. Stresses and convergences were examined at four entry locations near the face (during retreat of the second panel), as illustrated in figure 14. Threshold levels delineating expected conditions (from the 1-Left models) were established as follows:

Severe conditions:

Stress > 8,000 psi; convergence > 0.25 ft
PDI > 3.5; RDI > 3.5; FDI > 3.5

Borderline conditions:

Stress = 6,500 to 8,000 psi; convergence = 0.18 to 0.25 ft
PDI = 2.5 to 3.4; RDI = 2.5 to 3.4; FDI = 2.5 to 3.4

Desirable mining conditions:

Stress < 6,500 psi; convergence < 0.18 ft
PDI < 2.5; RDI < 2.5; FDI < 2.5

It was predetermined that good (desirable) mining conditions should exist at locations 3 and 4 since no supplemental supports (posts) would be installed in those areas. Borderline conditions could be tolerated at locations 1 and 2 (posts are set in this area),

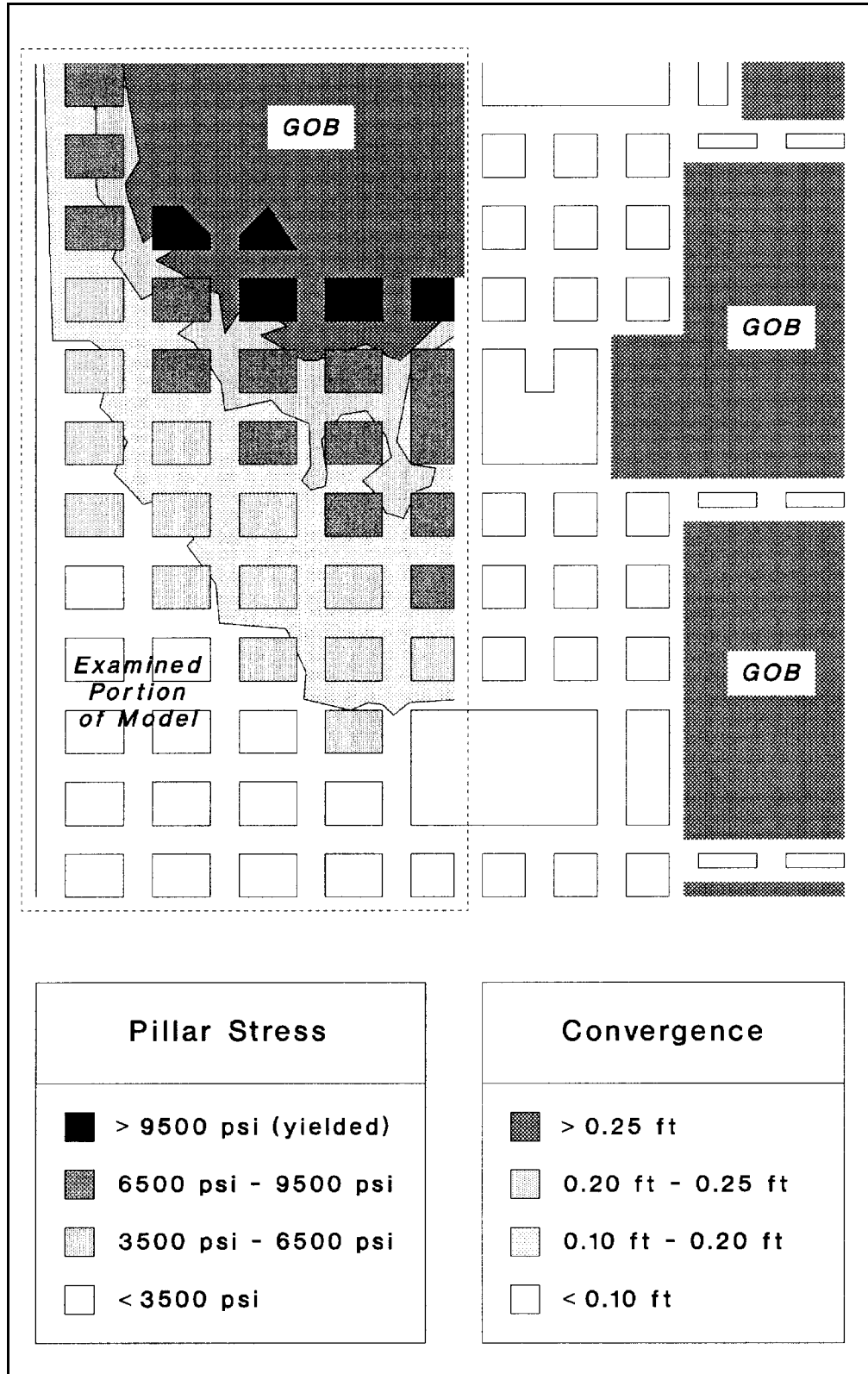


Figure 12.—Case study: BESOL output pillaring section - roof fall area.

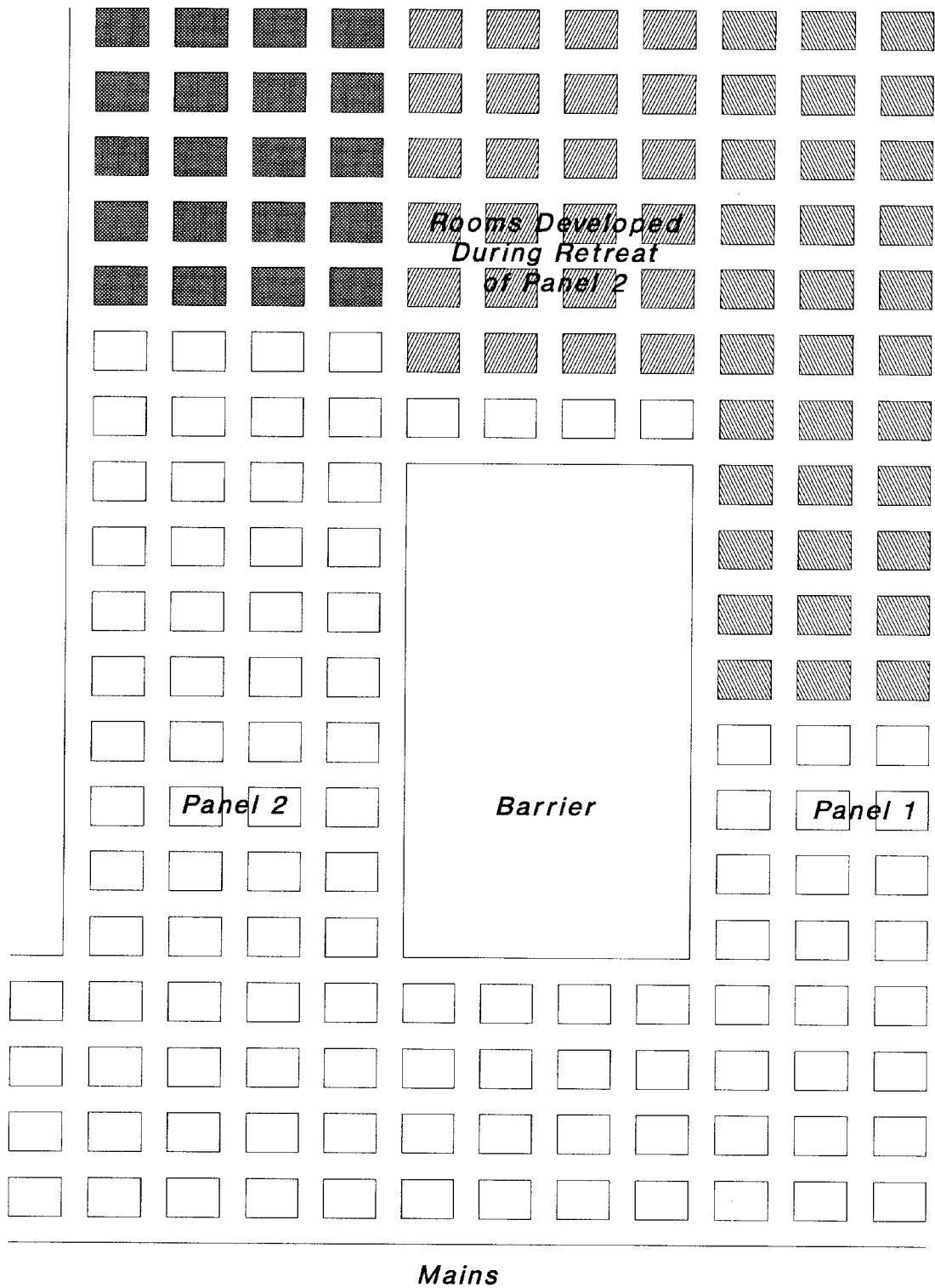


Figure 13.—Case study: full pillaring plan.

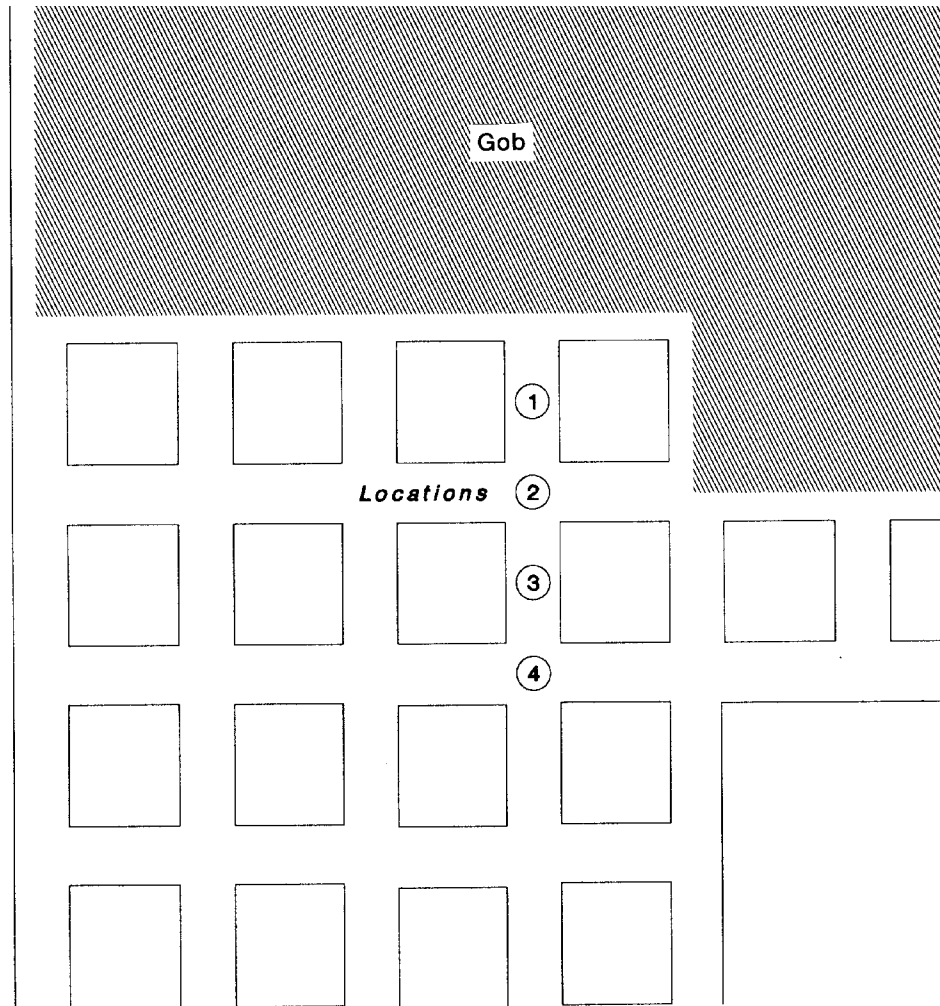


Figure 14.—Case study: full pillaring analysis locations.

but the occurrence of severe conditions should be avoided or at least limited to location 1.

Table 4 presents the BESOL and predicted deterioration index data for each of the four locations for a number of scenarios. The analysis indicated that the use of 40- by 30-ft

pillars would result in good conditions through a depth of 400 ft and that 40- by 40-ft pillars would be effective up to 600 ft of cover. Pillars 50- by 50-ft in size would be needed for deeper cover areas, although severe conditions could be possible at locations 1 and 2 as the depth approaches 900 ft.

CONCLUSION

Boundary-element modeling has proven to be an effective tool for mining engineers to resolve complex ground control problems. The techniques set forth in this paper describing coal, rock, and gob behavior have been effectively used to evaluate a variety of mining scenarios. Although they are supported by a number of in situ measurements and have resulted in near duplication of underground conditions in many instances, they provide only a first estimate of parameters that must be validated. Successful numerical simulation requires a substantial

effort, including the observation of conditions in many areas and the often repetitive process of calibrating model parameters. The use of techniques such as the deterioration index/regression method has greatly facilitated the linking observed and simulated mine conditions. It cannot be overemphasized, however, that in order to be of any value, a numerical model *must* be validated and provide a realistic representation of the underground environment for which it is applied.

REFERENCES

- Bieniawski ZT [1984]. Rock mechanics design in mining and tunneling. A. A. Balkema, 272 pp.
- Carr F, Wilson AH [1982]. A new approach to the design of multi-entry developments for retreat longwall mining. In: Proceedings of the Second Conference on Ground Control in Mining. Morgantown, WV: West Virginia University, pp. 1-21.
- Choi DS, McCain DL [1980]. Design of longwall systems. Trans Soc Min Eng AIME, Vol. 268, pp. 1761-1764.
- Crouch SL, Fairhurst C [1973]. The mechanics of coal mine bumps and the interaction between coal pillars, mine roof, and floor. U.S. Department of the Interior, Bureau of Mines, OFR 53-73, pp. 23-27.
- Crouch Research, Inc. [1988]. The BESOL system: boundary element solutions for rock mechanics problems: user's guide, version 2.01. St. Paul, MN: Crouch Research, Inc., pp. 5-19.
- Holland CT, Gaddy FL [1964]. The strength of coal in mine pillars. In: Proceedings of the 6th U.S. Symposium on Rock Mechanics. Rolla, MO: University of Missouri, pp. 450-466.
- Hsuing SM, Peng SS [1985]. Chain pillar design for U.S. longwall panels. Min Sci and Technol, Vol. 2, pp. 279-305.
- Mark C [1990]. Pillar design methods for longwall mining. Pittsburgh, PA: U.S. Department of the Interior, Bureau of Mines, IC 9247.
- Mark C, Chase FE [1997]. Analysis of retreat mining pillar stability (ARMPS). In: Proceedings - New Technology for Ground Control in Retreat Mining. Pittsburgh, PA: U.S. Department of Health and Human Services, Public Health Service, Centers for Disease Control and Prevention, National Institute for Occupational Safety and Health, DHHS (NIOSH) Publication No. 97-122, IC 9446, pp. 17-34.
- Mark C, Iannacchione AT [1992]. Coal pillar mechanics: theoretical models and field measurements compared. In: Proceedings of the Workshop on Coal Pillar Mechanics and Design. Pittsburgh, PA: U.S. Department of the Interior, Bureau of Mines, IC 9315, pp. 78-93.
- Molinda GM, Mark C [1993]. The coal mine roof rating (CMRR): a practical rock mass classification for coal mines. In: Proceedings of the 12th International Conference on Ground Control in Mining. Morgantown, WV: West Virginia University, pp. 92-103.
- Obert L, Duvall WI [1967]. Rock mechanics and the design of structures in rock. New York, NY: Wiley, pp. 542-545.
- Pappas DM, Mark C [1993]. Load deformation behavior of simulated longwall gob material. In: Proceedings of the 12th International Conference on Ground Control in Mining. Morgantown, WV: West Virginia University, pp. 184-193.

THE FRACTURE MECHANICS APPROACH TO UNDERSTANDING SUPPORTS IN UNDERGROUND COAL MINES

By James M. Kramer, Ph.D.,¹ George J. Karabin, P.E.,² and M. Terry Hoch³

ABSTRACT

This paper introduces the fracture mechanics approach—a unique way to predict the stability of a coal mine panel. The technique uses analytic equations to calculate the stress, strain, and yield characteristics of coal support systems. It uses fracture mechanics to model almost every type of mine support structure. Another feature is a method that incorporates field-tested knowledge into the analytical analysis. For example, this technique can model the yield characteristics of a coal seam by combining empirical pillar strength equations into the analytic analysis. It may be possible to simulate multiple-seam mining by incorporating subsidence methods into the analysis. The method is simple and quick, which makes it attractive for stress analysis software. It should be more accessible to those in the mining industry who do not have expertise in rock mechanics or numerical modeling. Although the purpose of this research is for modeling coal mines, it should be adaptable to any mine in a tabular deposit.

¹Mining engineer.

²Supervisory civil engineer.

³Chief.

Roof Control Division, Pittsburgh Safety and Health Technology Center, Mine Safety and Health Administration, Pittsburgh, PA.

INTRODUCTION

This paper presents a new way to analyze the mechanical behavior of underground coal mine supports. Included are analytic expressions describing the stress, strain, and yielding characteristics of a coal seam. The *fracture mechanics approach* (FMA) provides the capability to model almost every type of mine structure, including pillars, yield pillars, longwall gob, chocks, cribs, posts, and hydrostatic loads. In addition, it predicts pillar stability by combining empirical pillar strength equations into the analytic analysis. This makes the procedure useful for understanding how various support structures affect the mechanical performance of a mine panel.

Although the method is not as sophisticated as numerical analysis, it offers several advantages. The analytic equation

makes it as accurate as numerical modeling, but quicker and easier to use. Because of the few equations involved, it is easy to incorporate the process into a computer spreadsheet or programmable calculator. Real-time design analysis is possible by incorporating the technique into computer code. For example, one can change a design structure (e.g., add a crib) and see instantly the resultant stress effect. The coal yielding process uses empirical pillar strength equations derived from years of field measurements. Combining these equations into the analytic analysis provides insight into pillar stability. The system presented in this paper offers a unique perspective from which to study mine panel stability.

DESIGNING SUPPORT STRUCTURES FOR COAL MINES

There are several ways to analyze the stability of a mine layout. The easiest and, in some cases, most reliable is to use pillar strength equations. These equations are developed from extensive knowledge of coal seam behavior [Mark and Iannacchione 1992]. Most are based on physical stress measurements; however, some come from numerical studies or analytic equations. All of these methods use the pillar width-to-height ratio as the controlling factor. These strength equations can be accurate; however, they assume that the coal pillar is the single means of support. It is not possible to study the effects of cribs, posts, longwall gob, chocks, etc. Also, these equations do not predict the stress distribution through the panel, nor do they predict the extent of the yield zone in the coal.

There are other, more accurate, ways to analyze stability. Numerical modeling, if used properly, can be very accurate. It

can predict the stress distribution throughout the entire mine environment, including the coal seam, surrounding strata, slips, faults, and all types of supports. However, this method is time-consuming and requires a certain amount of technical skill. For example, using finite elements, it would take a skilled engineer a day or more to analyze the yield zone in a coal pillar based on data derived from field measurements.

This paper discusses a simple, quick, and accurate solution for predicting the stress distribution in coal pillars and other structures. It uses a combination of fracture mechanics and empirically derived techniques to predict the extent of the yield zone in a coal pillar. It can model nearly every structure used for mine support. Numerical modeling will validate the accuracy of the technique.

THE FRACTURE MECHANICS APPROACH

Understanding the FMA requires visualizing a coal seam as an extremely thin layer in the stratum of the Earth. A tunnel or opening in the coal would appear as a thin crack in an infinite mass.⁴ It should then make sense that it is possible to use the mechanics of cracks to analyze the stresses surrounding openings in coal seams.

Visualizing a mine opening as a crack is not new; others applied it to their research [Barenblatt 1962; Hackett 1959; Crouch and Fairhurst 1973; Berry 1960, 1963]. However, this paper describes a way to use the fracture mechanics directly to predict pillar stress. Combined with a superpositioning

technique, it is possible to obtain the complete stress distribution throughout the mine panel. A yielding technique completes the analysis by offering realistic characteristics to the coal pillars.

Westergaard's equation is fundamental to fracture mechanics theory and is also the basic equation for the FMA [Westergaard 1939]. The stress distribution at the crack tip is identical to the distribution adjacent to a mine opening. Westergaard describes the stress at the tip of a crack as

$$F_y(x) = \frac{F_x}{\sqrt{x^2 + a^2}}, \quad (1)$$

⁴In this paper, the term "crack" infers a mine opening and vice versa. Therefore, crack-tip stress is the same as rib or pillar stress.

where $F_y(x)$ ' stress distribution adjacent to a crack tip,
 a ' 1/2 the crack width,
 F ' in situ stress,
 and x ' distance from the center of the crack.

This equation implies that the only parameters needed to predict elastic rib stress are the entry width and the in situ stress (figure 1). Westergaard derived equation 1 by assuming that the stress field acting on the crack is located at an infinite distance from the crack surface. Another assumption is that the crack width must align with the planes of this stress field. In general, these conditions are similar to a mine environment. The Westergaard equation will accurately predict the stress distribution into the coal seam provided that the analysis remains within the elastic range.

NUMERICAL METHODS VALIDATE THE WESTERGAARD EQUATION FOR MINE ANALYSIS

Westergaard developed his stress function by making the following assumptions: the crack has a thickness of zero; it is contained in an infinite, homogeneous plate; and the plate is subjected to a uniform biaxial stress field. These conditions match fairly the conditions encountered in a coal mine opening. There are differences, however. A mine opening has an actual thickness. The structural properties of the coal differ from those of the surrounding rock mass. Also, a coal mine's environment is under the influence of a graduated, nonuniform, biaxial stress field controlled by gravity. It is necessary to consider all of these factors to validate the FMA. Previous research demonstrates the accuracy of the FMA by comparing it to numerical modeling output [Kramer 1996]. It is shown that the technique matches the numerical modeling predictions with a high degree of accuracy.

Figures 2 through 7 are plots that compare the stress prediction of the FMA with that of numerical modeling. The purpose is to show how well the FMA can predict stress even in conditions less ideal than those used by Westergaard to derive equation 1. Such conditions are similar to those encountered in an underground coal mine. All of the evaluations use FLAC⁵ as the numerical modeling software. Spreadsheet graphs are used to compare the FMA stress prediction with that determined by FLAC. Each demonstrates that the FMA compares reasonably well with the FLAC model for varying conditions of nonhomogeneity. Initially, the model is homogeneous and simple. The FMA matches extremely well with the numerical model [Kramer 1996]. Then, in order to introduce nonhomogeneity into the numerical model, each

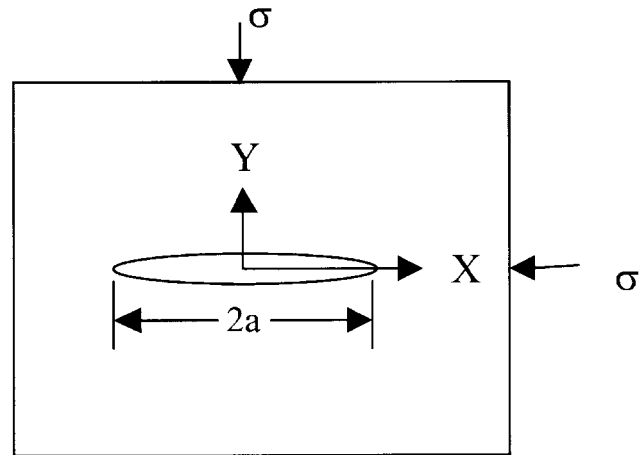


Figure 1.—Crack of width $2a$ subjected to a uniform biaxial stress field.

individual structural property is altered independently and the results are compared with the FMA. Finally, an evaluation is made between the FMA and a nonhomogeneous numerical model consisting of strata with properties even more variant than an actual mine environment.

Figure 2 charts the comparative stress predictions between the FMA and FLAC for a simple, elastic, and homogeneous model. Note that the stress distributions are nearly exact. The only real difference is at the edge of the mine opening. This difference is due to the approximation technique used in numerical analysis. The model in figure 3 has the same homogeneous properties as those for figure 2; it plots the stress distribution through various planes in the coal seam. This illustrates that the distribution, at any plane, remains consistent with the distribution through the center plane of the seam. Figures 4 and 5 demonstrate that the coal's modulus of elasticity or Poisson's ratio has little effect on the stress distribution through the center plane of the coal seam. The next step is to compare the accuracy of the FMA for predicting the stress of a nonhomogeneous numerical model. Figures 6 and 7 relate the results of the simulation.

Figure 6 shows the comparison between FLAC and the FMA for the stress distribution produced in a graduated, nonuniform, biaxial stress field similar to that encountered in an underground mine. For these studies, the horizontal stress is 0.3 times the vertical stress. The design of the model places the coal seam at a depth of 381 m. The structural parameters of the coal and rock are equivalent. This study also compares the Westergaard equation to the stress at various planes in the seam (figure 6).

It can be seen that the nonuniform stress field in the numerical model causes a deviation in stress from the Westergaard prediction; however, most of the difference is near the edge of the mine opening. In this portion of the mine rib, the coal is yielding. Analytical methods do not exist for predicting the stress distribution in this region. Introduced later in this paper is a method that uses field measurements to describe the stress distribution in the yield zone of a coal rib.

⁵ Fast Langrangian Analysis of Continuum, Itasca Corp., Minneapolis, MN.

**Comparing the Westergaard Equation to FLAC
(In situ stress = 6.9MPa, Entry width = 15.2m)**

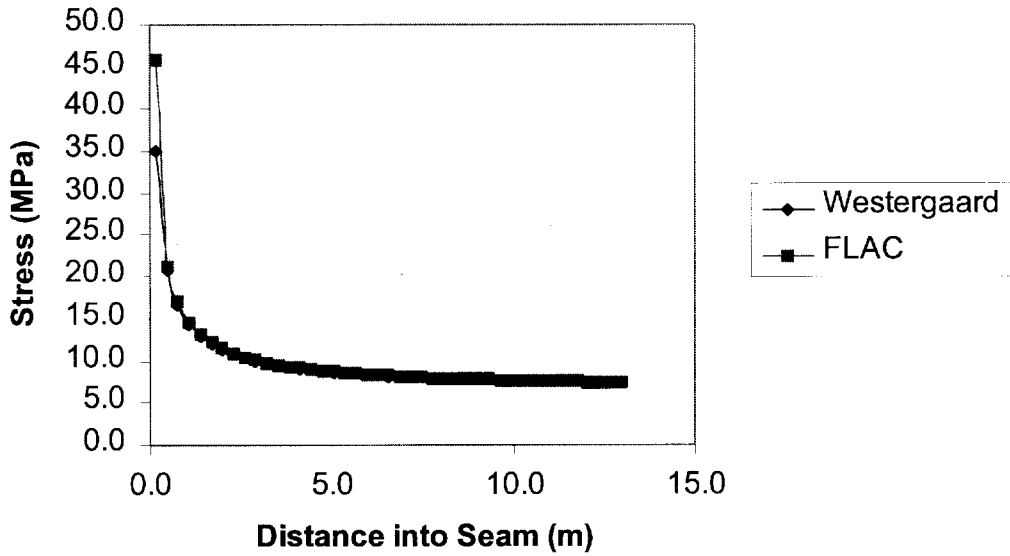


Figure 2.—Stress distribution in a coal seam next to a mine opening: comparison between numerical analysis and the Westergaard equation. Homogeneous model.

Stress Distribution in Various Planes in the Coal Seam

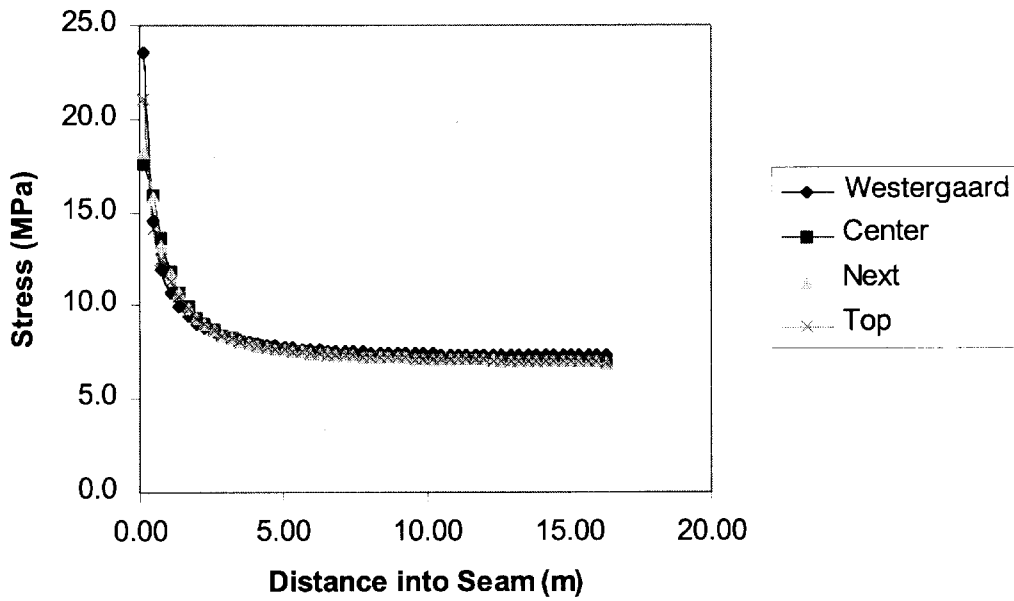


Figure 3.—Stress distribution at various levels in the coal seam. Properties similar to the model in figure 2.

Different Moduli of Elasticity in a Biaxial Stress Field

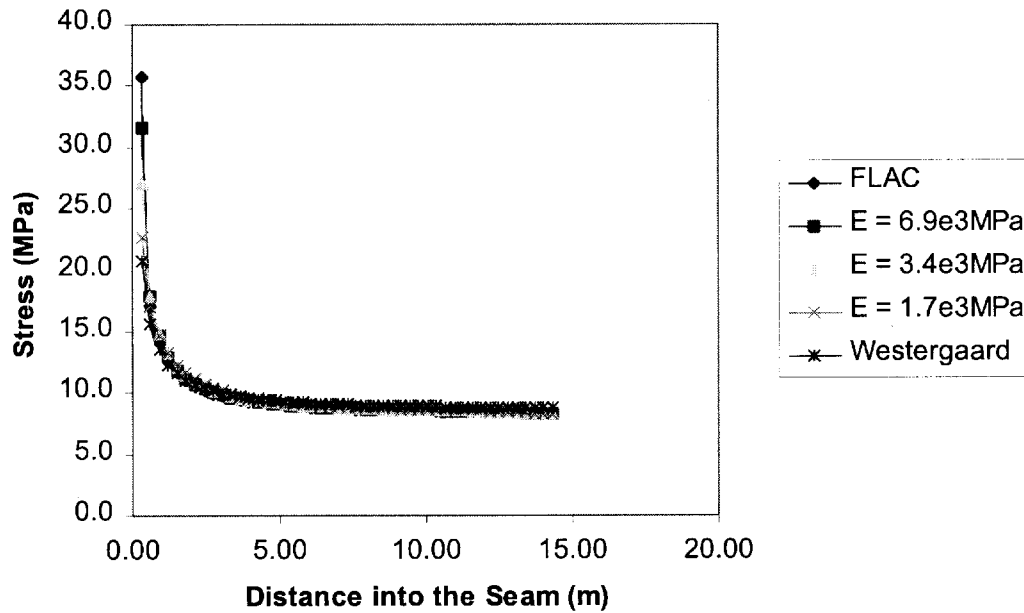


Figure 4.—Stress profile for coal with different moduli. Four separate FLAC models.

Poisson's Ratio Comparison in a Biaxial Stress Field

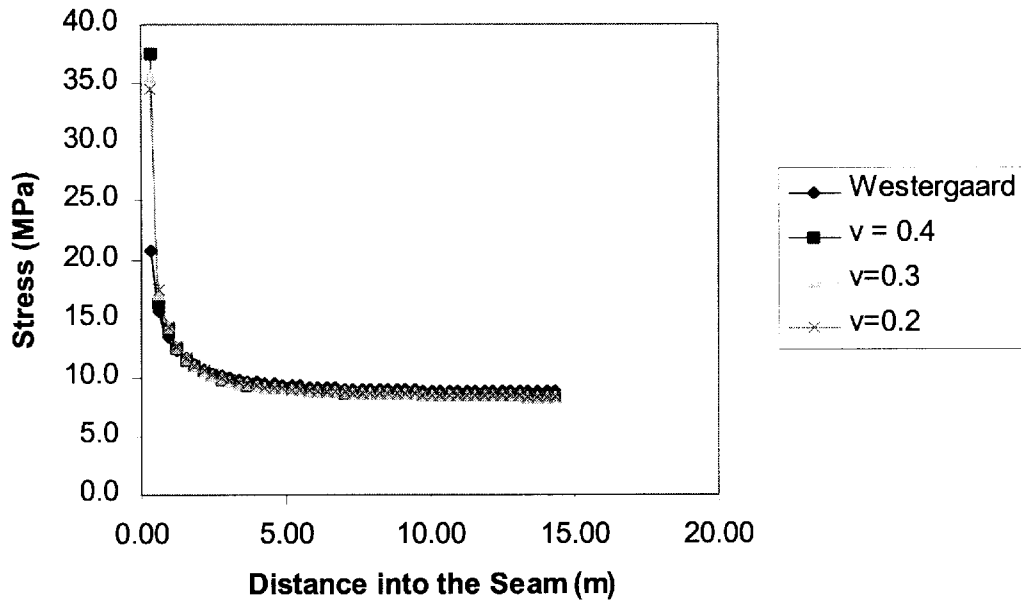


Figure 5.—How the Poisson ratio affects the stress distribution. Three separate FLAC models.

Stress at Various Planes in the Coal Seam

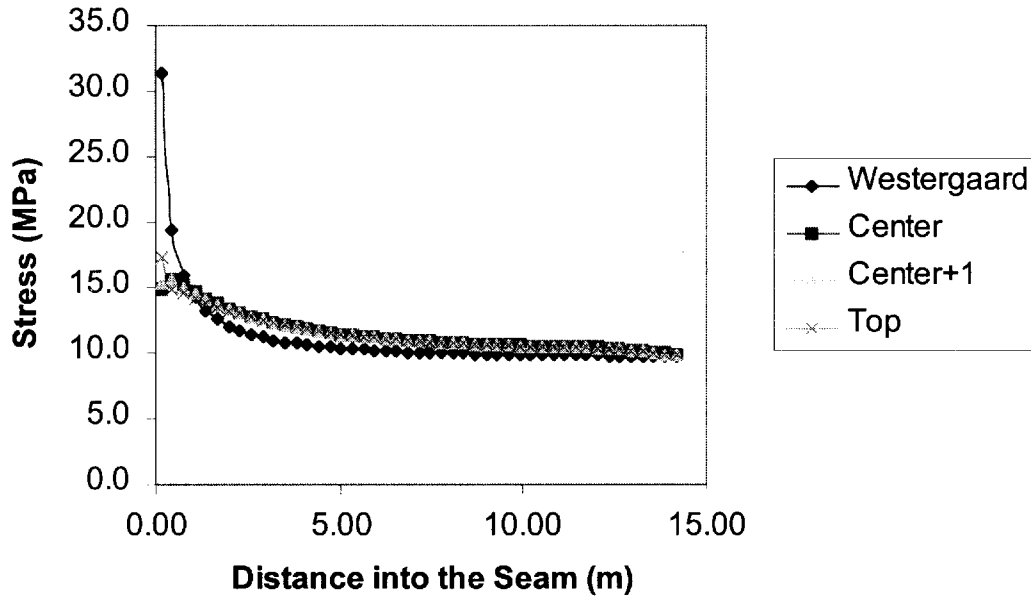


Figure 6.—The effect of a graduated, nonuniform biaxial stress distribution similar to conditions underground. Stress profile at various levels in the seam.

Conditions Similar to a Real Mining Environment

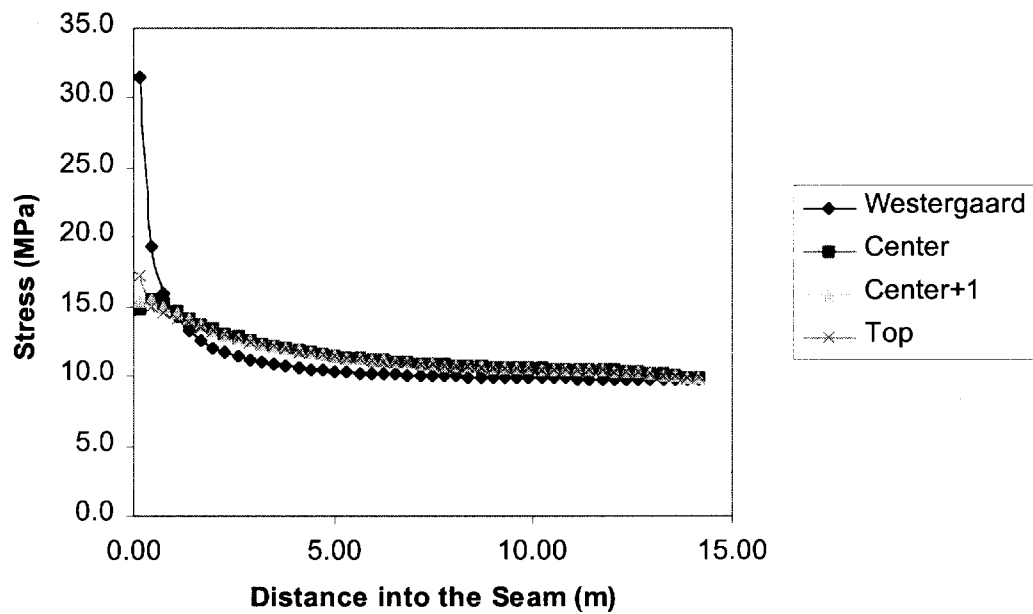


Figure 7.—Comparison of a model simulation of a real mine environment.

The numerical model described below will validate the FMA's ability to analyze structural variations found in a real mine environment. In this model, the strata are nonhomogeneous. In addition, the surrounding stress field is variable in both the vertical and horizontal planes. Such a model has structural variations greater than those encountered in most coal mines. The surrounding rock mass has a Young's modulus of 27,580 MPa and a Poisson's ratio of 0.2. The unit weight of this mass is 0.03 MN/m³. The coal seam has a Young's modulus of 3,448 MPa, a Poisson's ratio of 0.3, and a unit weight of 0.03 MN/m³. The unit weights are high to enhance the stress comparisons by increasing the effect of gravity

loading. To show the effect of mining in an area subjected to a high stress field, the model is initialized with a premining stress prior to adding the mine opening. Adding a mine opening to a model with a high biaxial stress field already in place would alter the stress in the areas adjacent to the mine opening. Figure 7 compares the Westergaard equation to FLAC's analysis for different levels in the coal seam. The distributions vary considerably; however, most of this deviation is near the mine opening. In this area, the coal will yield. A technique will be presented in this paper that describes the stress distribution in the yield zone of the coal.

THE POINT-FORCE METHOD USED TO SIMULATE MINE SUPPORTS

An essential concept of the FMA is the process by which a point force, acting on the surface of the crack, affects the stress intensity at the crack tip. In mining, this point force could be a mine post or hydraulic jack. A continuous series of point forces can model a yield pillar, longwall gob, the yield zone of the pillar, or any other type of mining supports [Kramer 1996]. Figure 8 depicts a crack with an internal point force, P , pushing out against the crack surface. This force P is at a distance x from the crack center. This force affects the stress intensity factor K at points A and B. The point force is similar to the loading from a single-point mine support, such as a post or hydraulic jack.⁶

Green functions are used to predict the stress intensity factors [Paris and Sih 1965]. The factors are:

$$K_A = \frac{P}{\sqrt{Ba}} \sqrt{\frac{a+x}{a-x}} \quad (2)$$

$$K_B = \frac{P}{\sqrt{Ba}} \sqrt{\frac{a-x}{a+x}} \quad (3)$$

where K_A = stress intensity at point A,

K_B = stress intensity at point B,

P = point force,

a = 1/2 the opening width,

and x = distance from opening center

⁶The stress intensity factor is of utmost importance in the study of fracture mechanics. It is a measure for the stress singularity at the crack tip. For the case of uniaxial compression with force P at infinity, K must be proportional to P . K_A and K_B must also be proportional to the square root of a length. For an infinite object, the only characteristic length is the crack size; thus, K must take the form: $K = F/(Ba)$.

YIELD PILLARS

Yield pillars are common in longwall mining; they control floor heave and/or fine tune roof behavior. As the name implies, the pillars yield, thus redistributing the load around a control area in the mine. It is possible to model yield pillars as a continuous series of point forces. Equations derived from in situ pillar strength measurements can determine the intensities of the point forces. However, for the present discussion, the point forces are considered uniform and equal to the yield strength of the coal (figure 9).

To illustrate the method, it is necessary to discuss only the stress effect at a single crack tip (e.g., point A in figure 9). Either equation 2 or equation 3 can describe the stress intensity at point A. The correct equation to use depends on the location of the point forces with respect to the a -origin. In the discussion below, the location of the point forces (figure 9) is chosen to provide the most complete example of the technique. Because the locations of the point forces are equally distributed on both sides of the origin, solution to the stress effect at point A requires using a combination of equations 2 and 3. In

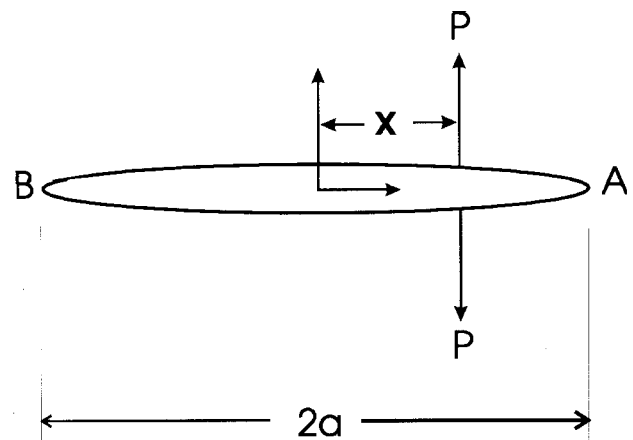


Figure 8.—Crack with wedge forces at x .

absence of the yield pillar, the stress intensity at point A is [Dugdale 1960]:

$$K_{insitu} = F_{insitu} \sqrt{Ba} \tag{4}$$

The yield pillar will act to reduce this intensity. The a-origin is located in the center of the point forces; thus, the distribution in the -x side is equal to the distribution in the +x side (figure 9). The stress intensity factor at point A caused by the continuous point forces on the +x side of the origin is

$$K_{+x} = K_A \int_0^d \frac{F_{ys}}{\sqrt{Ba}} \sqrt{\frac{a+x}{a-x}} dx \tag{5}$$

The stress intensity factor at point A caused by the continuous point forces on the -x side of the origin is

$$K_{-x} = K_A \int_0^d \frac{F_{ys}}{\sqrt{Ba}} \sqrt{\frac{a+x}{a-x}} dx \tag{6}$$

The stress intensity factor for the yield pillar becomes

$$K_{yield} = K_{+x} + K_{-x} \tag{7}$$

With the yield pillar in place, the stress intensity factor at point A becomes

$$K_{total} = K_{insitu} + K_{yield} \tag{8}$$

The Westergaard equation relates rib stress to the in situ stress and the width of the opening. Because K_{total} includes not only the in situ stress but also the effect of the yield pillar, it is necessary to modify the Westergaard equation to reflect this effect. It is necessary to modify the Westergaard equation by substituting a dummy variable in place of a real variable. The opening half-width variable "a" is the proper choice for the substitution.⁷ Solving for "a" in K_{total} and substituting it into the Westergaard equation as a dummy variable will provide the proper stress distribution at point A. The following demonstrates the concept.

The stress intensity factor is defined as

$$K = F \sqrt{Ba} \tag{9}$$

To modify the Westergaard equation, it is necessary to substitute values and solve for the unreal "a", making it a dummy variable such that

$$a_{dummy} = \frac{K_{total}^2}{BF_{insitu}^2} \tag{10}$$

The reduced Westergaard stress distribution at point A then becomes

$$F_{modified}(x) = \frac{F_{insitu} x}{\sqrt{x^2 + a_{dummy}^2}} \tag{11}$$

⁷Modifying F would result in the stress distribution leveling to a value below the in situ stress.

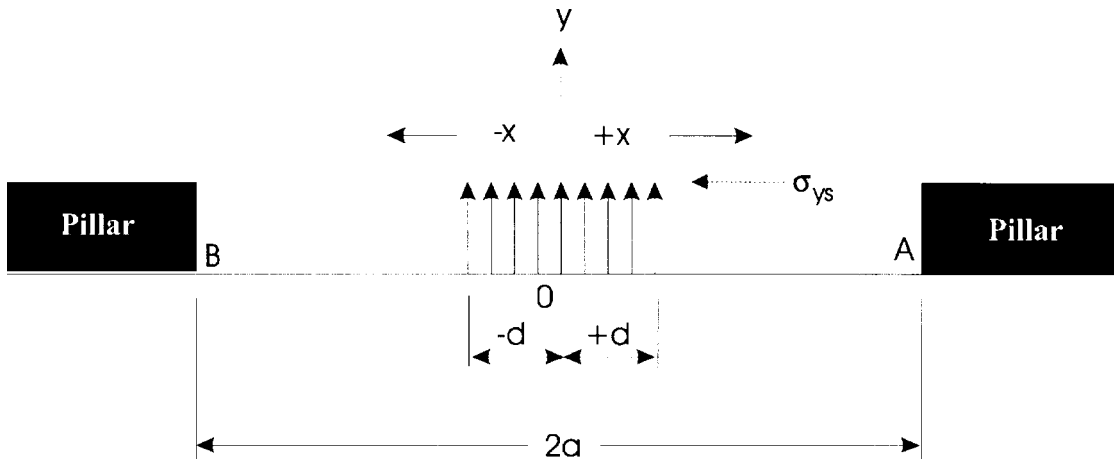


Figure 9.—Yielded pillar modeled as a continuous set of point forces.

LONGWALL GOB

The technique used to model longwall gob is similar to that for the yield pillar. An assumption can be made that the center of the gob is in contact with the roof and floor and the material is compacted completely. Due to symmetry, it is necessary to model only one-half the gob width to determine its effect on the stress intensity at the tip of the opening. Therefore, the opening extends from the gob center to edge of the gate pillar at point A (figure 10). The residual strength of this material is a function of the amount of compaction. Because the center of the gob has the greatest compaction, it has the greatest residual strength; the outside edge of the gob has the least. To simulate gob material, the point forces are high in the center of the gob and low at the edge. Originally, the following example was formulated using U.S. customary units of measurement. Conversion to the metric system makes some values appear awkward.

As usual, the a-origin and x-origin begin at a point equidistant from point A and the gob center. The point forces to the right of the origin (i.e., %x side) would use equation 5 to analyze the effect at point A; the point forces to the &x side of the origin will use equation 6. "Derive—A Mathematical Assistant"⁸ is used to solve for the integral in each equation. Included in table 1 are the input variables and resultant stress intensity factors for the gob depicted in figure 10. The gob material in the model is divided into six sections, each reflecting a different yield strength (YS₁ to YS₆). The first three sections are in the &x side (K_B side) of the origin; the other three are in the %x side (K_A side). The location of the section determines which point-force equation to use. The total effect of the gob is the summation of the K-values for all six sections:

$$K_{gob} = K_1 + K_2 + K_3 + K_4 + K_5 + K_6 \tag{12}$$

This value is subtracted from the K_{insitu} value (the stress intensity for the large opening without the gob material in place) to obtain the proper stress intensity factor at point A. The relation is

$$K_{total} = K_{insitu} - K_{gob} \tag{13}$$

EXAMPLE

Below is an example that demonstrates the technique. It analyzes the effect from two sections of the complete model shown in figure 10. These particular sections (sections 3 and 4) were chosen to illustrate forces on either side of the axis origin. The point forces in section 3 align in the &x direction; those in section 4 are in the %x direction. The stress intensity factor will be determined using a combination of equations 5 and 6. Table 1 lists the results from the complete analysis.

Input Parameters:

- Width of longwall face ' 232 m
- 1/2 width of longwall face ' 116 m
- 2a (width of longwall face plus gate entry) ' 122 m
- a ' 61 m
- F_{insitu} ' 13.8 MPa

Section 3:

The yield strength for section 3 is F_{ys3} ' 12.4 MPa. It occupies the &x portion of the a-axis for the 0- to (&)18.3-m segment. The effect on the stress intensity at point A due to section 3 of the gob is

$$K_3 = \frac{F_{ys}}{\sqrt{Ba}} \int_0^{18.3} \sqrt{\frac{a+x}{a-x}} dx$$

$$= \frac{12.4}{\sqrt{B61}} \int_0^{18.3} \sqrt{\frac{61+x}{61-x}} dx$$

$$= 14.1$$

NOTE: Although the point forces are in the -x region, the limits of the integral are from 0 to (%)18.3 m.

Section 4:

The yield strength for section 4 is F_{ys4} ' 10.3 MPa. This section occupies the %x portion of the a-axis for the 0- to (%)18.3-m segment. The effect on the stress intensity at point A due to section 4 of the gob is

$$K_4 = \frac{F_{ys}}{\sqrt{Ba}} \int_0^{18.3} \sqrt{\frac{a-x}{a+x}} dx$$

$$= \frac{10.3}{\sqrt{B61}} \int_0^{18.3} \sqrt{\frac{61-x}{61+x}} dx$$

$$= 15.9$$

"Derive—A Mathematical Assistant" solved both of these integrals. The solutions yield a rather cumbersome equation that is impractical to include in this paper; however, it can be incorporated into spreadsheet software or computer code. Table 1 includes the K factors for all six sections of the longwall gob. The effect on the stress intensity factor at point A caused by all six sections is

$$K_{gob} = K_1 + K_2 + K_3 + K_4 + K_5 + K_6$$

$$K_{gob} = 13.8 + 10.7 + 14.1 + 15.9 + 18.0 + 25.8$$

$$K_{gob} = 98.3$$

⁸Derive—A Mathematical Assistant," Soft Warehouse, Inc., 3660 Waiialae Ave., Honolulu, HI.

Table 1.—Input variables and stress intensity factors for each section of the longwall panel depicted in figure 10

	Section 1	Section 2	Section 3	Section 4	Section 5	Section 6
F_{ys} , MPa	13.8	13.1	12.4	10.3	8.3	6.9
x-range, m	61.0-36.6	36.6-18.3	18.3-0	0-18.3	18.3-36.6	36.6-55.0
Stress intensity at point A (%x side)	—	—	—	15.9	18.0	25.8
Stress intensity at point A (&x side)	13.8	10.7	14.1	—	—	—
K_{gob}	98.3	—	—	—	—	—

Input parameters:

Width of longwall face ' 232 m

1/2 width of longwall face ' 116 m

2a (width of longwall face plus gate entry) ' 122 m

a ' 61 m

F_{insitu} ' 13.8 MPa

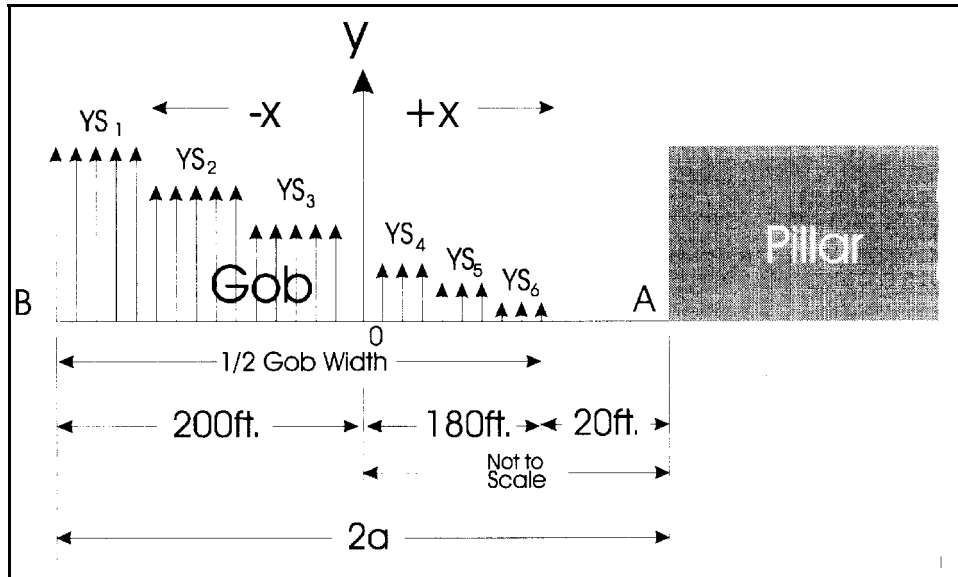


Figure 10.—Longwall gob simulated as point forces of different strengths.

Equation 4 determines the stress in absence of the gob (point forces) as

$$K_{insitu} ' F_{insitu} \sqrt{Ba}$$

$$K_{insitu} ' 13.8 \sqrt{B61}$$

$$K_{insitu} ' 191.0$$

$$a_{dummy} ' \frac{K_{total}^2}{BF_{insitu}^2}$$

$$a_{dummy} ' \frac{(92.7)^2}{B(13.8)^2}$$

$$a_{dummy} ' 14.4 \text{ m}$$

It is necessary to reduce this intensity to reflect the addition of the gob material. The stress intensity factor at point A now becomes

$$K_{total} ' K_{insitu} \& K_{gob}$$

$$K_{total} ' 92.7$$

The modified Westergaard distribution at point A becomes

$$F_{modified}(x) ' \frac{F_{insitu} x}{\sqrt{x^2 \& a_{dummy}^2}}$$

$$F_{modified}(x) ' \frac{13.8x}{\sqrt{x^2 \& 14.4^2}}$$

The dummy variable used to relate this stress reduction to the Westergaard equation is

This is the general technique used to model longwall gob. Luo significantly improved the above technique and developed a computer program to model the stability of longwall chain pillars [Kramer et al. 1998].

HYDROSTATIC FORCES

It is possible to measure the effect of hydrostatic forces on the coal seam. A hydrostatic force acts with equal strength in all three cardinal directions. It is similar to the pressure exerted from water or gas. To simulate a hydrostatic force, it is

necessary to fill the entire mine opening with a continuous distribution of point forces (figure 11). In order to test the hydrostatic effect, the point forces are set equal to the in situ stress (13.8 MPa). This situation should have the effect of flattening the stress distribution at point A to a level equal to the in situ stress.

Figure 12 is a plot of the stress distribution. It can be seen the distribution is almost uniform and equivalent to the in situ stress. This further demonstrates that the point-force method accurately describes the effective stress distribution at the mine rib.

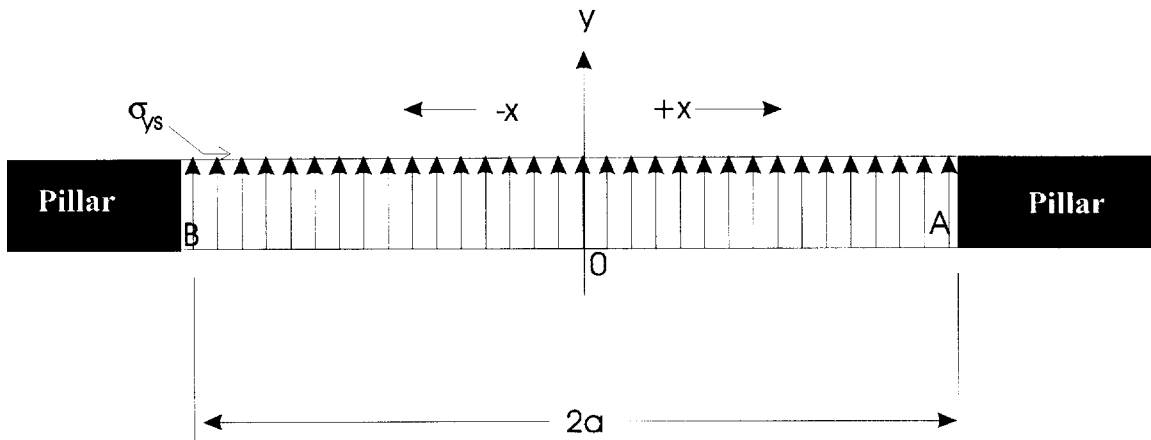


Figure 11.—Crack opening completely filled with point forces equal to the in situ stress.

**Crack Opening Filled with Point Loads
Equal to the In situ Stress**

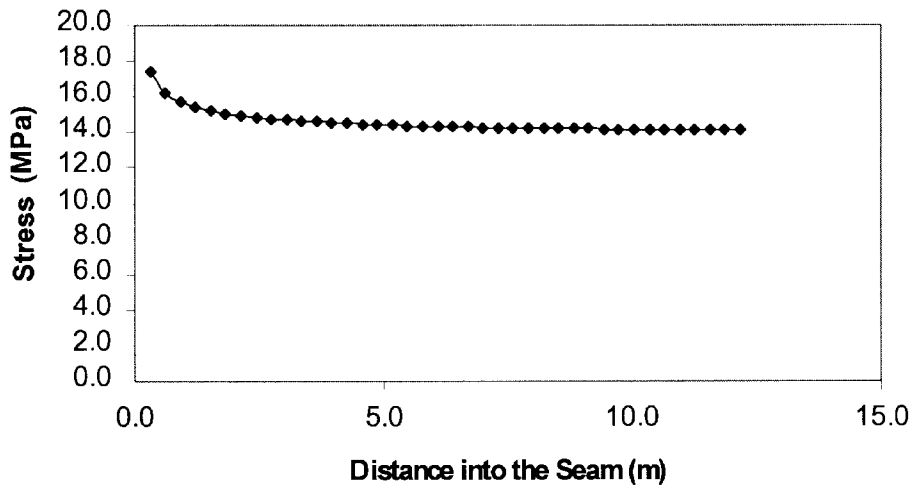


Figure 12.—Stress distribution at point A is nearly flat and equal to the in situ stress.

TECHNIQUE TO COMBINE DIFFERENT MINE SUPPORTS

It is possible to combine any type of mine supports and predict the resultant stress distribution in the coal seam. Figure 13 presents a typical mining environment combining the following structures: a longwall gob, a yield pillar, and a crib. Analyzing this arrangement requires a combination of the stress intensity factors for each support member. This combined value is used to reduce the total stress intensity at point A. The procedure for doing this is as follows:

- Calculate K_{insitu} for point A
- Calculate K_{gob} for point A
- Calculate K_{yield} for point A
- Calculate K_{crib} for point A
- Combine the stress intensity factors for each support, and use this value to reduce the stress intensity associated with the entire opening width:

$$K_{total} = K_{insitu} \& K_{gob} \& K_{yield} \& K_{crib}$$

EVALUATING PILLAR YIELD

Because coal mines are often located at a great depth below the surface, the stress levels often exceed the yield strength of the coal. It is necessary to account for yielding in the coal pillars to correctly assess structural stability. Fracture mechanics is useful in predicting the yielding characteristics of the coal.

The Westergaard equation introduces a singularity at the pillar edge. This is where the stress distribution approaches infinity. The pillar edge yields and redistributes the loading in order to eliminate the singularity. The yielded zone continues to offer residual support to the roof and floor.

Dugdale provides a way to estimate the length of this yield zone in the pillar [Dugdale 1960; Broek 1982]. The following sections describe how to determine the extent of the yield zone. Also described is a way to predict the stress distribution in the elastic core of the pillar. First, the basic technique used by Dugdale to arrive at his yield zone prediction is reviewed. Later, a technique is introduced that determines the extent of the yield zone specifically in coal.

THE EFFECT OF POINT LOADING ON THE STRESS INTENSITY AT THE CRACK TIPS

As mentioned previously, figure 8 depicts a crack with an internal wedge force P pushing out against the crack surface. This force P is at a distance x from the crack center. These wedge forces affect the stress intensity function, K, at points A and B. It is possible to use equations 2 and 3 to predict these stress intensity factors, K [Paris and Sih 1965]. A form of these equations is fundamental in the development of residual forces supporting the roof and floor in the yielded portion of the pillar.

DUGDALE'S APPROACH TO CRACK TIP YIELDING

Although the pillar edge yields, it has a residual strength that supports the roof and floor of the coal seam. Imagine this residual support as a continuous distribution of dislocated

point forces (figure 14). Dugdale determined the extent of the yielded zone by first assuming that the residual strength of each point force is equal to the yield strength, F_{ys} , of a material (in this case, coal) [Dugdale 1960; Broek 1982]. Because the yielded edge is significantly weaker, it would seem as though the mine opening becomes wider. The mine opening would theoretically extend into the pillar to the point where yielding stops. At this point, the singularity disappears because of the canceling effect of the residual stress in the yield zone. The effective mine width, $a_{eff} = a + D$, represents the distance to the new elastic crack tip, where D symbolizes the extent of the yielded zone.

The yielded zone, D, exerts a residual stress equal to the yield stress, F_{ys} . The yield zone, D, depicted as additional opening width, is not really an opening; the material can still bear the yield stress. The size of D is chosen so that the stress singularity disappears: K_{total} approaches zero. This means that the stress intensity, K_{insitu} , due to the uniform in situ stress, F, has to be compensated by the stress intensity, K_D , due to the residual wedge forces F_{ys} [Broek 1982]. In other words:

$$K_{insitu} = K_D \tag{14}$$

Satisfying equation 14 leads to the determination of D in the following manner. Equations 2 and 3 describe how a point load affects the stress intensity factor, K. If the wedge forces are distributed from s to the effective crack tip, the stress intensity becomes

$$K = \frac{P}{\sqrt{Ba}} \int_s^a \left(\sqrt{\frac{a-x}{a}} \cos \theta + \sqrt{\frac{a+x}{a}} \sin \theta \right) dx \tag{15}$$

Solution to this integral is

$$K = 2P \sqrt{\frac{a}{B}} \cos^2 \theta \frac{s}{a} \tag{16}$$

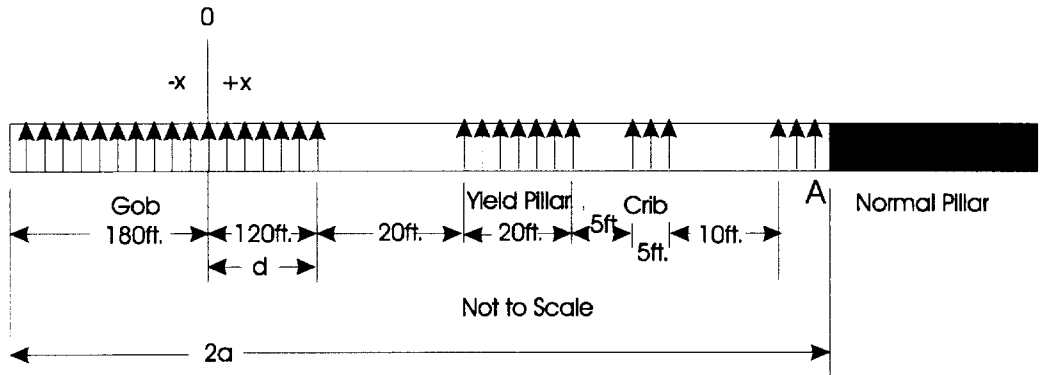


Figure 13.—Modeling various support structures using the point-force technique.

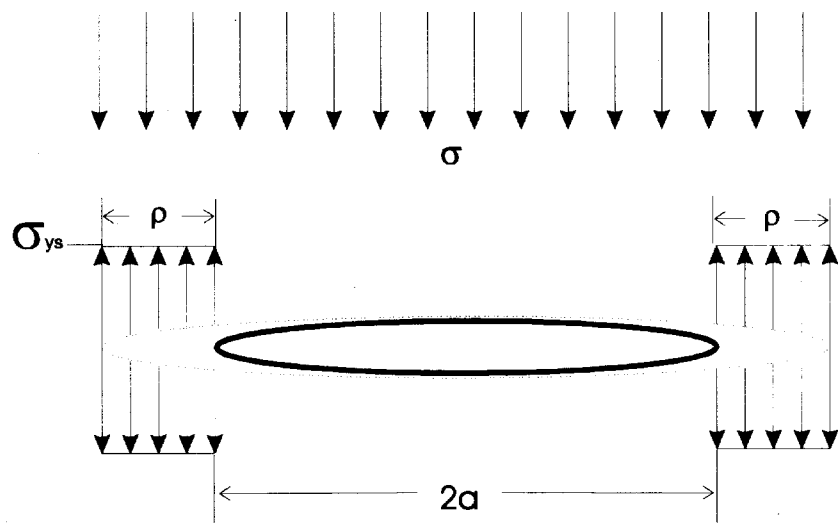


Figure 14.—Continuous point forces approximate the residual pillar strength in yielded zone preceding the elastic crack tip.

Applying this result to the crack in figure 14, the integral has to be taken from $s' - a$ to $a' - a$. Thus, "a" has to be substituted for "s" and "a % D" for "a" in equation 16, while P equals the yield strength, F_{ys} [Broek 1982]. This leads to the determination of the yield zone as

$$D = \frac{B^2 F^2 a}{8 F_{ys}^2}, \tag{17}$$

where D is the extent of the pillar yield zone.

Dugdale's description of the yield zone does not provide a simple way to predict the stress distribution in the elastic core adjacent the yielded edge. Irwin presents a method to predict the stress distribution in the elastic portion of the pillar [Broek 1982]. Irwin describes a yield zone that is similar in length to Dugdale's prediction; however, the crack tip extends only one-half the distance (figure 15).

The singularity vanishes if area A' area B. It was possible to verify this using spreadsheet software. It is particularly accurate for values of F/F_{ys} less than 0.75. Irwin's description produces the stress distribution shown in figure 16. This distribution is not representative with in situ measurements taken at underground mines [Mark and Iannacchione 1992].

PLAIN STRAIN

Dugdale's method concerns conditions of plane stress. Pillar analysis requires a plane strain condition. Studies indicate that for the case of plain strain, the effective yield stress can be as great as three times that for a similar plain stress analysis. This is due to confinement, which increases the triaxial yield strength. Broek suggests modifying the yield stress with the constraint factor:

$$p.c.f. = 1.68 F_{ys} \tag{18}$$

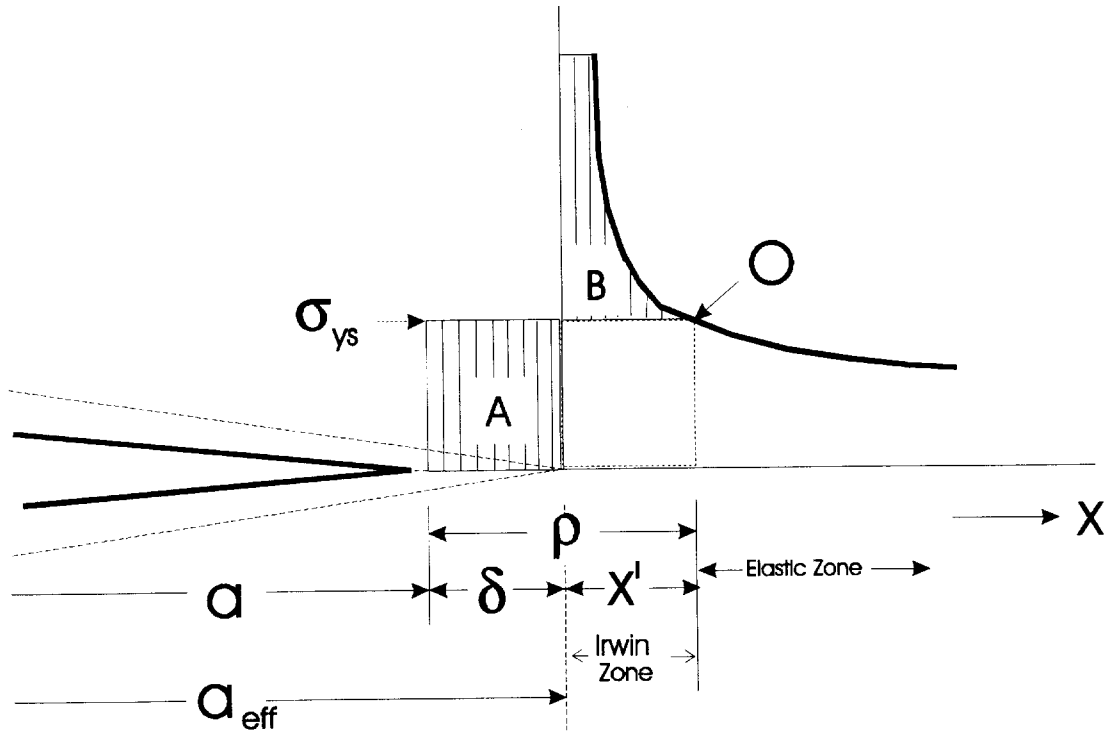


Figure 15.—The Westergaard distribution originates at the beginning of the Irwin zone, but does not take effect until the beginning of the elastic zone.

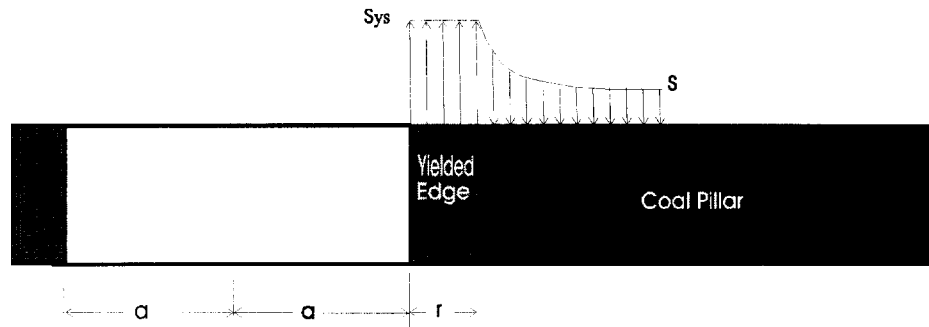


Figure 16.—Pillar stress distribution as predicted by the Dugdale-Irwin method.

THE DUGDALE-IRWIN METHOD AS IT RELATES TO A MINE ENVIRONMENT

Previous research indicates that confinement increases the yield strength of a pillar core [Crouch and Fairhurst 1973; Karabin and Evanto 1999; Sih 1966; Salamon and Munro 1967]. However, the measured pillar stress distribution does not resemble the distribution predicted by Dugdale-Irwin shown in figure 16. Underground measurements show the residual

strength should be low at the wall of the mine opening, but increase proportionally with the distance into the pillar core.

The mathematical model predicted by Dugdale-Irwin is accurate; only the visual perception is misleading. The residual stress distribution in the yielded area can take on any shape as long as area A equals area B (figure 17). A more realistic stress distribution such as that in figure 18 should then be possible.

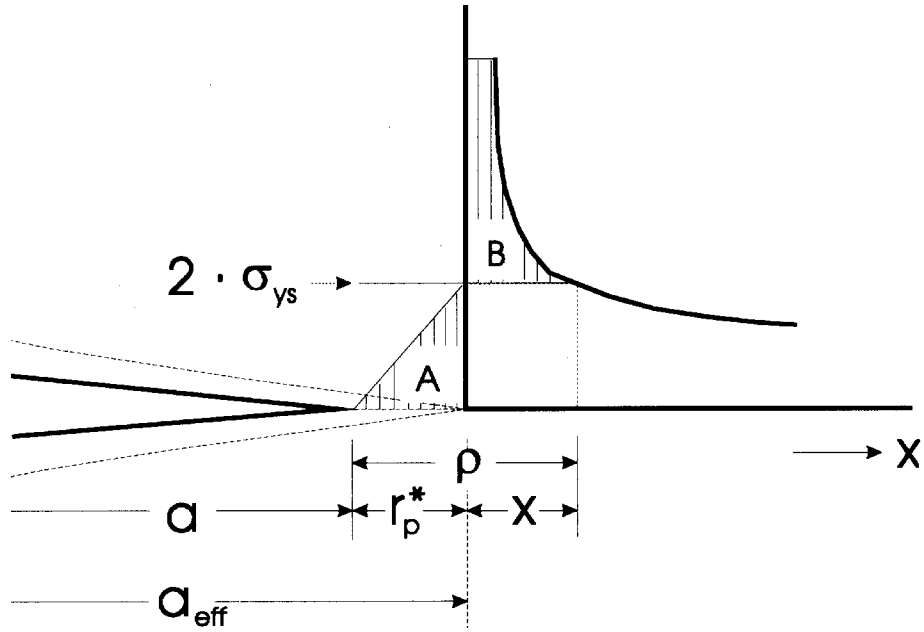


Figure 17.—Yield stress can assume any shape provided that area A equals area B.

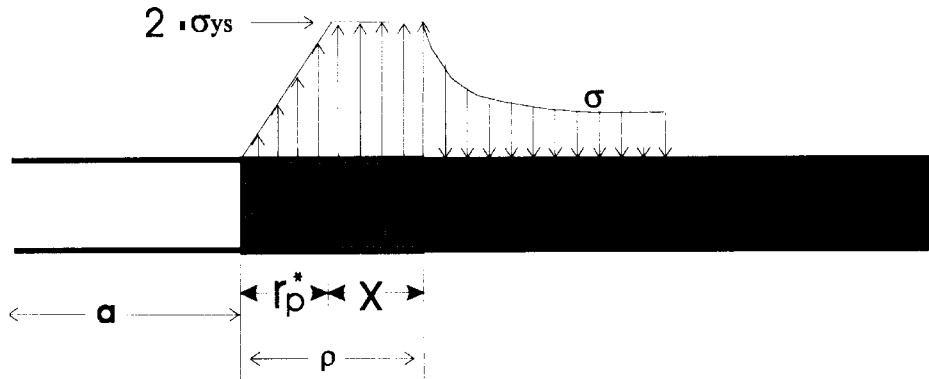


Figure 18.—Possible contour of pillar stress using the Dugdale-Irwin method.

COMBINING EMPIRICAL METHODS INTO THE ANALYTIC ANALYSIS

The Westergaard equation introduces a singularity at the pillar edge; this is where the stress approaches infinity. To eliminate this singularity, the edge must yield and redistribute the load. The yielded edge retains a residual strength that offers confinement to the core.

In situ field measurements demonstrate a nonlinear residual stress distribution in the yield zone of a coal pillar. The stress is low at the pillar rib and increases rapidly into the center of the pillar. This indicates that confinement makes the pillar strength higher than the unconfined compressive strength used by Dugdale-Irwin. It is possible to use the point-force method to model this residual strength and thus predict the extent of the yield zone. It is a common numerical technique to study the yielding coal

with a strain-softening model [Crouch and Fairhurst 1973; Wilson 1972]. Figure 19 depicts a model in terms of stress versus strain in a timeframe denoted by peak and post (residual) stress.

It is possible to use any of the popular pillar strength equations to predict the strain-softening characteristics of the coal. The equations of Bieniawski and Holland-Gaddy are the most accepted of these equations [Mark and Iannacchione 1992]. Mark and Iannacchione developed an equation that represents an average of these two equations. It predicts the pillar strength as a function of distance from the opening. This equation is:

$$F_v(x) = S_1 \times \left(0.78 + 1.74 \frac{x}{h} \right), \quad (19)$$

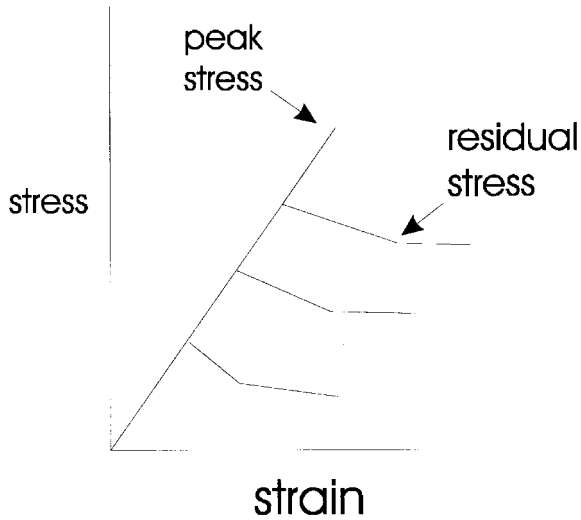


Figure 19.—The stress-strain characteristics in the yield zone of a coal seam.

where F_v ' peak stress at distance x , MPa,
 S_1 ' in situ coal strength, MPa,
 x ' distance to the free face, m,
 and h ' seam height, m.

It is possible to model the stress distribution in the yield zone as a series of point forces (figure 20). These

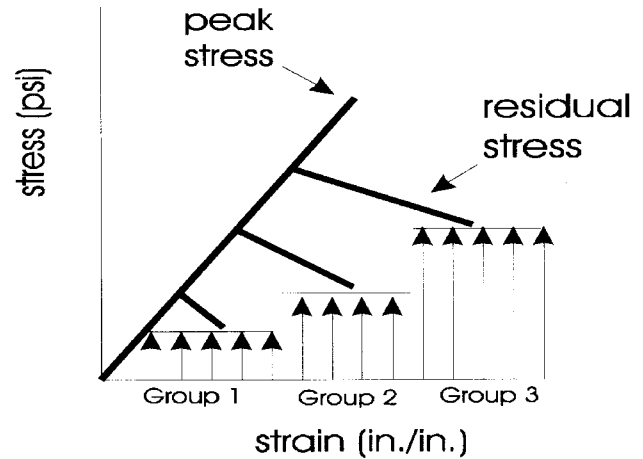


Figure 20.—It is possible to model peak or post stress as several groups of point forces.

continuous series of point forces has a uniform intensity within each group. Equation 19 will predict the average strength assigned to each group. It is necessary to use an iterative technique to determine the extent of the yield zone. This iterative technique progressively yields each group while testing for the disappearance of the singularity. When $K_p \leq K_{insitu}$, the yielding stops. Luo has eliminated the need for an iterative technique by providing the exact solution for the equation [Kramer et al. 1998].

EXAMPLE: USING STRAIN-SOFTENING TO DETERMINE THE EXTENT OF THE YIELD ZONE

Originally, this example was formulated using U.S. customary units of measurement. Conversion to the metric system makes some values appear awkward.

GROUP 1: 0-2 m INTO THE PILLAR

Input Parameters:

- S_1 ' 3.5 MPa
- F_{insitu} ' 6.9 MPa
- Entry width ($2a$) ' 6 m
- a ' 3 m
- Extension of group 1 (e_1) ' 2 m
- h ' 2 m
- a_{eff1} ' $a \% e_1$ ' 5 m

The first group of point forces simulates the post strength for group 1, which is the first 2 m into the pillar

(figure 20). These point forces are uniform; therefore, it is necessary to use equation 19 to determine an average strength value. This value will be assigned the point forces in group 1. An estimate of the average point force for group 1 would be determined from equation 19 for a point 1 m into the pillar.

$$F_{avg} = F_v(1\text{ m}) = 3.5 \left(0.78 \% 1.74 \frac{1}{2} \right) = 5.8 \text{ MPa}$$

The stress intensity relating to this average point force is taken from equation 15 as

$$K_{ps1,1} = \frac{F_{avg}}{\sqrt{Ba_{eff}}} \frac{a_{eff}}{a} \left(\sqrt{\frac{a_{eff} \% x}{a_{eff} \& x}} \% \sqrt{\frac{a_{eff} \& x}{a_{eff} \% x}} \right) dx .$$

Equation 16 solves this integral as

$$K_{ps_{1,1}} = 2F_{avg} \sqrt{\frac{a_{eff}}{B}} \cos^{0.1} \frac{a}{a_{eff}}$$

$$K_{ps_{1,1}} = 2 \left(5.8 \sqrt{\frac{5}{B}} \cos^{0.1} \frac{3}{5} \right)$$

= 13.6

$$K_{ps_{total}} = K_{ps_{1,1}}$$

= 13.6

The stress intensity for group 1 in absence of the point forces is

$$K_{a_{eff1}} = 6.9 \sqrt{B(3/2)}$$

= 27.3

$K_{ps_{total}}$ is less than $K_{a_{eff1}}$; therefore, this section is yielded and the crack extends to the end of the next section (group 2). The coal continues to yield until the residual pillar stress overcomes the in situ Westergaard stress.

GROUP 2: 2-4 m INTO THE PILLAR

Input Parameters:

$$e_2 = 2 \text{ m}$$

$$a_{eff1} = 5 \text{ m}$$

$$a_{eff2} = a_{eff1} + e_2 = 7 \text{ m}$$

Midpoint of group 2 is 3 m into the pillar

The crack tip is extended 4 m (i.e., $e_1 + e_2$) to the end of group 2. This makes a_{eff2} , the effective crack tip, equal to 7 m. Using equation 19, the average stress in this section is 11.9 MPa. This is the post strength determined for a location 3 m into the pillar. The stress intensity caused by the wedge forces in group 2 is

$$K_{ps_{2,2}} = 2 \left(11.9 \sqrt{\frac{7}{B}} \cos^{0.1} \frac{5}{7} \right)$$

= 27.5

It is necessary to also consider the stress intensity caused by the residual point forces in group 1. Because the crack tip extended into the 2-to 4-m (group 2) section of the yield zone, it is necessary to recalculate the effect of the 0- to 2-m (group 1) section of the yield zone:

$$K_{ps_{1,2}} = \frac{5.8}{\sqrt{B7}} \int_0^2 \left(\sqrt{\frac{7-x}{7}} + \sqrt{\frac{7-x}{7}} \right) dx$$

"Derive—A Mathematical Assistant" determined this value to be:

$$K_{ps_{1,2}} = 6.1$$

The total stress caused by the point forces is

$$K_{ps_{total}} = K_{ps_{2,2}} + K_{ps_{1,2}}$$

= 33.6

The stress intensity caused by the crack extension to the end of group 2 in absence of the residual point forces is

$$K_{a_{eff2}} = 6.9 \sqrt{B(5/2)}$$

= 32.3

This stress factor is less than the stress intensity due to the residual strength point forces ($K_{a_{eff2}} < K_{ps_{total}}$); thus, the yielding ceases in group 2. Because the values are nearly equal, the crack extended almost to the end of group 2 (i.e., 4 m into the pillar). It is possible to refine this distance, but it is unnecessary for this example. Equation 19 will predict the stress distribution in the yield zone; the Westergaard equation will predict the distribution in the elastic core.

Irwin suggests a way to use the Westergaard equation to predict the stress distribution in the pillar's elastic core (at the edge of the yield zone) [Broek 1982]. Irwin agrees with Dugdale's prediction for the extent of the yield zone, but he argues that the crack tip extends into this zone one-half the distance predicted by Dugdale such that

$$* = D/2 = 2 \text{ m (in the previous example).}$$

This increases the effective crack width to

$$a_{eff} = a + * = 5 \text{ m.}$$

This is the beginning of the Irwin zone—the region from which the Westergaard equation predicts the stress distribution into the core of the material (figure 21).

Extending the crack tip to the beginning of the Irwin zone, the Westergaard equation becomes

$$F_{Irwin \text{ zone}} = \frac{F_{insitu} x}{\sqrt{x^2 + (a + *)^2}} \quad (21)$$

Although the x-origin in the Westergaard equation begins in the Irwin zone, the stress distribution does not take effect until the beginning of the elastic zone. Equation

19 describes the stress distribution throughout the entire yield zone. Figure 22 shows the stress distribution for the combined strain-softening and analytic models.

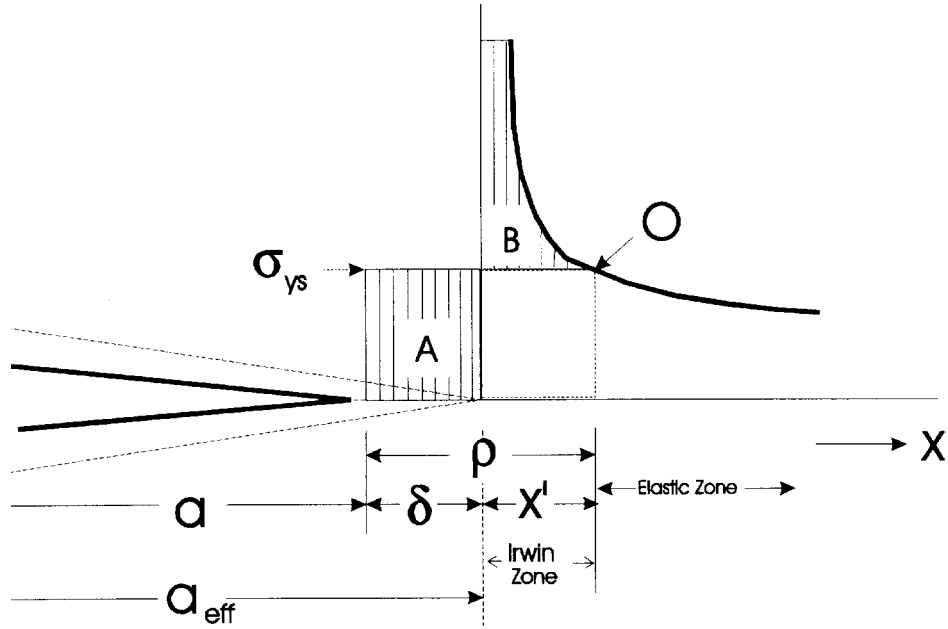


Figure 21.—The Westergaard equation begins in the Irwin zone; it takes effect in the elastic zone.

Combination of Strain-softening and Elastic Characteristics

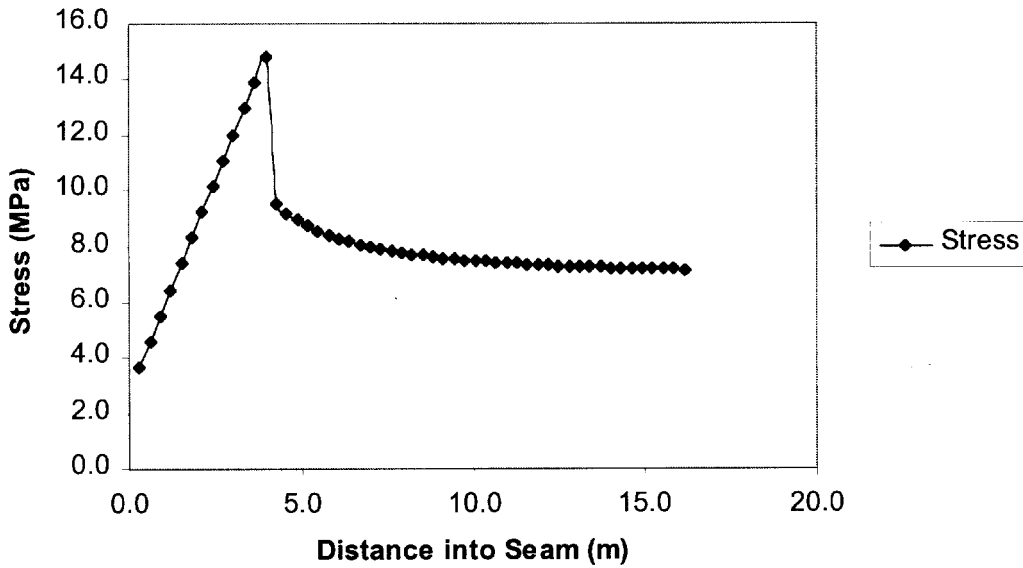


Figure 22.—Strain softening in the process zone and a Westergaard distribution in the elastic zone.

SUPERPOSITION

A mine opening affects the stress distribution at each of its sides. A mine panel is a gridwork of regularly or irregularly spaced entries and crosscuts.⁹ For a complete stress analysis, it is necessary to consider the stress influences caused by every mine passageway. A superposition technique makes this possible [Kramer 1996].

The superposition technique requires subdividing the stress distribution into its constitutive components (figure 23). Each side of the pillar is subjected to a

Westergaard stress distribution. Restricting the pillar model to two dimensions, as in the case of plane strain, limits these distributions to the left and right sides of the pillar. The basic components needed in the superposition are the uniform in situ stress, the stress component from the left opening, and the stress component from the right opening. The right and left stress components are each equal to the Westergaard equation with the in situ stress removed such that

$$F_{\text{component}} = \frac{F_{\text{insitu}}x}{\sqrt{x^2 + a^2}} + F_{\text{insitu}} \tag{22}$$

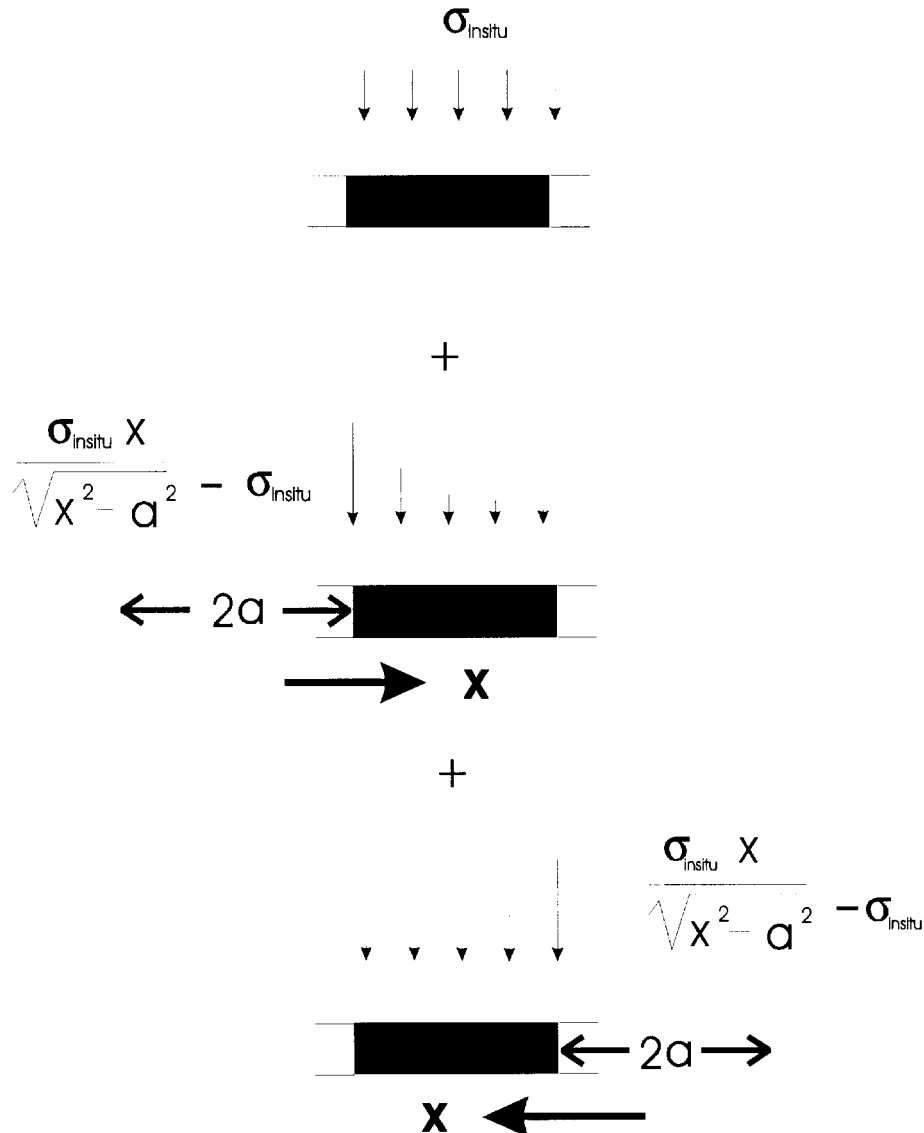


Figure 23.—Pillar stress broken down into three components.

⁹An entry is a tunnel aligned in the main direction of mining. A crosscut connects individual entries, usually at a right angle. Several entries and crosscuts comprise a mine panel. A pillar is coal remaining in place between two entries and crosscuts; it supports the mine roof.

The left stress component has the origin of its axis located to the left of the pillar. The positive direction, relative to this axis, is rightward from the origin into the pillar. The right component is the mirror image of the left. This component has the origin of its axis to the right of the pillar. The variable "a" can have a different value for each side of the pillar (figure 23). The total stress distribution on the pillar is equal to the left component plus the uniform

in situ stress plus the right component. As verified by FLAC, the superposition technique accurately predicts the stress distribution across a single pillar (figure 24).

A mine opening affects the stress distribution for a substantial distance. A mine panel consists of a gridwork of entries and crosscuts. It is necessary to superimpose the stress components from all mine passageways. FLAC compares the results of the superposition across an entire mine panel (figure 25).

Superposition Technique Across a Single Pillar

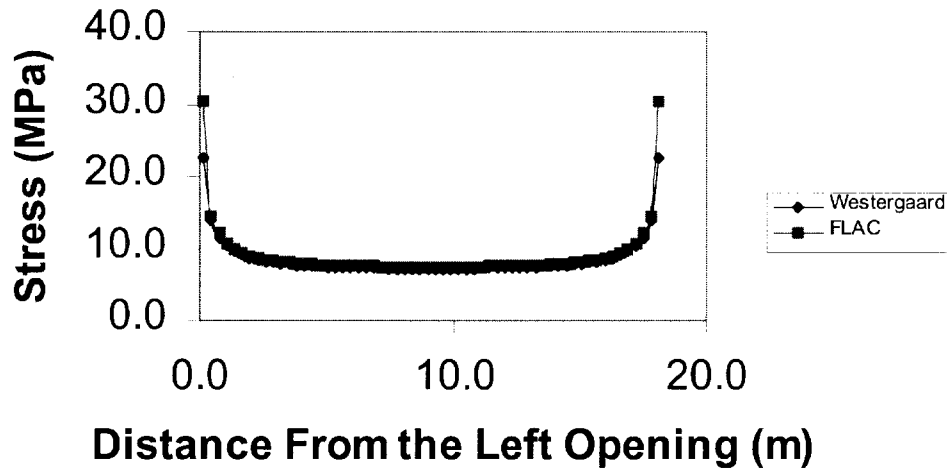


Figure 24.—Pillar with stress superimposed from both sides.

Superposition Comparison

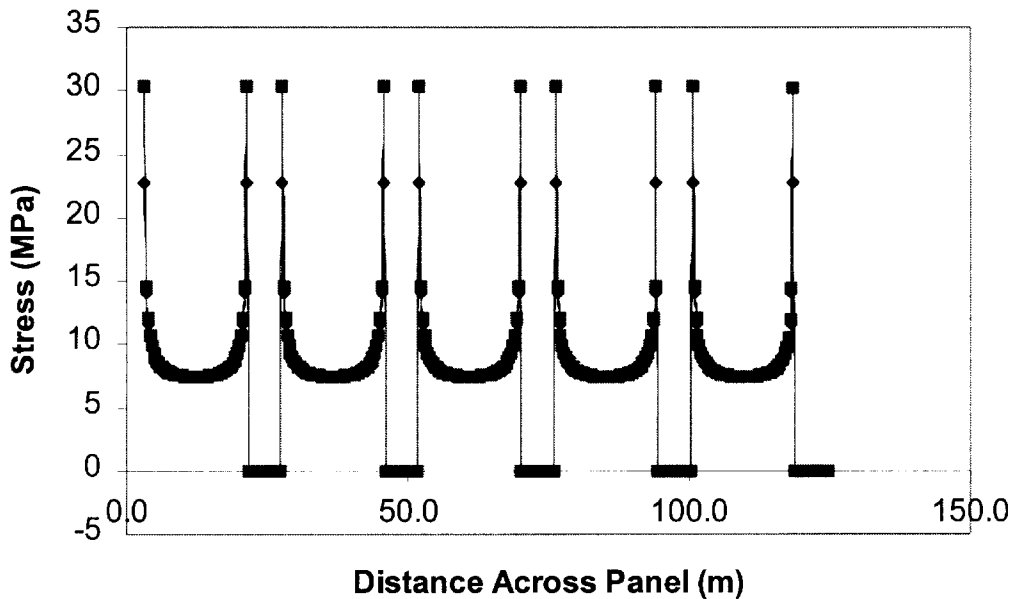


Figure 25.—Westergaard equation and superpositioning stress over an entire mine panel. Comparison with numerical model.

POSSIBLE ENHANCEMENTS

It is possible to enhance the modeling capabilities of the FMA. Adding other techniques would give the ability to analyze displacements in the strata, creep behavior in mine supports, and the effects of multiple-seam mining. Because the FMA is straightforward and easy to use, there is potential to model many different mining situations.

The following sections discuss some possible additions to the FMA. Although each technique presented seems reasonable, no comparison has been made with numerical analysis to qualify accuracy.

VIEW OF STRESS DISTRIBUTION FROM A PLANAR PERSPECTIVE

Sometimes it is desirable to study the stress distribution looking down on the coal seam (planar view) instead of into it (cross-sectional view). In a planar view, coal pillars are rectangular. The corners of the pillar generate mathematical singularities that create problems for analysis. One way to

eliminate the singularities is to assume the pillar is an ovaloid instead of a rectangle [Kramer 1996]. It is possible to segment the pillar into concentric ovaloid lines of equal distance (figure 26). Fracture mechanics predicts the stress distribution through the pillar centers, as indicated by the vertical and horizontal lines in figure 26. An interpolation technique can approximate the stress throughout the pillar by using the concentric ovaloid arcs as interpolation pathways. For instance, the arc segment between points A and B in figure 26 would be the interpolation path between the stresses at points A and B. It is easy to interpolate the stresses along ovaloid paths. The basic equations for mapping elliptical coordinates to Cartesian coordinates are:

$$\begin{aligned}x' &= a \cos 2 \\y' &= b \sin 2\end{aligned}\quad (23)$$

An example of the interpolation process follows.

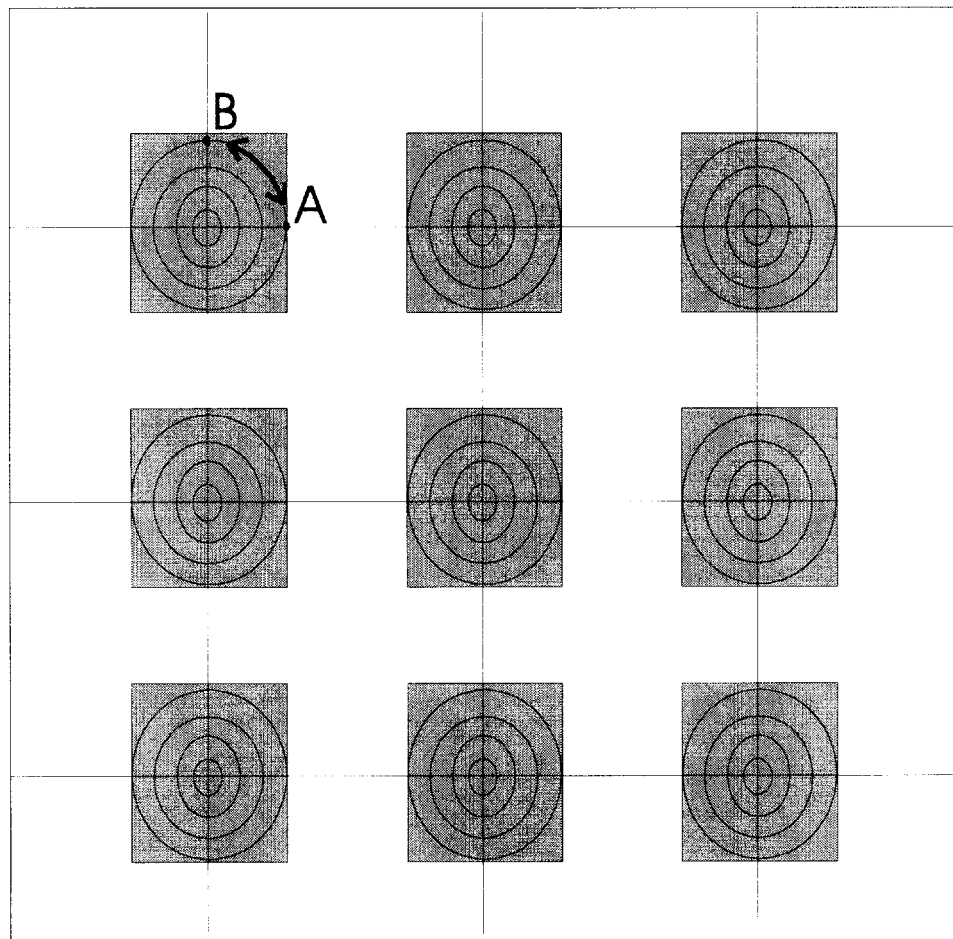


Figure 26.—Fracture mechanics predicts the center stress in both directions through the pillar. An interpolation technique translates the stress along the elliptical trajectories.

EXAMPLE OF INTERPOLATION

Considering the elliptical path shown in quadrant I of figure 27, interpolate the stresses along path A-B in the outer arc of quadrant I. For this example, assign the following properties:

$$F_A = 1,000 \text{ psi}$$

$$F_B = 1,500 \text{ psi}$$

$$a = 20$$

$$b = 10$$

Divide 2 into five equal angles:

$$\frac{90}{5} = 18^\circ \tag{24}$$

Determine the stress interpolation interval for each 18° arc:

$$\frac{1,500 \text{ psi} - 1,000 \text{ psi}}{5 \text{ intervals}} = 100 \text{ psi per interval} \tag{25}$$

Figure 28 illustrates the stress distribution along this arc. Equation 24 relates any point on the A and B axis to any point on the ovaloid (figure 27). Therefore, it is possible to approximate the stress distribution throughout the entire pillar.

VISCOELASTICITY

Sih [1966] and Paris and Sih [1965] discuss crack behavior in viscoelastic (time-dependent) material. For viscoelastic material, the crack-tip stress field is the same, only the stress intensity factors K_I are functions of time, such that

$$K_I = K_I(t) \tag{26}$$

This function shows promise for future applications using the FMA. For instance, it could be valuable for studying the behavior of salt.

DISPLACEMENTS

Fracture mechanics may also predict the displacement/strain in a mine environment. A common method to predict displacement is referred to as the "crack opening displacement" (COD) [Broek 1982]. The COD method takes into account the total displacement of the crack surface (figure 29). In mining, the COD predicts the combined displacement of the roof and floor of an opening, such that

$$COD = 2v = \frac{4F}{E} \sqrt{a^2 + x^2} \tag{27}$$

and at the center of the opening:

$$COD_{max} = 2v = \frac{4Fa}{E} \tag{28}$$

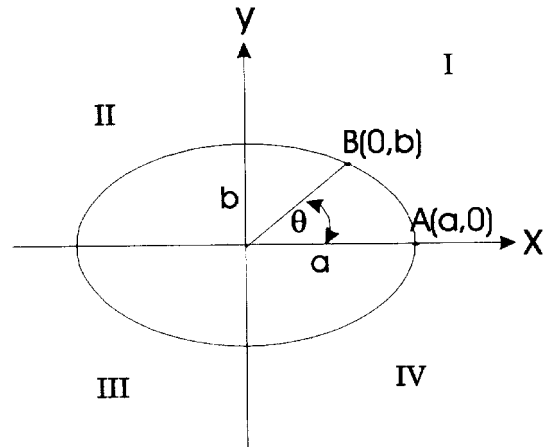


Figure 27.—Relationship between elliptical and rectangular coordinates.

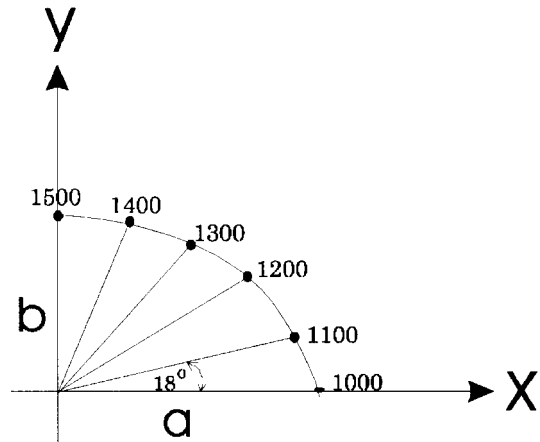


Figure 28.—Stresses distributed along interpolation arc.

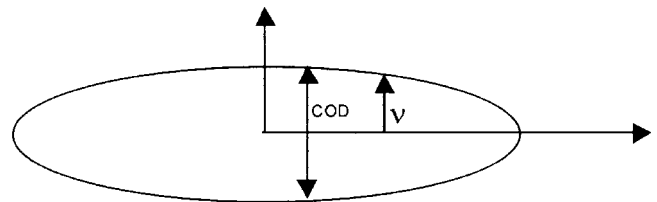


Figure 29.—The crack opening displacement (COD) method considers the displacement of the entire surface of a crack.

MULTIPLE-SEAM MINING

It may be possible to predict the effects on stress distribution caused by mining activity in seams above or below the area of interest. By using stress influence functions developed for mine subsidence prediction, it should be possible to predict multiple-seam influences with a respectable degree of accuracy

[Luo 1997]. This multiple-seam model could be more accurate than other numerical methods because most other methods use influence functions based on the theory of elasticity, which assumes infinitesimal displacements. Using influence functions based on mine subsidence profiles takes into account the well-documented, large-scale displacements measured at various mine locations.

CONCLUSION

This paper presents the FMA for predicting the stresses in a mine panel. It can model any combination of mine supports such as longwall gob, yield pillars, cribs, chocks, posts, automated temporary roof supports, and hydrostatic loads. The technique uses an analytic expression; thus, it is fast, simple, and accurate. It simulates pillar yield by combining the analytic equation with any empirical pillar strength equations. The procedure incorporates easily into spreadsheets or computer software. The FMA predicts pillar stress with a high degree of accuracy; however, it is no match to good numerical modeling

software. Its main function is to be quick and simple in order to encourage nonspecialized personnel to use it as a guide for studying mine supports.

The FMA works well for coal seams aligned along a horizontal plane. Additional effort is needed to assess its accuracy for seams aligning along inclined planes. More work is also necessary to develop FMA techniques for thick-seam mining, multiple-seam mining, and displacement prediction. Computer software featuring the FMA is available from the author.

REFERENCES

- Barenblatt G [1962]. The mathematical theory of equilibrium of cracks in brittle fracture. *Advances in Appl Mech* 7:55-129.
- Berry D [1960]. An elastic treatment of ground movement due to mining isotropic ground. *J Mech Phys Solids* 8:280-292.
- Berry D [1963]. Ground movement considered as an elastic phenomenon. *Trans Inst Min Eng* 123:28-41.
- Broek D [1982]. *Elementary engineering fracture mechanics*. 3rd ed. The Hague, The Netherlands: Martinus Nijhoff Publishers.
- Crouch SL, Fairhurst C [1973]. The mechanics of coal mine bumps and the interaction between coal pillars, mine roof, and floor. U.S. Department of the Interior, Bureau of Mines, OFR 53-73.
- Dugdale D [1960]. Yielding of steel sheets containing slits. *J Mech Phys* 8:100-108.
- Hackett P [1959]. Analytic analysis of rock movements caused by mining. *Trans Inst Min Eng* 118(7):421-433.
- Karabin GJ, Evanto MA [1999]. Experience with the boundary-element method of numerical modeling to resolve complex ground control problems. In: *Proceedings of the Second International Workshop on Coal Pillar Mechanics and Design*. Pittsburgh, PA: U.S. Department of Health and Human Services, Public Health Service, Centers for Disease Control and Prevention, National Institute for Occupational Safety and Health, DHHS (NIOSH) Publication No. 99-114, IC 9448.
- Kramer JM [1996]. The use of fracture mechanics to predict the stress distribution in coal mine pillars [Dissertation]. Morgantown, WV: West Virginia University, Department of Mining Engineering.
- Kramer JM, Luo Y, Peng SS [1998]. An analytic approach to determine the stress distribution in longwall chain pillars. In: *Proceedings of the 17th International Conference on Ground Control in Mining*. Morgantown, WV: University of West Virginia, pp. 162-168.
- Luo Y [1997]. Private conversation between J. Kramer, Mine Safety and Health Administration, and Y. Luo, West Virginia University, Morgantown, WV.
- Mark C, Iannacchione AT [1992]. Coal pillar mechanics: theoretical models and field measurements compared. In: *Proceedings of the Workshop on Coal Pillar Mechanics and Design*. Pittsburgh, PA: U.S. Department of the Interior, Bureau of Mines, IC 9315, pp. 78-93.
- Paris P, Sih G [1965]. Stress analysis of cracks. *ASTM STP* 391: 30-81.
- Salamon MDG, Munro AH [1967]. A study of the strength of coal pillars. *J S Afr Inst Min Metall* 68:55-67.
- Sih G [1966]. On the Westergaard method of crack analysis. *Inter J Fracture Mech* 2:628-631.
- Westergaard H [1939]. Bearing pressures and cracks. *ASME J of Appl Mech* 61:A49-53.
- Wilson AH [1972]. An hypothesis concerning pillar stability. *Min Eng (London)* 131(141):409-417.

A HYBRID STATISTICAL-ANALYTICAL METHOD FOR ASSESSING VIOLENT FAILURE IN U.S. COAL MINES

By Hamid Maleki, Ph.D.,¹ Eric G. Zahl,² and John P. Dunford³

ABSTRACT

Coal bumps are influenced by geologic conditions, the geometric design of coal mine excavations, and the sequence and rate of extraction. Researchers from private industry and government agencies around the world have studied mechanisms of violent failure and have identified individual factors that contribute to coal bumps. To develop predictive tools for assessing coal bump potential, the authors initiated a comprehensive study using information from 25 case studies undertaken in U.S. mines. Multiple linear regression and numerical modeling analyses of geological and mining conditions were used to identify the most significant factors contributing to stress bumps in coal mines.

Twenty-five factors were considered initially, including mechanical properties of strata, stress fields, face and pillar factors of safety, joint spacings, mining methods, and stress gradients. In situ strength was estimated in 12 coal seams where uniaxial compressive strength exceeded 2,000 psi. Allowances were made for favorable local yielding characteristics of mine roof and floor in reducing damage severity. Pillar and face factors of safety were calculated using displacement-discontinuity methods for specific geometries.

This work identified the most important variables contributing to coal bumps. These are (1) mechanical properties of strata, including local yield characteristics of a mine roof and floor, (2) gate pillar factors of safety, (3) roof beam thickness, joint spacing, and stiffness characteristics, which influence released energy, (4) stress gradients associated with the approach of mining to areas of higher stress concentrations, and (5) the mining method. By combining the strength of both analytical and statistical methods, new capabilities were developed for predicting coal bump potential and for building confidence intervals on expected damage.

¹Principal, Maleki Technologies, Inc., Spokane, WA.

²Civil engineer, Spokane Research Laboratory, National Institute for Occupational Safety and Health, Spokane, WA.

³Mining engineer, Spokane Research Laboratory, National Institute for Occupational Safety and Health, Spokane, WA.

INTRODUCTION

Coal bumps are sudden failures near mine entries that are of such a magnitude that they expel large amounts of coal and rock into the face area. These destructive events have resulted in fatalities and injuries to underground mine workers in the United States. Coal bumps are not only a safety concern in U.S. coal mines, but also have affected safety and resource recovery in other countries, including Germany, the United Kingdom, Poland, France, Mexico, the People's Republic of China, India, and the Republic of South Africa. Gradual or progressive failure, which is commonly experienced in coal mines, has less effect on mining continuity and safety and is generally controlled by timely scaling, cleaning, and bolting.

Researchers from private industry, government, and academia have studied the mechanisms of coal bumps [Crouch and Fairhurst 1973; Salamon 1984; Babcock and Bickel 1984; Iannacchione and Zelanko 1994; Maleki et al. 1995] and mine seismicity [Arabasz et al. 1997; McGarr 1984]. Seismic events are generated as mining activities change the stress field; they often result in either crushing of coal measure rocks (strain bump) or shearing of asperities along geological discontinuities (fault-slip). Sudden collapse of overburden rocks [Maleki 1981, 1995; Pechmann et al. 1995] has also been associated with large seismic events, triggering coal bumps in marginally stable pillars.

To differentiate between stable and violent failure of rocks, Crouch and Fairhurst [1973] and Salamon [1984] proposed a

comparison of postpeak stiffness of a coal seam and the loading system (mine roof and floor). Linkov [1992] proposed an energy criterion emphasizing that violent failure results when kinetic energy is liberated above that consumed during fracturing of the coal. In practice, it is difficult to estimate postpeak stiffness of coal for any geometry [Maleki 1995] or to calculate fracture energies. This led some practitioners to use either stored elastic strain energy or changes in energy release [Cook et al. 1966] to evaluate the likelihood of violent failure.

In view of limitations for unambiguous calculations of postpeak stiffness, many researchers have attempted to identify individual factors influencing coal bumps using the data from single-field measurement programs. Using such data analyses and in the absence of rigorous statistical treatment of all case studies, it is very difficult to identify geotechnical factors that influence coal bumps, to assign confidence intervals, and to develop predictive capabilities.

To identify the most significant factors contributing to coal bumps, the authors analyzed geometric and geologic data using both computational and statistical analysis techniques. The data included information on both violent and nonviolent failures from 25 mine sites in Colorado, Utah, Virginia, and Kentucky, where detailed geotechnical and in-mine monitoring results were available.

DATA ANALYSIS

The first step in developing a statistical model was to create suitable numerical values that express geologic, geometric, and geomechanical conditions. The second step was to reduce the number of independent variables by combining some existing variables into new categories and identify highly correlated independent variables. Reducing the number of variables is needed when there are too many variables to relate to the number of data points. The presence of highly correlatable variables influences which procedures are selected for multiple regression analyses. The third step was to develop a multivariate regression model and identify significant factors that contribute to coal bumps.

Some geologic variables were readily available in numerical format; other geomechanical factors had to be calculated using numerical and analytical techniques. These activities involved—

(1) Obtaining mechanical property values for roof, floor, and coal seams through laboratory tests of samples of near-seam strata. In situ strength of coal seams was estimated using the procedures suggested by Maleki [1992].

(2) Calculating both maximum and minimum secondary horizontal stresses using overcoring stress measurements from one to three boreholes [Bickel 1993].

(3) Calculating pillar and face factors of safety for individual case studies using both two- and three-dimensional boundary-element techniques [Maleki 1990; Crouch 1976; Zipf 1993]. Results were compared with field data when such data were available.

(4) Calculating energy release from a potential seismic event using boundary-element modeling and analytical formulations suggested by Wu and Karfakis [1994] for estimating energy accumulation in both roof and coal and energy release [McGarr 1984] in terms of Richter magnitude (M_1) using the following formula:

$$1.5 M_1 = a \times \log(E) + 11.8, \quad (1)$$

where E = total accumulated energy in roof and seam, erg,

and a = coefficient depending on joint density.

(5) Assessing the severity of coal bumps using a damage rating developed by and based on the authors' observations of physical damage to face equipment and/or injury to mine personnel, as well as observations by other researchers as cited in the literature. Damage levels were assigned a ranking between 0 and 3. Level 1 signifies interruptions in mining operations;

level 3 signifies damages to both face equipment and injuries to mine personnel.

The first step of the analyses involved the identification of 25 geologic, geometric, and geomechanical variables that had the potential to contribute to coal bump occurrence. Both

violent (bump-prone) and nonviolent conditions in 6 room-and-pillar mines and 19 longwall mines were studied. Tables 1-3 summarize these data and include averages, ranges, and standard deviations. Typical frequency histograms are presented in figures 1-3 and indicate that these case studies provided good coverage of the variables.

Table 1.—Statistical summary of geologic variables

Variable	Mean	Standard deviation	Range	No. of cases
Joint sets	1.4	0.6	1-3	25
Cleat sets	1.8	0.4	1-2	25
In-seam partings	1	0.9	0-3	21
Joint spacing, ft	22	18	5-50	24
Rock Quality Designation (RQD)	77	18	50-100	15
Depth, ft	1,640	440	900-2,700	25
Roof beam thickness, ft	14	11	5-40	25
Young's modulus, million psi	0.4-8	0.12	0.35-0.67	25
Young's modulus of roof and floor, million psi	3	1	1-4.8	25
Uniaxial strength, psi	3,240	750	2,000-4,600	25
Uniaxial strength of roof and floor, psi	14,700	3,460	8,000-22,000	25
Maximum horizontal stress, psi	1,920	1,100	100-3,800	25
Interacting seams	1.2	0.4	1-3	25
Local yield characteristics	0.8		0-2	25

Table 2.—Statistical summary of geometric variables

Variable	Mean	Standard deviation	Range	No. of cases
Pillar width, ft	63	34	30-140	23
Pillar height, ft	8.3	1	5.5-10	25
Entry span, ft	19	1	18-20	25
Barrier pillar width, ft	165	90	50-240	6
Face width, ft	550	130	200-800	25
Mining method	1.2	0.4	1-2	25
Stress gradient	0.9	0.6	0-2	25

Table 3.—Statistical summary of geomechanical variables

Variable	Mean	Standard deviation	Range	No. of cases
Pillar factor of safety	0.8	0.3	0.5-1.4	23
Face factor of safety	0.9	0.2	0.6-1.5	22
Energy (M _i)	3	0.5	2-4	22
Damage	1.4	1	0-3	25

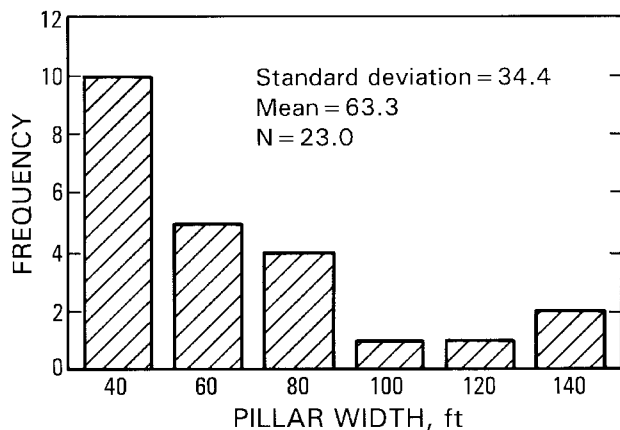


Figure 1.—Histogram frequency diagram for pillar width.

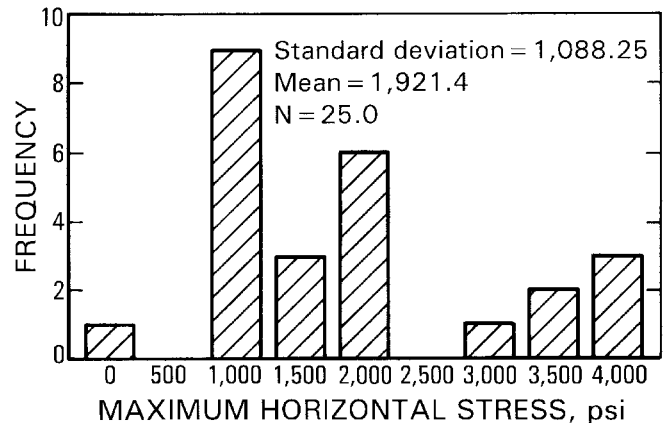


Figure 2.—Histogram frequency diagram for the maximum principal stress.

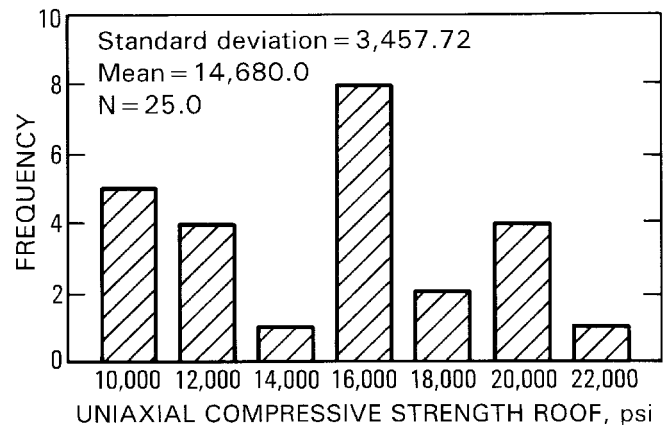


Figure 3.—Histogram frequency diagram for the uniaxial compressive strength of roof.

Roof beam thickness ranged from 5 to 40 ft. The beam chosen for the evaluation was the strongest beam of the near-seam strata located between one and four times the seam thickness in the mine roof. Although there is some evidence that massive upper strata have contributed to coal bumps in some mines [Maleki 1995], their influence was not directly evaluated in this study because of the lack of geological and mechanical property data.

Local yield characteristics of the immediate roof and floor strata influence coal pillar failure and the severity of coal

bumps. This factor varied from 0 to 2, where 0 indicates insignificant yielding in the roof and floor and 2 indicates favorable, gradual yielding in both roof and floor.

Stress gradients varied from 0 to 2, depending on whether mining proceeded toward an area of high stress (resulting from previous mining) and/or abnormal geologic conditions, such as those occasionally found near faults or grabens.

BIVARIATE CORRELATIONS AND DATA REDUCTION

The second step in the analyses involved correlations and variable reductions. Based on preliminary bivariate correlations among all geologic, geometric, and geomechanical variables, the number of variables was reduced by combining some variables into new ones. In addition, the cause-and-effect structure in the data was identified, helping to tailor the procedures for multiple regression analysis using forward stepwise inclusion of dependent variables, as described later in this paper. The new variables were as follows:

<i>Pqratio</i>	Ratio of maximum principal horizontal stress (P) to minimum stress (Q)
<i>Strenrc</i>	The ratio of uniaxial compressive strength of the roof to the coal
<i>Jointrf</i>	Joint spacing × roof beam thickness ÷ mining height
<i>Gradyield</i>	Ratio of roof and floor yield characteristics to stress gradient
<i>Panelwd</i>	Ratio of panel width to depth
<i>Youngrc</i>	Ratio of Young's modulus of the roof to the seam

Table 4 presents the bivariate correlation coefficients between the variable "damage" and selected geologic and

geometric variables. Energy (M_1), face factor of safety, stress gradient, pillar factor of safety, joint spacing, and uniaxial compressive strength of roof to coal were the most significant. Other variables were poorly correlated with damage, including the ratio of P to Q, pillar width, and Young's modulus of roof to coal.

Table 4.—Bivariate correlation coefficients between damage and selected variables

Variable	Coefficient
Significant variables: ¹	
Damage	1
Energy	0.65
<i>Gradyield</i>	0.57
<i>Jointrf</i>	0.52
Pillar factor of safety	0.44
Uniaxial strength of roof to coal	0.36
Face factor of safety	0.33
No. of interacting seams	0.33
Panel width to depth	0.31
Mining method	0.26
Insignificant variables:	
Pillar width	0.1
Ratio of P to Q	0.1
<i>Young's modulus roof to coal</i>	0.07

¹Two-tailed tests.

MULTIPLE LINEAR REGRESSION ANALYSIS

The last step in developing predictive capabilities was to complete multiple regression analyses using the numerical values obtained through measurements and numerical modeling. This is a hybrid approach where the strengths of both statistical and computational methods are combined. Computational methods have been used to assess the influence of a combination of geometric variables into single variables, such as pillar factor of safety and released energy. This was very useful for increasing goodness of fit and enhancing multiple regression coefficients. Statistical methods were used to identify significant variables, build confidence intervals, etc.

The multilinear regression procedure consisted of entering the independent variables one at a time into the equation using a forward selection methodology. In this method, the variable having the largest correlation with the dependant variable is entered into the equation. If a variable fails to meet entry requirements, it is not included in the equation. If it meets the criteria, the second variable with the highest partial correlation is selected and tested for entering into the equation. This procedure is very desirable when there is a cause-and-effect structure among the variables. An example of the cause-and-effect relationship is shown when a greater depth reduces pillar

factor of safety, contributes to an accumulation of energy, and ultimately results in greater damage. Using the above procedures, any hidden relationship between depth and pillar factor of safety, energy, and damage is evaluated and taken into account during each step of the analysis.

Several geomechanical variables (table 3) were initially used as dependent variables. The damage variable, however, resulted in the highest multiple regression coefficient. The multiple correlation coefficient (R), which is a measure of goodness of fit, for the last step was 0.87.

The assumptions of linear regression analysis were tested and found to be valid by an analysis of variance, F-statistics, and a plot of standardized residuals (figure 4). Residual plot did not indicate the need to include nonlinear terms because there was no special pattern in the residuals.

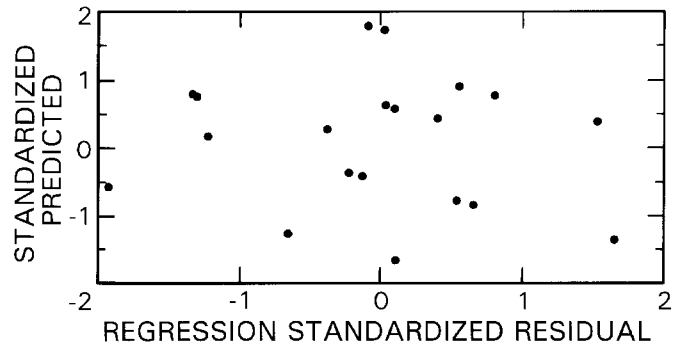


Figure 4.—Standardized scatterplot for the dependent variable "damage."

IMPORTANT VARIABLES CONTRIBUTING TO BUMP-PRONE CONDITIONS

Based on an examination of standardized regression coefficients (table 5), the following variables best explain the variations in damage and thus statistically have the most significant influence on coal bump potential:

- *Energy release.*—This variable includes the effects of the mechanical properties of the roof and coal, depth, stress field, and joint density and thus directly relates to damage.
- *Method.*—Mining method has a bearing on coal bump potential. The room-and-pillar method is associated with a higher degree of damage than longwall mining.
- *Pillar factor of safety.*—Gate pillar geometry contributes directly to the severity of damage.

- *Stress gradient and yield characteristics.*—Mining toward areas of high stress creates a potential for coal bumps; localized yielding roof and floor conditions encourage gradual failure, reducing the severity of damage.

Table 5.—Standardized regression coefficients and statistical significance

Variable	Standardized coefficient	T-significance
Energy	0.28	0.049
Pillar factor of safety . . .	0.34	0.011
Method	0.26	0.064
Gradyield	0.55	0.0004
Constant	NAP	0.234

NAP Not applicable.

CONCLUSIONS

A hybrid statistical-analytical approach was developed to identify the most significant factors contributing to coal bumps. By combining the strength of both analytical and statistical methods, the authors achieved new capabilities for predicting coal bump potential and for building confidence intervals on

expected damage. Because the method relies on an extensive amount of geotechnical data from 25 case studies in U.S. coal mines, it should be helpful to mine planners in identifying bump-prone conditions. This in turn will result in safer designs for coal mines.

REFERENCES

Arabasz WJ, Nava SJ, Phelps WT [1997]. Mining seismicity in the Wasatch Plateau and Book Cliffs coal mining districts, Utah, U.S.A. In: Gibowicz SJ, Lasocki S, eds. Proceedings of the Fourth International Symposium on Rockbursts and Seismicity in Mines. Balkema, pp. 111-116.

Babcock CO, Bickel DL [1984]. Constraint—the missing variable in the coal burst problem. In: Dowding CH, Singh MM, eds. Rock Mechanics in Productivity and Protection - Proceedings of the 25th Symposium on Rock Mechanics. Littleton, CO: Society for Mining, Metallurgy, and Exploration, Inc., pp. 639-647.

Bickel DL [1993]. Rock stress determinations from overcoring: an overview. Denver, CO: U.S. Department of the Interior, Bureau of Mines, Bulletin 694.

Cook NGW, Hook E, Petorius JPG, Ortlepp WD, Salamon MDG [1966]. Rock mechanics applied to the study of rock bursts. Int J S Afr Inst Min Metall, pp. 435-528.

Crouch SL [1976]. Analysis of stresses and displacements around underground excavations: an application of displacement discontinuity method. University of Minnesota Geomechanics Report.

Crouch SL, Fairhurst C [1973]. The mechanics of coal mine bumps and the interaction between coal pillars, mine roof, and floor. U.S. Department of the Interior, Bureau of Mines, OFR 53-73.

Iannacchione AT, Zelanko JC [1994]. Pillar mechanics of coal mine bursts: a control strategy. In: Proceedings of the 16th World Mining Congress, The Mining Industry on the Threshold of XXI Century (Sofia, Bulgaria). Vol. 5, pp. 15-23.

Linkov AM [1992]. Dynamic phenomena in mines and the problem of stability. University of Minnesota/MTS Systems Corp., lecture notes.

Maleki H [1981]. Coal mine ground control [Dissertation]. Golden, CO: Colorado School of Mines, Department of Mining Engineering.

Maleki H [1990]. Development of modeling procedures for coal mine stability evaluation. In: Hustrulid WA, Johnson GA, eds. Rock Mechanics Contributions and Challenges: Proceedings of the 31st U.S. Symposium. Balkema, pp. 85-92.

Maleki H [1992]. In situ pillar strength and failure mechanisms for U.S. coal seams. In: Proceedings of the Workshop on Coal Pillar Mechanics and Design. Pittsburgh, PA: U.S. Department of the Interior, Bureau of Mines, IC 9315, pp. 73-77.

Maleki H [1995]. An analysis of violent failure in U.S. coal mines: case studies. In: Proceedings - Mechanics and Mitigation of Violent Failure in Coal and Hard-Rock Mines. Spokane, WA: U.S. Department of the Interior, Bureau of Mines, SP 01-95, pp. 5-25.

Maleki H, Wopat PF, Repsher RC, Tuchman RJ, eds. [1995]. Proceedings - Mechanics and Mitigation of Violent Failure in Coal and Hard-Rock Mines. Spokane, WA: U.S. Department of the Interior, Bureau of Mines, SP 01-95.

McGarr A [1984]. Some applications of seismic source mechanism studies to assessing underground hazard. In: Gay NC, Wainwright EH, eds. Rock-bursts and Seismicity in Mines - Proceedings of the Symposium on Seismicity in Mines, Johannesburg, Republic of South Africa, 1982. South African Institute of Mining and Metallurgy, Symposium Series 6, pp. 199-208.

Pechmann JC, Walter WR, Arabasz W, Nava S [1995]. The February 3, 1995, M 5.1 seismic event in the trona mining district of southwestern Wyoming. Seismol Res Letter, Vol. 66, pp. 25-34.

Salamon MDG [1984]. Energy considerations in rock mechanics: fundamental results. Int J S Afr Inst Min Metall, pp. 237-246.

Wu X, Karfakis MG [1994]. An analysis of strain energy accumulation around longwall panels under strong roofs. In: Chugh YP, Beasley GA, eds. Proceedings of the Fifth Conference on Ground Control for Midwestern U.S. Coal Mines. Southern Illinois University, Department of Mining Engineering, pp. 230-253.

Zipf RK Jr. [1993]. Stress analysis in coal mines with MULSIM/NL. In: Proceedings of the 89th Meeting of the Rocky Mountain Coal Mining Institute. Lakewood, CO: Rocky Mountain Coal Mining Institute, pp. 38-43.

EMPIRICAL METHODS FOR COAL PILLAR DESIGN

By Christopher Mark, Ph.D.¹

ABSTRACT

Empirical methods involve the scientific interpretation of real-world experience. Many problems in ground control lend themselves to an empirical approach because the mines provide us with plenty of experience with full-scale rock structures. During the past 10 years, powerful design techniques have emerged from statistical analyses of large databases of real-world pillar successes and failures. These include the Analysis of Retreat Mining Pillar Stability (ARMPS), the Analysis of Longwall Pillar Stability (ALPS), the Mark-Bieniawski rectangular pillar strength formula, and guidelines for preventing massive pillar collapses. In the process, our practical understanding of pillar behavior has been greatly enriched.

¹Supervisory physical scientist, Pittsburgh Research Laboratory, National Institute for Occupational Safety and Health, Pittsburgh, PA.

INTRODUCTION

"Empirical" is defined by *Webster's Dictionary* [1988] as "relying upon or gained from experiment or observation." Until relatively recently, all pillar design methods used in the United States were empirical. The earliest, proposed by Bunting [1911], was based on case histories supplemented by laboratory testing. Later formulas followed the same basic pattern and were derived from laboratory tests (the Holland-Gaddy and Obert-Duvall formulas), large-scale in situ tests (the Bieniawski formula), or case histories (the Salamon-Munro formula).

Each of these "classic" pillar design formulas consisted of three steps:

- (1) Estimating the *pillar load* using tributary area theory;
- (2) Estimating the *pillar strength* using a pillar strength formula; and
- (3) Calculating the *pillar safety factor*.

In each case, the pillar strength was estimated as a function of two variables—the pillar's width-to-height (w/h) ratio and the coal seam strength. For many years, these classic formulas performed reasonably well for room-and-pillar mining under relatively shallow cover. Their key advantages were that they were closely linked to reality and were easy to use.

The greatest disadvantages of empirical formulas are that they cannot be easily extended beyond their original database, and they provide little direct insight into coal pillar mechanics. The growth of longwall mining exposed these shortcomings. Full extraction results in large abutment loads, which cannot be estimated by tributary area. More important is that longwall mining uses pillars that are much more "squat" (large w/h ratio) than those for which the classic formulas were developed. Testing such pillars in situ is prohibitively expensive, and laboratory tests of squat pillars are clearly inappropriate. Moreover, longwall mining raised some new issues even about the definition of what constitutes pillar "failure." The classic approach assumes that "pillars will fail when the applied load reaches the compressive strength of the pillars" and that "the load-bearing capacity of the pillar reduces to zero the moment the ultimate strength is exceeded" [Bieniawski 1992]. When large w/h longwall pillars "fail," however, their load-bearing capacity does not disappear. Rather, the gate roads become unserviceable.

During the 1970s, analytical methods began to emerge as an alternative to the classic formulas. Wilson [1972, 1983] of the British National Coal Board was the first to take a radically different approach to pillar design. He treated pillar design as a problem in mechanics, rather than one of curve-fitting to experimental or case history data. A pillar was analyzed as a complex structure with a nonuniform stress gradient, a buildup of confinement around a high-stress core, and progressive pillar failure. Although his mathematics were seriously limited [Mark

1987; Salamon 1992], Wilson's basic concepts are now broadly accepted.

The advent of powerful computer models gave a further boost to the analytical approach. The primary advantage of numerical models is that they can test assumptions about pillar behavior as affected by a variety of geometric and geologic variables. For example, independent studies reported by Gale [1992] and Su and Hasenfus [1997] concluded that for pillars whose $w/h > 6$, weak host rocks or partings have greater effects on pillar strength than the uniaxial compressive strength (UCS). Unfortunately, effective numerical modeling requires numerous assumptions about material properties, failure criteria, and post-failure mechanics.

In their insightful article, Starfield and Cundall [1988] introduced a classification of modeling problems (figure 1). One axis on the graph refers to the quality and/or quantity of the available data; the other measures the understanding of the fundamental mechanics of the problem to be solved. In many branches of mechanics, most problems fall into region 3, where there is both good understanding and reliable data. This is the region where numerical models can be built, validated, and used with conviction. Starfield and Cundall argued that problems in rock mechanics usually fall into the data-limited categories 2 or 4 and require a more experimental use of models.

In the field of coal mine ground control, however, many problems may actually fall into Starfield and Cundall's region 1. Our understanding of the complex mechanical behavior and properties of rock masses may be limited, but the potential for data collection is huge. Hundreds of longwall and room-and-pillar panels are mined each year, and each one can be considered a full-scale test of a pillar design. As Parker [1974] noted: "Scattered around the world are millions and millions of

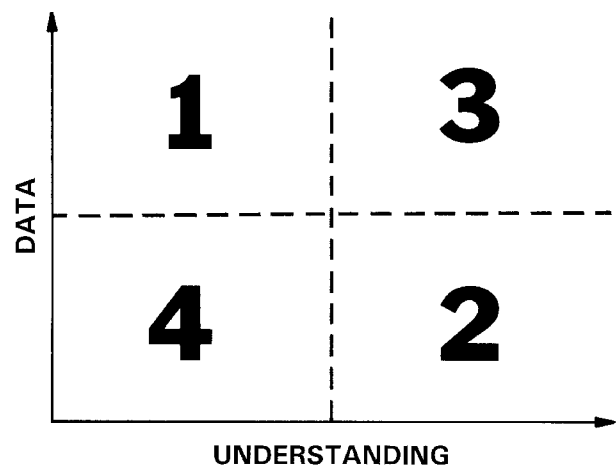


Figure 1.—Classification of modeling problems (after Starfield and Cundall [1988]).

pillars—the real thing—under all imaginable conditions; and tabulating their dimensions, the approximate loads, and whether they are stable or not would provide most useful guidelines for pillar design."

Actually, simply tabulating data does not necessarily lead to useful conclusions. Fortunately, today's data analysis techniques are far more powerful than those that were available to the pillar design pioneers. In the past 30 years, sciences like economics, sociology, psychology, anthropology, and epidemiology have all been transformed by quantitative data analysis using statistics [Encyclopedia Britannica 1989]. Sophisticated statistical packages enable researchers to efficiently comb large databases for significant relationships between the variables.

The empirical approach requires that the researcher begin with a clear hypothesis, often in the form of a simplified model

of the real world that abstracts and isolates the factors that are deemed to be important. It therefore requires, as Salamon [1989] indicated, "a reasonably clear understanding of the physical phenomenon in question." Without prudent simplification, the complexity of the problem will overwhelm the method's ability to discern relationships between the variables. However, a key advantage is that critical variables may be included, even if they are difficult to measure directly, through the use of "rating scales."

During the past 5 years, modern empirical techniques have been applied to a variety of problems in coal mine ground control. They have resulted in some very successful design techniques, as well as some new insights into pillar and rock mass behavior. This paper discusses some of them in more detail.

DESIGN OF LONGWALL GATE ENTRY SYSTEMS

In the 15 years after 1972, the number of U.S. longwall faces increased from 32 to 118 [Barczak 1992]. The new technology created a host of operational and safety problems, including the maintenance of stable travelways on the tailgate side. Researchers initially viewed gate entry ground control primarily as a pillar design issue. The clear correlation between larger pillars and improved conditions that had been established by trial and error at many mines supported this approach.

The most obvious difference between longwall pillars and traditional coal pillars is the abutment loading. The major contribution of the original Analysis of Longwall Pillar Stability (ALPS) was a formula for estimating the longwall pillar load based on numerous underground measurements [Mark 1990]. An evaluation of 100 case histories showed that 88% of the failed cases had stability factors <1.0 ; 76% of the successful cases had stability factors ≥ 1.0 [Mark 1992]. It was evident that ALPS had captured an essential element of the gate entry design problem.

On the other hand, there was a wide range of stability factors (approximately 0.5 to 1.2) in which both successful and unsuccessful designs occurred. Clearly, other variables in addition to the ALPS stability factor were influencing tailgate performance. A hypothesis was proposed stating that tailgate performance is determined by five factors:

- Pillar design and loading;
- Roof quality;
- Entry width;
- Primary support; and
- Supplemental support.

Attacking this extremely complex problem with traditional, deterministic rock mechanics using analytical or numerical models would have been extremely difficult. On the other hand, the problem was ideal for an empirical approach. The

empirical method could make full use of the wealth of full-scale case history data that had been collected. Moreover, it could focus directly on the variable of interest—tailgate performance.

It quickly became clear that roof quality was the key. Studies conducted as early as the 1960s had concluded that "whether or not the stress [from an extracted longwall panel] will influence a roadway depends more on the strength of the rocks which surround the roadway itself than on the width of the intervening pillar" [Carr and Wilson 1982]. Yet the variety and complexity of geologic environments had defied effective measurement.

The Coal Mine Roof Rating (CMRR) overcame this obstacle by providing a quantitative measure of the structural competence of coal mine roof [Molinda and Mark 1994; Mark and Molinda 1996]. The CMRR applies many of the principles of Bieniawski's Rock Mass Rating (RMR), with the following significant differences:

- The CMRR focuses on the characteristics of bedding planes, slickensides, and other discontinuities that determine the structural competence of sedimentary coal measure rocks.
- It is applicable to all U.S. coalfields and allows a meaningful comparison of structural competence, even where lithologies are quite different.
- It treats the bolted interval as a single structure while considering the contributions of the different lithologic units that may be present within it.

The CMRR weighs the importance of the geotechnical factors that determine roof competence and combines these values into a single rating on a scale from 0 to 100.

Data on tailgate performance were collected from approximately 55% of all U.S. longwall mines; these mines were selected to represent a geographic and geologic cross section of the U.S. longwall experience. A total of 64 case histories were

classified as "satisfactory" or "unsatisfactory" based on the conditions in the tailgate [Mark et al. 1994]. Each case history was described by the ALPS stability factor (SF), entry width, and primary support rating, as well as the CMRR.

Multivariate statistical analysis showed that when the roof is strong, smaller pillars can safely be used. For example, when the CMRR is 75, an ALPS SF of 0.7 is adequate. When the CMRR drops to 35, the ALPS SF must be increased to 1.3. Significant correlations were also found between the CMRR and both entry width and the level of primary support [Mark et al. 1994]. A simple design equation related the required ALPS SF to the CMRR:

$$\text{ALPS SF} = 1.76 - 0.014 \text{ CMRR} \quad (1)$$

THE ALPS database was recently revisited, with several new variables added. These include:

Rectangular pillar strength formula: All of the SFs were recalculated with the Mark-Bieniawski formula (see the section below on "Interactions With Numerical Models") substituted for the original Bieniawski formula. The new result is designated as the ALPS (R) SF.

Uniaxial compressive strength: Nearly 4,000 laboratory tests were compiled from the literature into the Database of Uniaxial Coal Strength (DUCS) [Mark and Barton 1996]. From these data, typical seam strength values were obtained for 60 U.S. coalbeds.

Width-to-height (w/h) ratio: The w/h of the largest pillar in the gate entry system was included as an independent variable to check if the pillar strength formula could be improved.

Depth of cover (H): H was included as an independent variable primarily to check the loading formulation.

The entry width and the primary support were included as before.

The statistical analysis showed that the ALPS (R) SF and the CMRR still correctly predicted 85% of the outcome, including

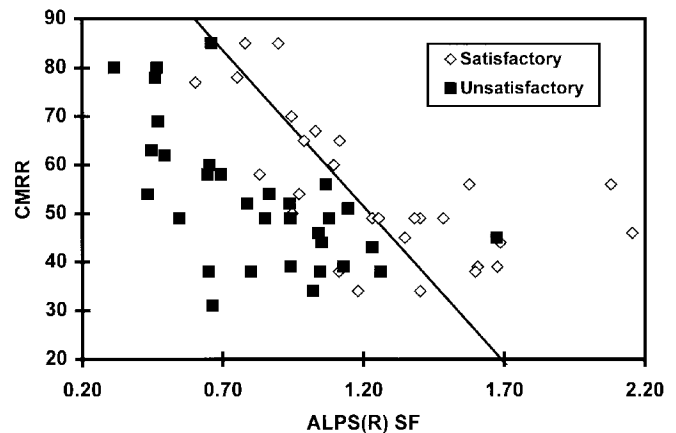


Figure 2.—U.S. longwall case histories showing the modified design equation for ALPS (R) with the Mark-Bieniawski pillar strength formula.

94% of the failures. None of the other new variables would be included even at the 50% confidence level (a 90% confidence level would be required for a covariate to be considered statistically significant). Figure 2 shows the distribution of the case histories and the revised design equation

$$\text{ALPS (R) SF} = 2.0 - 0.016 \text{ CMRR} \quad (2)$$

Since 1987, ALPS has become the most widely used pillar design method in the United States. The ALPS-CMRR method directly addresses gate entry performance and makes U.S. longwall experience available to mine planners in a practical form. ALPS reduces a multitude of variables (e.g., depth of cover, pillar widths, seam height, entry width, roof quality) into a single, meaningful design parameter—the stability factor. ALPS has been accepted because it is easy to use, its essential concepts are easy to grasp, and it has been thoroughly verified with case histories. Most importantly, ALPS gives reasonable answers that make sense in terms of experience. Tailgate blockages are far less common today than 10 years ago; ALPS can surely claim some of the credit.

PILLAR DESIGN FOR ROOM-AND-PILLAR MINING

Room-and-pillar mining still accounts for nearly 50% of the underground coal mined in the United States (even after excluding longwall development). Most room-and-pillar mines operate under relatively shallow depth, often working small, irregular deposits. Approximately 20% of room-and-pillar coal is won during pillar recovery operations [Mark et al. 1997b].

Room-and-pillar mines still suffer from large-scale pillar failures, including sudden collapses and the more common "squeezes." The classical empirical pillar strength formulas were developed precisely to prevent these types of failures, but they have never been entirely satisfactory. First, they did not consider the abutment loads that occur during pillar recovery

operations. Second, laboratory testing to determine coal strength has remained controversial despite the fact that textbooks have considered it an integral part of pillar design for 30 years. Third, because the empirical formulas were developed from tests on relatively slender specimens, their applicability to squat pillars has been open to question. Finally, attempts to verify the formulas' accuracy with U.S. case histories have been incomplete and conspicuously lacking in examples of pillar failure [Holland 1962; Bieniawski 1984].

An intensive research effort to develop an improved design method culminated in the Analysis of Retreat Mining Pillar

Stability (ARMPS). ARMPS employs many of the same basic constructs as ALPS, adapted to more complex and varied retreat mining geometries [Mark and Chase 1997]. The abutment load formulas were adapted to three dimensions to account for the presence of barrier pillars and previously extracted panels. Because the pillars used in retreat mining are often rectangular, the Mark-Bieniawski pillar strength formula was developed to estimate pillar strength. Features such as varied entry spacings, angled crosscuts, and slab cuts in the barrier can all be modeled.

To verify ARMPS, more than 200 retreat mining case histories were obtained from field visits throughout the United States. The case histories come from 10 States and cover an extensive range of geologic conditions, roof rock caveability, extraction methods, depths of cover, and pillar geometries. Ground conditions were characterized in each case as satisfactory or unsatisfactory. Where possible, data were also collected to assess the CMRR. Site-specific data on coal strength were not generally available for individual case histories, but DUCS again provided estimates of UCS for most coalbeds. Finally, the depth of cover and the w/h were also included as independent variables in the analysis. Details on the individual case histories have been presented elsewhere [Mark and Chase 1997].

When the entire data set was evaluated, it was found that 77% of the outcomes could be correctly predicted simply by setting the ARMPS SF to 1.46. Including either the depth or the w/h increased the correlation coefficient, r^2 , slightly without improving the accuracy (figure 3). The depth and the w/h ratio were strongly correlated with each other within the data set.

The accuracy improved when the data set was divided into two parts. One group included only cases where cover was shallow ($H < 200$ m (650 ft)) and where the pillars were not squat ($w/h < 8$). For this group, when the ARMPS SF = 1.5, 83% of the outcomes were correctly predicted. However, for the deep cover/squat pillar group, only 58% of the cases were correctly predicted at ARMPS SF = 0.93. No other variables could be included in either group at the 90% confidence level. It seems clear that ARMPS works quite well at shallow depth and moderate w/h ratios, but that other factors must be considered when squat pillars are used at greater depths.

The analysis also found that using laboratory UCS tests did not improve the accuracy of ARMPS at all. This finding confirms the results of a previously published study [Mark and

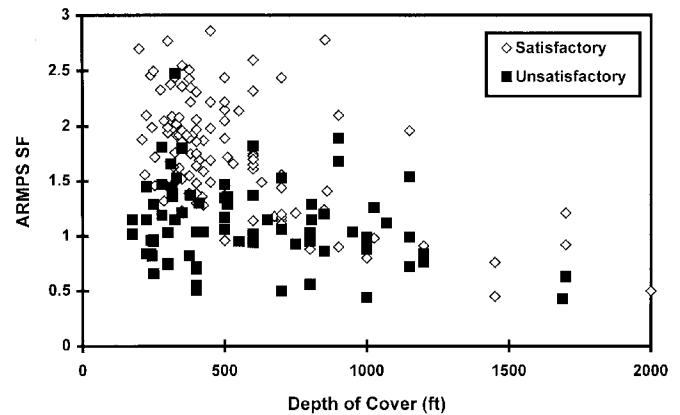


Figure 3.—U.S. room-and-pillar case histories.

Barton 1996], which showed that ARMPS was *more* reliable when the in situ coal strength was always assumed to be 6.2 MPa (900 psi). It also showed that the "size effect" varies dramatically from seam to seam depending on the coal cleat structure.

Studies in the Republic of South Africa and Australia have also found that a uniform coal strength worked reasonably well in pillar design formulas [Salamon 1991; Galvin and Hebblewhite 1995]. It has already been noted that ARMPS is significantly less reliable for squat pillars. It seems likely that while the strength of the intact coal (which is what is measured in a laboratory test) is not related to pillar strength, large-scale geologic features like bedding planes, clay bands, rock partings, and roof and floor rock may determine the strength of squat pillars. Such features influence the amount of confinement that can be generated within the pillar and therefore the load-bearing capacity of the pillar core. Similar conclusions have been reached by researchers using numerical models [Su and Hasenfus 1997; Gale 1992].

Although the CMRR was not found to be significant in the overall data set, one local study indicated that caveability may affect pillar design. More than 50 case histories were collected at a mining complex in southern West Virginia. Analysis showed that satisfactory conditions were more likely to be encountered under shale roof (figure 4) than under massive sandstone roof (figure 5). The implication is that better caving occurs with shale, resulting in lower pillar loads.

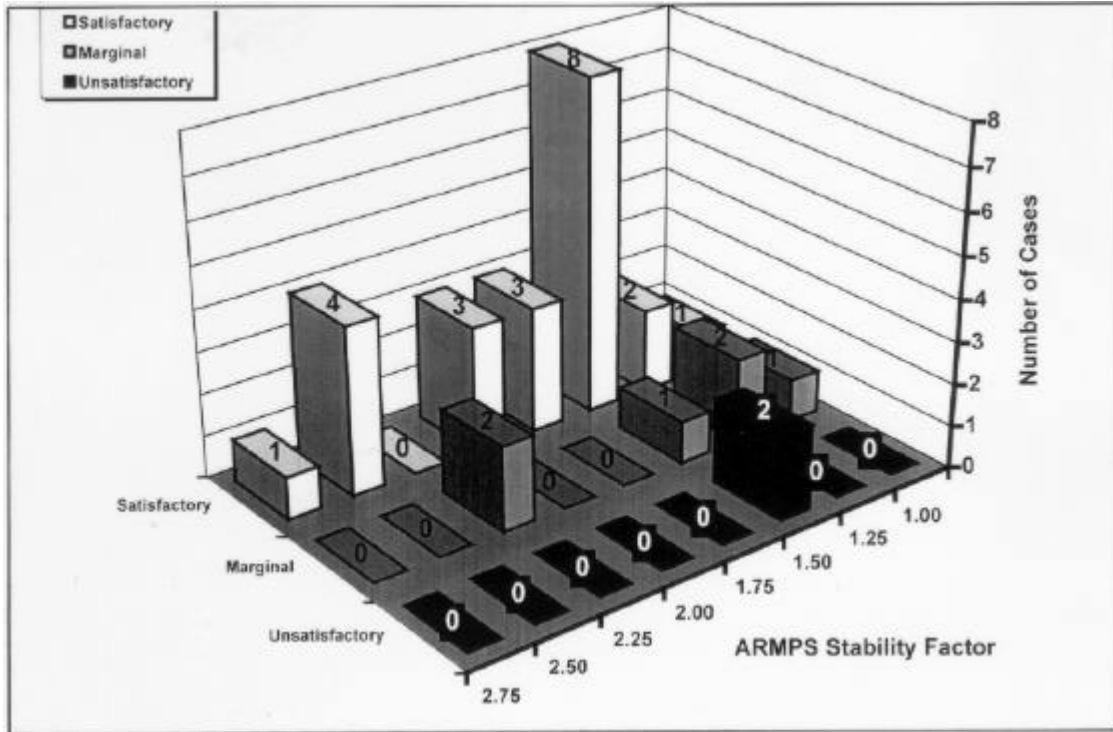


Figure 4.—Pillar performance under different roof geologies at a mining complex in West Virginia—shale roof.

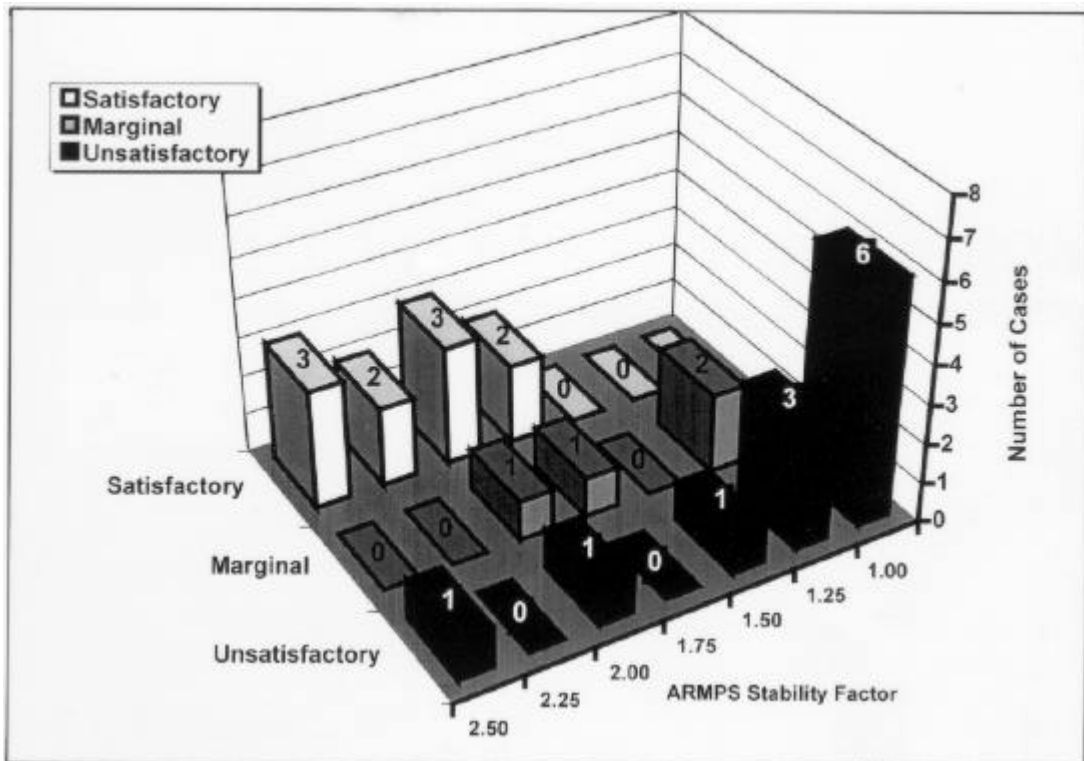


Figure 5.—Pillar performance under different roof geologies at a mining complex in West Virginia—sandstone roof.

MASSIVE PILLAR COLLAPSES

Most of the pillar failures included in the ARMPS database are "squeezes" in which the section converged over hours, days, or even weeks. There are also 15 massive pillar collapses that form an important subset [Mark et al. 1997a]. Massive pillar collapses occur when undersized pillars fail and rapidly shed their load to adjacent pillars, which in turn fail. The consequences of such chain-reaction failures typically include a powerful, destructive, and hazardous airblast.

Data collected at 12 massive collapse sites revealed that the ARMPS SF was <1.5 in every case and <1.2 in 81% of the cases (figure 6). What really distinguished the sudden collapses from the slow squeezes, however, was the pillar's w/h ratio. Every massive pillar collapse involved *slender* pillars whose w/h was <3. The overburden also included strong, bridging strata in every case.

In this instance, the empirical analysis led to a hypothesis about the mechanism of the failure. Laboratory tests have shown that slender coal specimens typically have little residual strength, which means that they shed almost their entire load when they fail. As the specimens become more squat, their residual strength increases, reducing the potential for a rapid domino-type failure. The mechanism of massive collapses was replicated in a numerical model [Zipf and Mark 1997], providing further support for the hypothesis.

Three alternative strategies were proposed to prevent massive pillar collapses:

- *Prevention:* With the prevention approach, the panel pillars are designed so that collapse is highly unlikely. This can be accomplished by increasing either the SF of the pillars or their w/h ratio.
- *Containment:* In this approach, high extraction is practiced within individual compartments that are separated by

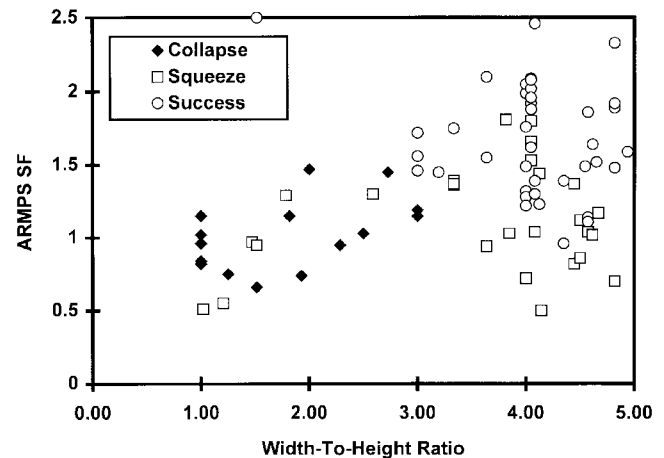


Figure 6.—A portion of the room-and-pillar case history database showing examples of pillar collapse.

barriers. The small pillars may collapse within a compartment, but because the compartment size is limited, the consequences are not great. The barriers may be true barrier pillars, or they may be rows of development pillars that are not split on retreat. The containment approach has been likened to the use of compartments on a submarine.

- *High extraction:* By removing enough coal during retreat mining, failure of the overburden may be induced, which would remove the airblast hazard.

The empirical analysis, using case histories, has allowed the first two of these approaches to be quantified in terms of the w/h ratio and the ARMPS SF. The guidelines are now being implemented in southern West Virginia, where the majority of these events have occurred.

INTERACTIONS WITH NUMERICAL MODELS

A number of important links have developed between empirical methods and numerical models. Because they were obtained from real-world data, empirical models are a good starting point for material property input to models. For example, Mark [1990] analyzed numerous field measurements of abutment stress and determined that the stress decay over the ribside could be approximated as an inverse square function. Karabin and Evanto [1999] adjusted the gob parameters in the BESOL boundary-element model to obtain a reasonable fit to the inverse square function. Similarly, Heasley and Salamon [1996a,b] used the same stress decay function to calibrate the LAMODEL program.

Empirical formulas have also helped provide coal properties for some models. Although empirical formulas do not explicitly consider the effect of internal pillar mechanics, it is apparent that they imply a nonuniform stress distribution because of the w/h effect. A derivation of the implied stress gradients was published by Mark and Iannacchione [1992]. For example, the Bieniawski formula

$$S_p = S_1 (0.64 - 0.36 w/h) \quad (3)$$

implies a stress gradient within the pillar at ultimate load of

$$S_v = S_1 (0.64 + 2.16 x/h), \quad (4)$$

where S_p = pillar strength,

S_1 = in situ coal strength,

S_v = vertical pillar stress,

and x = distance from pillar rib.

The stress gradient defines the vertical stress within the pillar at maximum load as a function of the distance from the nearest rib.

These empirical stress gradients have been widely used to estimate coal properties for use in boundary-element models that use strain-softening pillar elements. In the models, the peak stress increases the further the element is from the rib. The empirical stress gradients help ensure that the initial strength estimates are reasonable.

The same empirical stress gradient was used to extend a classic pillar strength formula to rectangular pillars. The original Bieniawski formula was derived for square pillars and underestimates the strength of rectangular pillars that contain proportionately more core area. By integrating equation 4 over

the load-bearing area of a rectangular pillar, the Mark-Bieniawski pillar strength formula is obtained:

$$S_p = S_1 (0.64 + 0.54 w/h + 0.18 (w^2/Lh)), \quad (5)$$

where L = pillar length.

The approach is illustrated in figure 7 and described in more detail by Mark and Chase [1997].

Other sections of this paper have indicated areas where numerical models and empirical methods have reached similar conclusions about important aspects of pillar mechanics. In light of these insights, old concepts of pillar "failure" have given way to a new paradigm that identifies three broad categories of pillar behavior:

- *Slender pillars* ($w/h < 3$), which have little residual strength and are prone to massive collapse when used over a large area;
- *Intermediate pillars* ($4 < w/h < 8$), where "squeezes" are the dominant failure mode in room-and-pillar mining and where empirical pillar strength formulas seem to be reasonably accurate; and
- *Squat pillars* ($w/h > 10$), which can carry very large loads and are strain-hardening, and which are dominated by entry failure (roof, rib, and floor) and by coal bumps.

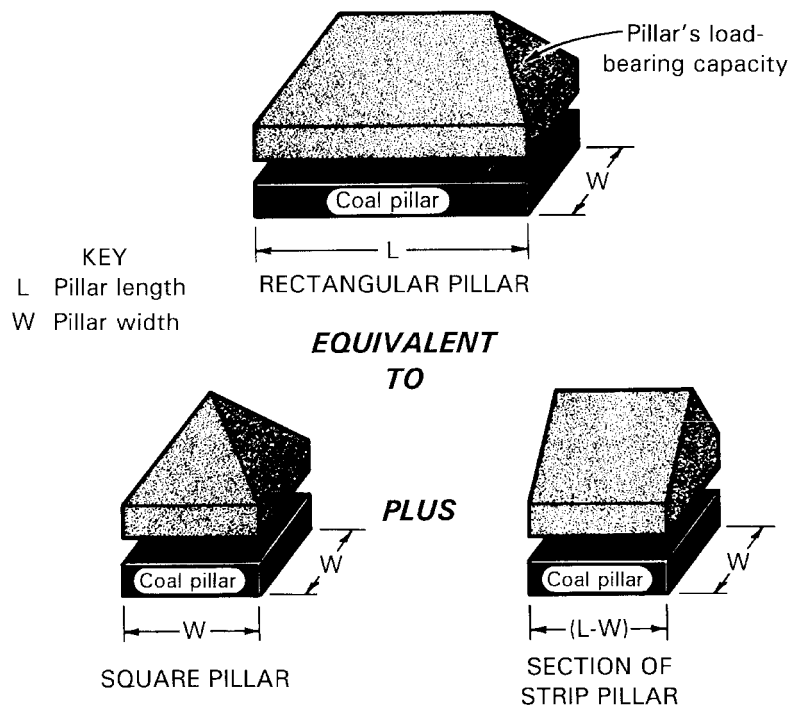


Figure 7.—Conceptual depiction of the Mark-Bieniawski pillar strength formula.

CONCLUSIONS

Empirical methods rely on the scientific interpretation of actual mining experience. Because they are so firmly linked to reality, they are particularly well suited to practical problems like pillar design. Empirical methods like ALPS and ARMPS have met the mining community's need for reliable design techniques that can be used and understood by the nonspecialist.

Successful empirical research has three central elements:

- A hypothesis or model that simplifies the real world, yet incorporates its most significant features;
- A large database of case histories, developed using consistent and thorough in-mine data collection techniques; and
- Quantitative analysis using appropriate statistical techniques.

Empirical techniques are not, of course, the only tool in the ground control specialist's kit. Indeed, one of the most satisfying developments in recent years is the synergy that has developed between empirical techniques and numerical modeling. The two approaches seem to have converged on a number of important conclusions, including:

- Laboratory testing of small coal samples, particularly UCS tests, are not useful for predicting pillar strength;
- The strength becomes more difficult to predict as the pillar becomes more squat;
- The w/h ratio is important for predicting not only the pillar strength, but also the mode of failure; and
- Many ground control problems must be considered from the standpoint of entry stability, where pillar behavior is just one component.

Certainly, more work remains before the age-old questions of pillar design are finally solved. In particular, much remains to be learned about the mechanics of squat pillars and roof-pillar-floor interactions. Currently, there is no accepted way to determine the frictional characteristics of the contacts, bedding planes, and partings that are so crucial to pillar strength. It is similarly difficult to characterize the bearing capacity of the floor. Simple, meaningful field techniques for estimating these properties will be necessary for further progress with either numerical or empirical techniques. Indeed, the cross-pollination between the numerical and empirical methods that has characterized the recent past can be expected to bear further fruit in the future.

REFERENCES

- Barczak TM [1992]. The history and future of longwall mining in the United States. Pittsburgh, PA: U.S. Department of the Interior, Bureau of Mines, IC 9316.
- Bieniawski ZT [1984]. Rock mechanics design in mining and tunneling. Balkema.
- Bieniawski ZT [1992]. A method revisited: coal pillar strength formula based on field investigations. In: Proceedings of the Workshop on Coal Pillar Mechanics and Design. Pittsburgh, PA: U.S. Department of the Interior, Bureau of Mines, IC 9315, pp. 158-165.
- Bunting D [1911]. Chamber pillars in deep anthracite mines. *Trans AIME*, Vol. 42, pp. 236-245.
- Carr F, Wilson AH [1982]. A new approach to the design of multi-entry developments for retreat longwall mining. In: Proceedings of the Second Conference on Ground Control in Mining. Morgantown, WV: West Virginia University, pp. 1-21.
- Encyclopedia Britannica [1989]. 15th ed. The social sciences. E. 27, p. 365.
- Gale WJ [1992]. A pillar design approach. In: Proceedings of the Workshop on Coal Pillar Mechanics and Design. Pittsburgh, PA: U.S. Department of the Interior, Bureau of Mines, IC 9315, pp. 188-195.
- Galvin JM, Hebblewhite BK [1995]. UNSW pillar design methodology. Sydney, Australia: University of New South Wales, Department of Mining Engineering, Research Release No. 1.
- Hesley KA, Salamon MDG [1996a]. New laminated displacement-discontinuity program. In: Aubertin M, Hassani F, Mitri H, eds. Proceedings of the Second North American Rock Mechanics Symposium: NARMS '96 (Montreal, Quebec, Canada), pp. 1879-1886.
- Hesley KA, Salamon MDG [1996b]. New laminated displacement-discontinuity program: fundamental behavior. In: Ozdemir L, Hanna K, Haramy KY, Peng S, eds. Proceedings of the 15th International Conference on Ground Control in Mining. Golden, CO: Colorado School of Mines, pp. 111-125.
- Holland CT [1962]. Design of pillars for overburden support: part II. *Min Cong J Apr*:66-71.
- Karabin GJ, Evanto MA [1999]. Experience with the boundary-element method of numerical modeling to resolve complex ground control problems. In: Proceedings of the Second International Workshop on Coal Pillar Mechanics and Design. Pittsburgh, PA: U.S. Department of Health and Human Services, Public Health Service, Centers for Disease Control and Prevention, National Institute for Occupational Safety and Health, DHHS (NIOSH) Publication No. 99-114, IC 9448.
- Mark C [1987]. Analysis of longwall pillar stability [Dissertation]. University Park, PA: The Pennsylvania State University, Department of Mining Engineering.
- Mark C [1990]. Pillar design methods for longwall mining. Pittsburgh, PA: U.S. Department of the Interior, Bureau of Mines, IC 9247.
- Mark C [1992]. Analysis of longwall pillar stability (ALPS): an update. In: Proceedings of the Workshop on Coal Pillar Mechanics and Design. Pittsburgh, PA: U.S. Department of the Interior, Bureau of Mines, IC 9315, pp. 238-249.
- Mark C, Barton TM [1996]. The uniaxial compressive strength of coal: should it be used to design pillars? In: Ozdemir L, Hanna K, Haramy KY, Peng S, eds. Proceedings of the 15th International Conference on Ground Control in Mining. Golden, CO: Colorado School of Mines, pp. 61-78.
- Mark C, Chase FE [1997]. Analysis of retreat mining pillar stability (ARMPS). In: Proceedings - New Technology for Ground Control in Retreat Mining. Pittsburgh, PA: U.S. Department of Health and Human Services, Public Health Service, Centers for Disease Control and Prevention, National Institute for Occupational Safety and Health, DHHS (NIOSH) Publication No. 97-122, IC 9446, pp. 17-34.

Mark C, Iannacchione AT [1992]. Coal pillar mechanics: theoretical models and field measurements compared. In: Proceedings of the Workshop on Coal Pillar Mechanics and Design. Pittsburgh, PA: U.S. Department of the Interior, Bureau of Mines, IC 9315, pp. 78-93.

Mark C, Molinda GM [1996]. Rating coal mine roof strength from exploratory drill core. In: Ozdemir L, Hanna K, Haramy KY, Peng S, eds. Proceedings of the 15th International Conference on Ground Control in Mining. Golden, CO: Colorado School of Mines, pp. 415-428.

Mark C, Chase FE, Molinda GM [1994]. Design of longwall gate entry systems using roof classification. In: New Technology for Longwall Ground Control - Proceedings: U.S. Bureau of Mines Technology Transfer Seminar. Pittsburgh, PA: U.S. Department of the Interior, Bureau of Mines, SP 01-94, pp. 5-17.

Mark C, Chase FE, Zipf RK Jr. [1997a]. Preventing massive pillar collapses in coal mines. In: Proceedings - New Technology for Ground Control in Retreat Mining. Pittsburgh, PA: U.S. Department of Health and Human Services, Public Health Service, Centers for Disease Control and Prevention, National Institute for Occupational Safety and Health, DHHS (NIOSH) Publication No. 97-122, IC 9446, pp. 35-48.

Mark C, McCall FE, Pappas DM [1997b]. A statistical overview of retreat mining of coal pillars in the United States. In: Proceedings - New Technology for Ground Control in Retreat Mining. Pittsburgh, PA: U.S. Department of Health and Human Services, Public Health Service, Centers for Disease Control and Prevention, National Institute for Occupational Safety and Health, DHHS (NIOSH) Publication No. 97-122, IC 9446, pp. 2-16.

Molinda GM, Mark C [1994]. Coal mine roof rating (CMRR): a practical rock mass classification for coal mines. Pittsburgh, PA: U.S. Department of the Interior, Bureau of Mines, IC 9387.

Parker J [1974]. Practical rock mechanics for the miner: part 7 - the logical way to design pillars. *Eng Min J Feb*:67.

Salamon MDG [1989]. Significance of strata control to the safety and efficiency of mining. In: Proceedings of the Eighth International Strata Control Conference (Düsseldorf, Germany).

Salamon MDG [1991]. Behavior and design of coal pillars. *Australian Coal J*, No. 32, pp. 11-22.

Salamon MDG [1992]. Strength and stability of coal pillars. In: Proceedings of the Workshop on Coal Pillar Mechanics and Design. Pittsburgh, PA: U.S. Department of the Interior, Bureau of Mines, IC 9315, pp. 94-121.

Starfield AM, Cundall PA [1988]. Towards a methodology for rock mechanics modelling. *Int J Rock Mech Min Sci* 25(3):99-106.

Su DWH, Hasenfus GJ [1997]. Effects of in-seam and near-seam conditions on coal pillar strength. Handout at the 16th International Conference on Ground Control in Mining (Morgantown, WV).

Webster's II New Riverside University Dictionary [1988]. Itasca, IL: The Riverside Publishing Co.

Wilson AH [1972]. An hypothesis concerning pillar stability. *Min Eng (London)* 131(141):409-417.

Wilson AH [1983]. The stability of underground workings in the soft rocks of the coal measures. *Int J Min Eng* 1:91-187.

Zipf RK Jr., Mark C [1997]. Design methods to control violent pillar failures in room-and-pillar mines. *Transactions of the Institution of Mining and Metallurgy* 106(Sept-Dec):A124-A132.

COAL PILLAR STRENGTH AND PRACTICAL COAL PILLAR DESIGN CONSIDERATIONS

By Daniel W. H. Su, Ph.D.,¹ and Gregory J. Hasenfus²

ABSTRACT

This paper demonstrates that finite-element modeling can be used to predict in situ coal pillar strength, especially under nonideal conditions where interface friction and roof and floor deformation are the primary controlling factors. Despite their differences in approach, empirical, analytical, and numerical pillar design methods have apparently converged on fundamentally similar concepts of coal pillar mechanics. The finite-element model results, however, are not intended to suggest a new pillar design criterion. Rather, they illustrate the site-specific and complex nature of coal pillar design and the value of using modeling procedures to account for such complex site-specific conditions. Because of the site-specific nature of coal pillar design, no single pillar design formula or model can apply in all instances. Understanding and accounting for the site-specific parameters are very important for successful coal pillar design. More work remains before the century-old problems related to pillar design are finally solved. Future research should focus on the cross-linkage of empirical, analytical, and numerical pillar design methods.

¹Senior research scientist.

²Group leader.

CONSOL, Inc., Research & Development, Liberty, PA.

INTRODUCTION

The strength of coal and coal pillars has been the subject of considerable research during the past 40 years. Coal strengths determined in the laboratory typically increase with increasing specimen width-to-height (w/h) ratio and decrease with increasing height and size. Based on the shape and size effect derived from testing of cubical specimens, a number of empirical pillar strength formulas [Gaddy 1956; Holland 1964; Obert and Duvall 1967; Salamon and Munro 1967; Bieniawski 1968] and closed-form analytical solutions for pillar strength [Wilson 1972; Barron 1984] were proposed during the past 4 decades and used by coal operators and regulatory authorities with varying degrees of success. However, empirical formulas may not be extrapolated with confidence beyond the data range from which they were derived, typically from pillars with w/h ratios of #5 [Mark and Iannacchione 1992], and these formulas inherently ignore roof and floor end constraint and subsequent interactions.

The importance of friction and end constraint on laboratory coal strength has been demonstrated by many researchers, including Khair [1968], Brady and Blake [1968], Bieniawski [1981], Salamon and Wagner [1985], Babcock [1990, 1994], and Panek [1994]. Practitioners and researchers alike,

including Mark and Bieniawski [1986], Hasenfuls and Su [1992], Maleki [1992], and Parker [1993], have noted the significance of roof and floor interactions on in situ pillar strength.

The importance of incorporating fundamental principles of rock material response and failure mechanics into a pillar strength model using a finite-element modeling (FEM) technique has been demonstrated by Su and Hasenfuls [1996, 1997]. To accurately assess pillar strength, a model should account not only for the characteristics of the coal, but also for those of the surrounding strata. The frictional end-constraint interaction between the pillar and the surrounding roof and floor has been demonstrated to be one of the most significant factors in the strength of very wide pillars. This paper summarizes the results of a series of FEM cases designed to evaluate the effect on pillar strength of end constraint or confinement over a wide range of pillar w/h ratios, as well as the effects of seam strength, rock partings, and weak floor. The interdependence among pillar design, entry stability, and ventilation efficiency in longwall mining is briefly discussed. Finally, the site-specific nature of coal pillar design is emphasized, and a direction of future research is suggested.

USE OF FINITE-ELEMENT MODELING IN PILLAR DESIGN

In recent years, FEM has been used to predict in situ coal pillar strength, especially under nonideal conditions in which interface friction and roof and floor deformation are the primary controlling factors. Practical coal pillar design considerations that incorporated the results of FEM and field measurements were presented by Su and Hasenfuls [1996]. Nonlinear pillar strength curves were first presented to relate pillar strength to w/h ratio under simulated strong mine roof and floor conditions (figure 1). Confinement generated by the frictional effect at coal-rock interfaces was demonstrated to accelerate pillar strength increase beginning at a w/h ratio of about 3. Thereafter, frictional constraint limitations and coal plasticity decelerate pillar strength increases beginning at a w/h of about 6. The simulated pillar strength curve under strong roof and floor compared favorably with measured peak strengths of four failed pillars in two coal mines in southwestern Virginia (figure 2) and is in general agreement with many existing coal pillar design formulas at $w/h < 5$.

FEM has also been used to evaluate the effect of in-seam and near-seam conditions, such as seam strength, rock partings, and weak floor rock, on pillar strength [Su and Hasenfuls 1997]. On

a percentage basis, seam strength was found to have a negligible effect on the peak strength for pillars at high w/h ratios (figure 3). For practical coal pillar design, exact determination of intact coal strength thus becomes unnecessary; for wide pillars, an average seam strength of 6.2 to 6.6 MPa may suffice for most U.S. bituminous coal seams. Rock partings within the coal seam, however, were found to have a variable effect on pillar strength, depending on the parting strength. A competent shale parting within the coal seam reduces the effective pillar height, thus increasing the ultimate pillar strength (figure 4). Conversely, a weak claystone parting slightly decreases pillar strength. In addition, weak floor rocks may decrease the ultimate pillar strength by as much as 50% compared to strong floor rock (figure 5). Field observations confirm pillar strength reduction in the presence of weak floor rocks.

Similar to CONSOL's studies, an earlier numerical study by the former U.S. Bureau of Mines employing a finite difference modeling technique concluded that pillar strength was highly dependent on the frictional characteristics of the coal-roof and coal-floor interfaces [Iannacchione 1990].

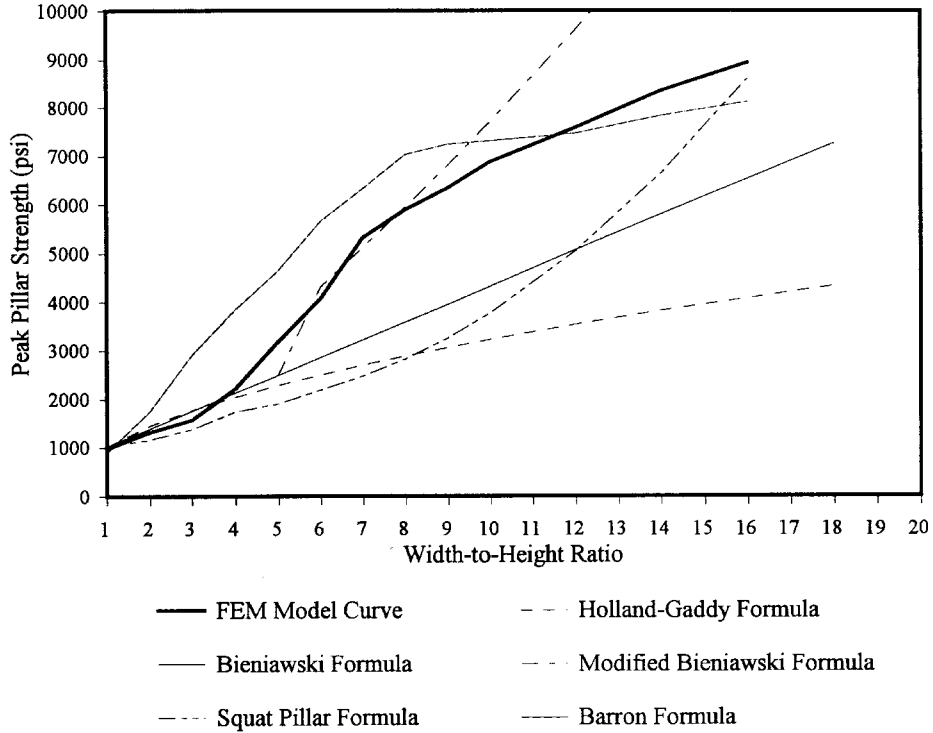


Figure 1.—Pillar strength comparison of FEM model results versus existing empirical formula.

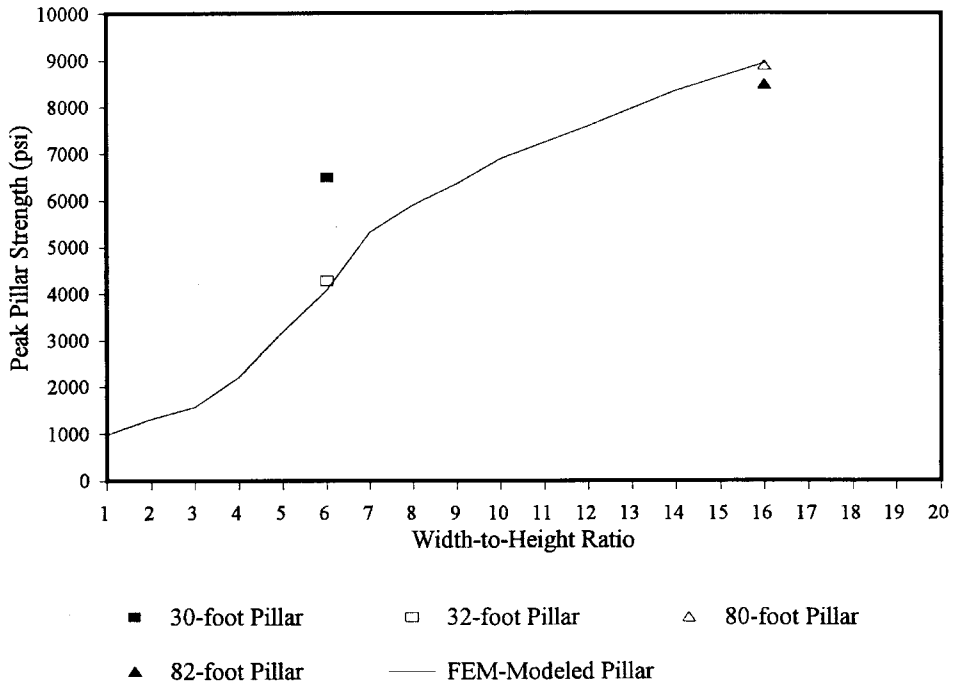


Figure 2.—Comparison of FEM modeled versus field pillar strength data (strong roof and strong floor conditions).

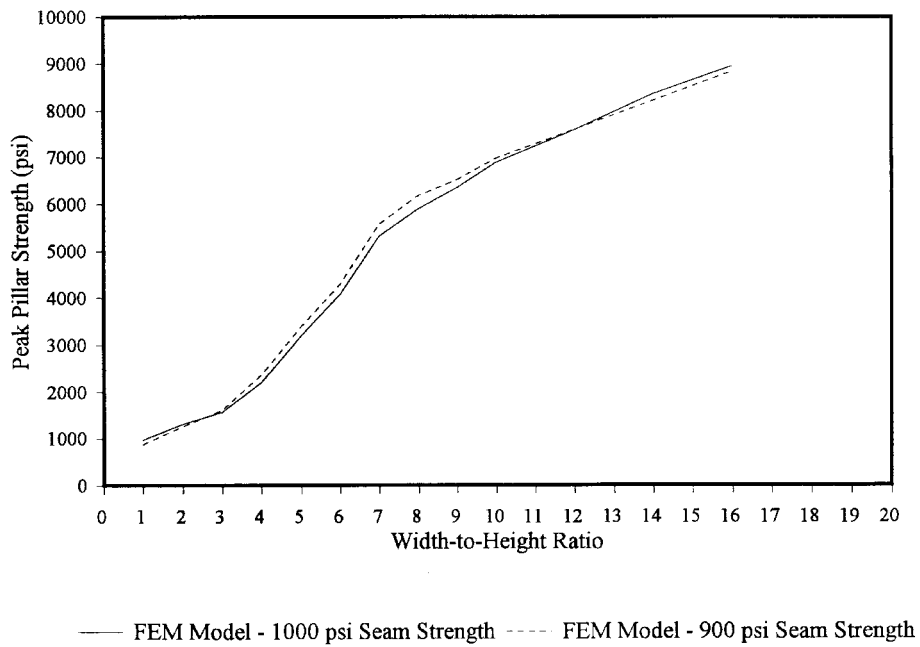


Figure 3.—Effect of seam strength on FEM model results.

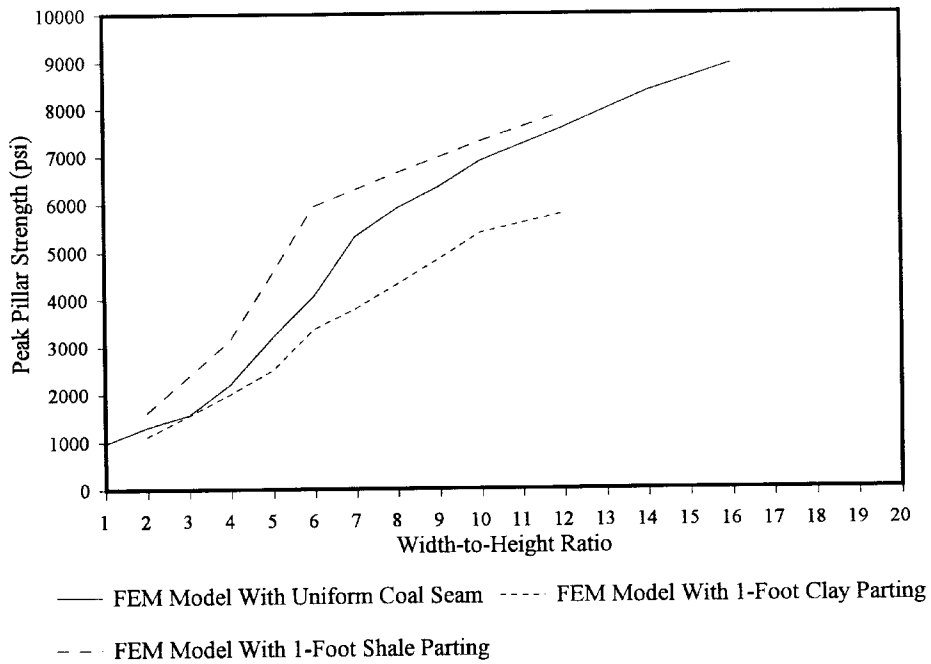


Figure 4.—Effect of claystone and shale parting on FEM model results.

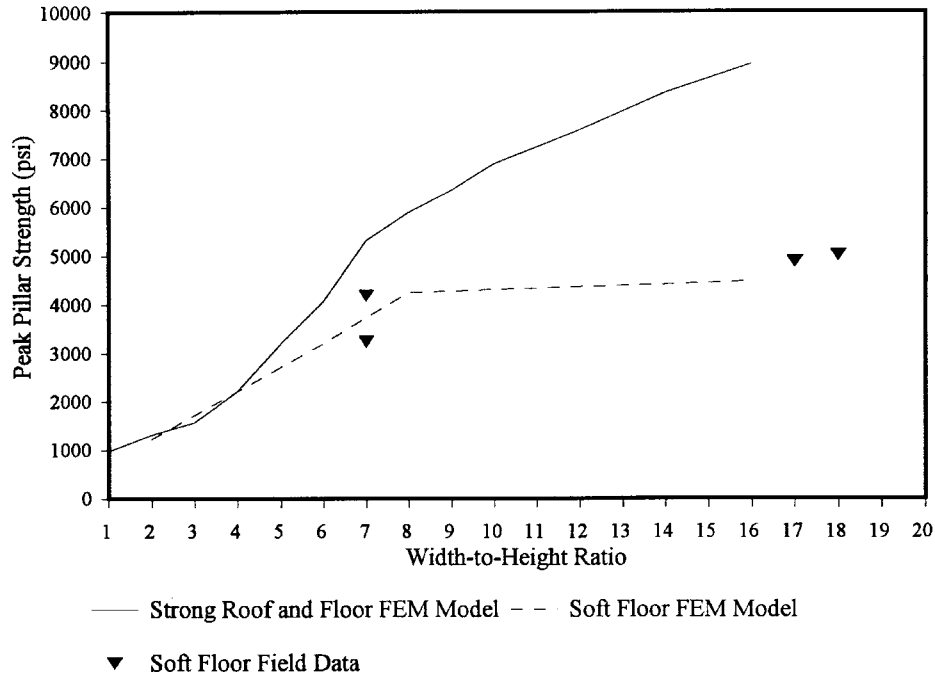


Figure 5.—Effect of weak claystone (soft) floor on pillar strength.

FUTURE PILLAR DESIGN CONSIDERATIONS RELATED TO SITE-SPECIFIC CONDITIONS

Because many coal pillar design formulas are empirical relationships that were developed under limited conditions, application of these formulas may be inappropriate when other factors not specifically addressed in these relationships are encountered. As demonstrated, pillar strength and therefore entry stability are extremely sensitive to the in situ characteristics of not only the coal, but also the adjacent and inclusive rock that comprise the coal pillar system. Unfortunately, a single site-specific empirical formula cannot accurately account for the variations of features that may significantly affect pillar and entry stability within a single coalfield or even a single mine. In addition, it is neither practical nor efficient to develop site-specific empirical formulas for all variations of roof, floor, and pillar characteristics that may occur within a mine.

Over the past decade, the Analysis of Longwall Pillar Stability (ALPS) approach to longwall pillar design has gained

wide acceptance for longwall pillar design analysis in U.S. coalfields [Mark and Chase 1993]. Although it has proven to be applicable for use in many mines and mining regions, ALPS, which relies solely on the Bieniawski formula for pillar strength calculation, does not always accurately represent pillar strength at high w/h ratios. For example, for the prevailing strong roof and floor conditions in the Virginia Pocahontas No. 3 Coalfield, ALPS significantly underestimates pillar strength (figure 6). Conversely, under very weak, "soft" conditions, ALPS may significantly overestimate pillar strength (figure 7). Although recent versions of ALPS provide a Coal Mine Roof Rating (CMRR) routine that modifies the safety factor requirement and better accommodates hard roof conditions, this routine does not correct the inherent error in pillar strength calculation, which may be important not only for entry stability and safety, but also for subsidence planning and design.

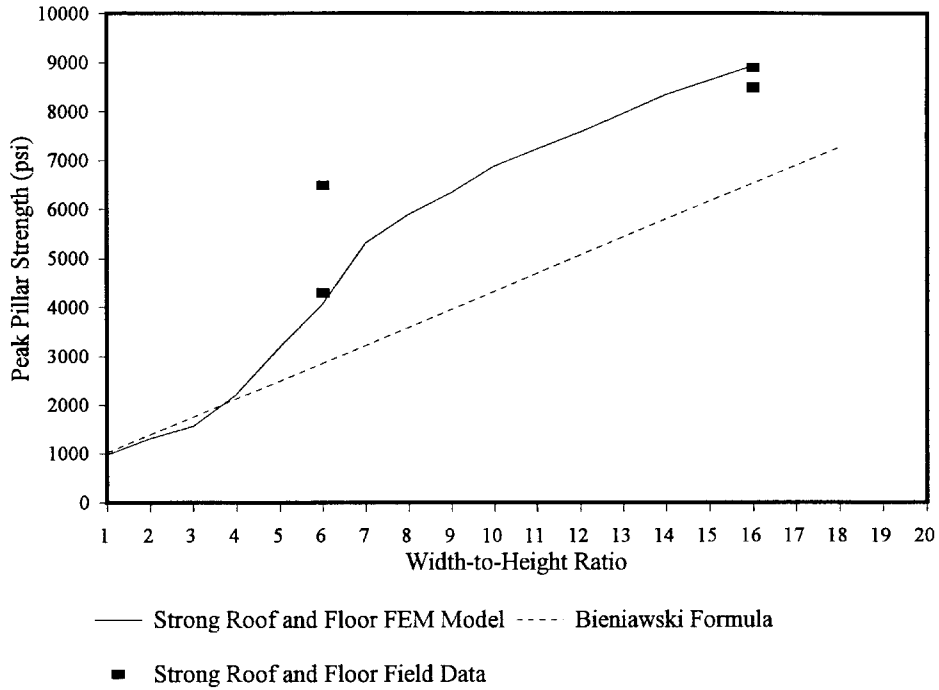


Figure 6.—FEM model and Bieniawski formula comparison with strong roof and floor data.

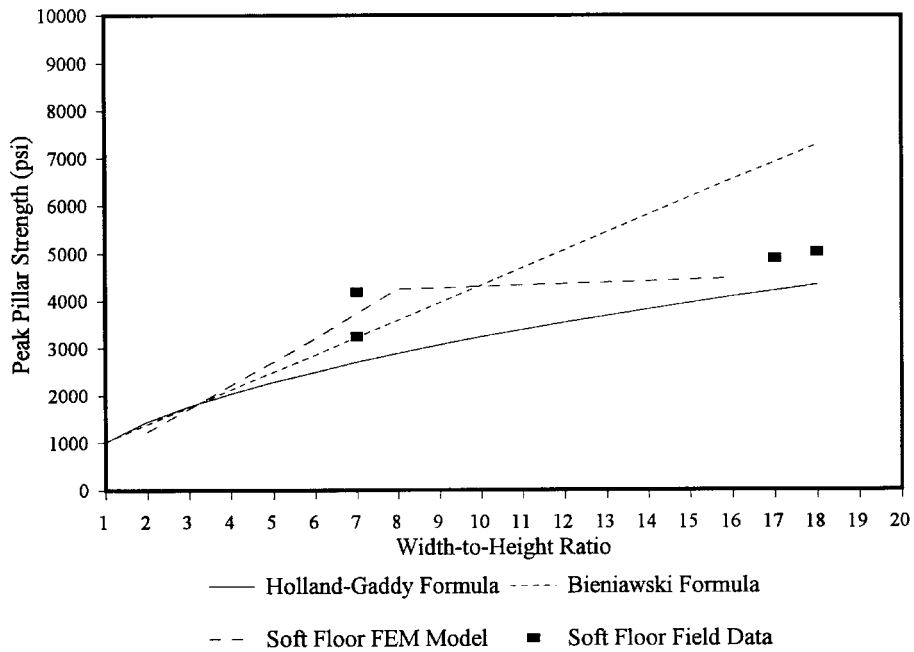


Figure 7.—Empirical pillar strength formula comparison with soft floor field data.

FUTURE PILLAR DESIGN CONSIDERATIONS RELATED TO ENTRY STABILITY AND VENTILATION EFFICIENCY

The ultimate goal of a successful pillar design is to achieve entry stability with optimum support. The classical pillar design approach focuses on determining safety factors from estimates of pillar strength and pillar load. This works well in room-and-pillar operations without second mining and in main entries not subject to abutment pressures. A successful longwall gate road design, on the other hand, requires stable headgate and tailgate entries under the influence of longwall abutment pressures. Headgate or tailgate entry failures, such as a roof fall, severe floor heave, or severe pillar spalling, may pose serious safety hazards and may stop longwall mining for days or weeks. Traditionally, headgate and tailgate stabilities have been correlated with pillar sizes, and many ground control researchers have focused on the design of longwall chain pillars for improving gate road stability. However, gate entry performance is influenced by a number of geotechnical and design factors, including pillar size, pillar loading, roof quality, floor quality, horizontal stresses, entry width, and primary and secondary supports [Mark and Chase 1993]. It suffices to say that pillar size is not the only factor affecting longwall headgate and tailgate stability. Therefore, strength of roof and floor rocks, state of in situ horizontal stresses, entry width, and support methodology are other important factors that should be included in any practical longwall chain pillar design methodology.

In the early 1990s, Mark and Chase [1993] used a back-calculation approach to suggest an ALPS stability factor for longwall pillars and gate entries based on a CMRR. The importance of floor stability and secondary support could not be determined from the data and were not included in the back-calculation. Nevertheless, their effort pioneered pillar design research that included roof rock strength and integrated pillar and entry roof stability. Although the floor strength, roof support, horizontal stresses, and entry width can theoretically be included in a numerical pillar design model, other issues, such as gob formation, load transfer, material properties, and

geological variations, may make model formulation difficult. It seems that a hybrid method of the back-calculation and numerical approaches may provide a more effective and versatile pillar design method in the future.

A more rigorous, yet practical pillar design methodology could be developed by incorporating a site-specific pillar strength formula obtained from numerical models or alternative field observations into the ALPS stability factor approach. As an example, for strong roof and floor, the FEM-based pillar strength curve, which incorporates site-specific roof and floor strength, predicts a strength for an 80-ft-wide pillar that closely emulates field results, but is nearly 40% higher than that predicted by the Bieniawski formula (figure 6). In addition, under very weak floor conditions, the Holland-Gaddy formula may better represent pillar strength than the Bieniawski formula (figure 7).

If such a combined approach is adopted, it could be done either on an independent basis or perhaps even as a modification to the overall ALPS design approach. Nevertheless, it is apparent that pillar design methodology could still benefit from a combination of empirical, analytical, and numerical methods to formulate practical pillar design based on site-specific roof, floor, and seam conditions.

An aspect of longwall gate road design that is often overlooked is its impact on ventilation. Specifically, for eastern U.S. coal mines that employ only three or four gate road entries, the ability to provide an effective internal bleeder system in the tailgate behind the face can be quite important. Obviously, effective ventilation area in the tailgate between two gobs is influenced by roof and floor geology, entry width and height, pillar load and pillar strength, and primary and secondary support. Where longwall chain pillar designs must provide an effective internal bleeder system, ground control engineers must account for the aforementioned factors in addition to pillar load and pillar strength.

CONCLUSIONS

With the capability of modeling interface friction and various boundary conditions, a finite-element code can be an effective tool for site-specific evaluation of in situ coal pillar strength that considers the complex failure mechanisms of in situ coal pillars. The modeling technique can be most useful for conditions where interface friction and roof and floor deformation are the primary controlling factors. Nonlinear pillar strength curves relate the increase of pillar strength to the w/h ratio. Confinement generated by frictional effects at the coal-rock interface is shown to increase the pillar strength more

rapidly at w/h ratios of about 3. The finite-element modeled in situ pillar strength curve for strong roof and floor conditions compares favorably with the measured peak strengths of five failed pillars in two southwestern Virginia coal mines and is in general agreement with many existing coal pillar design formulas at w/h ratios of <5. However, for wide pillars, modeling predicts a higher in situ coal pillar strength than most accepted formulas. Consequently, use of more conservative empirical formulas may lead to the employment of unnecessarily wide pillars or a lower estimated safety factor.

However, to accurately assess pillar strength, a model or formula should account not only for the characteristics of the coal, but also for those of the surrounding strata. Although seam strength is observed to have some effect on pillar strength, its significance is often overrated. In fact, for coal pillars with large w/h ratios, ultimate pillar strength is more dependent on end constraints than on seam strength. This reduces the significance of laboratory coal compressive strength determination for such conditions. For practical purposes, a uniform seam strength averaging about 6.2 to 6.6 MPa is adequate for most U.S. bituminous coal seams when employing finite-element models to simulate pillars with high w/h ratios.

The finite-element model results presented are not intended to suggest new pillar design relationships with w/h ratios. The primary objective of this paper is to emphasize the site-specific nature of coal pillar design and the value of using modeling procedures to account for such site-specific conditions. Understanding the site-specific parameters is an important ingredient for successful coal pillar design. Due to the variability of in situ properties, no currently available empirical,

analytical, or numerical pillar design formula is applicable in all cases. Utilization or imposition of pillar design formulas that do not, or cannot, account for site-specific variations in roof, floor, and parting conditions may lead to incorrect assessments of pillar strength, whether high or low, and incorrect estimates of pillar design safety factors. Empirical, analytical, or numerical design procedures should be validated by site-specific measurements or observational field studies whenever possible.

For longwall mining, pillar design is not the only factor affecting headgate and tailgate stability and ventilation efficiency. Strength of roof and floor rocks, state of in situ stresses, entry width, and support methodology are other important factors affecting longwall gate road stability and should be considered in practical longwall chain pillar design. Certainly, more work remains before the century-old problems related to pillar design are finally solved. Future pillar design methodology could benefit from a cross-linkage of empirical, analytical, and numerical pillar design methods.

REFERENCES

- Babcock CO [1990]. True uniaxial compressive strengths of rock or coal specimens are independent of diameter-to-length ratios. Denver, CO: U.S. Department of the Interior, Bureau of Mines, RI 9316.
- Babcock CO [1994]. Critique of pillar design equations from 1833 to 1990. Denver, CO: U.S. Department of the Interior, Bureau of Mines, IC 9398.
- Barron K [1984]. An analytical approach to the design of coal pillars. *CIM Bulletin* 77(868):37-44.
- Bieniawski ZT [1968]. The effects of specimen size on the compressive strength of coal. *Int J Rock Mech Min Sci* 5:325-335.
- Bieniawski ZT [1981]. Improved design of coal pillars for U.S. mining conditions. In: *First Annual Conference on Ground Control in Coal*. Morgantown, WV: West Virginia University, pp. 13-22.
- Brady BT, Blake W [1968]. An elastic solution of the laterally constrained circular cylinder under uniaxial loading. In: *10th U.S. Symposium on Rock Mechanics*, pp. 199-214.
- Gaddy FL [1956]. A study of the ultimate strength of coal as related to the absolute size of the cubical specimens tested. Blacksburg, VA: Virginia Polytechnic Institute and State University, *Bulletin VPI* 49(10), tables 6-10.
- Hasenfus GJ, Su DWH [1992]. A comprehensive integrated approach for longwall development design. In: *Proceedings of the Workshop on Coal Pillar Mechanics and Design*. Pittsburgh, PA: U.S. Department of the Interior, Bureau of Mines, IC 9315, pp. 225-237.
- Holland CT [1964]. The strength of coal in mine pillars. In: *Proceedings of the Sixth Symposium on Rock Mechanics*. Rolla, MO: University of Missouri, pp. 450-456.
- Iannacchione AT [1990]. The effect of roof and floor interface slip on coal pillar behavior. In: *Proceedings of the 31st U.S. Symposium on Rock Mechanics*, pp. 156-160.
- Khair AW [1968]. The effects of coefficient of friction on strength of model coal pillar [Thesis]. Morgantown, WV: West Virginia University, Department of Mining Engineering.
- Maleki H [1992]. In situ pillar strength and failure mechanisms for U.S. coal seams. In: *Proceedings of the Workshop on Coal Pillar Mechanics and Design*. Pittsburgh, PA: U.S. Department of the Interior, Bureau of Mines, IC 9315, pp. 73-77.
- Mark C, Bieniawski ZT [1986]. Field measurements of chain pillar response to longwall abutment loads. In: *Proceedings of the Fifth Conference on Ground Control in Mining*, pp. 114-122.
- Mark C, Chase FE [1993]. Gate entry design for longwall using the coal mine roof rating. In: *Proceedings of the 12th International Conference on Ground Control in Mining*. Morgantown, WV: West Virginia University, pp. 76-83.
- Mark C, Iannacchione AT [1992]. Coal pillar mechanics: theoretical models and field measurements compared. In: *Proceedings of the Workshop on Coal Pillar Mechanics and Design*. Pittsburgh, PA: U.S. Department of the Interior, Bureau of Mines, IC 9315, pp. 78-93.
- Obert L, Duvall WI [1967]. *Rock mechanics and the design of structures in rock*. New York, NY: John Wiley and Sons, pp. 542-545.
- Panek L [1994]. Sealing mine pillar size and slope with the R function. *SME preprint* 94-52. Littleton, CO: Society for Mining, Metallurgy, and Exploration, Inc.
- Parker J [1993]. Mine pillar design in 1993: computers have become the opiate of mining engineering, parts I and II. *Min Eng July*:714-717 and *Aug*:1047-1050.
- Salamon MDG, Munro AH [1967]. A study of the strength of coal pillars. *J S Afr Inst Min Metall* 68:55-67.
- Salamon MDG, Wagner H [1985]. Practical experiences in the design of coal pillars. In: Green AR, ed. *Proceedings of the 21st International Conference of Safety in Mines Research Institutes* (Sydney, Australia). Balkema, pp. 3-9.
- Su DWH, Hasenfus GJ [1996]. Practical coal pillar design considerations based on numerical modeling. Handout at the 15th International Conference on Ground Control in Mining (Golden, CO).
- Su DWH, Hasenfus GJ [1997]. Effects of in-seam and near-seam conditions on coal pillar strength. Handout at the 16th International Conference on Ground Control in Mining (Morgantown, WV).
- Wilson AH [1972]. An hypothesis concerning pillar stability. *Min Eng (London)* 131(141):409-417.

NEW STRENGTH FORMULA FOR COAL PILLARS IN SOUTH AFRICA

By J. Nielen van der Merwe, Ph.D.¹

ABSTRACT

For the last 3 decades, coal pillars in the Republic of South Africa have been designed using the well-known strength formula of Salamon and Munro that was empirically derived after the Coalbrook disaster. The database was recently updated with the addition of failures that occurred after the initial analysis and the omission of failures that occurred in a known anomalous area. An alternative method of analysis was used to refine the constants in the formula. The outcome was a new formula that shows that the larger width-to-height ratio coal pillars are significantly stronger than previously believed, even though the material itself is represented by a reduced constant in the new formula. The formula predicts lower strength for the smaller pillars, explaining the failure of small pillars that were previously believed to have had high safety factors. Application of the new formula will result in improved coal reserve utilization for deeper workings and enhanced stability of shallow workings.

¹Managing director, Itasca Africa (Pty.) Ltd., Johannesburg, Republic of South Africa.

INTRODUCTION

The Coalbrook disaster in January 1960, in which more than 400 men lost their lives when the mine's pillars collapsed, led to a concerted research effort that eventually resulted in the creation of two formulas for the prediction of coal pillar strength: the power formula of Salamon and Munro [1967] and the linear equation of Bieniawski [1968]. The Bieniawski formula was based on in situ tests of large coal specimens; the Salamon-Munro formula, on a statistical analysis of failed and stable pillar cases. The South African mining industry adopted the Salamon-Munro formula, even though the differences between the two formulas were not significant for the range of pillar sizes that were mined at the time.

It is characteristic of the Salamon-Munro formula that the strength increases at a lower rate as the width-to-height (w/h) ratios of the pillars increase. Later, this was rectified by the so-called squat pillar formula refined by Madden [1991]. This formula is valid for w/h ratios >5 and is characterized by an accelerating strength increase with increasing w/h ratios.

An intriguing aspect of the Salamon-Munro formula is the relatively high value of the constant in the formula that represents the strength of the coal material—7.2 MPa. This compares with the 4.3 MPa used in the Bieniawski formula. The question has always been why the statistical back-analysis yielded a higher value than the direct underground tests. An attempt by van der Merwe [1993] to explain the significantly higher rate of pillar collapse in the Vaal Basin yielded a constant for that area of 4.5 MPa, more similar to Bieniawski than to Salamon and Munro, but not directly comparable because it was valid for a defined geological district only.

In the process of analyzing coal pillar failures for other purposes, an alternative method of analysis was used that resulted in a formula that is 12.5% more effective in distinguishing between failed and stable pillars in the database. This paper describes the method of analysis and the results obtained.

REQUIREMENTS OF A SAFETY FACTOR FORMULA

A safety factor formula should satisfy two main requirements: (1) it should successfully distinguish between failed and stable pillars and (2) it should provide the means whereby relative stability can be judged. The third requirement, simplicity, has become less important with the widespread use of computers, but is still desirable.

These fundamental requirements are conceptually illustrated in figure 1. Figure 1A shows the frequency distributions of safety factors of the populations of failed and stable pillars,

respectively. The area of overlap between the populations can be seen as a measure of the success of the formula; the perfect formula will result in complete separation of the two populations. Figure 1B is a normalized cumulative frequency distribution of the safety factors of the failed cases plotted against safety factors. At a safety factor of 1.0, one-half of the pillars should have failed, or the midpoint of the distribution of failed pillars should coincide with a safety factor of 1.0.

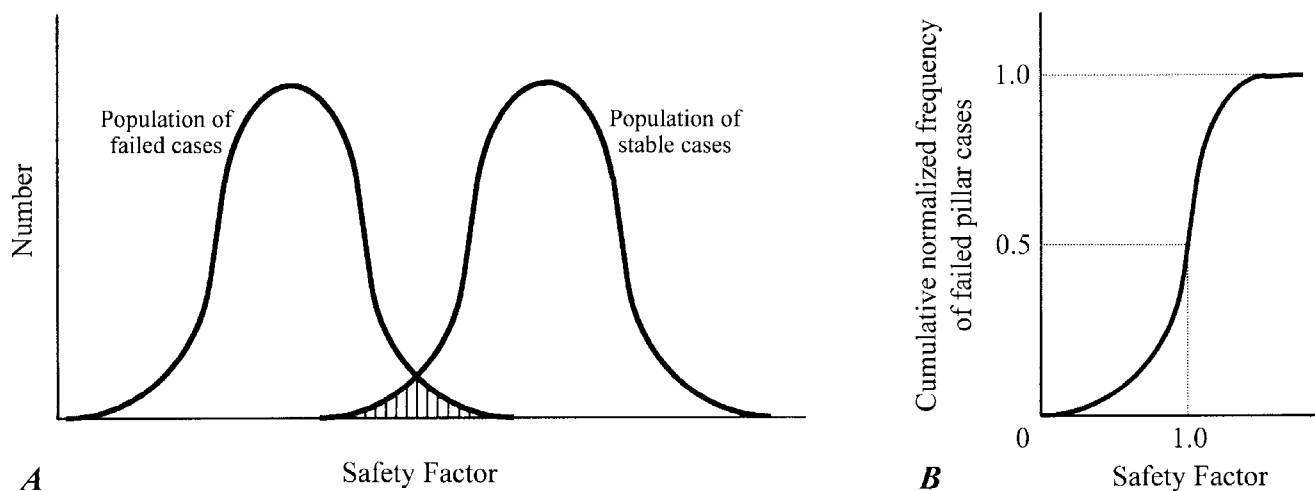


Figure 1.—Concept of the measure of success of a safety factor formula. *A*, The overlap area between the failed and stable cases should be a minimum. *B*, At a safety factor of 1.0, one-half of the pillars should have failed.

EXISTING FORMULAS IN SOUTH AFRICA

The safety factor is a ratio between pillar strength and pillar load. In its simplest form, the load is assumed to be the weight of the rock column overlying the pillar and the road around the pillar, i.e., the tributary area theory is normally used. This is widely held to be a conservative, and thus safe, assumption. However, it has at least one complication when this load is used to derive a safety factor empirically: if the load used to determine pillar strength is greater than the actual load, then the strength derived will also be greater than the actual pillar strength. If an alternative method is then used later to calculate pillar load, such as numerical modeling, and the strength is not modified, then the calculated safety factor will be greater than the real safety factor.

For purposes of this paper, the tributary area loading theory is used, and the restriction must then be added that the derived strength is only valid for situations where the tributary area load is used. This is not a unique restriction; even if not explicitly stated, it is also valid for any other empirical safety factor formula for which the tributary area loading assumption was used, such as the Salamon-Munro formula.

It then remains to determine a satisfactory formula for the calculation of pillar strength. The strength of a pillar is a function of the pillar dimensions, namely, width and height for a square pillar, and a constant that is related to the strength of the pillar material. According to Salamon and Munro [1967], the strength is

$$F = kw^a h^b, \quad (1)$$

where h = pillar height,

w = pillar width,

and k = constant related to material strength.

The parameters k , a , and b are interdependent. Salamon and Munro [1967] used the established greatest likelihood method to determine their values simultaneously and found:

$$k = 7.2 \text{ MPa},$$

$$a = 0.46,$$

$$\text{and } b = 0.66.$$

The linear formula of Bieniawski [1968] is

$$F = 4.3(0.64 + 0.36 w/h). \quad (2)$$

With the addition of new data on failures after 1966 to the Salamon and Munro database, Madden and Hardman [1992] found:

$$k = 5.24 \text{ MPa},$$

$$a = 0.63,$$

$$\text{and } b = 0.78.$$

These new values, however, did not result in sufficiently significant changes to safety factors to warrant changing the old formula, and they were not used by the industry. Note, however, the increases in values of a and b and reduction of k .

According to Madden [1991], the squat pillar formula, valid only for pillars with a $w/h > 5$, is

$$F = k \frac{R_0^b}{V^a} \left\{ \frac{b}{g} \left[\left(\frac{R}{R_0} \right)^g + 1 \right] \% 1 \right\}, \quad (3)$$

where R = pillar w/h ratio,

R_0 = pillar w/h ratio at which formula begins to be valid = 5.0,

and V = pillar volume.

Substituting $k = 7.2 \text{ MPa}$, $a = 0.0667$, $b = 0.5933$, $R_0 = 5.0$, and $g = 2.5$ results in a somewhat simplified form of the formula that is sometimes used:

$$F = \frac{0.0786}{V^{0.0667}} \{ R^{2.5} \% 181.6 \} \quad (4)$$

For quick calculations, equation 4 can be approximated with negligible error by

$$F = 0.0786 \frac{w^{2.366}}{h^{2.5667}} \% 9. \quad (5)$$

ALTERNATIVE METHOD OF ANALYSIS

Although μ , σ , and k are interdependent, they can be separated for purposes of analysis. It was found that changing μ and σ affected the overlap area of the populations of failed and stable pillars. Modifying k does not affect this relationship; it causes an equal shift toward higher or lower safety factors in both populations. Therefore, μ and σ can be modified independently to minimize the overlap area between the two populations; once that is done, k can be adjusted to shift the midpoint of the population of failed pillars to a safety factor of 1.0.

DETERMINATION OF μ AND σ

The data bank for failed pillars for the analysis described here was that quoted by Madden and Hardman [1992], which was the original Salamon and Munro data. The post-1966 failures were added to the data, and the three Vaal Basin failures were removed because the Vaal Basin should be treated as a separate group (see van der Merwe [1993]). (Note that a subsequent back-analysis indicated that the changes to the data bank did not meaningfully affect the outcome.)

For the first round of analysis, μ and σ were both varied between 0.3 and 1.2 with increments of 0.1. Safety factors were calculated for each case of failed and stable pillars. For each of the 100 sets of results, the area of overlap between the populations of failed and stable pillar populations was calculated. A standard procedure was used for this, taken from Harr [1987]. This involved the simplifying assumption that the distributions were both normal, but because it was only used for comparative purposes, the assumption is valid. Using the same procedure, the overlap area for the Salamon-Munro formula was also calculated. This was used as the basis from which an improvement factor was calculated for each of the new data sets.

The safety factor, S , was

$$S = \frac{\text{Strength}}{\text{Load}} \quad (6)$$

The tributary area theory was used to calculate the load:

$$\text{Load} = \frac{DgH(w\%B)^2}{w^2} \quad (7)$$

where H = mining depth,

w = pillar width,

and B = bord width.

Then, the strength was varied, as follows:

$$\text{Strength} = 7.2 \frac{w^\mu}{h^\sigma} \quad (8)$$

where w = pillar width,

h = pillar height,

μ = 0.3 to 1.2 with 0.1 increments,

and σ = 0.3 to 1.2 with 0.1 increments.

Equations 6 through 9 were applied to each of the cases of failed and stable populations, thus creating 100 sets of populations of safety factors of failed and stable cases. For each set, a comparative improvement factor was calculated. The first step was to calculate "f" for each of the 100 sets:

$$f = \frac{M_s \& M_f}{\sqrt{S_s^2 \& S_f^2}} \quad (9)$$

where M_s = mean safety factor of the population of stable pillars,

M_f = mean safety factor of the population of failed pillars,

S_s = standard deviation of the safety factors of the stable pillars,

and S_f = standard deviation of the safety factors of the failed pillars.

Then,

$$R = 0.5 \& \frac{1}{f} (2B)^{0.5} \exp\left(\frac{\&f^2}{2}\right) \quad (10)$$

and the overlap area between the two populations is

$$A = 0.5 \& R \quad (11)$$

Finally, the improvement factor, I , for each set is

$$I = \frac{A_s \& A_n}{A_c} \quad (12)$$

where A_s = overlap area with the original Salamon-Munro formula,

and A_n = overlap area with the new formula.

It was then possible to construct contours of the improvement factors for variations of α and β (figure 2). Figure 2 shows that the greatest improvement was for α between 0.7 and 0.8 and for β between 0.75 and 0.85. Fine tuning was then done by repeating the procedure with increments of 0.01 for α from 0.7 to 0.8 and for β between 0.75 and 0.85. The resulting contours are shown in figure 3.

On the basis of the contours of improvement factors in figure 3, it was concluded that for $\alpha = 0.81$ and $\beta = 0.76$, the improvement in efficiency of the formula to distinguish between failed and stable pillar cases is 12.5%.

DETERMINATION OF "k"

The last step was to determine k for the new exponents of α and β . This was done by adjusting k so that the midpoint of the population of failed pillars coincided with a safety factor of 1.0. It was found that a value of k = 4.0 MPa satisfied this condition; this is shown in figure 4.

FINAL NEW FORMULA

The full new formula for pillar strength in the Republic of South Africa is then as follows:

$$\text{Strength} = 4 \frac{W^{0.01}}{h^{0.76}} \tag{8}$$

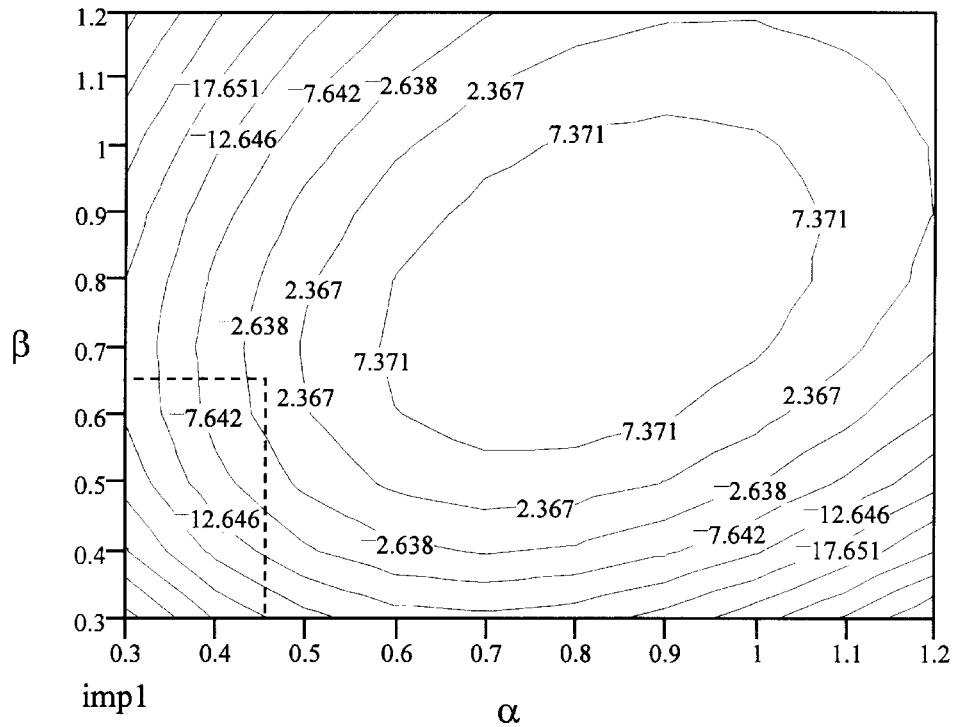


Figure 2.—Contour plot of percentage improvement in efficiency of formula to separate failed and stable pillar cases for variations of α between 0.3 and 1.2 and for β between 0.3 and 1.2. The Salamon and Munro [1967] combination is shown by the dotted lines.

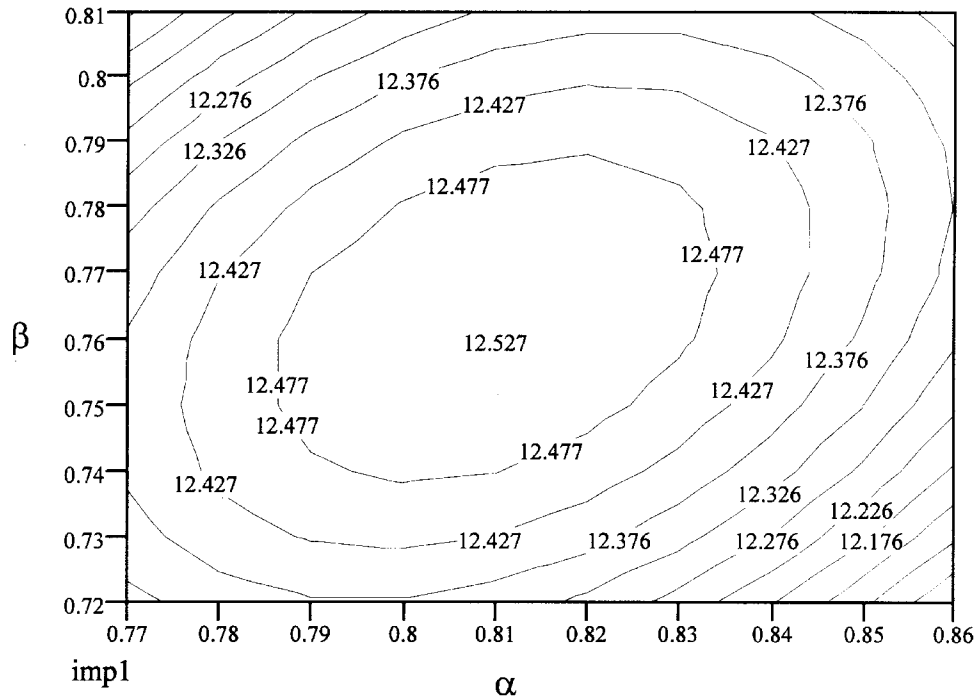


Figure 3.—Contour plot of percentage improvement in efficiency of formula to separate failed and stable pillar cases for variations of α between 0.77 and 0.86 and for β between 0.72 and 0.81.

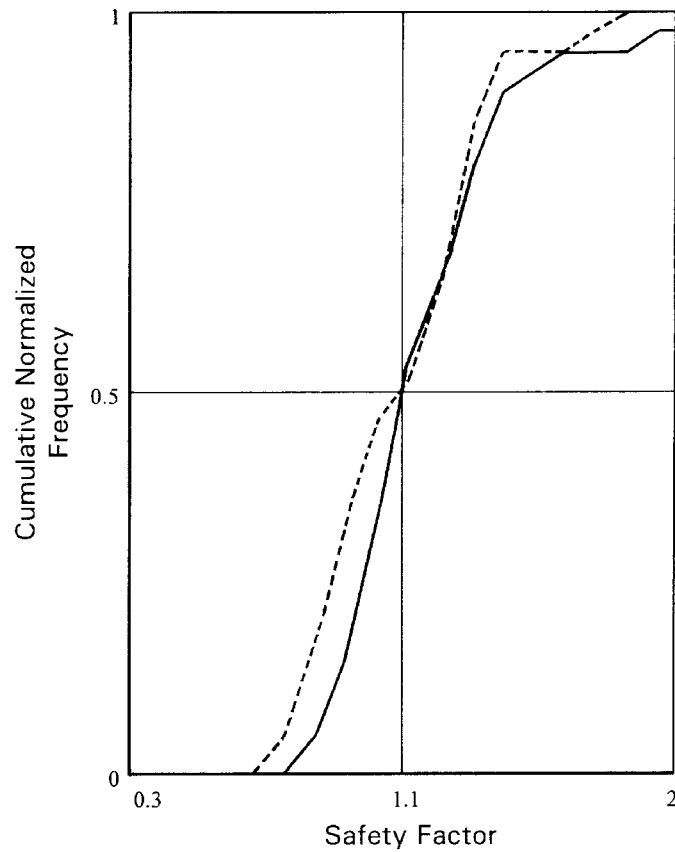


Figure 4.—Plot of cumulative normalized frequency against safety factors calculated with the Salamon-Munro formula (solid line) and the new formula (broken line). For the new formula, $k = 4$ MPa, $\alpha = 0.81$, and $\beta = 0.76$.

COMPARISON OF THE DIFFERENT FORMULAS

Again using the accepted Salamon-Munro formula as a basis, the formulas of Bieniawski [1968] and Madden and Hardman [1992] were also compared for relative changes in the overlap area of failed and stable pillar populations. The method used was the one described in the previous section. The relevant strength formulas were used in turn for the calculation of safety factors, and the overlap areas were calculated and compared with the original Salamon-Munro formula. The results are summarized below.

The table shows that the Bieniawski [1968] formula was only slightly less efficient than the Salamon-Munro formula; Madden and Hardman [1992] was slightly more efficient,

although the decision not to implement the latter was probably correct because the improvement is small. The formula derived in this paper, referred to in the table above as the "new formula," is, however, 12.5% more efficient, which is considered significant.

<i>Strength formula</i>	<i>Improvement factor, %</i>
<i>Bieniawski [1968]</i>	<i>&1.5</i>
<i>Madden and Hardman [1992] . .</i>	<i>% 2.3</i>
<i>New formula</i>	<i>%12.5</i>

DISCUSSION AND IMPLICATIONS FOR THE INDUSTRY

The new formula yields higher values of safety factors for most pillars than either of the formulas proposed previously for South African coals. The exceptions are the small pillars, such as those typically found at shallow depth. The new formula is more successful in explaining the "anomalous" pillar collapses of small pillars at shallow depth.

Figure 5 compares pillar strengths obtained with the various formulas for different w/h ratios of the pillars. Note that due to the different exponents of width and height, the relationships are ambiguous (except for the linear formula of Bieniawski [1968] and the Mark-Bieniawski formula described by Mark and Chase [1997]). For purposes of this comparison, the pillar heights were fixed at 3 m and the widths adjusted to obtain the different ratios.

An important feature of the comparison is the close correlation between the Mark-Bieniawski formula and the new formula. They were derived independently using different databases in different countries. Both predict stronger pillars for the same dimensions as the other formulas. The new

formula only deviates meaningfully from Mark-Bieniawski in the lower range of the w/h ratio, where it predicts weaker pillars. This is in accordance with observations where the failure of small pillars was previously regarded as anomalous.

The major implication for the coal mining industry is that higher coal extraction can be obtained without sacrificing stability. In effect, this is nothing more than a correction of the overdesign that has been implemented over the past decades. Figure 6 shows examples of the benefits with regard to the percentage extraction. The greater the depth and the higher the required safety factor, the greater the benefit.

As the new formula deals with underground pillar stability, it is inherently linked to the safety of underground mine personnel. In particular, it will enhance the stability of shallow workings, which has hitherto been a shortcoming of the Salamon-Munro formula. For deeper workings and for cases where surface structures are undermined, the new formula will enable mines to extract more coal without sacrificing stability.

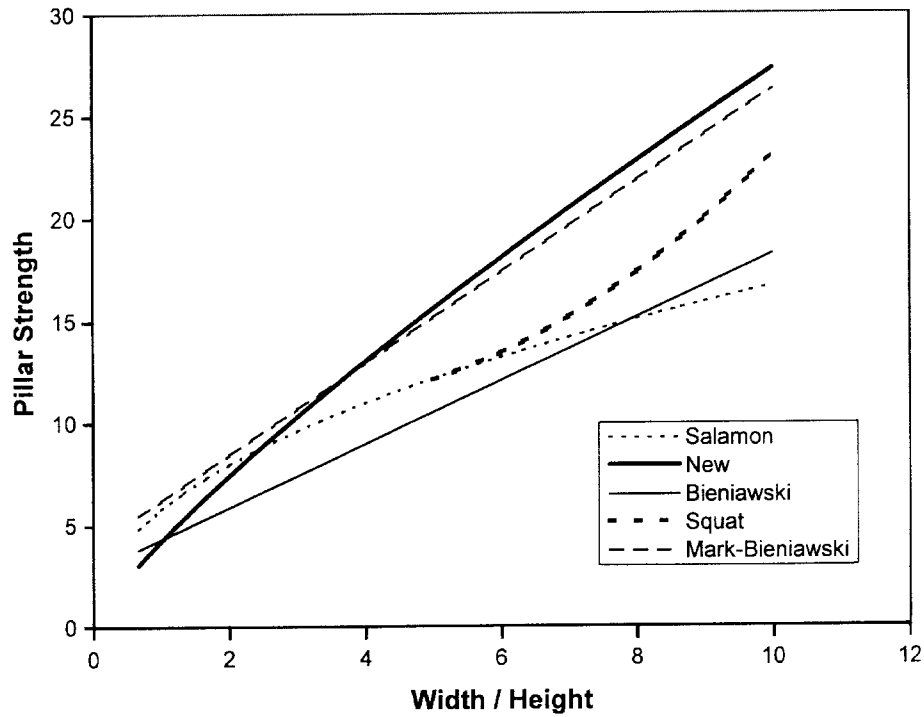


Figure 5.—Comparison of the strength increase with increasing width to height of pillars. The new formula results in higher strength values for most of the pillar sizes. This comparison is included for demonstration purposes only, because the relationship between width to height and pillar strength is ambiguous for all cases where the exponents of width and height are not equal. Note the similarity between the new formula and the Mark-Bieniawski formula.

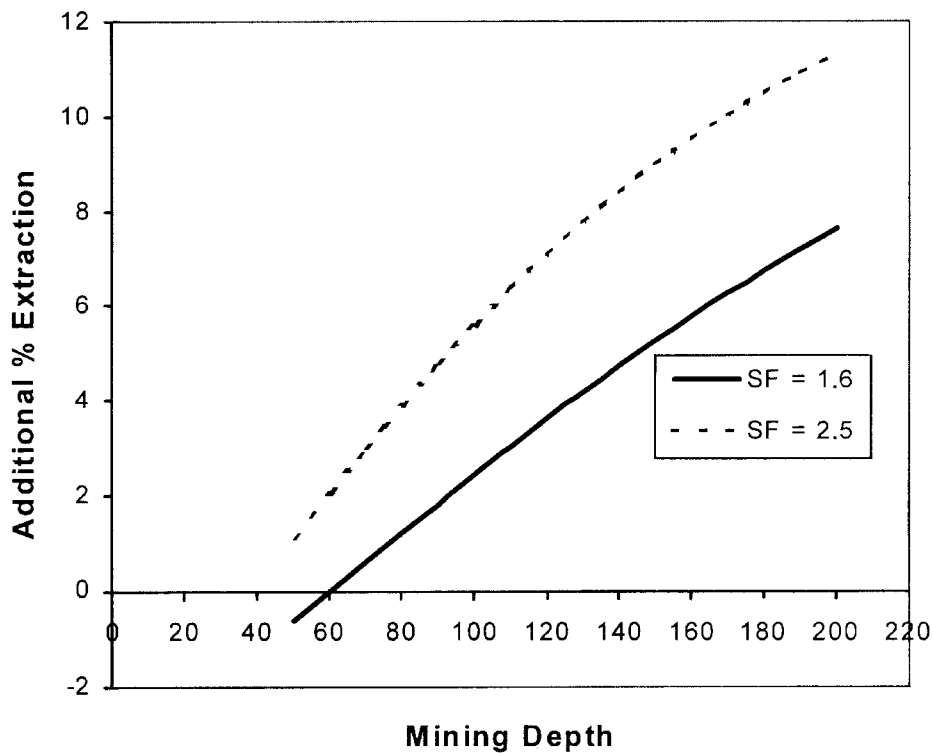


Figure 6.—Illustration of the benefit obtained by using the new formula. As the safety factors and depth of mining increase, more extraction can be obtained without sacrificing stability. For purposes of this comparison, the mining height was 3 m and the road width was 6.6 m.

ACKNOWLEDGMENTS

This work is part of a larger research project sponsored by Sasol Mining (Pty.) Ltd., whose support is gratefully acknowledged.

REFERENCES

- Bieniawski ZT [1968]. In situ strength and deformation characteristics of coal. *Eng Geol*, Vol. 2, pp. 325-340.
- Harr ME [1987]. Reliability-based design in civil engineering. McGraw-Hill Book Co., pp. 130-134.
- Madden BJ [1991]. A re-assessment of coal pillar design. *J S Afr Inst Min Metall* 91(1):27-37.
- Madden BJ, Hardman DR [1992]. Long-term stability of bord-and-pillar workings. In: Proceedings of the Symposium on Construction Over Mined Areas (Pretoria, Republic of South Africa, May 1992). Yeoville, Republic of South Africa: South African Institution of Civil Engineers.
- Mark C, Chase FE [1997]. Analysis of retreat mining pillar stability (ARMPS). In: Proceedings - New Technology for Ground Control in Retreat Mining. Pittsburgh, PA: U.S. Department of Health and Human Services, Public Health Service, Centers for Disease Control and Prevention, National Institute for Occupational Safety and Health, DHHS (NIOSH) Publication No. 97-122, IC 9446, pp. 17-34.
- Salamon MDG, Munro AH [1967]. A study of the strength of coal pillars. *J S Afr Inst Min Metall Sep*:55-67.
- Van der Merwe JN [1993]. Revised strength factor for coal in the Vaal Basin. *J S Afr Inst Min Metall* 93(3):71-77.

THE ROLE OF OVERBURDEN INTEGRITY IN PILLAR FAILURE

By J. Nielen van der Merwe, Ph.D.¹

ABSTRACT

The move toward partial pillar extraction versus full pillar extraction has necessitated a new approach to underground section stability. When pillars are mined too small to support the weight of the overburden, they will, in some cases, remain stable for a considerable period; in other cases, they will collapse unexpectedly and violently. There is no discernable difference between the pillar safety factors of the failed and stable cases. The explanation lies in the characteristics of the overburden layers.

A method is proposed that recognizes the overburden characteristics in the evaluation of stability. Two stability factors are calculated: one for the pillars, the other for the overburden. Using this method, it is possible to make use of the bridging capabilities of overburden layers to prevent pillar collapse. It is possible to scientifically design partial pillar extraction layouts that will be safe. Using energy considerations, it is also possible to prevent violent failure of pillars.

¹Managing director, Itasca Africa (Pty.) Ltd., Johannesburg, Republic of South Africa.

INTRODUCTION

In order for underground coal pillars to fail completely, two requirements must be met: (1) the pillars themselves must be loaded to beyond their load-bearing capacity, and (2) the overburden must deflect sufficiently to totally deform the pillars. In the consideration of pillar failure, the first requirement historically has received almost all of the attention; only scant mention is sometimes made of the role of the overburden.

Until recently, this has not been necessary. South African mining methods, longwalling apart, were either bord-and-pillar or pillar extraction methods with a number of variations. For bord-and-pillar, the pillars are sufficiently large to support the full weight of the overburden and the stiffness of the overburden is a bonus, merely decreasing the load on the pillars. In pillar extraction, the overburden usually fails completely, although there are situations where it is prone to be self-supporting for large enough distances to result in overloaded pillars and the well-known and understood negative consequences thereof.

Lately, however, there has been a move toward partial pillar extraction with a number of different names attached to the methods, like pillar robbing, pillar splitting, checkerboard extraction, etc. These methods all have in common the partial extraction of pillars, leaving self-supporting snooks (stubs) in the back area. They are usually larger than the ones left in normal stooping operations. These snooks are often stable for long

periods of time, even though their strengths are less than that required to support the full overburden. This in turn creates the impression that the pillars are much stronger than the prediction made with the strength formula.

There have also been occasions where the snooks failed after a period of time. The author has been involved in investigations into two of these. In both instances, the lack of serious accidents can only be ascribed to luck, both having occurred in the off-shift. In one case, ventilation stoppings were destroyed for a distance of several kilometers; in the other, the collapse overran unmined pillars and resulted in severe roof falls up to six lines of pillars beyond the end of the split pillars.

The difference between the cases that failed and those that remained stable is not to be found in the strengths of the pillars. The range of safety factors was from 0.5 to 0.7, and the stable ones were not the ones with the higher safety factors. The pillar safety factor alone does not explain stability in these marginal cases. There were, however, significant differences in the overburden composition and stability. The investigation indicated that in the stable cases, the overburden was strong enough to bridge the panels; in the failed cases, the overburdens failed. This resulted in the development of a concept that takes into account the overburden stability as well as pillar stability. This concept will be explained in this paper.

EFFECTS OF MINING ON THE OVERBURDEN

Mining results in increased loads on the unmined pillars. This causes the pillars to compress; the amount of compression is a function of the additional load on the pillars and the pillar's modulus of elasticity. The pillar compression is translated into deflection for the overburden. The higher the pillar loads, the greater the compression and the more the overburden will deflect. In the most simplistic view, coal mine overburdens can be regarded as a series of plates that can be conveniently simplified further to a series of beams in the general case where the panel lengths are several times greater than the panel widths.

The beam deflection results in induced tensile stress in the upper beam edges and the bottom center of the beam. The most simplistic view, adopted here as the starting point for the development of a more accurate model, is that the beam will fail when the induced tension exceeds the sum of the virgin horizontal stress and the tensile strength of the beam material.

However, it is well known that the overburden, consisting predominantly of sedimentary rock types often supplemented by a dolerite sill, is vertically jointed and therefore the tensile strength of the material can be ignored. Failure will thus occur when the induced tensile stress exceeds the virgin horizontal compressive stress.

The amount of deflection of any individual beam in the overburden is enhanced by the weight of the material on top of it and restricted by the resistance of the pillars underneath. There are no major differences in the moduli of the overburden rocks, dolerite sills apart, and the differential amounts of bending become a function of the thicknesses of the beams. In considering overburden stability, the identification of thick lithological units therefore is more important than the ratio of mining depth to panel width.

MATHEMATICAL RELATIONSHIP BETWEEN PILLAR LOAD AND OVERBURDEN DEFLECTION

The link between overburden deflection and pillar load is the pillar compression. The pillar cannot compress by a greater amount than the overburden deflection and vice versa. The maximum pillar deflection, δ , is

$$\delta = \frac{F}{E_c} h, \quad (1)$$

where h = pillar height,

F = load increase caused by mining,

and E_c = modulus of elasticity of coal.

The above is valid for the situation where the overburden is sufficiently soft not to restrict the compression of the pillars. There is general consensus that the modulus of elasticity of coal is around 4 GPa. However, the postfailure modulus is a

function of the pillar shape. According to data supplied by van Heerden [1975], the postfailure modulus, E_{cf} , appears to be²

$$E_{cf} = \frac{0.562w}{h} \approx 2.293. \quad (2)$$

Assuming tributary area loading conditions, the load increase on the pillars due to mining is

$$F_p = H \left(\frac{1}{1+e} + 1 \right), \quad (3)$$

where H = mining depth,

e = areal extraction ratio,

and C = Dg.

RELATIONSHIP BETWEEN PILLAR DEFLECTION AND INDUCED TENSION IN OVERBURDEN BEAM

The generic equation for beam deflection is

$$\delta = \frac{C_r L^4}{32E_r t^3}, \quad (4)$$

where L = panel width,

E_r = modulus of elasticity of the rock layer,

t = thickness of the rock layer,

and C_r = unit load on the rock layer.

The generic expression for the maximum generated tensile stress is

$$F_t = \frac{C_r L^2}{2t^2}. \quad (5)$$

By substituting δ by δ , the tension induced by bending can also be expressed in terms of the deflection, as follows:

$$F_t = \frac{16t}{L^2} h E_r \quad (6)$$

This is the tensile stress that will be generated in the overburden beam if the restriction to deflection is the resistance offered by the pillars underneath. It is also the upper limit of the generated tension because the resistance offered by the pillars will not allow further deflection. However, the overburden has inherent stiffness that will also restrict deflection. The maximum deflection that an unsupported beam will undergo is indicated by equation 4.

If F_t from equation 4 is greater than δ from equation 1, it means that the overburden is dependent on the pillars to restrict deflection and that the tensile stress generated in the beam is that found with equation 6. If δ is greater than F_t , it means that the beam is sufficiently stiff to control its own deflection and that the tension generated in the beam is that found with equation 5.

² Author's own linear fit to van Heerden's data.

OVERBURDEN FAILURE

The overburden beams will fail if the induced tension exceeds the virgin horizontal compression; this is conveniently expressed in terms of the vertical stress as

$$F_h = kF_v, \tag{7}$$

or

$$F_h = k(HH), \tag{8}$$

where HH is the depth at which the rock layer under consideration is located, not the depth of mining.

Next, define the overburden stability ratio (OSR) as

$$OSR = \frac{F_h}{F_t}. \tag{9}$$

PILLAR STABILITY

Pillar stability is evaluated by comparing pillar strength to pillar load; thus:

$$PSF = \frac{\text{Strength}}{\text{Load}} \tag{10}$$

The pillar load is conservatively estimated from the tributary area loading assumption as follows:

$$\text{Load} = \frac{DgH}{1 \& e}, \tag{11}$$

and the strength for South African pillars is [van der Merwe 1999]:

$$\text{Strength} = 4 \frac{w^{0.81}}{h^{0.76}}. \tag{12}$$

OVERALL STABILITY EVALUATION

To evaluate the overall stability of a coal mine panel, it is necessary to consider both the overburden and the pillar stability. This can be done by viewing the two stability parameters—the pillar safety factor (PSF) and the overburden stability ratio (OSR)—separately, or better, by plotting the two onto a plane. The concept is illustrated in figure 1.

The quadrants in figure 1 have different meanings for the stability evaluation. In quadrant I, both the overburden and the pillars are stable. This is the ideal situation for main development.

In quadrant II, the overburden is stable, although the pillars are unable to support the full weight of the overburden. This is potentially the most dangerous situation because there could be a false impression of stability when the OSR is not much greater than 1.0. The pillars will be stable for as long as the overburden remains intact; however, the moment that the overburden fails, the pillars will also fail. This may occur because of time-related strength decay of the stressed overburden or when mining progresses into an area with an unfavorably oriented unseen joint set in the overburden. The closer the OSR is to 1.0, the more dangerous the situation.

Quadrant III indicates a situation where both the pillars and the overburden will fail. This is again the ideal situation for the snooks in pillar extraction. One wants both to fail in this situation.

Quadrant IV indicates that the pillars are able to support the overburden, even though the overburden may fail. This is also a safe situation, although gradual failure may occur over a long period as the pillars lose strength.

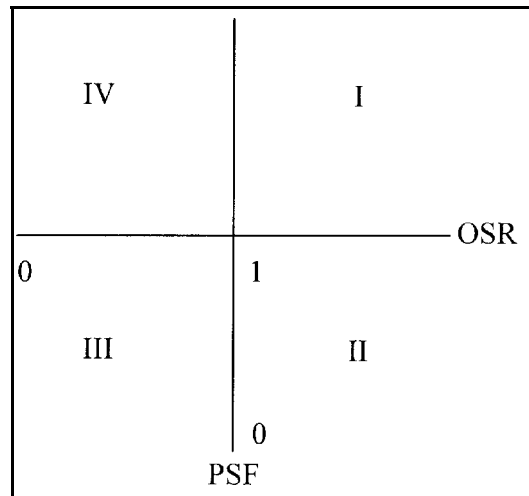


Figure 1.—Plot of OSR and PSF. Values of <1.0 for either indicate imminent instability.

PRACTICAL EXAMPLE

The following practical example is provided to indicate how the OSR/PSF procedure is applied in practice.

The mining depth is 143 m. The overburden consists of alternating layers of sandstones and shales. From the surface down, their thicknesses are as follows: 10, 5, 10, 20, 10, 50, 10, 10, 5, and 10 m. The mining height is 3 m; pillars are initially 18 m wide, and the roads are 6 m wide. The k-ratio is 2.0. The PSF is then 2.7, shown as point A in figure 2.

Pillars are then split by a 6-m-wide cut through the center, leaving remnants of 18 by 6 m, with an equivalent width (see Wagner [1980]) of 8 m. One line of pillars is left intact on either side of the panel, resulting in a width over which the pillars are split of 102 m. The PSF now decreases to 0.8. The OSR is calculated for each of the strata layers individually (see results in table 1).

It is seen from table 1 that because the pillars are beyond their failure limit, the overburden behavior is governed by the beam characteristics. Except for unit 6, all of the units will fail. Unit 6, however, is close to not failing and will probably be self-supporting for a short while. This combination of OSR and PSF is indicated by point B in figure 2.

During the time when they have not yet failed, it is probable that the pillars will have a stable visual appearance. Load cannot be seen. One's perception of pillar load is determined by the observed effects that accompany pillar compression, like slabbing. In this case, the pillar compression will be the greater of the deflection of unit 6 or the compression caused by the weight of the rock layers underneath unit 6. The deflection of unit 6 is 4 mm, and the compression of the pillars due to the weight of the strata underneath unit 6 is less than 2 mm. With the 4-mm compression of the pillars, the strain is 0.0013, which corresponds to a pillar load of 5.3 MPa. The strength of the snook is 8.4 MPa; the apparent safety factor is 1.6, and it will have the visual appearance of a stable pillar. However, the situation will change dramatically as soon as the overburden fails. At that moment, the pillars will be loaded by the full overburden weight. The safety factor will immediately decrease to 0.8.

Table 1.—OSR for the different strata layers with split pillars, panel width of 102 m

Unit No.	Thickness, m	0)h	OSR
1	10	0.028	31.5	0.038
2	5	0.564	31.5	0.01
3	10	0.113	31.5	0.038
4	20	0.025	31.5	0.154
5	10	0.282	31.5	0.038
6	50	0.004	31.5	0.961
7	10	0.62	31.5	0.038
8	10	0.677	31.5	0.038
9	5	5.75	31.5	0.01
10	10	0.761	31.5	0.038

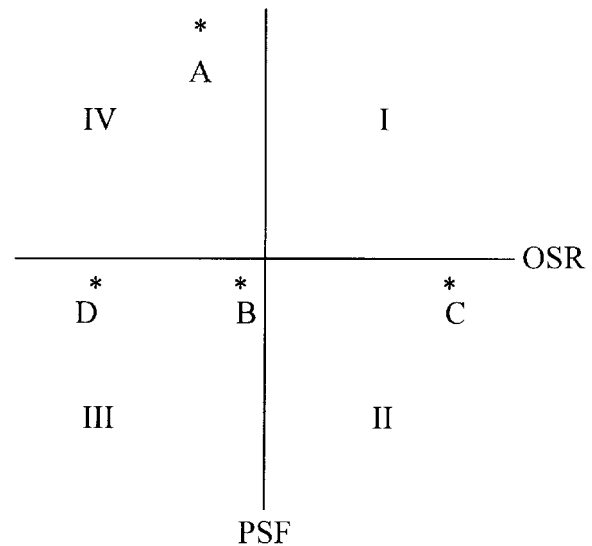


Figure 2.—OSR/PSF plot of the different options discussed in the example.

MODE OF FAILURE

Energy considerations indicate that failure will be violent if the stiffness of the pillars is less than that of the loading mechanism, which is the overburden. When the overburden fails, it loses continuity and, consequently, all stiffness as well. The stiffness of the loading mechanism is then 0. Therefore, the only way in which failure can be nonviolent in the situation where the overburden fails is where the pillars have a positive postfailure modulus. According to equation 2, this happens when the width-to-height (w/h) ratio of the pillars exceeds 4.08.

The w/h ratio of the pillars in this case is only 2.3; consequently, the failure will be violent, similar to what has been experienced on more than one occasion. This is similar to a conclusion reached by Chase et al. [1994], who analyzed pillar failures in the United States and found that massive collapses occurred where the w/h ratios of the pillars were less than 3. They also concluded that those collapses occurred where the overburden was able to bridge the excavation for a considerable distance before failure occurred.

The postfailure stiffness of coal with increasing w/h ratio of the pillars increases approximately linearly. There is thus no sudden distinction between what could be termed "violent" and "nonviolent" failure; rather, the relative degree of violence decreases with increasing w/h. It is suggested that the degree of violence be indicated by an index based on the magnitude of the postfailure stiffness of the coal, E_{cf} . It could be defined as follows:

$$I_v = 1 + \frac{E_{cf}}{4} \tag{13}$$

With the limited information at hand, mainly that of Chase et al. [1994], it appears that if $I_v > 1.15$, the failure may result in a dangerous situation. This obviously also depends on the area involved.

By substituting equation 2 into equation 13, the relative degree of violence may be expressed in terms of the w/h ratio as follows:

$$I_v \approx 1.57 \sqrt{0.14 w/h} \quad (14)$$

CONTROL MEASURES

There are a number of ways in which pillar splitting situations can be controlled using the OSR/PSF. One is to limit the width over which the pillars are split. For instance, if the width in the example is limited to 78 m (i.e., by splitting only three lines of pillars), the OSR of unit 6 increases to 1.6 and

there is a much higher probability that the unit will remain to be self-supporting, if only for a longer time. Note that when this is done, the PSF is not affected; it remains at a value of 0.8. This situation is indicated by point C in figure 2. This corresponds to other situations that have been observed, i.e., where split pillars with low apparent safety factors remain stable for considerable periods of time.

A second alternative is to do full extraction of every second pillar on a checkerboard pattern, leaving the alternating pillars intact. When this is done, the PSF decreases to 0.7. The OSR of the strongest unit, No. 6, is 0.3, indicating failure of the overburden. This is shown as point D in figure 2. However, the w/h ratio of the pillars is 6.0, which means that the pillars will not fail violently. The attraction of this option is that 50% of all of the coal contained in pillars is extracted, as opposed to 17% using the method in the previous paragraph.

INFLUENCE OF GEOLOGY

A cautionary note must be expressed at this point. The process of pillar failure for low safety factor pillars is driven by the overburden characteristics. It is thus very important to have detailed knowledge of the overburden composition. For instance, if the thickness of unit 6 in the example is 40 m instead of 50 m, then the control measure to restrict the number of pillars to be split to 78 m will not be effective; the OSR in that case will be 1.0, which places it back into the category with the highest uncertainty. The example in the previous section is nothing more than an example to illustrate the application of the method: it is not to be viewed as a guideline for panel widths, etc.

The full application of the method will require the establishment of guidelines for limit values of OSR and PSF. It seems reasonable to assume that there will be an area in the center of the plot shown in figure 1 that is to be avoided—the area of highest uncertainty, where the values of OSR and PSF are close to 1.0. Those limits need to be established; the best way of doing that will probably be through back-analysis in areas where there are examples of failed and stable cases for different periods of time.

CONCLUSIONS

- For underground workings to collapse, both the pillars and the overburden must fail. The model described here, simplified as it is, offers a method to evaluate the stability of pillar workings with low pillar safety factors by adding an evaluation of overburden stability to the evaluation of pillar stability.
- Even if the pillars are not strong enough to support the overburden, it is possible to prevent collapse by limiting the panel width, thereby allowing the overburden to be self-supporting.
- Refinement of the model will enable the scientific design of alternatives to full pillar extraction, avoiding the situation

where apparent stability caused by temporary bridging of the overburden leads to a false sense of security, only to be followed by catastrophic collapse.

- Quantification of the energy considerations can be done, leading to a design that will result in nonviolent failure of pillars.

- These conclusions are broadly similar to those reached by Chase et al. [1994]. The main difference is that this work offers a simple method of classifying the likelihood of failure occurring and the mode of failure should it occur.

ACKNOWLEDGMENTS

This work is part of a larger research project sponsored by Sasol Mining (Pty.) Ltd., whose support is gratefully acknowledged.

REFERENCES

Chase FE, Zipf RK Jr., Mark C [1994]. The massive collapse of coal pillars: case histories from the United States. In: Peng SS, ed. Proceedings of the 13th International Conference on Ground Control in Mining. Morgantown, WV: West Virginia University, pp. 69-80.

Van der Merwe JN [1999]. New strength formula for coal pillars in South Africa. In: Proceedings of the Second International Workshop on Coal Pillar Mechanics and Design. Pittsburgh, PA: U.S. Department of Health and

Human Services, Public Health Service, Centers for Disease Control and Prevention, National Institute for Occupational Safety and Health, DHHS (NIOSH) Publication No. 99-114, IC 9448.

Van Heerden WL [1975]. In situ determination of complete stress-strain characteristics of large coal specimens. *J S Afr Inst Min Metall* 75(8):207-217.

Wagner H [1980]. Pillar design in coal mines. *J S Afr Inst Min Metall* 80:37-45.

USING A POSTFAILURE STABILITY CRITERION IN PILLAR DESIGN

By R. Karl Zipf, Jr., Ph.D.¹

ABSTRACT

Use of Salamon's stability criterion in underground mine design can prevent the occurrence of catastrophic domino-type pillar failure. Evaluating the criterion requires computation of the local mine stiffness and knowledge of the postfailure behavior of pillars. This paper summarizes the status of the practical use of this important criterion and suggests important research to improve our capabilities.

Analytical and numerical methods are used to compute the local mine stiffness. Work to date in computing local mine stiffness relies mainly on elastic continuum models. Further work might investigate local mine stiffness in a discontinuous rock mass using alternative numerical methods.

Existing postfailure data for coal pillars are summarized, and a simple relationship for determining the postfailure modulus and stiffness of coal pillars is proposed. Little actual postfailure data for noncoal pillars are available; however, numerical models can provide an estimate of postfailure stiffness. Important factors controlling postfailure stiffness of rock pillars include the postfailure modulus of the material, end conditions, and width-to-height ratio.

Studies show that the nature of the failure process after strength is exceeded can be predicted with numerical models using Salamon's stability criterion; therefore, a method exists to decrease the risk of this type of catastrophic failure. However, the general lack of good data on the postfailure behavior of actual mine pillars is a major obstacle. Additional back-analyses of failed and stable case histories in conjunction with laboratory testing and numerical modeling are essential to improve our ability to apply the stability criterion.

¹Assistant professor, Department of Mining Engineering, University of Missouri-Rolla.

INTRODUCTION

As first noted by Cook and Hojem [1966], whether a test specimen in the laboratory explodes violently or crushes benignly depends on the stiffness of the testing system relative to the postfailure stiffness of the specimen. Full-scale pillars in mines behave similarly. Salamon [1970] developed the local mine stiffness stability criterion, which formalizes mathematically laboratory and field observations of pillar behavior in the postfailure condition. Although we understand the principles well, little is known by direct observation or back-calculation about the postfailure behavior of actual mine pillars.

The local mine stiffness stability criterion governs the mechanics of cascading pillar failure (CPF) [Swanson and Boler 1995], also known as progressive pillar failure, massive roof collapse, domino-type pillar failure, or pillar run. In this type of failure, when one pillar collapses, the load it carries transfers rapidly to its neighbors, causing them to fail and so forth. This failure mechanism can lead to the rapid collapse of very large mine areas. In mild cases, only a few tens of pillars fail; in extreme cases, hundreds, even thousands of pillars can fail.

Recent work by Chase et al. [1994] and by Zipf and Mark [1997] document 13 case histories of this failure mechanism in coal mines and 6 case histories in metal/nonmetal mines within the United States. Further work by Zipf [in press] has analyzed additional examples of this failure mechanism in the catastrophic collapse of web pillars in highwall mining operations. Reports by Swanson and Boler [1995], Ferriter et al. [1996], and Zipf and Swanson [in press] document the events and present analyses of the partial collapse at a trona mine in southwestern Wyoming, where one of the largest examples of this failure mechanism occurred.

Numerous instances of CPF have occurred in other parts of the world. The most infamous case is the Coalbrook disaster in the Republic of South Africa in which 437 miners perished when 2 km² of the mine collapsed within a few minutes on January 21, 1960 [Bryan et al. 1966]. Other instances occurred

recently at a coal mine in Russia and a large potash mine in Germany.

These collapses draw public interest for two reasons. First and foremost, a collapse presents an extreme safety hazard to miners. Obviously, the collapse area itself is the greatest hazard, but the collapse usually induces a devastating airblast due to displacement of air from the collapse area. An airblast can totally disrupt a mine's ventilation system by destroying ventilation stoppings, seals, and fan housings. Flying debris can seriously injure or kill mining personnel. The failure usually fractures a large volume of rock in the pillars and immediate roof and floor. In coal and certain other mines, this sudden rock fragmentation can release a substantial quantity of methane into the mine atmosphere that could result in an explosion.

Secondly, large mine collapses emit substantial seismic energy indicative of an implosional failure mechanism. For example, the seismic event associated with the collapse in southwestern Wyoming had a local magnitude of 5.3 [Swanson and Boler 1995]. Strong seismic signals of this type receive scrutiny from the international community because of U.S. obligations under the Comprehensive Test Ban Treaty (CTBT). Large collapses may initiate questions from the Federal Government and could result in further questions from other nations participating in the CTBT [Casey 1998; Heuze 1996].

The pillar failure mechanism considered in this paper (CPF or domino-type pillar failure) should not be confused with coal mine bumps and rock bursts, although both failure types are frequently associated with large seismic energy releases. Although the damage can seem similar, the underlying mechanics are completely different. The mechanism of pillar collapse largely depends on vertical stress and the postfailure properties of pillars. The mechanism for coal mine bumps and rock bursts is more complex. In these events, larger failures (seismic events) in the surrounding rock mass induce severe damage in susceptible mine workings.

LOCAL MINE STIFFNESS STABILITY CRITERION

When the applied stress on a pillar equals its strength, then the "safety factor" defined as the ratio strength over stress equals 1. Beyond peak strength when the strength criterion is exceeded, the pillar enters the postfailure regime, and the failure process is either stable or unstable. In this paper, *stability* refers

to the nature of the failure process after pillar strength is exceeded. Based on the analogy between laboratory test specimens and mine pillars, Salamon [1970] developed a criterion to predict stable or unstable failure of mine pillars. Figure 1 illustrates this well-known criterion.

Stable, nonviolent failure occurs when

$$|K_{LMS}| > |K_p|$$

and unstable, violent failure occurs when

$$|K_{LMS}| < |K_p|,$$

where $|K_{LMS}|$ is the absolute value of the local mine stiffness and $|K_p|$ is the absolute value of the postfailure stiffness at any point along the load convergence curve for a pillar. As long as this criterion is satisfied, CPF (domino-type pillar failure) cannot occur; however, when the criterion is violated, then unstable failure is possible.

Salamon's local mine stiffness stability criterion does not include the time variable and thus does not predict the rapidity of an unstable failure should it occur. CPF resides at the far end of the unstable pillar failure spectrum. At the other end are slow "squeezes" that develop over days or weeks. Workers and machinery have ample time to get out of the way of the failure. In a CPF, the failure is so rapid that workers and machinery cannot evacuate in time. Both CPF and squeezes violate a strength criterion and, somewhat later, the stability criterion; thus, unstable pillar failure can proceed. The rapidity of a failure may depend on the degree to which the local mine stiffness stability criterion is violated, i.e., the magnitude of the difference between K_{LMS} and K_p , as shown in figure 2.

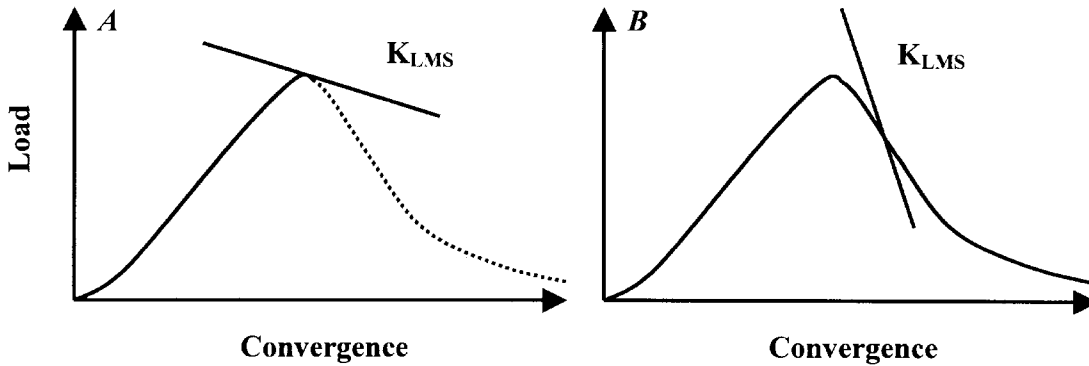


Figure 1.—Unstable, violent failure versus stable, nonviolent failure. Loading machine stiffness or local mine stiffness is represented by the downward sloping line intersecting the pillar load convergence (stress-strain) curve. *A*, Loading machine stiffness less than postfailure stiffness in a "soft" loading system. *B*, Loading machine stiffness greater than postfailure stiffness in a "stiff" loading system.

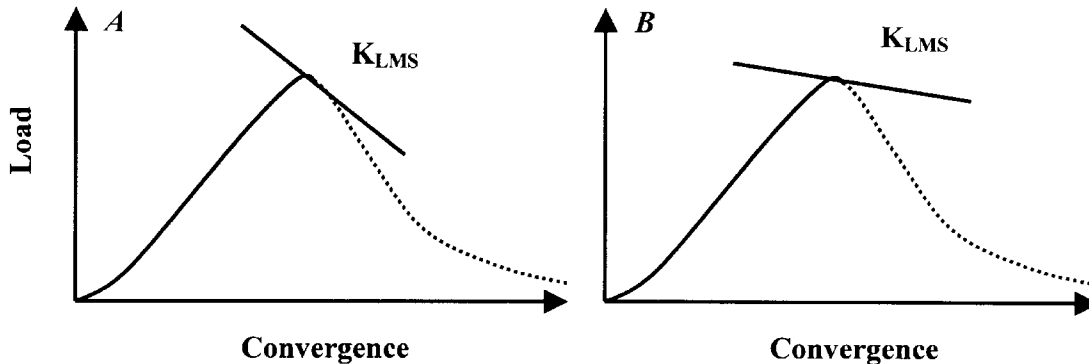


Figure 2.—Both cases violate the local mine stiffness stability criterion, i.e., $*K_{LMS}^* < *K_p^*$. *A*, Slow squeeze results when $*K_{LMS}^* < *K_p^*$. *B*, Rapid CPF results when $*K_{LMS}^* \ll *K_p^*$.

COMPUTING LOCAL MINE STIFFNESS

The local mine stiffness K_{LMS} relates deformation in the rock mass to changes in force on the rock mass. Force changes occur as stresses in the mined-out rock go from in situ values to zero as a result of mining. Deformations then occur in the rock mass. If a given amount of mining (and force change) results in small deformations, the system is "stiff"; if the resulting deformations are large, the system is "soft." The magnitude of the local mine stiffness depends in part on the modulus of the rock mass and in part on the geometry of the mining excavations. In general, the more rock that is mined out, the softer the system. Obtaining direct measurements of the local mine stiffness is generally not possible, since it is more of a mathematical entity than a measurable quantity for a rock mass. Numerical or analytical methods are employed to evaluate it for use in the stability criterion.

Figure 3 illustrates the behavior of the local mine stiffness for different mine layouts. This hypothetical example consists of an array of long narrow openings separated by similar pillars. An opening width to pillar width of 3 is assumed, implying 75% extraction. As the number of pillars increases from 3 to 15, stress concentration on the central pillar approaches its theoretical maximum of 4, and the local mine stiffness decreases as the panel widens. Local mine stiffness decreases as the extraction ratio increases. At sufficient panel width and high enough extraction, local mine stiffness decreases to zero, which is the worst possible condition for failure stability since it corresponds to pure dead-weight loading. If failure occurs, its nature is unstable and possibly violent.

An expression for local mine stiffness is

$$K_{LMS} = \frac{\Delta P}{\Delta D} = \frac{(S_u \& S_p)A}{D_u \& D_p}$$

where ΔP = change in force,

ΔD = change in displacement,

S_u = unperturbed stress,

S_p = perturbed stress,

D_u = unperturbed displacements,

D_p = perturbed displacements,

and A = element area.

This expression is easily implemented into boundary-element programs such as MULSIM/NL [Zipf 1992a,b; 1996], LAMODEL [Heasley 1997, 1998], and similar programs. Changes in stress and displacement are noted between adjacent mining steps, i.e., the "unperturbed" and "perturbed" state. By way of example, to compute the local mine stiffness associated with a pillar, first stresses and displacements are calculated at each element in the model in the usual way, giving the so-called unperturbed stresses and displacements. The pillar is then removed and all of the stresses and displacements are recomputed, giving the so-called perturbed stresses and displacements. In this case, S_p is identically zero. Local mine stiffness K_{LMS} is then calculated with the expression above.

Other numerical models can also be used to calculate K_{LMS} . Recent studies of web pillar collapses in highwall mining systems [Zipf, in press] used FLAC² to calculate local mine stiffness. Two-dimensional models of the web pillar geometry were used for the initial stress and displacement calculations. All elements comprising one pillar were removed, and stresses and displacements were recomputed. S_p is identically zero at the mined-out pillar. Local mine stiffness for the pillar is then evaluated for the pillar. When using FLAC, a simple FISH function can be constructed to facilitate the numerical computations.

²Fast Lagrangian Analysis of Continuum, Itasca Corp., Minneapolis, MN.

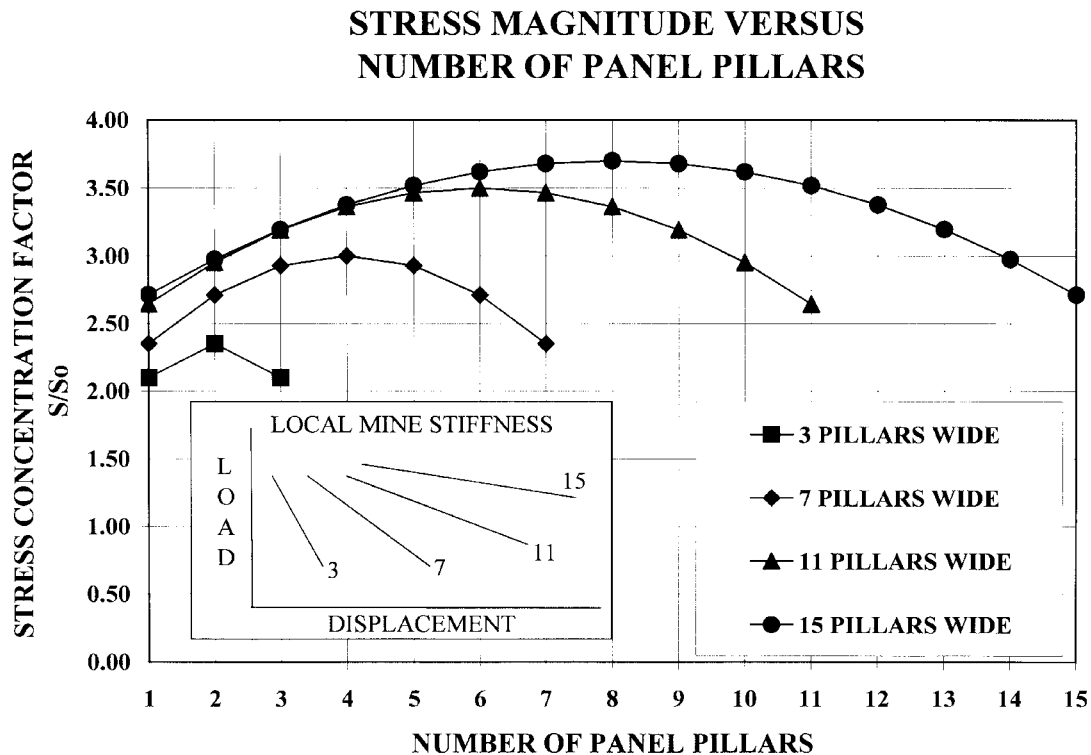


Figure 3.—Stress concentration factor versus number of panel pillars showing behavior of local mine stiffness as panel width increases.

POSTFAILURE STIFFNESS OF COAL PILLARS

In addition to the local mine stiffness parameter, Salamon's stability criterion also depends on the postfailure pillar stiffness, K_p , which is the tangent to the downward sloping portion of the complete load-deformation curves shown in figure 1. Jaeger and Cook [1979] discuss the many variables that affect the shape of the load convergence curve for a laboratory specimen, such as confining pressure, temperature, and loading rate. For many mining engineering problems of practical interest, the width-to-height (w/h) ratio of the test specimen is of primary interest. Figure 4 from Das [1986] shows how the magnitude of peak strength, slope of the postfailure portion of the stress-strain curve, and magnitude of the residual strength changes as w/h increases for tests on Indian coal specimens. Seedsman and Hornby [1991] obtained similar results for Australian coal specimens. Peak strength increases with w/h , and various well-known empirical coal strength formulas reflect this behavior

[Mark and Iannacchione 1992]. At low w/h , the postfailure portion of the stress-strain curve slopes downward, and the specimen exhibits strain-softening behavior. Postfailure modulus increases with w/h ; at a ratio of about 8, it is zero, which means that the specimen exhibits elastic-plastic behavior. Beyond a w/h of about 8, the postfailure modulus is positive and the specimen exhibits strain-hardening behavior.

Full-scale coal pillars behave similarly to laboratory test specimens; however, few studies have actually measured the complete stress-strain curve for pillars over a wide range of w/h . Wagner [1974], Bieniawski and Vogler [1970], and van Heerden [1975] conducted tests in the Republic of South Africa. Skelly et al. [1977] and more recently Maleki [1992] provide limited data for U.S. coal. Figure 5 summarizes the measurements of postfailure modulus for the full-scale coal pillars discussed above. The laboratory data shown in figure 4

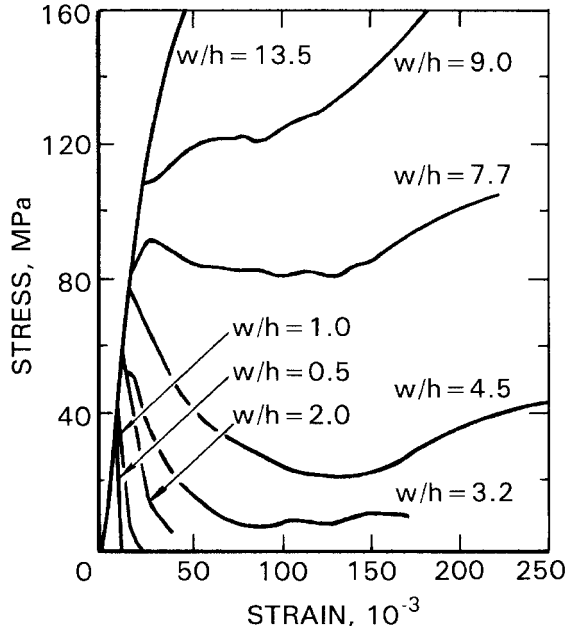


Figure 4.—Complete stress-strain curves for Indian coal specimens showing increasing residual strength and postfailure modulus with increasing w/h (after Das [1986]).

and the field data exhibit an upward trend as w/h increases, although the laboratory data show better definition. The laboratory postfailure modulus becomes positive at a w/h ratio of about 8, whereas the pillar data become positive at about 4.

Based on these field data, an approximate relationship for postfailure modulus of full-scale coal pillars is proposed as

$$E_p \text{ (MPa)} \approx 1,750 (w/h)^{0.1} + 437.$$

Assuming a unit width for the pillar, the postfailure stiffness is related to the postfailure modulus as

$$K_p = E_p (w/h)$$

or

$$K_p \text{ (MN/m)} \approx 1,750 + 437 (w/h).$$

As shown in figure 5, the simple relation for E_p decreases monotonically and becomes positive at a w/h of 4. The proposed relationship is not based on rigorous regression analysis. It is a simple, easy-to-remember equation that fits the general trend of the data.

POSTFAILURE MODULUS VERSUS PILLAR WIDTH-TO-HEIGHT RATIO

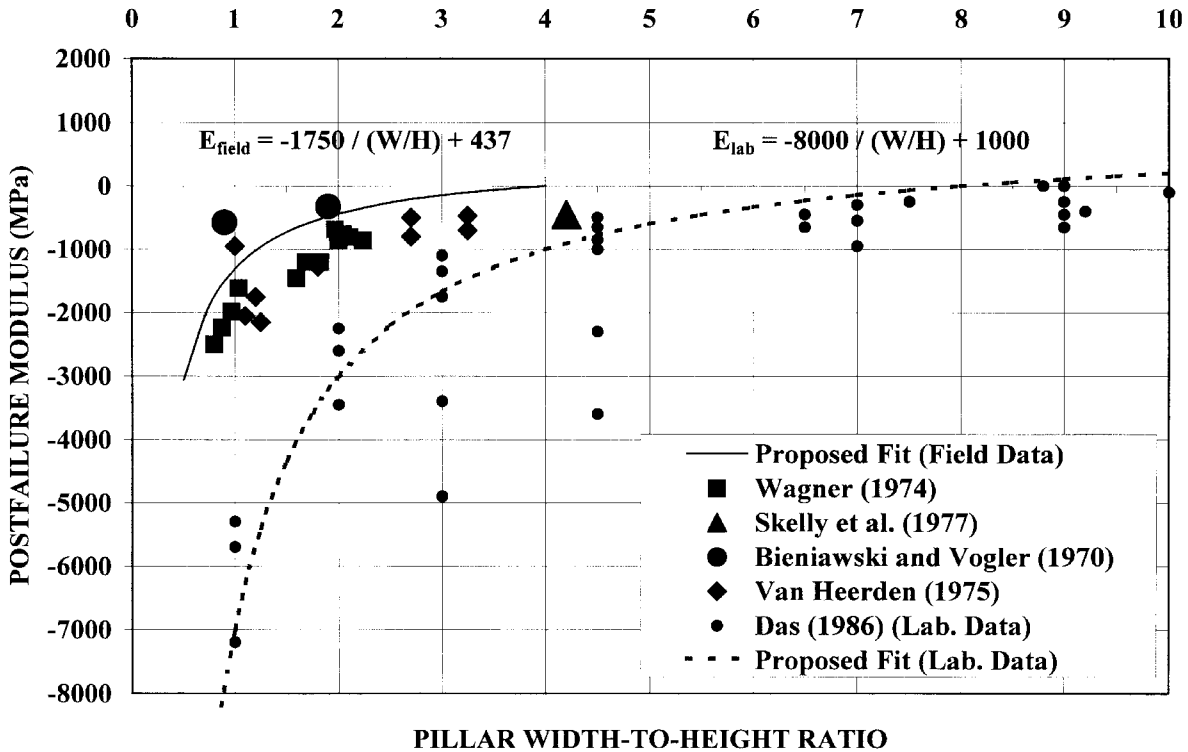


Figure 5.—Summary of postfailure modulus data for full-scale coal pillars and laboratory specimens. Also shown is proposed approximate equation for E_p .

POSTFAILURE STIFFNESS OF METAL/NONMETAL PILLARS

In comparison to coal, very little data exist for the postfailure behavior of pillars in various metal/nonmetal mines. Direct measurements of the complete stress-strain behavior of actual pillars are difficult, very expensive to conduct, and often simply not practical. Laboratory tests on specimens with various w/h can provide many useful insights similar to the coal data shown previously. Numerical methods seem to be the only recourse to estimate the complete load-deformation behavior of full-scale pillars where real data are still lacking. Work by Iannacchione [1990] in coal pillars and Ferriter et al. [1996] in trona pillars provides examples of numerical approaches to estimating K_p .

Ferriter et al. [1996] used FLAC to calculate the complete load-deformation behavior of the pillar-floor system in a trona mine. The objective for this modeling effort was to estimate postfailure stiffness of the pillar-floor system for a variety of pillar w/h ratios. Figure 6 shows the basic models considered. Each contained the same sequence of strong shale, trona, oil shale, and weak mudstone. A strain-softening material model was employed for these layers.

Figure 7 shows the computed rock movement after considerable deformation has occurred. The computed failure

involving the pillar resembles a classic circular arc. The computed deformations agree qualitatively with observations; however, the model deformations are much smaller than those observed in the field. The difference may arise because FLAC uses a continuum formulation to model a failure process that gradually becomes more and more discontinuous. Recognizing this limitation, the model results only apply up to the onset of failure and with caution a little beyond. Failure stability assessment is therefore possible in the initial computed postfailure regime.

The computations provide an estimate of the complete stress-strain behavior of the overall pillar-floor system. Using the "history" function within FLAC, the model recorded average stress across the middle layer of the pillar and the relative displacement between the top and bottom of the pillar from which strain was computed. Figure 8 shows the effective stress-strain curves determined for the pillar-floor system from these four models. The initial postfailure portion of these curves is an estimate of K_p for use in ascertaining the failure process nature, either stable or unstable, on the basis of the local mine stiffness stability criterion.

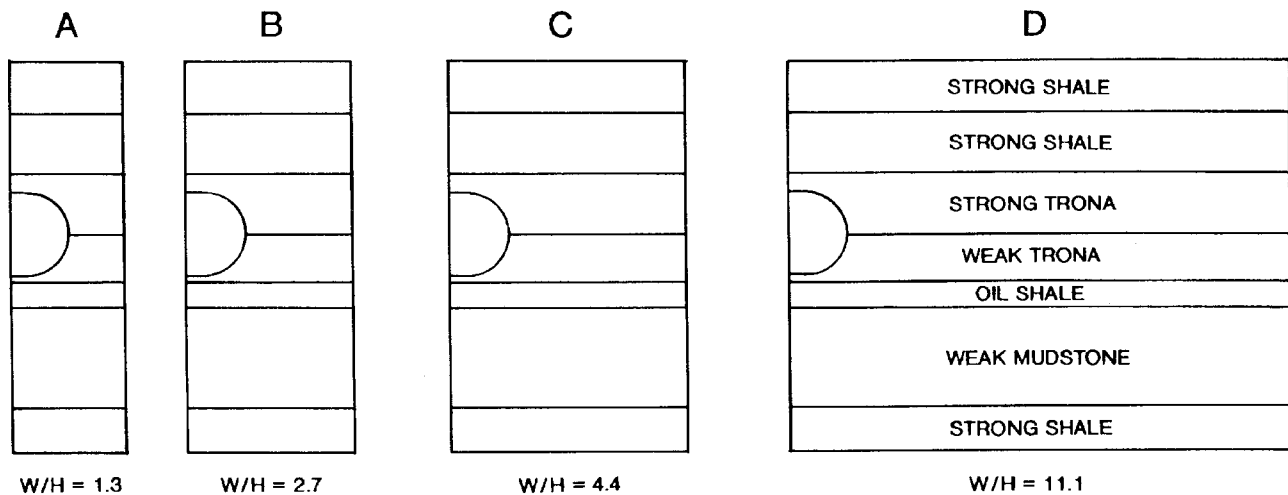


Figure 6.—FLAC models of pillar-floor system for increasing pillar width and w/h .

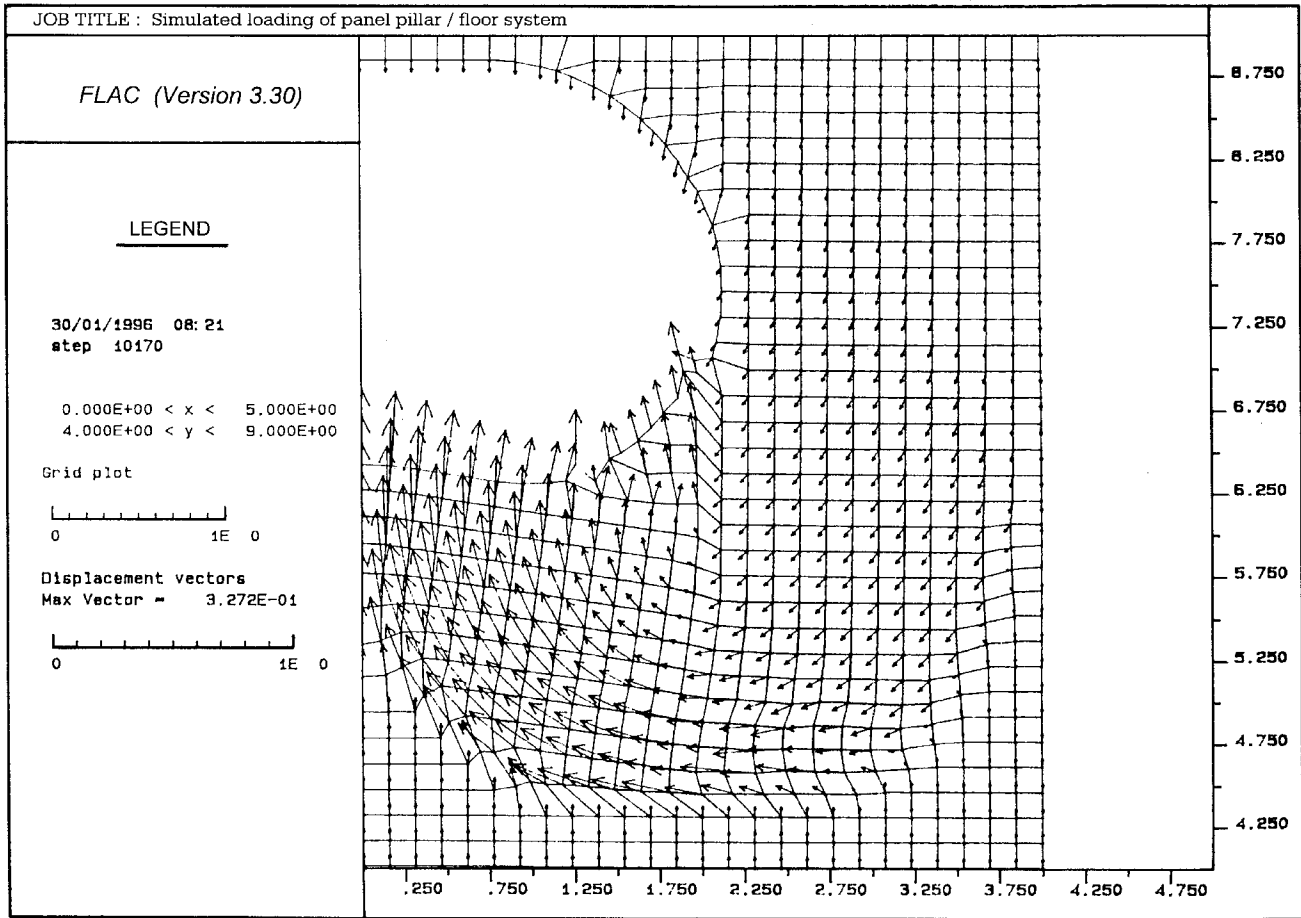


Figure 7.—Calculated deformation of pillar-floor system.

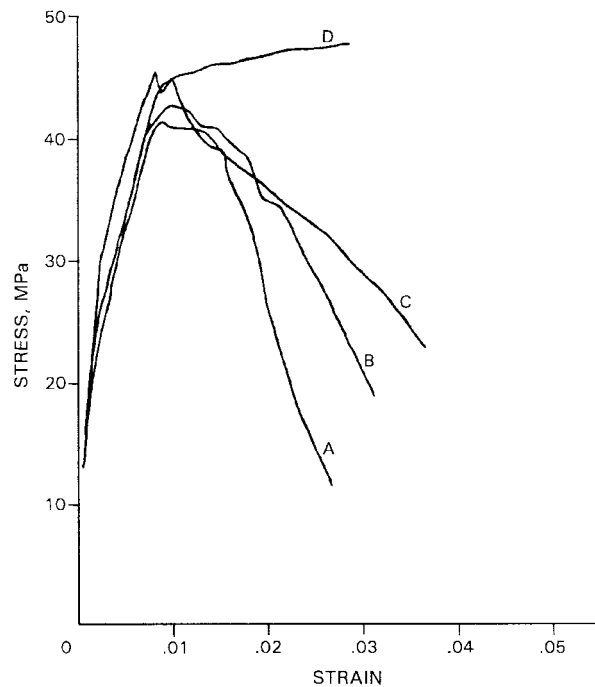


Figure 8.—Stress-strain behavior of pillar-floor for increasing pillar width and w/h.

USEFULNESS OF THE LOCAL MINE STIFFNESS STABILITY CRITERION

In practical mining engineering, we frequently want failure to occur. Failure usually means that we are extracting as much of a resource as practical. However, we want failure to occur in a controlled manner so that no danger is presented to mining personnel or equipment. The local mine stiffness stability criterion governs the nature of the failure process—stable and controlled or unstable and possibly violent. Field data in conjunction with numerical modeling enable calculation of local mine stiffness (K_{LMS}), estimation of postfailure stiffness (K_p), and thus evaluation of the local mine stiffness stability criterion.

The stability criterion was implemented into the boundary-element program MULSIM/NL and used to evaluate the nature of the failure process [Zipf 1996; Chase et al. 1994]. The following example shows results from two contrasting numerical models. Depending on whether the criterion is satisfied or violated, the stress and displacement calculations with MULSIM/NL behave in vastly different manners.

Figure 9 shows an unstable case, which violates the local mine stiffness stability criterion. In the initial model, calculations for an array of pillars show that stresses are close to peak strength and roof-to-floor convergence is still low. In

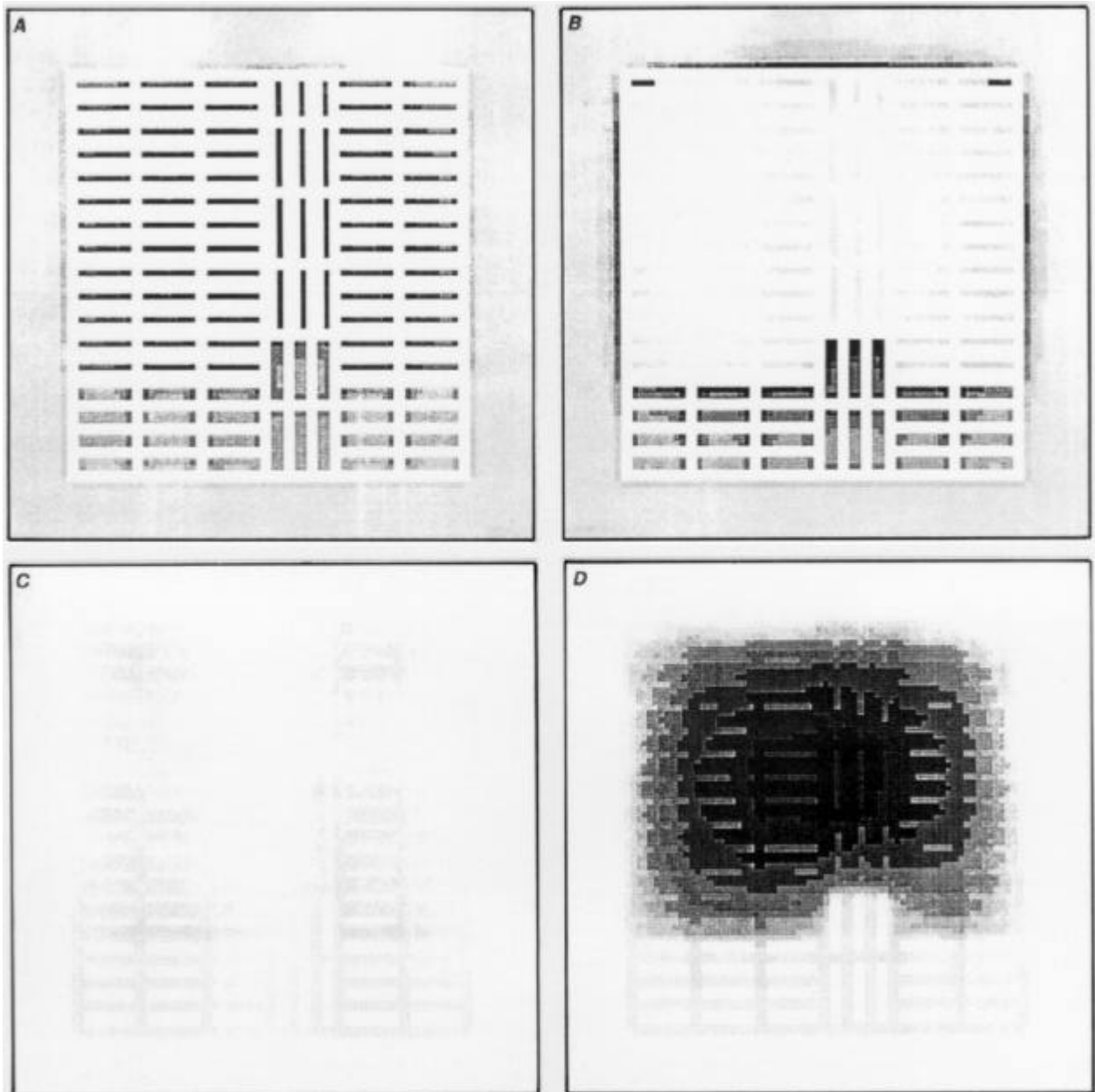


Figure 9.—Unstable case: (A), stress before pillar weakening, (B), convergence before pillar weakening, (C), stress after pillar weakening, (D), convergence after pillar weakening. Light to dark gray indicates increasing magnitude of calculated vertical stress and convergence.

the next modeling step, several pillars are removed to simulate mining or else initial pillar failure. This small change triggers dramatic events in the model. Convergence throughout the model increases dramatically, indicating that widespread failure has occurred. A small disturbance or increment of mining results in a much, much larger increment of failure in the model.

Figure 10 shows a stable case, which satisfies the stability criterion. As before, pillar stresses in the initial model are

everywhere near failure and convergence is low. In the next step, additional pillars are removed, as before. However, in the stable model, this significant change does not trigger widespread failure. An increment of mining results in a more or less equal increment of additional failure in the model.

The local mine stiffness stability criterion inspires three different design approaches to control CPF in mines: (1) containment, (2) prevention, and (3) full-extraction mining [Zipf and Mark 1997]. In the containment approach, panel

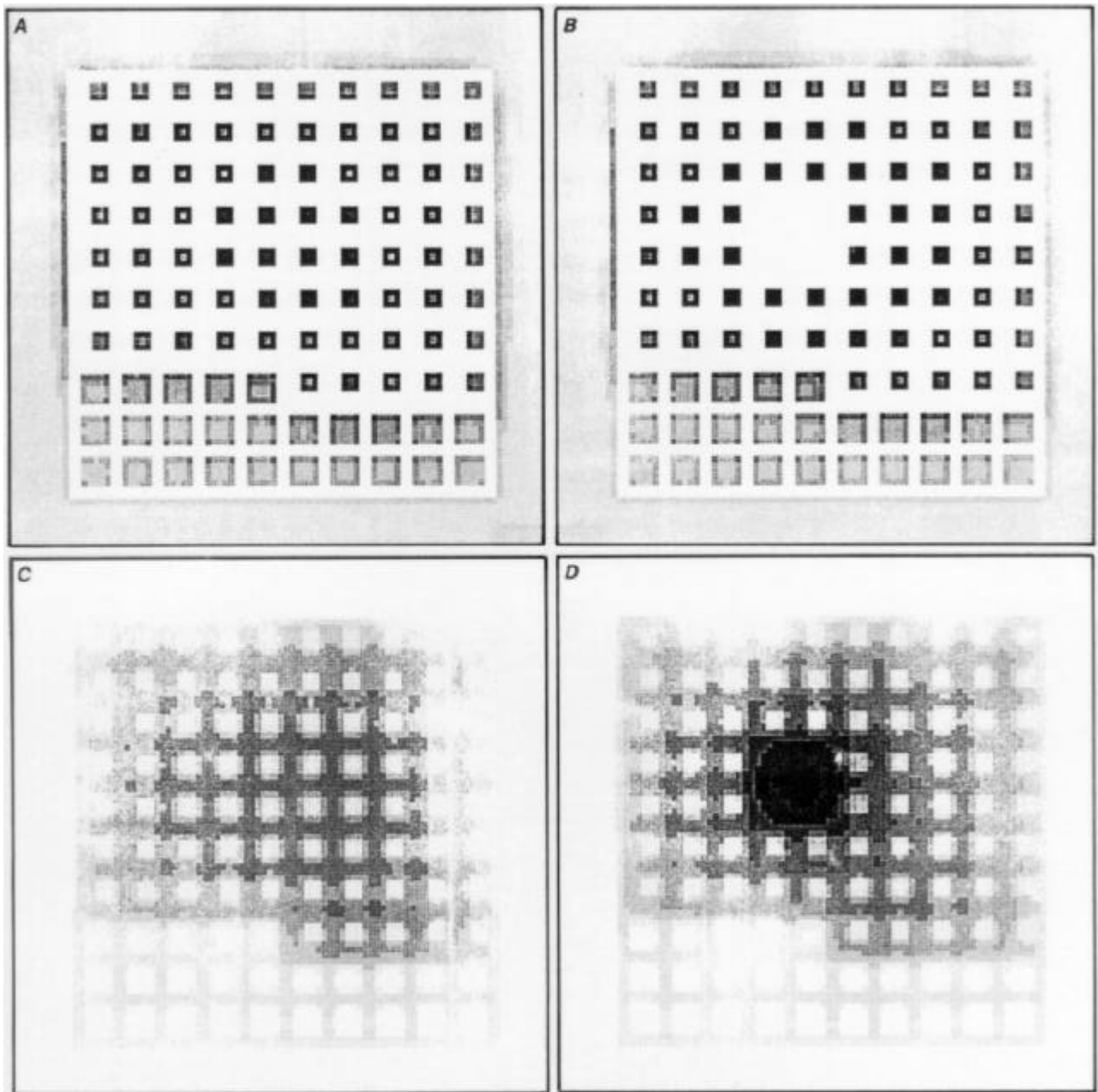


Figure 10.—Stable case: (A), stress before pillar weakening, (B), convergence before pillar weakening, (C), stress after pillar weakening, (D), convergence after pillar weakening. Light to dark gray indicates increasing magnitude of calculated vertical stress and convergence.

pillars must satisfy a strength-type design criterion, but they violate the stability criterion. Substantial barrier pillars "contain" the spread of potential CPF that could start. In the prevention approach, pillars must satisfy two design criteria—one based on strength, the other based on stability. This more

demanding approach ensures that should pillar failure commence, its nature is inherently stable. Finally, the full-extraction approach avoids the possibility of CPF altogether by ensuring total closure of the opening (and surface subsidence) upon completion of retreat mining.

SUMMARY AND RECOMMENDATIONS

Practical work to date with the local mine stiffness stability criterion reveals both the promises and shortcomings of the criterion in the effort to prevent catastrophic failures in mines. Back-analysis of case histories in various mines demonstrates the possibilities of using the criterion in predictive design to decrease the risk of catastrophic collapse [Swanson and Boler 1995; Zipf 1996; Chase et al. 1994; Zipf, in press]. The tool could have wide application in metal, nonmetal, and coal room-and-pillar mines, as well as other mining systems. However, a larger database of properly back-analyzed case histories of collapse-type failure is required. In addition to collapse-type failures, the criterion could evaluate the nature of shear-type failure and have applications in rock burst and coal mine bump mitigation.

Practical calculations of the local mine stiffness (K_{LMS}) term in the stability criterion have been done using analytical methods [Salamon 1970; 1989a,b] and, more recently, numerical methods [Zipf, in press]. Major factors affecting K_{LMS} are rock mass modulus; mine geometry, including panel and barrier pillar width; and the percentage extraction, i.e., the overall amount of mining. Analytical and numerical K_{LMS} calculations done to date assume an elastic continuum and neglect the presence of major discontinuities. The effect of these discontinuities is certain to decrease K_{LMS} ; however, the magnitude of these effects requires further numerical study.

Other numerical approaches, such as discrete-element or discontinuous deformation analysis, may provide useful insight into the K_{LMS} for practical mine design.

Better understanding of the postfailure behavior of mine pillars requires additional effort. Experiments on full-scale pillars are generally not practical; however, careful laboratory and numerical studies could provide justifiable estimates of K_p for mine pillars. Tests in the laboratory should examine the complete stress-strain behavior of various roof-pillar-floor composites at a variety of w/h ratios. Other variables to consider include the effect of horizontal discontinuities and water in the rock mass. Laboratory experiments can provide the necessary benchmark data for numerical studies that extrapolate to the field.

This paper summarizes the status of practical evaluation of the local mine stiffness stability criterion for prevention of certain types of catastrophic ground failures in mines. Back-analyses of collapse case histories show that the stability criterion can predict the possibility of these catastrophic failures. Evaluating the criterion depends on numerical computation of K_{LMS} and limited knowledge of the postfailure behavior of pillars. Further laboratory and numerical studies of the input parameters K_{LMS} and K_p should increase our confidence in predicting failure nature with the local mine stiffness stability criterion.

REFERENCES

- Bieniawski ZT, Vogler UV [1970]. Load-deformation behavior of coal after failure. In: Proceedings of the Second ISRM Congress on Rock Mechanics, ISRM (Belgrade, Yugoslavia). Vol. 1, paper No. 2-12.
- Bryan A, Bryan JG, Fouche J [1966]. Some problems of strata control and support in pillar workings. *The Mining Engineer* 123:238-254.
- Casey LA [1998]. Comprehensive test ban treaty research and development plans and accomplishments...from signature to entry into force. Washington, DC: U.S. Department of Energy, Office of Nonproliferation and National Security, Office of Research and Development, Report No. DOE/NN-98001802.
- Chase FE, Zipf RK Jr., Mark C [1994]. The massive collapse of coal pillars: case histories from the United States. In: Peng SS, ed. Proceedings of the 13th International Conference on Ground Control in Mining. Morgantown, WV: West Virginia University, pp. 69-80.
- Cook NGW, Hojem JPM [1966]. A rigid 50-ton compression and tension testing machine. *J S Afr Inst Mech Eng* 1:89-92.
- Das MN [1986]. Influence of width/height ratio on postfailure behavior of coal. *Int J of Mining and Geol Eng* 4:79-87.
- Ferriter RL, Zipf RK Jr., Ropchan DM, Davidson J [1996]. Report of Technical Investigation, Underground Nonmetal Mine, Mine Collapse Accident, Solvay Mine, Solvay Minerals, Inc., Green River, Sweetwater County, Wyoming, February 3, 1995. Denver, CO: U.S. Department of Labor, Mine Safety and Health Administration.
- Heasley KA [1997]. A new laminated overburden model for coal mine design. In: Proceedings - New Technology for Ground Control in Retreat Mining. Pittsburgh, PA: U.S. Department of Health and Human Services, Public Health Service, Centers for Disease Control and Prevention, National Institute for Occupational Safety and Health, DHHS (NIOSH) Publication No. 97-122, IC 9446, pp. 60-73.
- Heasley KA [1998]. Numerical modeling of coal mines with a laminated displacement-discontinuity code [Dissertation]. Golden, CO: Colorado School of Mines, Department of Mining and Earth Systems Engineering.
- Heuze F [1996]. LLNL's partnership with selected U.S. mines for CTBT verification: a pictorial and some reflections. UCRL-ID-122577.
- Iannacchione AT [1990]. Behavior of a coal pillar prone to burst in the southern Appalachian Basin of the United States. In: Fairhurst C, ed. Proceedings of Rockbursts and Seismicity in Mines. Balkema, pp. 295-300.
- Jaeger JC, Cook NGW [1979]. Fundamentals of rock mechanics. 3rd ed. Chapman and Hall.

Maleki H [1992]. In situ pillar strength and failure mechanisms for U.S. coal seams. In: Proceedings of the Workshop on Coal Pillar Mechanics and Design. Pittsburgh, PA: U.S. Department of the Interior, Bureau of Mines, IC 9315, pp. 73-77.

Mark C, Iannacchione AT [1992]. Coal pillar mechanics: theoretical models and field measurements compared. In: Proceedings of the Workshop on Coal Pillar Mechanics and Design. Pittsburgh, PA: U.S. Department of the Interior, Bureau of Mines, IC 9315, pp. 78-93.

Salamon MDG [1970]. Stability, instability, and design of pillar workings. *Int J of Rock Mech Min Sci* 7:613-631.

Salamon MDG [1989a]. Some applications of the frictionless laminated model. In: Proceedings of the 30th U.S. Rock Mechanics Symposium (Morgantown, WV). Balkema: pp. 891-898.

Salamon MDG [1989b]. Subsidence prediction using a laminated model. In: Proceedings of the 30th U.S. Rock Mechanics Symposium (Morgantown, WV). Balkema: pp. 503-510.

Seedsman RW, Hornby P [1991]. Controlled and uncontrolled pillar collapse. NERDDC project report No. 1440. Australia: ACIRL Ltd.

Skelly WA, Wolgamott J, Wang FD [1977]. Coal pillar strength and deformation prediction through laboratory sample testing. In: Proceedings of the 18th U.S. Rock Mechanics Symposium. Golden, CO: Colorado School of Mines, pp. 2B5-1 to 2B5-5.

Swanson PL, Boler FM [1995]. The magnitude 5.3 seismic event and collapse of the Solvay trona mine: analysis of pillar/floor failure stability. U.S. Department of the Interior, Bureau of Mines, OFR 86-95.

Van Heerden WL [1975]. In situ determination of complete stress-strain characteristics of large coal specimens. *J S Afr Inst Min Metall* 75(8):207-217.

Wagner H [1974]. Determination of the complete load-deformation characteristics of coal pillars. In: Proceedings of the Third International Congress on Rock Mechanics. National Academy of Sciences, Vol. 2B, pp. 1076-1081.

Zipf RK Jr. [1992a]. MULSIM/NL application and practitioner's manual. Pittsburgh, PA: U.S. Department of the Interior, Bureau of Mines, IC 9322.

Zipf RK Jr. [1992b]. MULSIM/NL theoretical and programmer's manual. Pittsburgh, PA: U.S. Department of the Interior, Bureau of Mines, IC 9321.

Zipf RK Jr. [1996]. Simulation of cascading pillar failure in room-and-pillar mines using boundary-element method. In: Proceedings of the Second North American Rock Mechanics Symposium. Balkema, pp. 1887-1892.

Zipf RK Jr. [in press]. Catastrophic collapse of highwall web pillars and preventative design methods. In: Proceedings of the 18th International Conference on Ground Control in Mining. Morgantown, WV: West Virginia University.

Zipf RK Jr., Mark C [1997]. Design methods to control violent pillar failures in room-and-pillar mines. *Transactions of the Institution of Mining and Metallurgy* 106(Sept-Dec):A124-A132.

Zipf RK Jr., Swanson PL [in press]. Description of a large catastrophic failure in a southwestern Wyoming trona mine. In: Proceedings of the 37th U.S. Rock Mechanics Symposium (Vail, CO).



- Delivering on the Nation's promise:
Safety and health at work for all people
through research and prevention.

To receive other information about occupational safety and health problems, call
1-800-35-NIOSH (1-800-356-4674), or
visit the NIOSH Home Page on the World Wide Web at
<http://www.cdc.gov/niosh>

DHHS (NIOSH) Publication No. 99-114

June 1998